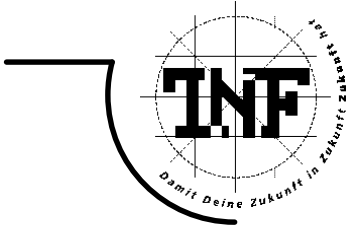




JOHANNES KEPLER
UNIVERSITÄT LINZ
Netzwerk für Forschung, Lehre und Praxis



Finite and Boundary Element Tearing and Interconnecting Methods for Multiscale Elliptic Partial Differential Equations

DISSERTATION

zur Erlangung des akademischen Grades

DOKTOR DER TECHNISCHEN WISSENSCHAFTEN

Angefertigt am *Institut für Numerische Mathematik*

Begutachtung:

O. Univ. Prof. Dipl. Ing. Dr. Ulrich Langer, Universität Linz

Prof. Dr. Axel Klawonn, Universität Duisburg-Essen

Eingereicht von:

Dipl.-Ing. Clemens Pechstein

Linz, Dezember 2008

*für Astrid,
meine lieben Eltern,
und in Erinnerung an Großvater Gerhard*

Abstract

Finite and boundary element discretizations of elliptic partial differential equations result in large linear systems of algebraic equations. In this dissertation we study a special class of domain decomposition solvers for such problems, namely the finite and boundary element tearing and interconnecting (FETI/BETI) methods. We generalize the theory of FETI/BETI methods in two directions, unbounded domains and highly heterogeneous coefficients.

The basic idea of FETI/BETI methods is to subdivide the computational domain into smaller subdomains, where the corresponding local problems can still be handled efficiently by direct solvers, if feasible, in parallel. The global solution is then constructed iteratively from the repeated solution of local problems. Here, suitable preconditioners are needed in order to ensure that the number of iterations depends only weakly on the size of the local problems. Furthermore, the incorporation of a coarse solve ensures the scalability of the method, which means that the number of iterations is independent of the number of subdomains.

For scalar second-order elliptic equations given in a bounded domain where the diffusion coefficient is constant on each subdomain, FETI/BETI methods are proved to be quasi-optimal. In particular, the condition number of the corresponding preconditioned system is bounded in terms of a logarithmic expression in the local problem size. Furthermore, the bound is independent of jumps in the diffusion coefficient across subdomain interfaces.

First, we consider the case of unbounded domains, where one subdomain corresponds to an exterior problem, while the other subdomains are bounded. The exterior problem is approximated using the boundary element method. The fact that this exterior domain can touch arbitrarily many interior subdomains and that the diameter of its boundary is larger than those of the interior subdomains leads to special difficulties in the analysis. We provide explicit condition number bounds that depend on a few geometric parameters, and which are quasi-optimal in special cases. Our results are confirmed in numerical experiments.

Second, we consider elliptic equations with highly heterogeneous coefficient distributions. We prove rigorous bounds for the condition number of the preconditioned FETI system that depend only on the coefficient variation in the vicinity of the subdomain interfaces. To be more precise, if the coefficient varies only moderately in a layer near the boundary of each subdomain, the method is proved to be robust with respect to arbitrary variation in the interior of each subdomain and with respect to coefficient jumps across subdomain interfaces. In our analysis we develop and use new technical tools such as generalized Poincaré and discrete Sobolev inequalities. Our results are again confirmed in numerical experiments. We also demonstrate that FETI preconditioners can lead to robust behavior even for certain coefficient distributions that are highly varying in the vicinity of the subdomain interfaces.

Finally, we consider nonlinear stationary magnetic field problems in two dimensions, as an important application of our preceding analysis. There, the Newton linearization leads to problems with highly heterogeneous coefficients, which can be efficiently solved using the proposed FETI/BETI methods.

Zusammenfassung

Die Finite-Elemente-Methode und die Randelementmethode sind Standardverfahren zur Diskretisierung elliptischer partieller Differentialgleichungen. Beide Verfahren führen auf großdimensionierte, lineare algebraische Gleichungssysteme, deren schnelle Lösung ganz wesentlich die Effizienz dieser numerischen Methoden bestimmt. In dieser Arbeit betrachten wir eine spezielle Klasse von Gebietszerlegungsmethoden zur Lösung derartiger Probleme, genannt FETI/BETI-Methoden (*Finite/Boundary Element Tearing and Interconnecting Methods*). Wir erweitern die bekannte Theorie dieser Methoden in zwei Richtungen, auf unbeschränkte Gebiete und auf Probleme mit stark variierenden Koeffizienten.

Die Grundidee der FETI/BETI-Methoden ist eine Zerlegung des Rechengebiets in kleinere Teilgebiete, auf denen lokalisierte Gleichungen effizient durch direkte Verfahren gelöst werden können. Dabei bietet sich zudem die Möglichkeit der Parallelisierung. Die globale Lösung wird dann schrittweise durch wiederholtes Lösen lokaler Probleme rekonstruiert. Hier werden Vorkonditionierer benötigt, damit die Größe der lokalen Probleme die Anzahl der Iterationsschritte nur schwach beeinflusst. Weiters stellt erst die Einbeziehung eines sogenannten Grobgitter-Problems die Skalierbarkeit sicher, was bedeutet dass die Anzahl der Schritte *nicht* mit der Anzahl der Teilgebiete anwächst.

Für skalare elliptische partielle Differentialgleichungen zweiter Ordnung auf beschränkten Gebieten ist bekannt, dass FETI/BETI-Methoden quasi-optimal sind, sofern der Diffusionskoeffizient der Gleichung auf jedem Teilgebiet konstant ist oder nur schwach variiert. Genauer gesagt ist die Konditionszahl des zugehörigen vorkonditionierten Systems durch einen logarithmischen Term in der lokalen Problemgröße beschränkt. Diese Schranke ist unabhängig von möglichen Sprüngen des Diffusionskoeffizienten zwischen den einzelnen Teilgebieten.

Zunächst betrachten wir den Fall eines unbeschränkten Gebiets, in welchem eines der Teilgebiete den Außenraum umfasst. Dort wird die Lösung mit Hilfe der Randelementmethode berechnet. Die Tatsache, dass dieses äußere Teilgebiet beliebig viele innere Teilgebiete berühren kann und dass der Durchmesser seines Randes im Allgemeinen größer ist als die der inneren Teilgebiete, führt auf Schwierigkeiten in der Analysis. Wir leiten explizite Schranken für die zugehörigen Konditionszahlen her, die von geometrischen Parametern abhängen und für Spezialfälle quasi-optimal sind. Unsere theoretischen Resultate werden in numerischen Experimenten bestätigt.

Weiters betrachten wir den Fall skalarer elliptischer partieller Differentialgleichungen mit stark variierenden Koeffizienten, deren Werte insbesondere auch innerhalb jedes Teilgebiets schwanken können. Wir zeigen explizite Schranken für die Konditionszahl der vorkonditionierten FETI-Systeme, welche nur von der Koeffizientenvariation in der Nähe der Teilgebietsränder abhängen. Genauer gesagt, falls der Koeffizient pro Teilgebiet in einem Bereich nahe des jeweiligen Randes nur schwach variiert, ist die FETI-Methode robust in jeglicher Variation im Inneren der Teilgebiete und in Koeffizientensprüngen zwischen den einzelnen Teilgebieten. Für unsere Analysis entwickeln wir neuartige technische Hilfsmittel, wie etwa verallgemeinerte Poincaré- und diskrete Sobolev-Ungleichungen. Unsere theoretischen Ergebnisse werden wiederum in numerischen Experimenten bestätigt.

Zuletzt wenden wir die zuvor diskutierten Methoden auf nichtlineare zweidimensionale stationäre Magnetfeldprobleme an. Hier führt die Newton-Linearisierung auf Problemstellungen mit stark variierenden Koeffizienten, welche durch geeignete FETI/BETI-Methoden effizient gelöst werden können.

Preface

This thesis covers results that were achieved within my research at the Institute of Computational Mathematics and the special research program SFB F013 at the Johannes Kepler University Linz. Hereby, I gratefully acknowledge the support by the Austrian Science Funds (FWF) and the Austrian Grid project.

My deep gratitude goes to my advisor Ulrich Langer, who arose my interest in this subject, motivated and encouraged me, and who organized the financial support for my research. At the same time I would like to thank Axel Klawonn for showing so much interest in my work and for co-refereeing this thesis. I am also deeply indebted to my collaborator and friend Robert Scheichl, who invested his time and energy for our joint research, encouraged and pushed me.

Special thanks go to Olaf Steinbach, who never hesitated to help me and spent his time for enlightening discussions. I would also like to express my thanks to Olof Widlund for showing his strong interest in my results and for the fruitful discussions with him. For their helpful hints I want to thank Ernst Stephan and Norbert Heuer.

My research would not have been successful without the discussions, helpful hints, and the support by Astrid Sinwel, Sabine Zaglmayr, Veronika Pillwein, Günther Of, Sven Beuchler, Walter Zulehner, Bert Jüttler, Joachim Schöberl, Ivan Graham, Dylan Copeland, Tino Eibner, David Pusch, Christoph Koutschan, Stefan Reitzinger, and Oliver Rheinbach.

I gratefully acknowledge the scientific environment at both the Institute of Computational Mathematics and the SFB F013, and want to thank my colleagues there for their hospitality. Additionally I would like to thank the Radon Institute for Computational and Applied Mathematics (RICAM), Austrian Academy of Sciences (ÖAW) at Linz for the permission to use their high end computer “thebrain” for many of my numerical experiments.

Private life is so much important to have a good balance with work. Therefore I want to thank in particular all the jazz musicians with whom I shared my spare time.

Finally, I would like to express my sincere thanks to my family, who supported me through all the years, and to my girlfriend Astrid for her understanding, her faith in me, and her love.

Linz
December 2008

Clemens Pechstein

Contents

Introduction	1
1 Preliminaries	11
1.1 Basic concepts	11
1.1.1 Basic notation and auxiliary results	11
1.1.2 Projections	14
1.2 The potential equation	14
1.3 Variational methods	16
1.3.1 Sobolev spaces	16
1.3.2 Variational formulation	24
1.3.3 Existence of unique solutions to abstract variational problems	25
1.3.4 Galerkin's method	26
1.4 Boundary integral equations	27
1.4.1 Boundary integral operators and the Calderón system	27
1.4.2 Representation formulae	30
1.4.3 Steklov-Poincaré operators	30
1.4.4 Newton potentials and Dirichlet-to-Neumann maps	33
1.5 Discretization techniques	34
1.5.1 Triangulations	34
1.5.2 Finite element method	35
1.5.3 Boundary element method	41
1.6 Estimates for approximate Steklov-Poincaré operators	44
2 Hybrid one-level methods	47
2.1 Variational skeleton formulations	48
2.1.1 Continuous skeleton formulations	48
2.1.2 Discrete skeleton formulations	51
2.2 Standard one-level and all-floating FETI/BETI methods	52
2.2.1 Formulation of standard one-level FETI/BETI methods	52
2.2.2 Formulation of all-floating FETI/BETI methods	61
2.2.3 Implementation issues	64
2.2.4 Analysis of the methods	69
2.2.5 Numerical results	84
2.2.6 A reformulation of the FETI/BETI PCG algorithm	87
2.3 Interface-concentrated FETI methods	93
2.3.1 Boundary-concentrated FEM	93

2.3.2	Interface-concentrated FETI	94
2.3.3	Numerical results	95
3	One-level methods for unbounded domains	97
3.1	Model problem and skeleton formulation	98
3.1.1	Continuous formulation	98
3.1.2	Discrete formulation	101
3.2	Difficulties in the case of unbounded domains	102
3.3	Formulation of FETI/BETI methods in unbounded domains	102
3.4	Condition number estimates	104
3.4.1	The extension indicator	104
3.4.2	Main result	109
3.4.3	Additional technical tools	110
3.4.4	The P_D estimates	113
3.5	Numerical results	119
3.6	Implementation issues	121
4	Dual-primal methods	123
4.1	Formulation of FETI/BETI-DP methods	124
4.1.1	Dual-primal spaces	124
4.1.2	The actual dual-primal methods	126
4.2	Condition number bounds for dual-primal methods	127
4.3	Implementation issues of dual-primal methods	132
4.3.1	Handling of edge and face constraints	132
4.3.2	Realization of the operators	133
4.3.3	Comparison of dual-primal and one-level methods	136
5	Multiscale coefficients	137
5.1	Problem formulation of multiscale elliptic PDEs	138
5.2	Formulation of FETI methods for multiscale PDEs	139
5.2.1	Different scaling operators and preconditioners	140
5.3	Robustness analysis	142
5.3.1	A straightforward condition number bound	142
5.3.2	New coefficient-robust condition number bounds	143
5.4	Proof of the theoretical results	145
5.4.1	A cut-off result	146
5.4.2	Generalized Poincaré, Friedrichs, and discrete Sobolev inequalities	147
5.4.3	Proof of the P_D -estimate (5.15)	154
5.4.4	Proof of Corollary 5.16	158
5.5	Numerical results	158
6	Applications to nonlinear magnetic field problems	165
6.1	Problem formulation	165
6.1.1	Constitutive laws	166
6.1.2	Interface and boundary conditions	167
6.1.3	Vector potential formulation	167
6.1.4	Reduction to two dimensions	168

6.1.5	Existence and uniqueness of solutions	169
6.1.6	Approximation of B - H -curves	170
6.2	Newton-FETI/BETI methods	172
6.2.1	Newton's method	173
6.2.2	The linearized problem	174
6.2.3	Error control	174
6.3	Numerical results	175
Bibliography		181
Eidesstattliche Erklärung		197
Curriculum Vitae		199

Introduction

State of the Art

PDEs, FEM, and BEM

Partial differential equations (PDEs) appear almost everywhere in the modeling of physical processes, e. g., heat transfer, fluid dynamics, structural mechanics, and electromagnetics, to name just some important applications. In this thesis we will mostly be concerned with the potential equation

$$-\operatorname{div} [\alpha(x) \nabla u(x)] = f(x), \quad x \in \Omega,$$

with the unknown function u , the given coefficient α , the source term f , and the computational domain $\Omega \subset \mathbb{R}^d$. In only a few cases the solution of PDEs can be computed analytically. In the remaining cases the solution has to be approximated using discretization techniques. In the past decades—besides the finite difference method (FDM), the finite volume method (FVM), and the finite integration technique (FIT)—the finite element method (FEM) and the boundary element method (BEM) have been established as probably the most powerful tools in the numerical simulation of PDEs.

The finite element method is based on the variational formulation of boundary value problems for PDEs. Its main advantages are the general applicability to linear and nonlinear PDEs, coupled multi-physics systems, complex geometries, varying material coefficients, and different kinds of boundary conditions. Furthermore, the FEM is based on a profound functional analytical framework (cf. BRAESS [16], BRENNER AND SCOTT [26], and CIARLET [35]), allowing for a rigorous error analysis. The main idea is to subdivide the computational domain into small simple domains called elements, which altogether form a triangulation (mesh) of the domain. On the elements the solution is approximated by local finite dimensional spaces, e. g., polynomials. The unknown coefficients with respect to a chosen basis are called degrees of freedom (DOFs) or unknowns. For well-posed linear boundary value problems, the FEM discretization leads to a linear system of algebraic equations that uniquely determines the unknowns, and therefore the approximate solution.

For many PDEs, e. g., the potential equation, the Stokes, Lamé, Helmholtz, and also Maxwell equations, analytical fundamental solutions are known. In some cases, e. g., constant coefficients and vanishing source terms of the PDE, by using the fundamental solution, one can derive integral equations that completely describe the underlying boundary value problem involving the unknown function (here u) only on the boundary of the computational domain. The solution in the interior can then be calculated directly from a representation formula involving the fundamental solution. The boundary element method (BEM) discretizes these integral equations on the boundary. Here, as an obvious advantage, only

boundary meshes have to be constructed in contrast to the volume meshes when using the FEM. A particular difficulty of the BEM is the non-locality of the boundary integral operators which have to be approximated by data-sparse techniques in order to obtain efficient solvers. For a comprehensive mathematical theory on boundary integral equations see, e. g., MCLEAN [134] and HSIAO AND WENDLAND [90]. For boundary integral equations and BEM see, e. g., SAUTER AND SCHWAB [164], STEINBACH [175], and also RJASANOW AND STEINBACH [158]. For data-sparse approximation techniques we additionally refer to the recently published monograph by BEBENDORF [8] and the references therein.

Domain decomposition methods and parallelization

If the number N of DOFs gets large, direct solvers for linear systems result in non-optimal complexity, i. e., $\mathcal{O}(N^\beta)$ with $\beta > 1$. In the case of standard Gaussian elimination for banded FEM systems the complexity is as bad as $\mathcal{O}(N^2)$ in two and $\mathcal{O}(N^{7/3})$ in three space dimensions, which can be enhanced to $\mathcal{O}(N^{3/2})$ resp. $\mathcal{O}(N^2)$ for sparse systems using special elimination strategies, cf., e. g., ZUMBUSCH [197]. Therefore, iterative solvers become the key ingredient to fast simulation. In this field, domain decomposition (DD) solvers have proved to be a powerful technique. Among them are overlapping and non-overlapping DD methods (also called substructuring methods), which subdivide the computational domain into (overlapping or non-overlapping) subdomains. The underlying algorithms are built from a number of local solves of smaller problems on the subdomains. This concept is embedded in the more general *abstract Schwarz theory*, coined by SCHWARZ [169], where the solution space is subdivided into *subspaces*. This theory covers additive, multiplicative, and hybrid Schwarz methods; among them multilevel and multigrid methods. Some of these methods result in quasi-optimal solvers with a computational complexity $\mathcal{O}(N(1 + \log N)^\beta)$. In certain cases they can even lead to optimal complexity $\mathcal{O}(N)$. Particularly in the context of elliptic PDEs, the incorporation of a coarse space has proved to be the key ingredient to achieve solvers which are robust in the number of subdomains. For a comprehensive account of the theory and the algorithms in domain decomposition but also of the general Schwarz theory, we refer to the monograph by TOSELLI AND WIDLUND [184], see also QUARTERONI AND VALLI [150] and SMITH, BJØRSTAD, AND GROPP [171]. For multigrid and multilevel methods we refer to BRAMBLE AND ZHANG [18], HACKBUSCH [80], and VASSILEVSKI [187].

The abstract framework of non-overlapping domain decomposition methods allows us (i) to couple different discretization techniques, such as BEM and FEM, and (ii) to parallelize solution algorithms on a mathematical level. Furthermore, there is a great potential to treat multi-physics problems (see, e. g., QUARTERONI AND VALLI [150]).

In many situations, it is of interest to couple FEM and BEM to exploit the advantages of both methods, also known as *marriage a la mode – the best of both worlds* (see ZIENKIEWICZ, KELLY, AND BETTESS [195]). For instance, the finite element method is suitable for heterogeneous coefficients, source terms, and nonlinearities, whereas one can model subdomains with constant coefficients (such as large air regions or small air gaps) and even unbounded regions very suitably using the boundary element method. A remarkable work is the article by COSTABEL [38] on the symmetric coupling of FEM and BEM, which was successfully used in (hybrid) domain decomposition methods, see, e. g., CARSTENSEN, KUHN, AND LANGER [30], HAASE, HEISE, KUHN, AND LANGER [78], HSIAO, STEINBACH, AND WENDLAND [91], HSIAO AND WENDLAND [89], LANGER [115], LANGER AND STEINBACH [120], STEINBACH [174].

In the last decades parallel computing has become more and more important, since the physical speed barrier has almost been reached by today's computer chips. However, parallelization is often only added as an afterthought in software design, which usually results in the fact that the parallel speed-up is limited to just a few processors. Far more efficiency can be gained using algorithms that can be parallelized on a mathematical level, and for which a profound mathematical analysis of the parallel scalability on massively parallel computers is available. This means that parallelization must already enter the *design* of numerical algorithms. Here, domain decomposition methods serve as a natural framework: In the simplest case, each processor treats one subdomain of the decomposition of the computational domain. Since communication between processors is still the dominant part, it should by all means be minimized, and so the mathematical algorithm should only require a relatively weak coupling between the subdomain problems. On the other hand, as described above, a global coupling via a coarse problem is essential when dealing with elliptic PDEs. Finding algorithms without any loss of efficiency has been a very active topic of research since thirty years. Here we refer, e. g., to BASTIAN [5], DOUGLAS, HAASE, AND LANGER [47], HAASE [77], SMITH, BJØRSTAD, AND GROPP [171], TOSELLI AND WIDLUND [184], ZUMBUSCH [197], the references therein, the more recent works by KLAWONN AND RHEINBACH [105, 106, 107] and RHEINBACH [154], and to the software projects *Hypre* (<http://acts.nersc.gov/hypre/>), *PETSc* (<http://www-unix.mcs.anl.gov/petsc/petsc-as/>), and *UG* (<http://sit.iwr.uni-heidelberg.de/~ug/>), see also *DUNE* (<http://www.dune-project.org/>).

Iterative substructuring methods

Among the most successful non-overlapping domain decomposition methods (at least for elliptic PDEs) are the balancing Neumann-Neumann methods, the finite element tearing and interconnecting (FETI) methods, the dual-primal FETI (FETI-DP) methods, and a method called balanced domain decomposition by constraints (BDDC). The classical FETI method, nowadays called the *one-level FETI method*, was introduced by FARHAT AND ROUX [55, 56] in 1991 as a dual iterative substructuring method, where it was first used for computational mechanics. In contrast to primal iterative substructuring methods, the finite element subspaces are given on each subdomain including its boundary, and in the first instance this leads to a discontinuous approximation space. The global continuity of the solution is enforced by pointwise algebraic constraints, modeled by Lagrange multipliers. The resulting saddle point problem is equivalent to a dual problem which is symmetric positive semidefinite. Using a preconditioned conjugate gradient (PCG) subspace iteration this dual problem can be solved iteratively. FARHAT, MANDEL, AND ROUX [57] proposed the first preconditioner for this dual problem, called *Dirichlet preconditioner*, which results in a weak growth of the number of iterations with respect to the number of degrees of freedom in the local problems. The main ingredients of FETI are local Dirichlet and Neumann solves, as well as an algebraic coarse solve.

We note that the pioneering work for iterative substructuring methods is a series of papers by BRAMBLE, PASCIAK, AND SCHATZ [19, 20, 21, 22], and that many of the tools developed there are essential in the FETI theory. Secondly we mention that the basic ideas in FETI and Neumann-Neumann methods can be tracked back to early work by GLOWINSKI AND WHEELER [70] on certain mixed methods.

Nowadays, an extensive mathematical framework for FETI methods is available. In their

pioneering work, MANDEL AND TEZAUR [131] published the first convergence proof for the one-level FETI method with non-redundant Lagrange multipliers for two-dimensional elliptic problems with homogeneous coefficients. They showed that the spectral condition number of the corresponding preconditioned system is bounded by $C(1 + \log(H/h))^\beta$, with $\beta \leq 3$, where H denotes the subdomain diameter, h the local mesh size, and C is a generic constant independent of H , h , and the number of subdomains. For a special two-dimensional case, they could show $\beta \leq 2$. Another breakthrough was the work by KLAWONN AND WIDLUND [109, 108] who introduced and analyzed new one-level FETI methods for three-dimensional elliptic problems with heterogeneous coefficients. They could prove the spectral bound $C(1 + \log(H/h))^2$, including also the case of redundant Lagrange multipliers, which are more commonly used in parallel implementations. Furthermore, provided that the coefficients of the PDE are constant (or at most mildly varying) in each subdomain, Klawonn and Widlund showed that the constant C is also independent of possible jumps in the coefficients across subdomain interfaces when a special scaling of the preconditioner is applied.

Using the basic idea of FETI methods, LANGER AND STEINBACH [118, 119] introduced the boundary element tearing and interconnecting (BETI) method and coupled FETI/BETI methods. The coupling of BEM and FEM in the tearing and interconnecting framework is possible mainly for two reasons: (i) the domain decomposition is non-overlapping, and (ii) FETI acts on the subdomain interfaces and relies on the finite element Schur complement on the local boundaries which is an approximation of the Steklov-Poincaré operator, also known as the Dirichlet-to-Neumann map. This operator can also be approximated using the BEM. Due to spectral arguments, the condition number of the BETI and the coupled FETI/BETI methods is also bounded by $C(1 + \log(H/h))^2$.

One-level FETI methods involve an algebraic coarse problem which is built from a special projection that deals with the local kernel of elliptic operators in *floating subdomains* that have no contribution from the Dirichlet boundary. In fact, the solution of the local Neumann problem $-\operatorname{div}[\alpha_i \nabla u] = f$ in Ω_i , with the conormal derivative $\alpha_i \frac{\partial u}{\partial n_i}$ prescribed on the whole of the boundary $\partial\Omega_i$, is only unique up to an additive constant, and this constant spans the kernel of the operator. In the construction of the coarse problem that guarantees parallel scalability of one-level FETI, we rely heavily on these non-trivial kernels of the local Neumann problems. The exact characterization of these local kernels is a non-trivial task for some more complicated PDEs, e. g., linear elasticity. There, the local kernel can have a dimension up to six in three dimensions. For local Neumann problems that are always uniquely solvable, e. g., for the equation $-\operatorname{div}[\alpha_i \nabla u] + \beta_i u = f$, the one-level FETI method has to be modified in order to get a coarse problem which ensures scalability. Such a modification has been proposed by FARHAT, CHEN, AND MANDEL [58] for time-dependent problems, see also TOSELLI AND KLAWONN [182] for problems arising in electromagnetics.

These technical and implementational difficulties led to the introduction of the dual-primal FETI (FETI-DP) methods by FARHAT, LESOINNE, LE TALLEC, PIERSON, AND RIXEN [63]. Here, not all of the continuity constraints are imposed by Lagrange multipliers, but some of the DOFs are designated as *primal* DOFs and eliminated from the system like in a block Cholesky factorization, cf. LI AND WIDLUND [125]. This way the local Neumann problems are always uniquely solvable and the size of the coarse problem is then the number of such primal DOFs. The first analysis was given by MANDEL AND TEZAUR [132] for two-dimensional problems with homogeneous coefficients. KLAWONN, WIDLUND, AND

DRYJA [111] gave a full analysis for the three-dimensional case with heterogeneous coefficients. As already observed numerically by FARHAT, LESOINNE, AND PIERSON [61] in three dimensions, fixing only a few vertices as primal DOFs is not sufficient and leads to a linear growth of the condition number in H/h . This is due to the fact that finite element vertex evaluations in two dimensions are almost continuous with a logarithmic dependency on H/h , whereas vertex evaluations in three dimensions have a linear dependency on H/h . The quasi-optimal bound can be obtained by introducing more primal constraints, such as edge or face constraints, which enforce edge or face averages of the solution to be continuous. The BEM counterpart of FETI-DP is called BETI-DP and was first introduced in LANGER, POHOAȚĂ, AND STEINBACH [121].

A convenient alternative to FETI-DP, when dealing with PDEs with no elliptic operators such as Laplace or linear elasticity with no zero-order terms, is a modification of the one-level FETI method that simplifies the characterization of the local kernels. Such an approach was independently introduced for finite elements by DOSTÁL, HORÁK, AND KUČERA [46], named *total FETI*, and for boundary elements by OF [138, 139], referred to as *all-floating BETI* (AF-BETI). Here, the Dirichlet boundary conditions are not incorporated into the FE or BE spaces, but rather imposed by additional Lagrange multipliers. Therefore, all subdomains become floating, and one can work uniformly with the full kernel.

Let us make a few remarks on Neumann-Neumann methods and the more recent balancing domain decomposition by constraints (BDDC). Neumann-Neumann methods (see BOURGAT, GLOWINSKI, LETALLEC, AND VIDRASCU [15], DE ROECK AND LETALLEC [41], DRYJA AND WIDLUND [48], LE TALLEC [124], MANDEL AND BREZINA [129], SARKIS [162]) provide a preconditioner to the Schur complement system by solving local Neumann problems using the jumps in the flux on each subdomain and then correcting the previous iterate with the corresponding function values. With the incorporation of a coarse space, the number of iterations becomes independent of the number of subdomains. For piecewise constant coefficients with respect to the subdomains, the method can be made robust using a partition of unity related to the coefficient values, which is also central in the FETI theory. As shown by KLAWONN AND WIDLUND [109], FETI and Neumann-Neumann methods are very closely related and can be considered as dual to each other.

BDDC, introduced by DOHRMANN [42] and analyzed by MANDEL AND DOHRMANN [130], is a balancing Neumann-Neumann method with a special coarse space that is derived from primal constraints in the same way as in FETI-DP methods. Indeed, it was shown by MANDEL, DOHRMANN, AND TEZAUER [133] and BRENNER AND SUNG [27] that the FETI-DP and the BDDC methods have essentially the same spectrum. For further references on BDDC methods see, e. g., DOHRMANN [43] and LI AND WIDLUND [126].

We mention that FETI type and Neumann-Neumann type methods have been generalized to structural mechanics (see, e. g., BRENNER [24], FARHAT, CHEN, MANDEL, AND ROUX [59], FARHAT AND MANDEL [54], KLAWONN AND WIDLUND [108, 110]), Helmholtz problems (FARHAT, MACEDO, AND LESOINNE [62], FARHAT, MACEDO, AND TEZAUER [60]), eddy current problems (TOSELLI AND KLAWONN [182], TOSELLI [180, 181]), and also to non-conforming (mortar) discretizations (KIM AND LEE [103], KIM [101, 102], STEFANICA [172], STEFANICA AND KLAWONN [173]). Inexact FETI-DP methods were introduced in KLAWONN AND RHEINBACH, RHEINBACH [106, 154]; here preconditioners on the saddle point formulation of FETI-DP methods are used to allow for an inexact solution of the coarse

problem. For extensions of FETI type methods to high-order (*hp* and spectral element) methods, see, e. g., Klawonn, Pavarino, and Rheinbach [112, 112], Pavarino [141], Toselli and Vasseur [183], and the references in Toselli and Widlund [184, Chap. 7]. A special *hp* method called *interface-concentrated* FETI has been introduced by Beuchler, Eibner, and Langer [11], building on a work by Khormskij and Melenk [100] for boundary-concentrated *hp*-FEM discretizations.

Highly heterogeneous coefficients

In many applications, the coefficients of the underlying PDE are heterogeneous in the sense that they jump across material interfaces while being homogeneous within a single material. The analysis of FETI type methods in this case can be covered by the theory in Klawonn and Widlund [109] and Klawonn, Widlund, and Dryja [111], as long as the material interfaces are resolved by the subdomain partitioning. However, there are other applications where the coefficient varies also within the subdomains, among them the simulation of complicated layered, heterogeneous, porous, or stochastic media, and nonlinear problems. We call such coefficients *highly heterogeneous* or *multiscale* coefficients. The development of fast and robust iterative solvers for problems with (highly) heterogeneous coefficients has been a very active area of research, specifically in the setting of multiscale solvers, and in the domain decomposition and multigrid communities. In the following we first review results on the heterogeneous case (apart from [109, 111]), where the coefficient is resolved by the subdomains or the coarsest mesh. Secondly, we review known results for the much more difficult highly heterogeneous case.

An important contribution concerning the heterogeneous case was the one by Sarkis [162, 163, 161] building on earlier works by Dryja and Widlund [48], Dryja, Smith, and Widlund [49], and Widlund [190] who used non-standard (sometimes known as *exotic*) coarse spaces to obtain robust additive and multiplicative Schwarz type solvers for coefficients which are piecewise constant with respect to the subdomains, see also Bjørstad, Dryja, and Vainikko [12], Chan and Mathew [31], and Toselli and Widlund [184]. We note that Sarkis introduced the concept of *quasi-monotone* coefficient distributions on cross points. The quasi-monotonicity is violated, e. g., in case of a checkerboard distribution with two different coefficient values. It turns out that for many methods, non-quasi-monotone coefficient distributions form indeed the harder case.

In their recent article [192], Xu and Zhu consider the conjugate gradient method with various multilevel preconditioners. If the coefficient is constant in M connected regions that are resolved by the coarsest mesh, the convergence is uniform in the coefficient jumps. In particular, the case of non-quasi-monotone coefficient distributions is covered as well. Although the condition number of the preconditioned system deteriorates in general, the number of small eigenvalues can be shown to be equal to M while the other eigenvalues form a cluster. Therefore, the number of iterations of the CG method depends only on M and the ratio of the extremal eigenvalues of the cluster. Robustness analysis for algebraic multilevel methods can be found in Kraus and Margenov [114].

Let us now come to works on highly heterogeneous coefficient distributions which are not resolved by subdomains or the coarse mesh. Graham and Hagger [71, 72] discovered and analyzed clustering effects (similar to those later exploited by Xu and Zhu) in the spectrum of FEM systems for high contrast coefficients, and they used additive Schwarz

preconditioned CG methods to exploit these effects. For similar computational results see VUIK, SEGAL, AND MEIJERINK [189]. If the coefficient is constant on M different regions, the number of small eigenvalues is equal to M . Graham and Hagger proved the convergence of CG with an additive Schwarz preconditioner for such coefficient distributions, where the iteration number depends only on M and is independent of the jumps in the coefficient. In contrast to previous works, the jumps need be resolved neither by the subdomains nor by the coarse grid.

In the articles by GRAHAM, LECHNER, AND SCHEICHL [75], GRAHAM AND SCHEICHL [73, 74], and SCHEICHL AND VAINIKKO [165] we find theory for Schwarz type domain decomposition solvers for highly heterogeneous coefficients, which adjust the basis functions of the coarse space according to the coefficients. The authors come up with very general bounds for the condition number in terms of one or two indicators which describe the relationship between the coefficients, the subdomain partitioning, and the coarse basis functions. In order to obtain robust bounds the authors specialize on certain “island” configurations. By an “island” we understand a region of heterogeneity in the coefficient which is fully contained in another homogeneous region where the coefficient is constant. Under certain assumptions on these islands, the indicators mentioned above can be estimated in terms of accessible geometric parameters, such as the overlap parameter, diameters of the islands, and distances between islands and element or subdomain interfaces. Here we must point out that in spite of the rather special assumptions, islands may still cut through subdomain facets or can be included in their interior. Indeed, the theoretical analyses are rather involved, which is for sure associated to the difficulty of the problem of highly heterogeneous coefficients.

Numerical robustness results for (algebraic) multigrid and multilevel methods can be found, e. g., in ALCOUFFE, BRANDT, DENDY, JR., AND PAINTER [4], RUGE AND STÜBEN [160], and VANEK, MANDEL, AND BREZINA [186]. Theoretical results are given in AKSOYLU, GRAHAM, KLIE, AND SCHEICHL [3], GEORGIEV, KRAUS, AND MARGENOV [68].

As observed numerically by several authors, FETI type methods seem to be robust even when coefficient jumps are not aligned with the subdomain partitioning, see RIXEN AND FARHAT [155, 156] for one-level methods and KLAWONN AND RHEINBACH [104, 107] for FETI-DP methods. A theoretical foundation is so far still lacking.

On this work

The aims of this work are to investigate FETI/BETI type methods for the case of

- (i) unbounded domains, i. e., coupling to exterior problems, and
- (ii) highly heterogeneous coefficients.

The aspect of exterior problems and highly heterogeneous coefficients is mainly driven by the application to nonlinear magnetic field computations as they will be explained in more detail in the sequel. In two dimensions, the linearization of such equations results in potential equations. Similar equations arise in nonlinear electrostatics, see, e. g., IDA AND BASTOS [92, Chap. 3] or KALTENBACHER [93, Sect. 4.3]. Therefore the potential equation (in two and three dimensions) will serve as our model problem throughout. In the following we describe some phenomena which occur in the context of these magnetic field problems in order to motivate our investigations on FETI/BETI type methods.

Exterior problems Except for special cases, electromagnetic fields radiate to infinity, although they might decay rather fast according to *radiation conditions*, such as the Silver-Müller radiation condition for the Maxwell equations or the Sommerfeld radiation condition for the Helmholtz equation, cf., e. g., MONK [136]. Henceforth, the computational domain is at first sight unbounded. There are many techniques to deal with such unbounded domains in connection with magnetic field computations. Besides the use of Dirichlet boundary conditions on an artificial boundary exploiting the fast decay far away from the sources, infinite elements, conformal mappings, perfectly matched layers, etc., the boundary element method can handle radiation conditions in homogeneous media with high accuracy. Here, one introduces an artificial interface away from the sources and can find boundary integral equations which exactly model the entire PDE in the exterior of that interface. In particular, the exterior Steklov-Poincaré operator, i. e., the exterior Dirichlet-to-Neumann map, for Laplace’s equation can be fully described by means of such integral operators.

Since the FETI/BETI methods for bounded domains can be described very naturally by Steklov-Poincaré operators on the subdomains, it seems straightforward to treat unbounded domains with FETI/BETI type methods. From a practical point of view this is indeed the case. However, new questions concerning robustness arise which are usually not present in the bounded case. In the standard theory of FETI/BETI type methods, it is assumed that each subdomain has a finite, uniformly bounded number of neighbors, and that neighboring subdomains are of comparable size. In the context of our theory, the “size” of the exterior subdomain is measured by the diameter of its boundary (which is finite), in the following denoted by H_0 . Therefore, the standard assumption requires that all the neighboring subdomains of the exterior domain have a diameter proportional to H_0 which implies that there can only be very few of them. In general, using the known theory in its basic form, the condition number depends on the ratios H_0/H_i and on the number of neighbors of the exterior domain, which would be rather limiting. In practice, we are interested in problems where the exterior domain can have arbitrarily many neighboring subdomains and in solvers which are robust with respect to the number of neighbors and the different sizes of the subdomains.

Nonlinearity and heterogeneity In two-dimensional nonlinear magnetic field computations the coefficient of the PDE, called *reluctivity* ν , depends nonlinearly on the gradient of the solution, or equivalently on the magnetic flux density $|\mathbf{B}|$. For many materials, such as ferromagnetic ones, this dependency is nonlinear. In other materials, such as air or insulators, the reluctivity coefficient can be modeled as constant. In any case, we expect jumps in the coefficient across material interfaces, and these jumps can be of order $\mathcal{O}(10^3)$ and more. If we apply a Newton type method to the nonlinear equation, the linearized equation in each iterative step is again a potential equation with a tensor-valued coefficient, denoted by ζ , that depends on the gradient of the current iterate. Since such gradients can grow arbitrarily large near singularities which arise at material corners (cf., e. g., GRISVARD [76]), the coefficient ζ can become highly heterogeneous, even within a homogeneous (but nonlinear) material. In summary, for such nonlinear problems we have

- large jumps in the coefficient ζ across material interfaces, and
- smooth but large variation in ζ within an individual material due to nonlinear effects.

Iterative solvers for the linearized problems should be robust with respect to the variation in the coefficient ζ . The existing theory on FETI methods covers only the case of coefficients

that are piecewise constant on the subdomains or only slightly varying. If we apply the methods naively to highly heterogeneous coefficients as described above, the rate of variation will enter the condition number bound, i. e., the method is, in its basic form, not robust with respect to the variation. However, RIXEN AND FARHAT [155, 156] introduced modified scaling strategies for one-level FETI methods, known as *superlumping*, which are proved to be rather effective for coefficient jumps which are *not* aligned with interfaces, at least numerically. A similar scaling has been numerically tested for nonlinear magnetostatic field problems in LANGER AND PECHSTEIN [116]. Scalings for related FETI-DP together with numerical results can be found in KLAWONN AND RHEINBACH, KLAWONN AND RHEINBACH [104, 107]. However, a theoretical proof of all these robustness results has so far been lacking.

Main achievements The main emphasis of this thesis is not on computations but on theory. Nevertheless we have also confirmed our theoretical results by numerical experiments and applied the methods to nonlinear magnetic field problems. Our main achievements are the following ones.

Exterior problems. We provide explicit condition number bounds for standard one-level and all-floating FETI/BETI methods in the unbounded case, which we summarize in the following. Let Γ_0 denote the artificial interface separating the exterior domain from the interior subdomains. If in addition to the radiation condition, no further Dirichlet boundary conditions are imposed (e. g., on parts of the interior subdomain boundaries), the condition number κ of the preconditioned FETI/BETI system is bounded by

$$C \max_{i \in \mathcal{I}_{\text{int}}} (1 + \log(H_i/h_i))^2,$$

where \mathcal{I}_{int} is the index set of the interior subdomain and the constant C is independent of H_0 , H_i , h_i , the number of subdomains, and in particular of the ratio H_0/H_i and the number of neighbors of the exterior subdomain. If additionally, the coefficient corresponding to the exterior subdomain is larger or equal to those of the interior subdomains, the constant C is independent of the values of the (piecewise constant) subdomain coefficients. In case of a Dirichlet boundary in the interior that is separated from Γ_0 by a distance $\eta > 0$, we obtain

$$\kappa \leq C \frac{H_0}{\eta} \max_{i \in \mathcal{I}_{\text{int}}} (1 + \log(H_i/h_i))^2.$$

Similar estimates hold true if the Dirichlet boundary touches Γ_0 . In the worst case, we can prove the same estimate as above where η equals the minimal diameter of the subdomains neighboring the exterior domain. Then the constant C is independent of the coefficients and the location of the Dirichlet boundary. We note that in three dimensions, the factor H_0/H_j is a measure for the square root of the number of neighbors of the exterior domain.

We prove that dual-primal FETI/BETI methods for unbounded domains result always in the quasi-optimal condition number bound $C \max_{i \in \mathcal{I}_{\text{int}}} (1 + \log(H_i/h_i))^2$, with C independent of H_0 , H_i , h_i , the number of subdomains, the neighbors of the exterior domain, and the values of the (piecewise) coefficients. We discuss implementation issues of both the one-level and the dual-primal methods for unbounded domains.

Highly heterogeneous coefficients. As previously discussed, there are only very few theoretical results for domain decomposition methods for highly heterogeneous coefficients. Our work is

mainly inspired by the articles by GRAHAM, LECHNER, AND SCHEICHL [75] and SCHEICHL AND VAINIKKO [165].

Using energy minimization and cut-off arguments, and by proving some new generalized Sobolev inequalities, we can show a rigorous bound for the condition number of the preconditioned FETI system that depends only on the coefficient variation in the vicinity of subdomain interfaces. To be more precise, for suitably chosen parameters $\eta_i > 0$, let Ω_{i,η_i} denote the layer of width η_i near the boundary of each subdomain Ω_i . Then, for a general (positive) coefficient function $\alpha \in L^\infty(\Omega)$, the condition number of the preconditioned one-level FETI system is bounded by

$$C \max_{k \in \mathcal{I}} \left(\frac{H_k}{\eta_k} \right)^\beta \max_{i \in \mathcal{I}} \max_{x,y \in \Omega_{i,\eta_i}} \frac{\alpha(x)}{\alpha(y)} (1 + \log(H_i/h_i))^2,$$

where \mathcal{I} is the index set of the subdomain, and the constant C is independent of $\alpha(\cdot)$. In general, $\beta = 2$; if the coefficient in the interior is always larger than in the boundary layers, $\beta = 1$. In particular the dependency of the condition number is restricted to the boundary layers only, i. e., the coefficient may vary a lot in the interior of each subdomain. Our condition number bound holds also in case of the all-floating and the dual-primal method.

Application to nonlinear magnetic field problems. We apply the one-level FETI/BETI method to nonlinear stationary magnetic field problems in two dimensions, where in particular the highly heterogeneous case is of strong relevance.

The analyses of our theoretical results will be treated in the more interesting three-dimensional case. The corresponding proofs for the two-dimensional case can be obtained easily from the three-dimensional ones. As a matter of fact, we need to enter and modify the known theory on a rather deep level. This is why we have decided to review this theory in detail. We present numerical experiments that illustrate and confirm our results on one-level (including all-floating) FETI/BETI methods.

Outline

This dissertation is structured as follows.

- Chapter 1 provides some preliminaries, such as Sobolev spaces, the variational formulation, FEM, BEM, and Steklov-Poincaré operators. The experienced reader may bypass this chapter.
- In Chapter 2 we discuss hybrid one-level tearing and interconnecting methods, presenting a unified theory for standard one-level and all-floating FETI/BETI methods.
- Chapter 3 investigates the extension of one-level FETI/BETI methods to unbounded domains.
- In Chapter 4 we discuss dual-primal FETI/BETI methods for bounded and unbounded domains.
- Chapter 5 deals with FETI type methods for highly heterogeneous coefficients.
- In Chapter 6, we apply the FETI/BETI methods to nonlinear magnetic field problems in two dimensions and provide some numerical results.

Chapter 1

Preliminaries

This chapter contains the preliminaries for our thesis. Section 1.1 introduces some basic concepts. In Section 1.2 we briefly discuss the potential equation. Section 1.3 deals with Sobolev spaces, variational formulations and Galerkin's method. In Section 1.4 we introduce boundary integral equations related to the interior and exterior Laplace equation as well as the corresponding Steklov-Poincaré operators, which are among the key tools of non-overlapping domain decomposition methods. Section 1.5 briefly covers two discretization techniques, the finite element method (FEM) and the boundary element method (BEM). Furthermore, we introduce approximations of Steklov-Poincaré operators. We very briefly address solvers for finite element systems and data-sparse techniques for the BEM, such as \mathcal{H} -matrices. Finally, Section 1.6 contains spectral estimates relating the approximate and the continuous Steklov-Poincaré operators.

1.1 Basic concepts

1.1.1 Basic notation and auxiliary results

Vectors and matrices For two vectors $p, q \in \mathbb{R}^n$, we denote the Euclidean inner product by $p \cdot q := (p, q)_{\ell^2} := \sum_{i=1}^n p_i q_i$, and the Euclidean norm by $|p| := (p \cdot p)^{1/2}$. If it is clear from the context we simply denote the vector of zero entries by 0 . When not pointed out explicitly, all vectors are understood as column vectors. The transpose p^\top of a column vector p is a row vector. Similarly, we denote the transpose of a matrix $A \in \mathbb{R}^{n \times m}$ by A^\top . A matrix $A \in \mathbb{R}^{n \times n}$ is called *symmetric positive definite* (SPD) if it is symmetric and $(Ap) \cdot p > 0$ for all $p \in \mathbb{R}^n \setminus \{0\}$. The identity matrix is denoted by I . A number $\lambda \in \mathbb{R}$ is called *eigenvalue* of A if there exists a vector $z \neq 0$ such that $Az = \lambda z$. If A is SPD, all eigenvalues are strictly positive. Denote by $\lambda_{\max}(A)$ and $\lambda_{\min}(A)$ the largest and smallest eigenvalue, respectively, which can be characterized by

$$\lambda_{\max}(A) = \max_{z \neq 0} \frac{(Az, z)_*}{(z, z)_*}, \quad \lambda_{\min}(A) = \min_{z \neq 0} \frac{(Az, z)_*}{(z, z)_*},$$

for any inner product $(\cdot, \cdot)_*$ on \mathbb{R}^n . The *spectral condition number* of an SPD matrix A is defined by

$$\kappa(A) := \frac{\lambda_{\max}(A)}{\lambda_{\min}(A)}.$$

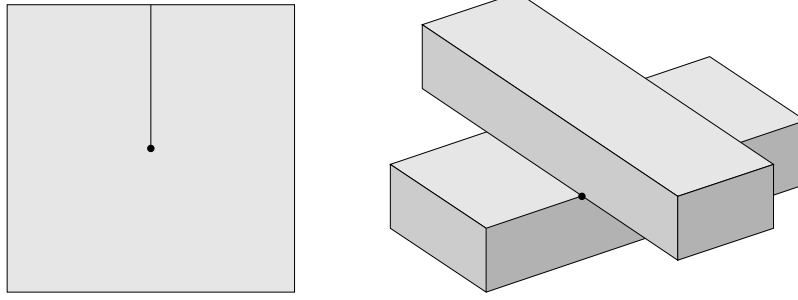


Figure 1.1: Two domains that fail to be Lipschitz.

Banach spaces and linear operators We denote the *dual* of a Banach space V by V^* . The dual is the space of the linear and bounded functionals on V . The duality product on $V^* \times V$ is denoted by $\langle \cdot, \cdot \rangle$, i. e., for a functional $f \in V^*$, we have $\langle f, v \rangle = f(v) \in \mathbb{R}$. For subspace $U \subset V$ we define its *polar space* $U^\circ \subset V^*$ by

$$U^\circ := \{f \in V^* : \langle f, v \rangle = 0 \quad \forall v \in U\}.$$

Let W be another Banach space and $A : V \rightarrow W^*$ a bounded linear operator. We define the *adjoint* $A^\top : W \rightarrow V^*$ by the relation $\langle A^\top w, v \rangle = \langle Av, w \rangle$ for all $v \in V, w \in W$. An operator $S : V \rightarrow V^*$ is said to be *self-adjoint* if $S^\top = S$. If in addition, there exists a constant $c > 0$ with $\langle Sv, v \rangle \geq c\|v\|_V^2$ for all $v \in V$, we call S *elliptic*. As it is well-known in the elliptic case, the inverse $S^{-1} : V^* \rightarrow V$ is linear, bounded, and elliptic as well. In case that V is of finite dimension, we may call the operator S symmetric positive definite (SPD) as well, since it can be represented by an SPD matrix. As a convention, we call a general self-adjoint elliptic operator $S : V \rightarrow V^*$ SPD as well. Any such SPD operator S defines an inner product $\langle v, w \rangle_S := \langle Sv, w \rangle$ on V . For a subset $U \subset V$, we define the orthogonal complement of U with respect to V by

$$U^{\perp_S} := \{w \in U : \langle w, v \rangle_S = 0 \quad \forall v \in V\}.$$

The kernel and range of a general linear operator $A : V \rightarrow W$ are denoted by

$$\ker A := \{v \in V : Av = 0\}, \quad \text{range } A := \{w \in W : \exists v \in V : w = Av\}.$$

If V and W are of finite dimension, we have $(\ker A)^\circ = \text{range } A^\top$ because $\text{range } A$ is closed, cf. BREZZI AND FORTIN [29, Chap. II]. The identity operator on a space V is denoted by I_V , where we omit the subscript V if the corresponding space is clear from the context.

Domains and manifolds We call an open and connected subset $\Omega \subset \mathbb{R}^d$ a *domain*. In most cases, a domain Ω will be bounded, too. The boundary of a domain is denoted by $\partial\Omega$. We call a non-empty boundary $\partial\Omega$ *Lipschitz* if it can be represented by a finite family of Lipschitz continuous functions, see, e. g., EVANS [53] or MCLEAN [134]. We call a domain Lipschitz if its boundary is Lipschitz. Note that for each bounded Lipschitz domain Ω , its open complement $\mathbb{R}^d \setminus \bar{\Omega}$ is Lipschitz too. Due to Rademacher's theorem (see the references in MCLEAN [134, p. 96f]), Lipschitz domains have a unique outward unit normal vector to the boundary in the L^∞ sense. Figure 1.1 shows two famous examples of domains which

fail to be Lipschitz. However, both are the union of two Lipschitz domains. A manifold $\Gamma \subset \partial\Omega$ is called *relatively open* (relatively closed), if its open (closed) in the topology of the $(d-1)$ -dimensional boundary $\partial\Omega$. A manifold is called *closed* if it has no boundary in the $\partial\Omega$ -topology. If clear from context we will often write open, but meaning relatively open. For a domain or manifold \mathcal{M} , let $\mathbf{1}_{\mathcal{M}}$ denote the function which is identical to 1 on \mathcal{M} , and let $\mathbf{0}_{\mathcal{M}}$ denote the function being identical to 0 on \mathcal{M} . Finally, we define the diameter $\text{diam}(\mathcal{M}) := \sup_{x, y \in \mathcal{M}} |x - y|$.

Integrals All domain integrals are Lebesgue integrals and will be written in the form $\int_{\Omega} f(x) dx$ or in short $\int_{\Omega} f dx$. Integrals on hypersurfaces are understood as Lebesgue integrals with respect to the corresponding surface measure or arc length and are written in the form $\int_{\Gamma} f(x) ds_x$ or in short $\int_{\Gamma} f ds$.

Constants in estimates Throughout this work the notion $a \lesssim b$ means that some (generic) constant $C > 0$ exists with $a \leq Cb$. Such a constant C will never depend on the relevant parameters such as mesh size, (sub)domain diameters, coefficients, number of subdomains, etc., but it may depend on the geometric shapes of subdomains, elements, etc. Similarly, $a \gtrsim b$ is short hand for $b \lesssim a$, and $a \simeq b$ stands for $a \lesssim b$ and $b \lesssim a$.

Suprema and infima We agree on the convention that we write

$$\sup_{x \in X} \frac{a(x)}{b(x)} \quad \text{as short hand for} \quad \sup \left\{ \frac{a(x)}{b(x)} : x \in X, b(x) \neq 0 \right\},$$

i. e., we exclude those $x \in X$ where the denominator vanishes. Similarly, we write

$$\inf_{x \in X} \frac{a(x)}{b(x)} \quad \text{as short hand for} \quad \inf \left\{ \frac{a(x)}{b(x)} : x \in X, b(x) \neq 0 \right\}.$$

Auxiliary result

Lemma 1.1. *Let V be a Hilbert space and $A : V \rightarrow V^*$ a self-adjoint and elliptic operator with its self-adjoint and elliptic inverse $A^{-1} : V^* \rightarrow V$. Then*

$$\langle w, A^{-1}w \rangle = \sup_{v \in V} \frac{\langle w, v \rangle^2}{\langle Av, v \rangle} \quad \forall w \in V^*.$$

Proof. The operator A^{-1} defines an inner product $(u, v)_{A^{-1}} := \langle u, A^{-1}v \rangle^{1/2}$ on V^* with associated norm $\|\cdot\|_{A^{-1}}$. The Cauchy-Schwarz inequality implies

$$\|w\|_{A^{-1}} = \sup_{u \in V^*} \frac{(w, u)_{A^{-1}}}{\|u\|_{A^{-1}}} = \sup_{v \in V} \frac{\langle w, v \rangle}{\langle Av, v \rangle^{1/2}},$$

where we have substituted $v := A^{-1}u$. □

1.1.2 Projections

Let U and Z be finite-dimensional Hilbert spaces with $\dim Z < \dim U$, and let $G : Z \rightarrow U^*$ be an injective linear operator. Due to our assumptions $\ker G = \{0\}$ but $\ker G^\top \neq \{0\}$. We are interested in operators $P : U \rightarrow U$ and their adjoints $P^\top : U^* \rightarrow U^*$ of the form

$$\begin{aligned} P &= I - QG(G^\top QG)^{-1}G^\top, \\ P^\top &= I - G(G^\top QG)^{-1}G^\top Q, \end{aligned} \quad (1.1)$$

where the operator $Q : U^* \rightarrow U$ is SPD and therefore defines inner products $\langle v, w \rangle_Q = \langle v, Qw \rangle$ and $\langle v, w \rangle_{Q^{-1}} = \langle Q^{-1}v, w \rangle$ on U and U^* , respectively. Note, that the term $(G^\top QG)^{-1}$ is well-defined because G is injective and Q is SPD. By construction we have

$$\begin{aligned} G^\top P &= 0, & PQG &= 0, & PQ &= QP^\top, \\ P^\top G &= 0, & G^\top QP^\top &= 0, & Q^{-1}P &= P^\top Q^{-1}. \end{aligned} \quad (1.2)$$

The operator P is a *projection*, i. e., $P^2 = P$. Also P^\top , $I - P$, and $I - P^\top$ are projections, which implies

$$\begin{aligned} \langle Pv, (I - P)w \rangle_{Q^{-1}} &= 0 & \forall v, w \in U, \\ \langle P^\top v, (I - P^\top)w \rangle_Q &= 0 & \forall v, w \in U^*, \end{aligned} \quad (1.3)$$

i. e., P and $I - P$ are *orthogonal* in the inner product defined by Q^{-1} , and P^\top as well as $I - P^\top$ are Q -orthogonal. From the identities in (1.2) we obtain

$$\begin{aligned} \text{range } P &= \ker G^\top, \\ \text{range } (I - P) &= (\ker G^\top)^{\perp_{Q^{-1}}} = \text{range } (QG), \\ \text{range } P^\top &= \ker(G^\top Q), \\ \text{range } (I - P^\top) &= \ker(G^\top Q)^{\perp_Q} = \text{range } G. \end{aligned} \quad (1.4)$$

We note that the above projections remain well-defined if Q is only SPD on $\text{range } G$.

1.2 The potential equation

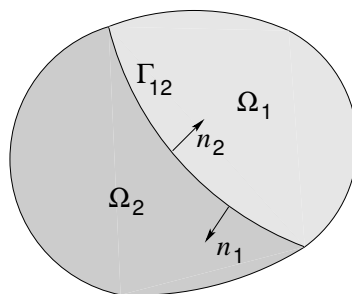
This section introduces the classical potential equation (sometimes also called heat equation or diffusion equation) together with interface and boundary conditions. Let $\Omega \subset \mathbb{R}^d$ (with $d = 2$ or 3) be a bounded Lipschitz domain.

Differential operators Let the following fields be sufficiently smooth. For *scalar fields* $u : \Omega \rightarrow \mathbb{R}$ we define the *gradient*,

$$\nabla u := \left(\frac{\partial u}{\partial x_1}, \dots, \frac{\partial u}{\partial x_d} \right)^\top. \quad (1.5)$$

For *vector fields* $\mathbf{v} = (v_1, \dots, v_d)^\top : \Omega \rightarrow \mathbb{R}^d$, which, with a few exceptions, will be denoted by boldface symbols, we define the *divergence*,

$$\text{div } \mathbf{v} := \sum_{k=1}^d \frac{\partial v_k}{\partial x_k}. \quad (1.6)$$

Figure 1.2: Two subdomains Ω_1, Ω_2 with interface Γ_{12} .

The *Laplace operator* Δ is defined by

$$\Delta u := \operatorname{div}(\nabla u) = \sum_{k=1}^d \frac{\partial^2 u}{\partial x_k^2}. \quad (1.7)$$

The potential equation The *potential equation* reads: Find a sufficiently smooth function $u : \Omega \rightarrow \mathbb{R}$ such that

$$-\operatorname{div}[\mathcal{A}\nabla u] = f \quad \text{in } \Omega, \quad (1.8)$$

for a given *source* function $f : \Omega \rightarrow \mathbb{R}$ and a sufficiently smooth coefficient matrix $\mathcal{A} : \Omega \rightarrow \mathbb{R}^{d \times d}$. If $\mathcal{A} = \alpha I$ for some scalar function α we can write

$$-\operatorname{div}[\alpha \nabla u] = f \quad \text{in } \Omega. \quad (1.9)$$

In case $\alpha \equiv 1$ we call (1.8) *Poisson's equation*. If additionally $f \equiv 0$, we call (1.8) *Laplace's equation* since it reads

$$-\Delta u = 0 \quad \text{in } \Omega. \quad (1.10)$$

Boundary conditions We consider Dirichlet and Neumann boundary conditions. Let the boundary $\partial\Omega$ split into two disjoint parts, a Dirichlet boundary Γ_D and a Neumann boundary Γ_N . For technical reasons we assume that Γ_D is a relatively closed manifold, whereas Γ_N is open. The boundary conditions read

$$u = g_D \quad \text{on } \Gamma_D, \quad (1.11)$$

$$(\mathcal{A}\nabla u) \cdot n = g_N \quad \text{on } \Gamma_N, \quad (1.12)$$

where g_D and g_N are given, and n is the outward unit normal vector to $\partial\Omega$. The term $(\mathcal{A}\nabla u) \cdot n$ is called *conormal derivative*.

Interface conditions So far we have assumed that the coefficient \mathcal{A} (or α) is sufficiently smooth, in particular continuous. Suppose now that Ω is composed of two disjoint subdomains Ω_1, Ω_2 , so that $\bar{\Omega} = \bar{\Omega}_1 \cup \bar{\Omega}_2$. Then we call the manifold $\Gamma_{12} = \partial\Omega_1 \cap \partial\Omega_2$ the *interface*, see Figure 1.2. If \mathcal{A} is smooth on each of the subdomains Ω_1, Ω_2 but discontinuous across Γ_{12} , and if f is piecewise smooth too, the potential equation can only be formulated in each

of the subdomains. On the interface Γ_{12} we have to introduce interface conditions. The entire system reads

$$-\operatorname{div}[\mathcal{A}\nabla u_i] = f \quad \text{in } \Omega_i, \quad i = 1, 2 \quad (1.13)$$

$$u_1 = u_2 \quad \text{on } \Gamma_{12}, \quad (1.14)$$

$$(\mathcal{A}\nabla u_1) \cdot n_1 + (\mathcal{A}\nabla u_2) \cdot n_2 = 0 \quad \text{on } \Gamma_{12}, \quad (1.15)$$

where u_1, u_2 are the restrictions of the global solution u to Ω_1, Ω_2 respectively, and n_1 and $n_2 = -n_1$ are the outward unit normal vectors to $\partial\Omega_1$ and $\partial\Omega_2$, respectively. The interface conditions (1.14)–(1.15) state that both the solution and the conormal derivative are continuous.

Remark 1.2. Note that, here the source function f may be discontinuous across Γ_{12} , later on we can allow for $f \in L^2(\Omega)$. For less regularity, as in the case of surface sources, the condition (1.15) needs to be changed accordingly.

Interface conditions for the case of many subdomains are straightforward.

Mixed boundary value problem Summarizing we state the *mixed boundary value problem* for the potential equation, here again for the case of two subdomains. For given \mathcal{A}, f, g_D , and g_N sufficiently (piecewise) smooth find a function $u : \bar{\Omega} \rightarrow \mathbb{R}$ such that

$$\begin{aligned} -\operatorname{div}[\mathcal{A}\nabla u] &= f & \text{in } \Omega_i & \quad i = 1, 2, \\ (\mathcal{A}\nabla u) \cdot n_1 + (\mathcal{A}\nabla u) \cdot n_2 &= 0 & \text{on } \Gamma_{12}, \\ u|_{\Gamma_D} &= g_D & \text{on } \Gamma_D, \\ (\mathcal{A}\nabla u) \cdot n &= g_N & \text{on } \Gamma_N. \end{aligned} \quad (1.16)$$

1.3 Variational methods

In this section we introduce the concept of weak solutions to the potential equation. To this end, Section 1.3.1 introduces Sobolev spaces, trace operators, and some important results such as Friedrichs' and Poincaré's inequalities. Section 1.3.2 contains the variational formulation of the potential equation, Section 1.3.3 discusses existence and uniqueness thereof, and finally we state Galerkin's method in Section 1.3.4

1.3.1 Sobolev spaces

1.3.1.1 Definition

Comprehensive introductions to Sobolev spaces can be found, e. g., in ADAMS AND FOURNIER [1], EVANS [53], or MCLEAN [134]. In the following let $\Omega \subset \mathbb{R}^d$ be a (possibly unbounded) domain with Lipschitz boundary $\partial\Omega$, or $\Omega = \mathbb{R}^d$. We start with a list of some basic spaces:

- $\mathcal{C}(\Omega)$ space of continuous functions in Ω
- $\mathcal{C}^k(\Omega)$ space of k -times continuously differentiable functions in Ω ($\mathcal{C}^0(\Omega) := \mathcal{C}(\Omega)$)
- $\mathcal{C}^\infty(\Omega)$ space of infinitely many times continuously differentiable functions in Ω

$\mathcal{C}_0^\infty(\Omega)$	space of functions from $\mathcal{C}^\infty(\Omega)$ with compact support in Ω
$\mathcal{D}(\Omega)$	functions from $\mathcal{C}_0^\infty(\Omega)$ equipped with a special topology
$\mathcal{D}'(\Omega)$	space of distributions in Ω
$L^p(\Omega)$	space of Lebesgue-measurable functions v on the domain Ω where $\int_\Omega v ^p dx$ is bounded
$L^\infty(\Omega)$	space of Lebesgue-measurable functions with bounded essential supremum
$L_{loc}^1(\Omega)$	space of locally Lebesgue-integrable functions, i. e., absolutely integrable on every compact subset of Ω
$H^k(\Omega)$	closure of $\mathcal{C}^\infty(\Omega)$ in the norm $\ u\ _{H^k(\Omega)} = (\sum_{ \alpha \leq k} \int_\Omega D^\alpha u ^2 dx)^{1/2}$
$H_0^1(\Omega)$	closure of $\mathcal{C}_0^\infty(\Omega)$ in the norm $\ \cdot\ _{H^1(\Omega)}$
$H^{-1}(\Omega)$	the dual of $H_0^1(\Omega)$

Occasionally, we make use of the spaces $\mathcal{C}^k(\mathcal{M})$, $\mathcal{C}^\infty(\mathcal{M})$, and $L^p(\mathcal{M})$ on a manifold \mathcal{M} . We need the following notion of *weak derivatives*.

Definition 1.3. A function $u \in L_{loc}^1(\Omega)$ has weak derivative $v \in L_{loc}^1(\Omega)$ with respect to x_i if and only if

$$\int_\Omega v \varphi dx = - \int_\Omega u \frac{\partial \varphi}{\partial x_i} dx \quad \forall \varphi \in \mathcal{C}_0^\infty(\Omega).$$

We write $\frac{\partial u}{\partial x_i} = v$. If all weak derivatives of a function u of order one exist, we write $\nabla u = (\frac{\partial u}{\partial x_1}, \dots, \frac{\partial u}{\partial x_d})^\top$. This is justified by the fact that if additionally $u \in \mathcal{C}^1(\Omega)$ the weak derivative coincides with the classical derivative. Higher order derivatives are defined recursively.

This definition gives rise to the *distributional derivative*. A *distribution* $f \in \mathcal{D}'(\Omega)$ is a linear functional on the space $\mathcal{D}(\Omega)$ which is continuous in a special topology. Distributions are *generalized functions* in the sense that every locally integrable function $f \in L_{loc}^1(\Omega)$ naturally defines a distribution $\tilde{f} \in \mathcal{D}'(\Omega)$ by $\langle \tilde{f}, \varphi \rangle = \int_\Omega f \varphi dx$. In the following we identify f and \tilde{f} . Finally, Definition 1.3 can be generalized to distributions, resulting in the fact that all derivatives of distributions (or functions) are well-defined in the distributional sense.

For Lipschitz domains Ω , the space $H^1(\Omega)$ defined as above contains those functions in $L^2(\Omega)$ whose distributional derivatives up to order 1 can be represented by functions in $L^2(\Omega)$. Equipped with the inner product

$$(u, v)_{H^1(\Omega)} := \int_\Omega u v dx + \int_\Omega \nabla u \cdot \nabla v dx, \quad (1.17)$$

and with the seminorm $|\cdot|_{H^1(\Omega)}$ and norm $\|\cdot\|_{H^1(\Omega)}$ defined by

$$|u|_{H^1(\Omega)}^2 := \int_\Omega |\nabla u|^2 dx \quad \text{and} \quad \|u\|_{H^1(\Omega)}^2 := \|u\|_{L^2(\Omega)}^2 + |u|_{H^1(\Omega)}^2, \quad (1.18)$$

respectively, $H^1(\Omega)$ becomes a Hilbert space.

If Ω is bounded and Lipschitz, denote its open complement by $\Omega^{\text{ext}} := \mathbb{R}^d \setminus \overline{\Omega}$. We define the space $H_{\text{loc}}^1(\Omega^{\text{ext}})$ which is more general than $H^1(\Omega^{\text{ext}})$ by

$$H_{\text{loc}}^1(\Omega^{\text{ext}}) := \{u \in \mathcal{D}'(\Omega^{\text{ext}}) : u \in H^1(\Omega^{\text{ext}} \cap B_R) \quad \forall R > 0\}, \quad (1.19)$$

where B_R is the open ball with center in the origin and radius R , cf. [134, Chap. 7, p. 234ff].

Sobolev spaces $H^s(\Omega)$ with real indices $s > 0$ can be defined using the Sobolev-Slobodeckii norm (see also the next paragraph), the Fourier transform, or an interpolation method, cf. [134, Sect. 3]. As long as Ω is bounded and Lipschitz we have $H^s(\Omega) \subset H^t(\Omega) \subset L^2(\Omega)$ for $1 \geq s > t > 0$, and the inclusions are compact (by Rellich's theorem, cf. [134, Theorem 3.27]).

Sobolev spaces on manifolds For a bounded manifold $\tilde{\Gamma}$ (open or closed) recall that $L^2(\tilde{\Gamma})$ is the space of square-integrable functions with respect to the Lebesgue surface measure. For a bounded domain Ω with Lipschitz boundary $\partial\Omega$ we define the space

$$H^{1/2}(\partial\Omega) := \{u \in L^2(\partial\Omega) : \|u\|_{H^{1/2}(\partial\Omega)} < \infty\}, \quad (1.20)$$

using the Sobolev-Slobodeckii norm

$$\|u\|_{H^{1/2}(\partial\Omega)} := \left(\|u\|_{L^2(\partial\Omega)}^2 + |u|_{H^{1/2}(\partial\Omega)}^2 \right)^{1/2}, \quad (1.21)$$

with the seminorm

$$|u|_{H^{1/2}(\partial\Omega)} := \left(\int_{\partial\Omega} \int_{\partial\Omega} \frac{|u(x) - u(y)|^2}{|x - y|^d} ds_x ds_y \right)^{1/2}. \quad (1.22)$$

For an open hypersurface $\tilde{\Gamma} \subset \partial\Omega$, we define the space

$$H^{1/2}(\tilde{\Gamma}) := \{u \in L^2(\tilde{\Gamma}) : \exists \tilde{u} \in H^{1/2}(\partial\Omega), \tilde{u}|_{\tilde{\Gamma}} = u\}, \quad (1.23)$$

with the norm

$$\|u\|_{H^{1/2}(\tilde{\Gamma})} := \inf \{ \|\tilde{u}\|_{H^{1/2}(\partial\Omega)} : \tilde{u} \in H^{1/2}(\partial\Omega), \tilde{u}|_{\tilde{\Gamma}} = u \}. \quad (1.24)$$

As a matter of fact, the space $\overline{\mathcal{C}_0^\infty(\tilde{\Gamma})}^{\|\cdot\|_{H^{1/2}(\tilde{\Gamma})}}$ coincides with $H^{1/2}(\tilde{\Gamma})$. We define

$$H_{00}^{1/2}(\tilde{\Gamma}) := \{u|_{\tilde{\Gamma}} : u \in H^{1/2}(\partial\Omega), u|_{\partial\Omega \setminus \tilde{\Gamma}} = 0\}, \quad (1.25)$$

which is in general a genuine subspace of $H^{1/2}(\tilde{\Gamma})$ and contains those functions whose extension by zero from $\tilde{\Gamma}$ to $\partial\Omega$ has still a bounded $H^{1/2}(\partial\Omega)$ -norm. Alternatively, the space is characterized as the interpolation of $H_0^1(\tilde{\Gamma})$ and $L^2(\tilde{\Gamma})$ with interpolation parameter $1/2$, cf. TOSELLI AND WIDLUND [184, Lemma A.8]. An intrinsic norm for $H_{00}^{1/2}(\tilde{\Gamma})$ is given by

$$\|u\|_{H_{00}^{1/2}(\tilde{\Gamma})} := \left\{ \|u\|_{H^{1/2}(\tilde{\Gamma})}^2 + \int_{\tilde{\Gamma}} \frac{u(x)^2}{d(x, \partial\tilde{\Gamma})} ds_x \right\}^{1/2}, \quad (1.26)$$

where $d(x, \partial\tilde{\Gamma})$ denotes the distance from x to the boundary of $\tilde{\Gamma}$, see, e.g., LIONS AND MAGENES [127, Theorem 11.7]. Obviously, for a closed hypersurface Γ , the spaces $H_{00}^{1/2}(\Gamma)$ and $H^{1/2}(\Gamma)$ coincide. We define

$$H^{-1/2}(\tilde{\Gamma}) := [H_{00}^{1/2}(\tilde{\Gamma})]^*. \quad (1.27)$$

Note that in the literature, $H^{-1/2}(\tilde{\Gamma})$ is sometimes denoted by $\tilde{H}_{00}^{-1/2}(\tilde{\Gamma})$, and $[H^{1/2}(\tilde{\Gamma})]^*$ is often denoted by $\tilde{H}^{-1/2}(\tilde{\Gamma})$.

1.3.1.2 Trace operators

In the following let Ω be a bounded domain with Lipschitz boundary $\partial\Omega$.

The Dirichlet trace

Theorem 1.4 (Trace theorem). *Let Ω be a bounded domain with Lipschitz boundary $\partial\Omega$. Then the Dirichlet trace operator $\gamma_0 : \mathcal{C}^\infty(\Omega) \rightarrow \mathcal{C}^\infty(\partial\Omega)$ defined by*

$$\gamma_0 u := u|_{\partial\Omega},$$

has a unique continuous extension as a linear operator from $H^1(\Omega)$ to $H^{1/2}(\partial\Omega)$, i. e., there exists a constant $C_T > 0$ with

$$\|\gamma_0 u\|_{H^{1/2}(\partial\Omega)} \leq C_T \|u\|_{H^1(\Omega)} \quad \forall u \in H^1(\Omega).$$

Proof. See, e. g., MCLEAN [134, Theorem 3.37]. □

Notation. In the sequel we will often write $u|_{\partial\Omega}$ instead of $\gamma_0 u$, even if u is only from $H^1(\Omega)$.

Theorem 1.5 (Inverse trace theorem). *Let Ω be a bounded domain with Lipschitz boundary $\partial\Omega$. Then there exists a linear extension operator $\mathcal{E} : H^{1/2}(\partial\Omega) \rightarrow H^1(\Omega)$ and a constant $C_{IT} > 0$ such that*

$$\gamma_0(\mathcal{E}u) = u, \quad \|\mathcal{E}u\|_{H^1(\Omega)}^2 \leq C_{IT} \|u\|_{H^{1/2}(\partial\Omega)}^2 \quad \forall u \in H^{1/2}(\partial\Omega),$$

i. e., \mathcal{E} is a continuous right inverse of γ_0 . The same inequality holds if we replace the norms by the respective seminorms.

Proof. See, e. g., MCLEAN [134, Theorem 3.37]. □

It is important to note that

$$\|u\|_{H^{1/2}(\partial\Omega)} := \inf \{ \|\tilde{u}\|_{H^1(\Omega)} : \tilde{u} \in H^1(\Omega), \tilde{u}|_{\partial\Omega} = u \} \quad (1.28)$$

is an equivalent norm to the $H^{1/2}(\partial\Omega)$ -norm, and that the characterization

$$H_0^1(\Omega) = \overline{\mathcal{C}_0^\infty(\Omega)}^{\|\cdot\|_{H^1(\Omega)}} = \{u \in H^1(\Omega) : u|_{\partial\Omega} = 0\} \quad (1.29)$$

holds; see, e. g., [134, Theorem 3.40]. In particular, functions from $H_0^1(\Omega)$ can be extended by zero to $H^1(\mathbb{R}^d)$.

The Neumann trace Let $n : \partial\Omega \rightarrow \mathbb{R}^d$ denote the outward unit normal vector to $\partial\Omega$ which is piecewise smooth for Lipschitz domains. For a function $u \in \mathcal{C}^\infty(\Omega)$, we can define the *normal derivative*

$$\gamma_1 u := \frac{\partial u}{\partial n} := \nabla u \cdot n, \quad (1.30)$$

also called *Neumann trace* of u . This definition can be directly extended to H^2 -functions, but not to arbitrary H^1 -functions. Solutions to the potential equation, however, *do* have a well-defined Neumann trace. For $u \in \mathcal{D}'(\Omega)$ we define the distributional Laplacian Δu by

$$\langle \Delta u, v \rangle := \langle u, \Delta v \rangle \quad \forall v \in \mathcal{C}_0^\infty(\Omega).$$

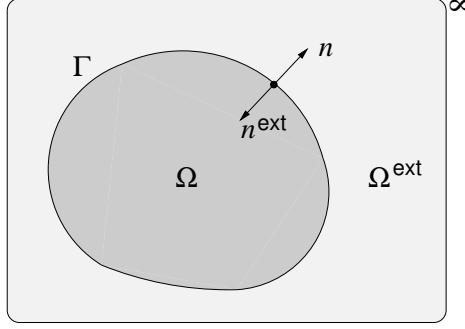


Figure 1.3: Interior domain Ω , exterior domain Ω^{ext} and the two outward unit normal vector n and n^{ext} to the boundary Γ .

Theorem 1.6. *Let $f \in (H^1(\Omega))^*$ and let $u \in H^1(\Omega)$ be a solution of*

$$-\Delta u = f,$$

as an equation in $(H^1(\Omega))^$. Then, there exists a unique functional $g \in H^{-1/2}(\partial\Omega)$ such that*

$$(\nabla u, \nabla v)_{L^2(\Omega)} = \langle f, v \rangle_{\Omega} + \langle g, \gamma_0 v \rangle_{\partial\Omega} \quad \forall v \in H^1(\Omega),$$

and

$$\|g\|_{H^{-1/2}(\partial\Omega)} \leq C \left(\|u\|_{H^1(\Omega)} + \|f\|_{(H^1(\Omega))^*} \right).$$

Proof. See, e. g., [134, Lemma 4.3]. □

It is important to note that, in general, the functional g , which is the generalization of the normal derivative, depends not alone on u , but also on $f \in (H^1(\Omega))^*$. If f is clear from the context, we write $\gamma_1 u := g$.

If $f \in L^2(\Omega)$, i. e., $\Delta u \in L^2(\Omega)$, we have

$$(\nabla u, \nabla v)_{L^2(\Omega)} = (-\Delta u, v)_{L^2(\Omega)} + \langle g, \gamma_0 v \rangle_{\partial\Omega} \quad \forall v \in H^1(\Omega).$$

This is Green's first identity which is known to hold for $u, v \in C^\infty(\Omega)$ with $g = \gamma_1 u$. The discussion shows that g depends only on u , and that the Neumann trace operator γ_1 is continuous as a linear operator

$$\gamma_1 : H_\Delta^1(\Omega) \rightarrow H^{-1/2}(\partial\Omega),$$

where

$$H_\Delta^1(\Omega) := \{u \in H^1(\Omega) : \Delta u \in L^2(\Omega)\}.$$

An alternative argument is that if $f \in L^2(\Omega)$, the gradient ∇u is in $H(\text{div}, \Omega)$ and therefore its normal trace $\nabla u \cdot n$ is well-defined in $H^{-1/2}(\partial\Omega)$; see, e. g., GIRAULT AND RAVIART [69], MONK [136].

The *conormal derivative* $(\mathcal{A}\nabla u) \cdot n$ can be generalized in a similar way, using the equation $-\text{div}(\mathcal{A}\nabla u) = f$, see [134, Lemma 4.3].

Exterior traces Let Ω be a bounded Lipschitz domain with Lipschitz boundary Γ and outward unit normal vector n , and set $\Omega^{\text{ext}} := \mathbb{R}^d \setminus \bar{\Omega}$. Let furthermore $\mathcal{C}_0^\infty(\bar{\Omega})$ denote the space of restrictions of functions from $\mathcal{C}_0^\infty(\mathbb{R}^d)$ to Ω , i. e., the functions can have non-trivial values at $\partial\Omega$ but they need to have compact support in \mathbb{R}^d . Let $n^{\text{ext}} := -n$ denote the unit normal vector on Γ pointing into Ω , i. e., the outside of Ω^{ext} , cf. Figure 1.3. Similarly to the interior case, we define the trace operators

$$\gamma_0^{\text{ext}} : \mathcal{C}_0^\infty(\bar{\Omega}^{\text{ext}}) \rightarrow \mathcal{C}^\infty(\Gamma) : u \mapsto u|_\Gamma, \quad (1.31)$$

$$\gamma_1^{\text{ext}} : \mathcal{C}_0^\infty(\bar{\Omega}^{\text{ext}}) \rightarrow L^2(\Gamma) : u \mapsto \frac{\partial u}{\partial n^{\text{ext}}} := \nabla u|_\Gamma \cdot n^{\text{ext}}. \quad (1.32)$$

The space $L^2(\Gamma)$ is justified here, because the gradient ∇u is $\mathcal{C}^\infty(\Gamma) \subset L^2(\Gamma)$ and n^{ext} is $L^\infty(\Gamma)$. Note, that the alternative definition $\gamma_1^{\text{ext}} u = -\frac{\partial u}{\partial n^{\text{ext}}}$ is used often in the literature. The exterior Dirichlet trace operator can be continuously be extended to

$$\gamma_0^{\text{ext}} : H^1(\Omega^{\text{ext}}) \rightarrow H^{1/2}(\Gamma). \quad (1.33)$$

As in the interior case, γ_0^{ext} is surjective and there exists a continuous right inverse. This is intuitively clear, because we can restrict the function u to a suitable subset of Ω^{ext} and apply the interior trace theorem. This way, also functions from $H_{\text{loc}}^1(\Omega^{\text{ext}})$ have a well-defined Dirichlet trace. For details see, e. g., SAUTER AND SCHWAB [164, Sect. 2.6] and the references therein.

Applying MCLEAN [134, Lemma 4.1] we find that for each function $u \in H^1(\Omega^{\text{ext}})$ satisfying the equation

$$-\Delta u = 0 \quad \text{in } \Omega^{\text{ext}},$$

to be read in the distributional sense, there exists a unique functional $g \in H^{-1/2}(\Gamma)$ with satisfies

$$(\nabla u, \nabla v)_{L^2(\Omega^{\text{ext}})} = \langle g, \gamma_0^{\text{ext}} v \rangle_\Gamma \quad \forall v \in H^1(\Omega^{\text{ext}}).$$

However, in general solutions to exterior boundary value problems are *not* in $H^1(\Omega^{\text{ext}})$ but only in $H_{\text{loc}}^1(\Omega^{\text{ext}})$. In order to make use of Green's identity, we need to prescribe a *radiation condition*, i. e., some assumption about the behavior of the solution at infinity. We will return to this issue in Section 1.4.

More notes on traces With the Dirichlet trace being defined on the whole of Γ , it is also well-defined on any part $\tilde{\Gamma}$ of the boundary Γ , as a function in $H^{1/2}(\tilde{\Gamma})$. As stated before, the restriction of the Neumann trace from $H^{-1/2}(\Gamma)$ is well-defined as a functional in $H^{-1/2}(\tilde{\Gamma})$, i. e., with test functions from $H_{00}^{1/2}(\tilde{\Gamma})$.

Notation. We write γ_0^{int} , γ_1^{int} if we want to emphasize the use of the interior trace operators γ_0 , γ_1 . We will often write $u|_\Gamma$ as a short hand for $\gamma_0^{\text{int}} u$ or $\gamma_0^{\text{ext}} u$ when the context allows to do so, and we write $u|_{\tilde{\Gamma}}$ for the restriction of a function u from H^1 to the hypersurface $\tilde{\Gamma} \subset \partial\Omega$.

1.3.1.3 Friedrichs and Poincaré type inequalities

Friedrichs and Poincaré type inequalities are powerful tools for the analysis of variational problems, finite element approximations, and domain decomposition methods. They can be derived from the following general result.

Theorem 1.7. *Let Ω be a bounded and connected domain with Lipschitz boundary $\partial\Omega$. Let $\psi : H^1(\Omega) \rightarrow \mathbb{R}$ a bounded linear functional which reproduces the constants, i. e.,*

$$z \in \mathcal{P}_0(\Omega), \psi(z) = 0 \implies z = 0.$$

Then

$$\|u\|_{H^1(\Omega)} := \left\{ |u|_{H^1(\Omega)}^2 + \psi(u)^2 \right\}^{1/2}$$

is a norm on $H^1(\Omega)$ equivalent to $\|\cdot\|_{H^1(\Omega)}$. Furthermore there exists a constant $C_\psi > 0$ depending only on Ω and on ψ such that

$$\|u\|_{L^2(\Omega)} \leq C_\psi |u|_{H^1(\Omega)} \quad \forall u \in H^1(\Omega), \psi(u) = 0.$$

Proof. The proof is performed by *reductio ad absurdum* using an embedding argument due to Rellich; see e. g., BRENNER AND SCOTT [26, Sect. 5.3], NEČAS [137], and also TOSELLI AND WIDLUND [184, Theorem A.12]. \square

Theorem 1.8 (Friedrichs' inequality). *Let Ω be a bounded Lipschitz domain and let Γ_D be a connected part of $\partial\Omega$ with positive surface measure. Then there exists a constant $C_F > 0$ depending only on Ω and Γ_D such that for all $u \in H^1(\Omega)$ with $u|_{\Gamma_D} = 0$ we have*

$$\|u\|_{L^2(\Omega)} \leq C_F |u|_{H^1(\Omega)}.$$

Proof. Follows from Theorem 1.7 by setting $\psi(u) = \int_{\Gamma_D} u \, ds$, cf. TOSELLI AND WIDLUND [184, Lemma A.14]. \square

Theorem 1.9 (Poincaré's inequality). *Let Ω be a bounded Lipschitz domain. Then there exists a constant $C_P > 0$ depending only on Ω such that for all $u \in H^1(\Omega)$ with $\int_{\Omega} u \, dx = 0$, we have*

$$\|u\|_{L^2(\Omega)} \leq C_P |u|_{H^1(\Omega)}.$$

Proof. Follows from Theorem 1.7, see BRENNER AND SCOTT [26, Sect. 5.3] or TOSELLI AND WIDLUND [184, Lemma A.13]. \square

Note that since constants C_F and C_P stem from a *reductio ad absurdum*, we only know about their existence, but nothing on their magnitude. For a certain class of simply shaped domains, such as simplices, rectangles, hexagons, star-shaped domains, etc. some direct proofs with explicit constants exist; see, e. g., MICHLIN [135], ZHENG AND QI [194]. Nevertheless, the dependence of C_F , C_P on the size (i. e., the diameter) of Ω can be made explicit using a simple scaling argument.

Corollary 1.10. *There exist a constant $\tilde{C}_F > 0$ depending on Ω and Γ_D but not on the size of Ω , and a constant $\tilde{C}_P > 0$ depending only on the shape of Ω such that*

$$\|u\|_{L^2(\Omega)} \leq \tilde{C}_F (\text{diam } \Omega) |u|_{H^1(\Omega)} \quad \forall u \in H^1(\Omega), u|_{\Gamma_D} = 0, \quad (1.34)$$

$$\|u\|_{L^2(\Omega)} \leq \tilde{C}_P (\text{diam } \Omega) |u|_{H^1(\Omega)} + |\Omega|^{-1/2} \left| \int_{\Omega} u \, dx \right| \quad \forall u \in H^1(\Omega). \quad (1.35)$$

Proof. The proof is easily worked out by an argument called *dilation*. We represent the domain Ω as a transformed domain $\widehat{\Omega}$ of unit diameter by a simple scaling of the coordinates. The L^2 -norm and the H^1 -seminorm scale differently because of the derivatives in $|\cdot|_{H^1(\Omega)}$. For a detailed presentation see TOSELLI AND WIDLUND [184, Sect. 3.4]. To show (1.35) we apply Theorem 1.9 (with the dilation argument) to the function $u - \bar{u}$ where $\bar{u} = |\Omega|^{-1} \int_{\Omega} u \, dx$:

$$\|u\|_{L^2(\Omega)} \leq \|u - \bar{u}\|_{L^2(\Omega)} + \|\bar{u}\|_{L^2(\Omega)} \leq \tilde{C}_P |u|_{H^1(\Omega)} + |\Omega|^{1/2} |\bar{u}|.$$

□

Remark 1.11. In particular for Poincaré's inequality it is essential that Ω is *connected*. The inequality does in general not hold for sets with more than one component.

Corollary 1.12. *Let Ω be a bounded Lipschitz domain. Then the following (squared) norms are equivalent,*

$$\begin{aligned} & |u|_{H^1(\Omega)}^2 + \frac{1}{(\text{diam } \Omega)^2} \|u\|_{L^2(\Omega)}^2 \\ & |u|_{H^1(\Omega)}^2 + \frac{1}{\text{diam } \Omega} \|u\|_{L^2(\partial\Omega)}^2, \\ & |u|_{H^1(\Omega)}^2 + \frac{1}{|\partial\Omega| \text{diam } \Omega} \left(\int_{\partial\Omega} u \, ds \right)^2, \end{aligned}$$

and the equivalence constants depend only on the shape of Ω .

Proof. Follows from a variant of Theorem 1.7, see TOSELLI AND WIDLUND [184, Lemma A.17], and a dilation argument. □

Lemma 1.13 (Bramble-Hilbert). *Let Ω be a bounded and connected domain with Lipschitz boundary $\partial\Omega$. Let $\psi : H^1(\Omega) \rightarrow \mathbb{R}$ be a bounded linear functional which satisfies*

$$|\psi(u)| \leq C_\psi \|u\|_{H^1(\Omega)} \quad \forall u \in H^1(\Omega),$$

for some $C_\psi > 0$, and vanishes on the constants, i. e.,

$$\psi(z) = 0 \quad \forall z \in \mathcal{P}_0(\Omega).$$

Then we also have

$$|\psi(u)| \leq C_\psi C_P |u|_{H^1(\Omega)} \quad \forall u \in H^1(\Omega),$$

where C_P is the constant from Theorem 1.9.

Proof. For the proof of the original more general result on functions in $H^k(\Omega)$ for domains that satisfy a strong cone condition see BRAMBLE AND HILBERT [17], for a proof on domains which are star-shaped with respect to a ball see BRENNER AND SCOTT [26, Lemma 4.3.8]. Here we give a proof (for the case $k = 1$) using Poincaré's inequality: Due to the linearity and boundedness of ψ we have

$$|\psi(u)| = |\psi(u + z)| \leq C_\psi \|u + z\|_{H^1(\Omega)} \quad \forall z \in \mathcal{P}_0(\Omega),$$

i. e., for all constant z . Choosing $z := \frac{1}{|\Omega|} \int_{\Omega} u \, dx$ we have $\int_{\Omega} u + z \, dx = 0$, and Poincaré's inequality yields $\|u + z\|_{H^1(\Omega)} \leq C_P |u + z|_{H^1(\Omega)} \leq |u|_{H^1(\Omega)}$. □

Remark 1.14. The dependence of the factor $C_\psi C_P$ in Lemma 1.13 on the diameter of Ω can be made explicit by dilation.

1.3.2 Variational formulation

We start with the potential equation from Section 1.2 in classical form for the case of two subdomains: Find $u \in \mathcal{C}(\bar{\Omega})$ with $u \in \mathcal{C}^2(\Omega_i) \cap \mathcal{C}^1(\Omega_i \cup (\Gamma_N \cap \bar{\Omega}_i) \cup \Gamma_{12})$ for $i = 1, 2$, such that

$$\begin{aligned} -\operatorname{div}[\mathcal{A}\nabla u] &= f && \text{in } \Omega_i && i = 1, 2, \\ (\mathcal{A}\nabla u) \cdot n_1 + (\mathcal{A}\nabla u) \cdot n_2 &= 0 && \text{on } \Gamma_{12}, \\ u|_{\Gamma_D} &= g_D && \text{on } \Gamma_D, \\ (\mathcal{A}\nabla u) \cdot n &= g_N && \text{on } \Gamma_N. \end{aligned} \tag{1.36}$$

We call solutions of (1.36) *classical solutions*. Multiplying the first equation by a trial function v , integrating subdomain-wise, using integration by parts, the interface conditions, and the boundary conditions, we obtain the *variational formulation*: Find $u \in H^1(\Omega)$ with $u|_{\Gamma_D} = g_D$ such that

$$a(u, v) = \langle F, v \rangle \quad \forall v \in H_D^1(\Omega), \tag{1.37}$$

where

$$H_D^1(\Omega) := \{v \in H^1(\Omega) : v|_{\Gamma_D} = 0\},$$

with the bilinear form $a(\cdot, \cdot) : H^1(\Omega) \times H^1(\Omega) \rightarrow \mathbb{R}$ defined by

$$a(u, v) := \int_{\Omega} (\mathcal{A}\nabla u) \cdot \nabla v \, dx,$$

and the linear form $F : H^1(\Omega) \rightarrow \mathbb{R}$ defined by

$$\langle F, v \rangle := \int_{\Omega} f v \, dx + \int_{\Gamma_N} g_N v \, ds.$$

We call solutions u of (1.37) *weak solutions* to (1.36). If a weak solution and the data \mathcal{A} , f , g_D , g_N are sufficiently smooth, the weak solution is also a classical solution. Note that the case of multiple interfaces is straightforward.

In the following, we assume with out loss of generality that $g_D = 0$. Indeed, if $g_D \neq 0$ we can homogenize (1.37) by choosing an arbitrary extension $\tilde{g} \in H^1(\Omega)$ with $\tilde{g}|_{\Gamma_D} = g_D$. Such extensions must exist due to Theorem 1.5. If we solve

$$a(u_0, v) = \underbrace{\langle F, v \rangle - a(\tilde{g}, v)}_{=: \langle \tilde{F}, v \rangle} \quad \forall v \in H_D^1(\Omega), \tag{1.38}$$

for $u_0 \in H_D^1(\Omega)$, the solution u of (1.37) is given by $u = \tilde{g} + u_0$. Obviously, $\tilde{F} \in (H_D^1(\Omega))^*$.

Lemma 1.15. *Let the Dirichlet boundary Γ_D be of positive surface measure, $\mathcal{A} \in (L^\infty(\Omega))^{d \times d}$, $f \in L^2(\Omega)$, $g_D \in H^{1/2}(\Gamma_D)$, and $g_N \in L^2(\Gamma_N)$. Furthermore, assume that there exist uniform bounds of the coefficient matrix, i. e., there exist constants $\underline{\alpha}, \bar{\alpha} > 0$ with*

$$\underline{\alpha}|p|^2 \leq (\mathcal{A}(x)p) \cdot p \leq \bar{\alpha}|p|^2 \quad \text{for all } p \in \mathbb{R}^d \text{ and almost all } x \in \Omega.$$

Then the bilinear form is elliptic (coercive) and bounded on $H_D^1(\Omega)$, i. e., there exist constants $\underline{c}_a, \bar{c}_a > 0$ with

$$\begin{aligned} a(v, v) &\geq \underline{c}_a \|v\|_{H^1(\Omega)}^2 & \forall v \in H_D^1(\Omega), \\ a(u, v) &\leq \bar{c}_a \|u\|_{H^1(\Omega)} \|v\|_{H^1(\Omega)} & \forall u, v \in H_D^1(\Omega), \end{aligned}$$

and the linear form is bounded, i. e., there exists a constant $\bar{c}_F > 0$ with

$$\langle F, v \rangle \leq \bar{c}_F \|v\|_{H^1(\Omega)} \quad \forall v \in H_D^1(\Omega).$$

Proof. The ellipticity of $a(\cdot, \cdot)$ follows from our assumptions on \mathcal{A} and from Friedrichs' inequality. The boundedness of $a(\cdot, \cdot)$ and $\langle F, \cdot \rangle$ follow basically using the Cauchy-Schwarz inequality. \square

1.3.3 Existence of unique solutions to abstract variational problems

Let V be a Hilbert space and let $a(\cdot, \cdot) : V \times V \rightarrow \mathbb{R}$ be an elliptic and bounded bilinear form, and $F \in V^*$. For the time being, V , $a(\cdot, \cdot)$, and F can be arbitrary, but we keep our model problem in mind. Consider the abstract variational problem: Find $u \in V$ such that

$$a(u, v) = \langle F, v \rangle \quad \forall v \in V. \quad (1.39)$$

Theorem 1.16 (Lax-Milgram). *Let V be a Hilbert space. Let $a(\cdot, \cdot) : V \times V \rightarrow \mathbb{R}$ be an elliptic and bounded bilinear form, and let $F \in V^*$ be a bounded linear form. Then the variational formulation (1.39) has a unique solution $u \in V$ which fulfills the a priori estimate*

$$\frac{1}{\bar{c}_a} \|F\|_{V^*} \leq \|u\|_V \leq \frac{1}{\underline{c}_a} \|F\|_{V^*},$$

where \underline{c}_a and \bar{c}_a are the constants of ellipticity and boundedness of $a(\cdot, \cdot)$, respectively.

Proof. Follows directly from the variational problem, the ellipticity and boundedness, and the definition of the dual norm, see, e. g., BRENNER AND SCOTT [26, Sect. 2.7]. \square

Lemma 1.15 shows that the assumptions of the Lax-Milgram theorem are fulfilled. Hence, under suitable assumptions the potential equation (1.36) has a unique weak solution.

Introducing the operator

$$A : V \rightarrow V^* : u \mapsto a(u, \cdot), \quad (1.40)$$

we can rewrite (1.39) as operator equation: Find $u \in V$ such that

$$A u = F \quad \text{in } V^*. \quad (1.41)$$

The operator A is linear and elliptic. The statement of the Lax-Milgram theorem can be generalized to nonlinear strongly monotone and Lipschitz continuous operators; for a proof see ZEIDLER [193].

Theorem 1.17 (Zarantonello). *Let V be a Hilbert space. Let the operator $A : V \rightarrow V^*$ be strongly monotone, i. e., there exists $\underline{c}_A > 0$ with*

$$\langle A(u) - A(v), u - v \rangle \geq \underline{c}_A \|u - v\|_V^2 \quad \forall u, v \in V,$$

and Lipschitz continuous, i. e., there exists $\bar{c}_A > 0$ with

$$\|A(u) - A(v)\|_{V^*} \leq \bar{c}_A \|u - v\|_V \quad \forall u, v \in V.$$

Then, the (nonlinear) operator equation

$$A(u) = F \quad \text{in } V^* \tag{1.42}$$

has a unique solution $u \in V$.

1.3.4 Galerkin's method

Let V be a Hilbert space with a closed subspace $V_0 \subset V$, and let $g \in V$. We consider the abstract variational problem: Find $u \in V_g := g + V_0$ such that

$$a(u, v) = \langle F, v \rangle \quad \forall v \in V_0, \tag{1.43}$$

with the bounded and V_0 -elliptic bilinear form $a(\cdot, \cdot) : V \times V \rightarrow \mathbb{R}$ and $F \in V_0^*$. *Galerkin's method* is as follows. Choose a finite dimensional subspace $V_0^h \subset V_0$ and consider the projected problem: Find $u_h \in V_g^h := g + V_0^h$ such that

$$a(u_h, v_h) = \langle F, v_h \rangle \quad \forall v_h \in V_0^h. \tag{1.44}$$

The following a-priori estimate (see, e. g., [26, Sect. 2.8]) states that the discretization error is controlled in terms of the approximation error of the space V^h .

Lemma 1.18 (Céa). *Let $u \in V_g$ be the solution of (1.43) and let $u_h \in V_g^h$ be the solution of (1.44). Then we have*

$$\|u - u_h\|_V \leq \frac{\bar{c}_a}{\underline{c}_a} \inf_{v_h \in V_g^h} \|u - v_h\|_V,$$

where \underline{c}_a and \bar{c}_a are the constants of V_0 -ellipticity and boundedness of $a(\cdot, \cdot)$, respectively.

In the case that the bilinear form is symmetric and $F \in V^*$, the solutions u of (1.39) and u_h of (1.44) are characterized via the *Ritz energy functional*,

$$J(v) := \frac{1}{2}a(v, v) - \langle F, v \rangle, \tag{1.45}$$

and the following result (cf., e. g., BRENNER AND SCOTT [26, Sect. 2.5]).

Lemma 1.19. *Let V be a Hilbert space, let $a(\cdot, \cdot) : V \times V \rightarrow \mathbb{R}$ be symmetric, bounded, and V_0 -elliptic, and assume $F \in V^*$. Then the solutions u and u_h of (1.39) and (1.44), respectively, fulfill*

$$\begin{aligned} u &= \operatorname{argmin}_{v \in V_g} J(v), & J(u) &\leq J(u_h), \\ u_h &= \operatorname{argmin}_{v_h \in V_g^h} J(v_h), & a(u_h, u_h) &\leq a(u, u). \end{aligned}$$

1.4 Boundary integral equations

In this section we embrace the concept of boundary integral equations and Steklov-Poincaré operators. Using fundamental solutions, the partial differential equation on a domain can be reformulated in terms of integral equations on the boundary. For a comprehensive discussion see, e. g., MCLEAN [134], SAUTER AND SCHWAB [164], or STEINBACH [175].

1.4.1 Boundary integral operators and the Calderón system

Let $\Omega \subset \mathbb{R}^d$ ($d = 2$ or 3) be a bounded domain with a simply connected Lipschitz boundary $\Gamma := \partial\Omega$. In the following we consider the interior $\Omega^{\text{int}} := \Omega$ and the exterior $\Omega^{\text{ext}} := \mathbb{R}^d \setminus \overline{\Omega}$ of Γ . Let n and n^{ext} denote the outward unit normal vectors on Γ pointing into Ω^{ext} and Ω^{int} , respectively, see Figure 1.3 on page 20. We consider the interior and exterior Laplace problem

$$-\Delta u = 0 \quad \text{in } \Omega^{\text{int}}, \quad (1.46)$$

$$-\Delta u = 0 \quad \text{in } \Omega^{\text{ext}}, \quad (1.47)$$

respectively. A fundamental solution to (1.46) and (1.47) is given by

$$U^*(x, y) := \begin{cases} -\frac{1}{2\pi} \log|x-y| & \text{for } d = 2, \\ \frac{1}{4\pi} \frac{1}{|x-y|} & \text{for } d = 3, \end{cases} \quad (1.48)$$

see, e. g., EVANS [53], MCLEAN [134, Theorem 8.1]. In fact, in two dimensions, we could use $1/(2\pi) \log(r/|x-y|)$ for any $r > 0$. Note that for other classes of domains, such as the half space $\mathbb{R}^{d-1} \times \mathbb{R}^+$ or the domain $\mathbb{R}^d \setminus \{0\}$, other fundamental solutions must be used, cf. COSTABEL AND DAUGE [40].

As mentioned in Section 1.3.1.2, exterior problems require special care. Solutions to (1.47) are in general only in the space $H_{\text{loc}}^1(\Omega^{\text{ext}})$ and in order to make use of Green's identity we need a *radiation condition*. To this end we follow an approach by COSTABEL AND DAUGE [40], see also MCLEAN [134, pp. 234ff].

Lemma 1.20. *Let $u \in \mathcal{D}'(\Omega^{\text{ext}})$ fulfill equation (1.47) in the distributional sense, and let $U^*(x, y)$ be a fundamental solution for the Laplace operator on Ω^{ext} . Then the distribution u is in $\mathcal{C}^\infty(\Omega^{\text{ext}})$, and there exists a unique function $\mathcal{M}u \in \mathcal{C}^\infty(\mathbb{R}^d)$ such that for each bounded Lipschitz domain Ω_1 with $\mathbb{R}^d \setminus \Omega^{\text{ext}}$ is compactly contained in Ω_1 ,*

$$(\mathcal{M}u)(x) = \int_{\partial\Omega_1} U^*(x, y) \gamma_1^{\text{ext}} u(y) ds_y - \int_{\partial\Omega_1} \gamma_{1,y}^{\text{ext}} U^*(x, y) u(y) ds_y \quad \forall x \in \Omega_1.$$

Proof. See MCLEAN [134, Theorem 6.4 and Lemma.7.11]. □

In particular, the lemma ensures that solutions u of (1.47) with $\gamma_0^{\text{ext}} u \in H^{1/2}(\Gamma)$ are in $H_{\text{loc}}^1(\Omega^{\text{ext}})$. Furthermore, $-\Delta \mathcal{M}u = 0$. The radiation condition we will use throughout reads

$$\mathcal{M}u = 0, \quad (1.49)$$

and it is characterized by the following lemma.

Lemma 1.21. *Let $u \in \mathcal{D}'(\Omega^{\text{ext}})$ fulfill equation (1.47) in the distributional sense. Then the following statements hold.*

(i) *If $d = 3$, $\mathcal{M}u = 0$ if and only if*

$$u(x) = \mathcal{O}(|x|^{-1}) \quad \text{as } |x| \rightarrow \infty.$$

(ii) *If $d = 2$, $\mathcal{M}u = 0$ if and only if there exists a constant b such that*

$$u(x) = b \log |x| + \mathcal{O}(|x|^{-1}) \quad \text{as } |x| \rightarrow \infty.$$

(iii) *If $d = 2$, then $u(x) = \mathcal{O}(1)$ as $|x| \rightarrow \infty$ if and only if there exists a constant b such that*

$$u(x) = b + \mathcal{O}(|x|^{-1}) \quad \text{as } |x| \rightarrow \infty.$$

In this case $\mathcal{M}u = b$.

Proof. See MCLEAN [134, Theorem 8.9]. □

If the radiation condition (1.49) holds, each $H_{\text{loc}}^1(\Omega^{\text{ext}})$ solution of (1.47) exhibits a well-defined Neumann trace $\gamma_1^{\text{ext}}u \in H^{-1/2}(\Gamma)$, cf. MCLEAN [134, Theorem 7.15], which fulfills the identity

$$\langle \gamma_1^{\text{ext}}u, \varphi \rangle_{\Gamma} = \int_{\Omega^{\text{ext}}} \nabla u \cdot \nabla \varphi \, dx \quad \forall \varphi \in \mathcal{C}_0^{\infty}(\overline{\Omega^{\text{ext}}}). \quad (1.50)$$

In order to come up with integral equations that characterize the solutions of the interior and exterior Laplace problem, we define the single layer potential operator $V : H^{-1/2}(\Gamma) \rightarrow H^{1/2}(\Gamma)$, the double layer potential operator $K : H^{1/2}(\Gamma) \rightarrow H^{1/2}(\Gamma)$, and the hypersingular integral operator $D : H^{1/2}(\Gamma) \rightarrow H^{-1/2}(\Gamma)$ by

$$\begin{aligned} (Vt)(x) &:= \int_{\Gamma} U^*(x, y) t(y) \, ds_y, \\ (Ku)(x) &:= \int_{\Gamma} \frac{\partial}{\partial n_y} U^*(x, y) u(y) \, ds_y, \\ (Du)(x) &:= -\frac{\partial}{\partial n_x} \int_{\Gamma} \frac{\partial}{\partial n_y} U^*(x, y) u(y) \, ds_y, \end{aligned} \quad (1.51)$$

where $x \in \Gamma$. The adjoint double layer potential $K^{\top} : H^{-1/2}(\Gamma) \rightarrow H^{-1/2}(\Gamma)$ is given by

$$(K^{\top}t)(x) = \int_{\Gamma} \frac{\partial}{\partial n_x} U^*(x, y) t(y) \, ds_y. \quad (1.52)$$

The integral representations for V , K , and D in (1.51) are to be understood as weakly singular, Cauchy singular, and hypersingular surface integrals, respectively; for details see, e. g., STEINBACH [175]. Note also, that $H^{1/2}(\Gamma)$ and $H^{-1/2}(\Gamma)$ are dual to each other as long as Γ is a closed hypersurface. The following assumption is needed for the ellipticity of the single layer potential operator V in two dimensions.

Assumption 1.22. *Throughout this work, we assume that*

$$\text{diam } \Omega < 1 \quad \text{if } d = 2,$$

which can always be obtained by a simple scaling of the coordinates.

In two dimension, instead of scaling one could also use an alternative fundamental solution $U^*(x, y) = 1/(2\pi) \log(r/|x - y|)$ with a suitably chosen parameter $r > 0$, cf. MCLEAN [134, pp. 264f].

The results summarized in the next Lemma can essentially be found in STEINBACH [175], where the reader can also find the corresponding references to the original papers.

Lemma 1.23. *The boundary integral operators defined in (1.51) are linear and bounded operators with the following properties:*

(i) *Every weak solution of the interior Laplace problem (1.46) fulfills the Calderón system*

$$\begin{pmatrix} \gamma_0^{\text{int}} u \\ \gamma_1^{\text{int}} u \end{pmatrix} = \begin{pmatrix} \frac{1}{2}I - K & V \\ D & \frac{1}{2}I + K^\top \end{pmatrix} \begin{pmatrix} \gamma_0^{\text{int}} u \\ \gamma_1^{\text{int}} u \end{pmatrix}. \quad (1.53)$$

For weak solutions to the exterior Laplace problem (1.47) which fulfill the radiation condition (1.49), the same equations hold, where we have to take the exterior traces and flip the signs in front of K and K^\top .

(ii) *The single layer potential operator V is self-adjoint and elliptic, i. e., there exists a constant $c_V > 0$ such that*

$$\langle V w, w \rangle \geq c_V \|w\|_{H^{-1/2}(\Gamma)}^2 \quad \forall w \in H^{-1/2}(\Gamma).$$

Consequently, the inverse $V^{-1} : H^{1/2}(\Gamma) \rightarrow H^{-1/2}(\Gamma)$ is self-adjoint, elliptic, and bounded, and $\|v\|_{V^{-1}} := \langle V^{-1}v, v \rangle^{1/2}$ defines a norm on $H^{1/2}(\Gamma)$ which is equivalent to $\|\cdot\|_{H^{1/2}(\Gamma)}$.

(iii) *The single layer potential operator V is an isomorphism between the subspaces $H_*^{-1/2}(\Gamma)$ and $H_*^{1/2}(\Gamma)$, defined by*

$$\begin{aligned} H_*^{-1/2}(\Gamma) &:= \{w \in H^{-1/2}(\Gamma) : \langle w, \mathbf{1}_\Gamma \rangle = 0\}, \\ H_*^{1/2}(\Gamma) &:= \{v \in H^{1/2}(\Gamma) : \langle V^{-1}v, \mathbf{1}_\Gamma \rangle = 0\}. \end{aligned} \quad (1.54)$$

(iv) *The hypersingular integral operator D is self-adjoint and there exists an ellipticity constant $c_D > 0$ such that*

$$\begin{aligned} \langle D v, v \rangle &\geq c_D \|v\|_{H^{1/2}(\Gamma)}^2 & \forall v \in H_*^{1/2}(\Gamma), \\ \langle D v, v \rangle &\geq c_D |v|_{H^{1/2}(\Gamma)}^2 & \forall v \in H^{1/2}(\Gamma). \end{aligned}$$

Moreover, we have $\ker D = \text{span}\{\mathbf{1}_\Gamma\}$.

(v) The double layer potential operator K admits the contraction properties

$$\begin{aligned} (1 - c_K)\|v\|_{V^{-1}} &\leq \|(\tfrac{1}{2}I \pm K)v\|_{V^{-1}} \leq c_K \|v\|_{V^{-1}} && \forall v \in H_*^{1/2}(\Gamma), \\ (1 - c_K)\|v\|_{V^{-1}} &\leq \|(\tfrac{1}{2}I - K)v\|_{V^{-1}} \leq \|v\|_{V^{-1}} && \forall v \in H^{1/2}(\Gamma), \\ 0 &\leq \|(\tfrac{1}{2}I + K)v\|_{V^{-1}} \leq c_K \|v\|_{V^{-1}} && \forall v \in H^{1/2}(\Gamma), \end{aligned}$$

where

$$c_K := \frac{1}{2} + \sqrt{\frac{1}{4} - c_0} < 1, \quad c_0 := \inf_{v \in H_*^{1/2}(\Gamma)} \frac{\langle Dv, v \rangle}{\langle V^{-1}v, v \rangle} \in \left(0, \frac{1}{4}\right).$$

Additionally,

$$\ker(\tfrac{1}{2}I + K) = \text{span}\{\mathbf{1}_\Gamma\}, \quad \ker(\tfrac{1}{2}I - K) = \{\mathbf{0}_\Gamma\}, \quad (\tfrac{1}{2}I - K)\mathbf{1}_\Gamma = \mathbf{1}_\Gamma.$$

Remark 1.24. The constants c_0 and c_K do not depend on the size of the domain Ω^{int} but only on its shape. This can be shown by introducing a simple scaling of the domain and transforming the energy forms induced by D and V . In two dimensions the logarithm occurring in the fundamental solution yields an additive term in the V -form; nevertheless this term vanishes for functions in the space $H_*^{1/2}(\Gamma)$. We note that an important contribution to the contraction properties is the article by STEINBACH AND WENDLAND [177], see also COSTABEL [39] for a historical remark.

The two boundary integral equations appearing in the Calderón system (1.53) can be used to solve Dirichlet, Neumann, and mixed boundary value problems in the sense that we determine the complete Cauchy data $(\gamma_0^{\text{int}}u, \gamma_1^{\text{int}}u)$. We do not go into details here, because we will mainly use Steklov-Poincaré operators in this work, which are introduced in Section 1.4.3. For the corresponding theory and other approaches see, e. g., STEINBACH [175, Sect. 7].

1.4.2 Representation formulae

With the help of the Cauchy data $(\gamma_0^{\text{int}}u, \gamma_1^{\text{int}}u)$, the actual solution $u \in H^1(\Omega^{\text{int}})$ of (1.46) is given by the representation formula

$$u(x) = \int_\Gamma U^*(x, y) \gamma_1^{\text{int}}u(y) ds_y - \int_\Gamma \gamma_1^{\text{int}}U^*(x, y) \gamma_0^{\text{int}}u(y) ds_y \quad \text{for } x \in \Omega^{\text{int}}. \quad (1.55)$$

For the exterior problem (1.47), (1.49) we have

$$u(x) = \int_\Gamma U^*(x, y) \gamma_1^{\text{ext}}u(y) ds_y - \int_\Gamma \gamma_1^{\text{ext}}U^*(x, y) \gamma_0^{\text{ext}}u(y) ds_y \quad \text{for } x \in \Omega^{\text{ext}}. \quad (1.56)$$

For details see, e. g., MCLEAN [134, Theorem 7.5, Theorem 7.12].

1.4.3 Steklov-Poincaré operators

The properties of the boundary integral operators justify the following definition of the *interior Steklov-Poincaré operator* $S^{\text{int}} : H^{1/2}(\Gamma) \rightarrow H^{-1/2}(\Gamma)$ and the *exterior Steklov-Poincaré operator* $S^{\text{ext}} : H^{1/2}(\Gamma) \rightarrow H^{-1/2}(\Gamma)$,

$$S^{\text{int}} := V^{-1}(\tfrac{1}{2}I + K), \quad S^{\text{ext}} := V^{-1}(\tfrac{1}{2}I - K), \quad (1.57)$$

which are linear and bounded. We find that for every solution u of (1.46) we have $\gamma_1^{\text{int}} u = S^{\text{int}} \gamma_0^{\text{int}} u$, and for every solution u of (1.47) we have $\gamma_1^{\text{ext}} u = S^{\text{ext}} \gamma_0^{\text{ext}} u$. In other words, S^{int} (resp. S^{ext}) is the Dirichlet to Neumann map for the interior (resp. exterior) Laplace equation. Furthermore, the Calderón system (1.53) yields the symmetric representations

$$\begin{aligned} S^{\text{int}} &= D + \left(\frac{1}{2}I + K^\top\right)V^{-1}\left(\frac{1}{2}I + K\right), \\ S^{\text{ext}} &= D + \left(\frac{1}{2}I - K^\top\right)V^{-1}\left(\frac{1}{2}I - K\right), \end{aligned} \quad (1.58)$$

which imply that S^{int} and S^{ext} are self-adjoint operators. We define the interior energy form

$$a_{\Omega^{\text{int}}}(u, v) := \int_{\Omega^{\text{int}}} \nabla u \cdot \nabla v \, dx \quad \text{for } u, v \in H^1(\Omega^{\text{int}}).$$

Due to Theorem 1.6,

$$\langle S^{\text{int}} v, w \rangle_\Gamma = a_{\Omega^{\text{int}}}(u, w) \quad \forall w \in H^1(\Omega^{\text{int}}), \quad (1.59)$$

where $u \in H^1(\Omega^{\text{int}})$ solves $-\Delta u = 0$ (in the distributional sense) and $u|_\Gamma = v$. Using the minimizing property Lemma 1.19, we obtain that

$$\langle S^{\text{int}} v, v \rangle = \min_{\substack{u \in H^1(\Omega^{\text{int}}) \\ u|_\Gamma = v}} a_{\Omega^{\text{int}}}(u, u), \quad (1.60)$$

see also STEINBACH [175]. The function \tilde{u} where the minimum is attained is called *harmonic extension* of u from Γ to Ω^{int} .

For the exterior problem, we can show a similar minimizing property. We define the linear functional

$$\|u\|_{H_*^1(\Omega^{\text{ext}})} := \left\{ \int_{\Omega^{\text{ext}}} |\nabla u(x)|^2 \, dx + \int_{\Omega^{\text{ext}}} |u(x)|^2 \frac{dx}{\rho(x)} \right\}^{1/2} \quad \text{for } u \in H_{\text{loc}}^1(\Omega^{\text{ext}}),$$

where $\rho(x) = |x|^2$ if $d = 3$ and $\rho(x) = |x|^2 (\log |x|)^2$ if $d = 2$, and we assume that $0 \notin \overline{\Omega^{\text{ext}}}$. The subspace

$$H_*^1(\Omega^{\text{ext}}) := \{v \in H_*^1(\Omega^{\text{ext}}) : \|u\|_{H_{\text{loc}}^1(\Omega^{\text{ext}})} < \infty\}$$

equipped with $\|\cdot\|_{H_*^1(\Omega^{\text{ext}})}$ as norm is a Hilbert space because it is equivalent to a weighted Sobolev space. Furthermore, one can show that $C_0^\infty(\overline{\Omega^{\text{ext}}})$ is dense in $H_*^1(\Omega^{\text{ext}})$. Obviously, the solution u to our exterior problem subject to the radiation condition is in $H_*^1(\Omega^{\text{ext}})$. By a density argument, one can even show that $|\cdot|_{H^1(\Omega^{\text{ext}})}$ is a norm equivalent to $\|\cdot\|_{H_*^1(\Omega^{\text{ext}})}$ on $H_*^1(\Omega^{\text{ext}})$. Consequently, we have existence and uniqueness of the variational problem to find $u \in H_*^1(\Omega^{\text{ext}})$ with some prescribed Dirichlet data such that

$$a_{\Omega^{\text{ext}}}(u, w) = 0 \quad \forall w \in H_*^1(\Omega^{\text{ext}}), \quad w|_\Gamma = 0.$$

where

$$a_{\Omega^{\text{ext}}}(u, w) := \int_{\Omega^{\text{ext}}} \nabla u \cdot \nabla w \, dx \quad \text{for } u, w \in H_*^1(\Omega^{\text{ext}})$$

denotes the exterior energy form. Finally, an application of Lemma 1.19 yields

$$\langle S^{\text{ext}} v, v \rangle = \min_{\substack{u \in H_*^1(\Omega^{\text{ext}}) \\ u|_{\Gamma} = v}} a_{\Omega^{\text{ext}}}(u, u). \quad (1.61)$$

For details, see LUNG-AN AND YING [128] and SAUTER AND SCHWAB [164]. Summarizing, if u solves the interior Laplace equation or the exterior one with the radiation condition, then

$$\begin{aligned} \langle S^{\text{int}} \gamma_0^{\text{int}} u, \gamma_0^{\text{int}} u \rangle &= a_{\Omega^{\text{int}}}(u, u), \\ \langle S^{\text{ext}} \gamma_0^{\text{ext}} u, \gamma_0^{\text{ext}} u \rangle &= a_{\Omega^{\text{ext}}}(u, u), \end{aligned} \quad (1.62)$$

respectively. Moreover, (1.57) implies

$$\langle V^{-1} v, v \rangle = \langle S^{\text{int}} v, v \rangle + \langle S^{\text{ext}} v, v \rangle \quad \forall v \in H^{1/2}(\Gamma), \quad (1.63)$$

and if u solves (separately) the interior and the exterior Laplace equation, we have

$$\langle V^{-1} u, u \rangle = a_{\Omega^{\text{int}}}(u, u) + a_{\Omega^{\text{ext}}}(u, u). \quad (1.64)$$

One can quite easily show that the semi-norm induced by S^{int} is equivalent to the V^{-1} -norm on the subspace $H_*^{1/2}(\Gamma)$, and that there are similar estimates for the S^{ext} norm. The following lemma which summarizes results by STEINBACH AND WENDLAND [177] and COSTABEL [39] gives such estimates with more or less explicit constants which depend only on the shape of Γ .

Lemma 1.25. (i) *The following estimates hold for the Steklov-Poincaré operators:*

$$\begin{aligned} (1 - c_K) \langle V^{-1} v, v \rangle &\leq \langle S^{\text{int}/\text{ext}} v, v \rangle \leq c_K \langle V^{-1} v, v \rangle & \forall v \in H_*^{1/2}(\Gamma), \\ (1 - c_K) \langle V^{-1} v, v \rangle &\leq \langle S^{\text{ext}} v, v \rangle \leq \langle V^{-1} v, v \rangle & \forall v \in H^{1/2}(\Gamma), \\ 0 &\leq \langle S^{\text{int}} v, v \rangle \leq c_K \langle V^{-1} v, v \rangle & \forall v \in H^{1/2}(\Gamma), \end{aligned}$$

with the contraction constant $c_K > 0$ from Lemma 1.23(v). In particular, S^{ext} is $H^{1/2}(\Gamma)$ -elliptic and S^{int} is $H_*^{1/2}(\Gamma)$ -elliptic with $\ker S^{\text{int}} = \text{span}\{\mathbf{1}_{\Gamma}\}$.

(ii) *Poincaré's fundamental theorem holds (cf. COSTABEL [39]):*

$$\begin{aligned} \langle S^{\text{ext}} v, v \rangle &\leq \frac{c_K}{1 - c_K} \langle S^{\text{int}} v, v \rangle & \forall v \in H_*^{1/2}(\Gamma), \\ \langle S^{\text{int}} v, v \rangle &\leq \frac{c_K}{1 - c_K} \langle S^{\text{ext}} v, v \rangle & \forall v \in H^{1/2}(\Gamma), \end{aligned}$$

where $c_K/(1 - c_K) > 1$.

(iii) *For $v \in H^{1/2}(\Gamma)$, the decomposition $v = \tilde{v} + v_0 \mathbf{1}_{\Gamma}$ with $v_0 \in \mathbb{R}$ and $\tilde{v} \in H_*^{1/2}(\Gamma)$ is unique and orthogonal in the inner products induced by V^{-1} and S^{ext} ,*

$$\langle V^{-1} \tilde{v}, v_0 \mathbf{1}_{\Gamma} \rangle = 0, \quad \langle S^{\text{ext}} \tilde{v}, v_0 \mathbf{1}_{\Gamma} \rangle = 0.$$

(iv) *For all $v \in H^{1/2}(\Gamma)$, we have*

$$\frac{1 - c_K}{c_K} \langle S^{\text{ext}} v, v \rangle \leq \langle S^{\text{int}} v, v \rangle + \frac{\langle V^{-1} v, \mathbf{1}_{\Gamma} \rangle^2}{\langle V^{-1} \mathbf{1}_{\Gamma}, \mathbf{1}_{\Gamma} \rangle} \leq \frac{c_K}{1 - c_K} \langle S^{\text{ext}} v, v \rangle.$$

Proof. The proof follows mainly from Lemma 1.23. We start with (iii): For $v \in H^{1/2}(\Gamma)$, the relations $\tilde{v} = v - v_0 \mathbf{1}_\Gamma$ and $\langle V^{-1}(v - v_0 \mathbf{1}_\Gamma), \mathbf{1}_\Gamma \rangle = 0$ imply

$$v_0 = \frac{\langle V^{-1}v, \mathbf{1}_\Gamma \rangle}{\langle V^{-1}\mathbf{1}_\Gamma, \mathbf{1}_\Gamma \rangle}, \quad (1.65)$$

which proves the uniqueness of the decomposition. Using that $(\frac{1}{2}I - K)\mathbf{1}_\Gamma = \mathbf{1}_\Gamma$ (Lemma 1.23(v)) we obtain

$$S^{\text{ext}} \mathbf{1}_\Gamma = V^{-1}(\frac{1}{2}I - K)\mathbf{1}_\Gamma = V^{-1}\mathbf{1}_\Gamma, \quad (1.66)$$

and thus

$$\langle S^{\text{ext}} v_0 \mathbf{1}_\Gamma, \tilde{v} \rangle = \langle V^{-1}v_0 \mathbf{1}_\Gamma, \tilde{v} \rangle = 0,$$

which proves the orthogonality in (iii).

Part (i): For $v \in H_*^{1/2}(\Gamma)$, the Cauchy-Schwarz inequality and the contraction properties stated in Lemma 1.23(v) yield

$$\langle S^{\text{int/ext}} v, v \rangle = \langle V^{-1}(\frac{1}{2}I \pm K)v, v \rangle \leq \|(\frac{1}{2}I \pm K)v\|_{V^{-1}} \|v\|_{V^{-1}}^2 \leq c_K \|v\|_{V^{-1}}^2.$$

On the other hand, for all $v \in H_*^{1/2}(\Gamma)$ we have

$$\begin{aligned} \langle S^{\text{int/ext}} v, v \rangle &= \langle V^{-1}(\frac{1}{2}I \pm K)v, v \rangle = \langle V^{-1}v, v \rangle - \langle V^{-1}(\frac{1}{2}I \mp K)v, v \rangle \\ &\geq \langle V^{-1}v, v \rangle - c_K \|v\|_{V^{-1}}^2 \geq (1 - c_K) \langle V^{-1}v, v \rangle. \end{aligned}$$

The inequalities on the full space $H^{1/2}(\Gamma)$ can be derived using the decomposition (iii) and the mapping properties of $(\frac{1}{2}I \pm K)$, see Lemma 1.23(v).

Statement (ii) is an immediate consequence of (i). Since $c_K \in (\frac{1}{2}, 1)$ one easily proves $c_K/(1 - c_K) > 1$.

Finally, with the decomposition from (iii) and formula (1.66) we obtain

$$\langle S^{\text{ext}} v, v \rangle = \langle S^{\text{ext}} \tilde{v}, \tilde{v} \rangle + \langle S^{\text{ext}} v_0 \mathbf{1}_\Gamma, v_0 \mathbf{1}_\Gamma \rangle = \langle S^{\text{ext}} \tilde{v}, \tilde{v} \rangle + \langle V^{-1} v_0 \mathbf{1}_\Gamma, v_0 \mathbf{1}_\Gamma \rangle.$$

Using formula (1.65), Poincaré's fundamental theorem (ii), and $c_k/(1 - c_K) > 1$, we can easily show the desired estimates (iv). \square

To summarize, we have

$$\langle S^{\text{int}} v, v \rangle \simeq |v|_{H^{1/2}(\Gamma)}^2, \quad \langle S^{\text{ext}} v, v \rangle \simeq \|v\|_{H^{1/2}(\Gamma)}^2 \quad \forall v \in H^{1/2}(\Gamma),$$

where in two dimensions we have to fix $\text{diam } \Gamma < 1$.

1.4.4 Newton potentials and Dirichlet-to-Neumann maps

Let Ω be a bounded domain with Lipschitz boundary Γ and let $f \in H^{-1}(\Omega) = (H_0^1(\Omega))^*$ and let $u \in H_0^1(\Omega)$ be the weak solution to

$$\begin{aligned} -\Delta u &= f & \text{in } \Omega, \\ u &= 0 & \text{on } \Gamma. \end{aligned}$$

Due to Theorem 1.6, there exists a unique functional $g \in H^{-1/2}(\Gamma)$ which depends on f , such that

$$(\nabla u, \nabla v)_{L^2(\Omega)} = \langle f, v \rangle_{\Omega} + \langle g, v \rangle_{\Gamma} \quad \forall v \in H^1(\Omega),$$

which generalizes the normal derivative $\frac{\partial u}{\partial n}$. We define the *Newton potential* N by

$$N : H^{-1}(\Omega) \rightarrow H^{-1/2}(\Gamma) : f \mapsto -g. \quad (1.67)$$

In other words, Nf gives the negative flux induced by the source f subject to homogeneous Dirichlet boundary conditions. Obviously, the Newton potential is linear and continuous, see also STEINBACH [174].

The complete Dirichlet to Neumann map corresponding to the boundary value problem

$$\begin{aligned} -\Delta u &= f && \text{in } \Omega, \\ u &= g_D && \text{on } \Gamma \end{aligned}$$

is given by

$$g_D \mapsto \gamma_1^{\text{int}} u = \frac{\partial u}{\partial n} = S^{\text{int}} g_D - Nf. \quad (1.68)$$

1.5 Discretization techniques

1.5.1 Triangulations

Let $\Omega \subset \mathbb{R}^d$ ($d = 2$ or 3) be a bounded domain with Lipschitz boundary $\partial\Omega$. A *triangulation* $\mathcal{T} = \{\tau\}$ of Ω or $\partial\Omega$ is a non-overlapping partition into finitely many *elements*. In this work we consider only simplicial elements, i. e., line segments, triangles, and tetrahedra. For a simplex $\tau \in \mathcal{T}$, we set $h_\tau := \text{diam } \tau$, and we define ρ_τ by the diameter of the largest ball contained in τ . Furthermore, for a triangulation \mathcal{T} we set $h := \max_{\tau \in \mathcal{T}} h_\tau$. We introduce the notions of geometrically conforming, shape-regular, and quasi-uniform triangulations following TOSELLI AND WIDLUND [184, Appendix B].

Definition 1.26. *A triangulation \mathcal{T} of Ω or $\partial\Omega$ is called geometrically conforming (in brief: conforming) if the intersection of the closure of two different elements is either empty, a vertex, an edge, or a face that is common to both elements.*

A family of triangulations \mathcal{T}^h of Ω or $\partial\Omega$ is called shape-regular if there exists a constant $C > 0$ independent of h such that

$$h_\tau \leq C \rho_\tau \quad \forall \tau \in \mathcal{T}^h.$$

A family of triangulations \mathcal{T}^h of Ω or $\partial\Omega$ is called quasi-uniform if it is shape-regular and if there exists a constant $c > 0$ independent of h such that

$$h_\tau \geq ch \quad \forall \tau \in \mathcal{T}^h.$$

Notation. For a given triangulation $\mathcal{T}^h(\Omega)$, let Ω^h denote the set of nodes (vertices) of the triangulation, including the nodes on the boundary $\partial\Omega$, and let $\partial\Omega^h$ denote the set of nodes of the triangulation that lie on $\partial\Omega$. Finally, we define the set of Dirichlet nodes $\Gamma_D^h := \partial\Omega^h \cap \Gamma_D$ (note that Γ_D is relatively closed). A typical node will be denoted by x^h .

1.5.2 Finite element method

In this subsection we briefly show the concept of the finite element method. For more details we refer the reader, e. g., to BRAESS [16], BRENNER AND SCOTT [26], CIARLET [35], and ZULEHNER [196].

1.5.2.1 Formulation

In this work we consider mainly linear finite elements. For a given family of triangulations $\mathcal{T}^h(\Omega)$ of Ω , we define the family of spaces

$$V^h(\Omega) := \{v \in \mathcal{C}(\bar{\Omega}) : v|_{\tau} \in \mathcal{P}_1(\tau) \quad \forall \tau \in \mathcal{T}^h(\Omega)\}, \quad (1.69)$$

where \mathcal{P}_1 is the space of affine linear polynomials. It can be shown that $V^h(\Omega) \subset H^1(\Omega)$. For each node $x^h \in \Omega^h$, define the *nodal finite element basis function* $\varphi_{x^h} \in V^h(\Omega)$ by

$$\varphi_{x^h}(y^h) = \begin{cases} 1 & \text{for } y^h = x^h, \\ 0 & \text{else.} \end{cases} \quad (1.70)$$

Then, $\{\varphi_{x^h}\}_{x^h \in \Omega^h}$ is a basis for V^h .

The mixed boundary value problem Let Γ_D be a relatively closed part of $\partial\Omega$ with positive surface measure and set $\Gamma_N = \partial\Omega \setminus \Gamma_D$. Consider the variational formulation of the potential equation with homogeneous boundary conditions on Γ_D . For simplicity, we choose the coefficient in the PDE equal to one although everything works for more general coefficients. The infinite-dimensional problem reads: Find $u \in H_D^1(\Omega)$ such that

$$a(u, v) = \langle F, v \rangle \quad \forall v \in H_D^1(\Omega), \quad (1.71)$$

where $H_D^1(\Omega) = \{v \in H^1(\Omega) : v|_{\Gamma_D} = 0\}$ and

$$a(u, v) = \int_{\Omega} \nabla u \cdot \nabla v \, dx, \quad \langle F, v \rangle = \int_{\Omega} f v \, dx + \int_{\Gamma_N} g_N v \, ds.$$

The corresponding Galerkin equation reads: Find $u_h \in V_D^h(\Omega)$ such that

$$a(u_h, v_h) = \langle F, v_h \rangle \quad \forall v_h \in V_D^h(\Omega), \quad (1.72)$$

where $V_D^h(\Omega) := V^h(\Omega) \cap H_D^1(\Omega)$. We introduce a suitable enumeration of the nodes, $\Omega^h = \{x_1, \dots, x_{n_N}\}$, such that the nodes on Γ_D are given by $\{x_{n_F+1}, \dots, x_{n_N}\}$. Consequently, $\{\varphi_1, \dots, \varphi_{n_F}\}$ is a basis for $V_D^h(\Omega)$. Furthermore, we define the *stiffness matrix* \mathbf{K} and the *load vector* \mathbf{f} by

$$\mathbf{K}_{ij} = a(\varphi_{x_j}, \varphi_{x_i}), \quad \mathbf{f}_i = \langle F, \varphi_{x_i} \rangle \quad \text{for } i, j = 1, \dots, n_F. \quad (1.73)$$

We can transform equation (1.72) to the following system of linear equations: Find $\mathbf{u} \in \mathbb{R}^{n_F}$ such that

$$\mathbf{K} \mathbf{u} = \mathbf{f}. \quad (1.74)$$

Due to the fact that the basis functions have local support and due to the structure of the bilinear form $a(\cdot, \cdot)$, the stiffness matrix is *sparse*, i. e., there are only a few non-zero entries per row. The solution u_h is finally given by

$$u_h := \sum_{i=1}^{n_F} \mathbf{u}_i \varphi_{x_i}.$$

Note that the homogeneous Dirichlet boundary conditions are fulfilled automatically because the basis functions corresponding to the Dirichlet nodes are excluded. The entries \mathbf{u}_i of the coefficient vector \mathbf{u} are associated to the nodes x_i and called degrees of freedom (DOFs). The map between u_h and \mathbf{u} is one-to-one and called *Ritz isomorphism*.

Later on in this chapter we will make use of the *full stiffness matrix* $\bar{\mathbf{K}}$ and the *full load vector* $\bar{\mathbf{f}}$ defined by

$$\bar{\mathbf{K}}_{ij} = a(\varphi_{x_j}, \varphi_{x_i}), \quad \bar{\mathbf{f}}_i = \langle F, \varphi_{x_i} \rangle \quad \text{for } i, j = 1, \dots, n_N, \quad (1.75)$$

i. e., incorporating the complete set of nodes and basis functions. When the context allows we may drop the bars.

The pure Neumann problem If $\Gamma_D = \emptyset$, i. e., $\Gamma_N = \partial\Omega$, the continuous problem is not uniquely solvable. Testing the variational equation with the constant function $\mathbf{1}_\Omega$ we obtain the *compatibility condition*

$$\int_{\Omega} f \, dx + \int_{\partial\Omega} g_N \, ds = 0. \quad (1.76)$$

Let us assume that the data (f, g_N) fulfills this condition, then the solution is unique up to an additive constant. A particular solution u can be found by applying some *gauge*, e. g.,

$$\int_{\Omega} u \, dx = 0, \quad (1.77)$$

or alternatively, $\int_{\partial\Omega} u \, ds = 0$. Using the regularized bilinear form

$$\tilde{a}(u, v) := a(u, v) + \beta \int_{\Omega} u \, dx \int_{\Omega} v \, dx, \quad (1.78)$$

for some regularization parameter $\beta > 0$, the Galerkin equation $\tilde{a}(u, v) = \langle F, v \rangle$ is always solvable, and if the data (f, g_N) fulfills the compatibility condition, the solution fulfills the gauge condition (1.77).

The same concept carries over to the discrete setting. The stiffness matrix \mathbf{K} (which coincides with the full stiffness matrix) has a kernel of dimension 1 and is spanned by the vector $\mathbf{1}$ of ones. To obtain a unique solution we can use the modified stiffness matrix $\tilde{\mathbf{K}}$ corresponding to the bilinear form $\tilde{a}(\cdot, \cdot)$. However, this might affect the sparsity of $\tilde{\mathbf{K}}$. Alternatively, we can use any discrete regularization,

$$\tilde{a}(u_h, v_h) := a(u_h, v_h) + \beta_h (u_h, \mathbf{1}_\Omega)_{\mathcal{R}_h} (v_h, \mathbf{1}_\Omega)_{\mathcal{R}_h} \quad \forall u_h, v_h \in V^h, \quad (1.79)$$

for some $\beta_h > 0$ where $(\cdot, \cdot)_{\mathcal{R}_h} : V^h \times V^h \rightarrow \mathbb{R}$ needs to be SPD only on $\text{span}\{\mathbf{1}_\Omega\} \subset V^h(\Omega)$. For instance we can use

$$(u_h, v_h)_{\mathcal{R}_h} := u_h(y^h) u_h(y^h), \quad \text{or} \quad (u_h, v_h)_{\mathcal{R}_h} := \int_L u_h ds \int_L v_h ds, \quad (1.80)$$

for a vertex $y^h \in \Omega^h$ or a curve $L \subset \bar{\Omega}_i$. In three dimensions, vertex regularizations might cause numerical stability problems. No matter which regularization we take, $\tilde{\mathbf{K}}^{-1}$ is a pseudo-inverse of \mathbf{K} .

1.5.2.2 Properties of the stiffness matrix

Let us consider again the mixed boundary value problem with a non-trivial Dirichlet boundary Γ_D . With the Ritz isomorphism $u_h \leftrightarrow \mathbf{u}$, $v_h \leftrightarrow \mathbf{v}$ we have that

$$a(u_h, v_h) = (\mathbf{K} \mathbf{u}, \mathbf{v}) \quad \forall u_h, v_h \in V_D^h(\Omega),$$

from which we that properties of the bilinear form $a(\cdot, \cdot)$ (such as symmetry, SPD, etc.) carry over to the stiffness matrix \mathbf{K} . It can be shown that for a quasi-uniform triangulation $\mathcal{T}^h(\Omega)$, the spectral condition number $\kappa(\mathbf{K})$ of the stiffness matrix fulfills

$$\kappa(\mathbf{K}) = \mathcal{O}(h^{-2}) \quad \text{as } h \rightarrow 0, \quad (1.81)$$

i. e., it grows with the number of DOFs. The bound is sharp in general; see, e. g., BRENNER AND SCOTT [26].

1.5.2.3 Solvers for finite element systems

In order to solve a system of the form

$$\mathbf{K} \mathbf{u} = \mathbf{f},$$

with a sparse stiffness matrix $\mathbf{K} \in \mathbb{R}^{n \times n}$, where n is the number of DOFs, we can use *direct* and *iterative* solvers.

Direct solvers It is known that the complexity of Gauss' method, the LU -factorization or the Cholesky-factorization of a dense matrix is $\mathcal{O}(n^3)$ as $n \rightarrow \infty$. For sparse matrices pivoting and reordering techniques can be used to obtain a matrix with small bandwidth, which enhances the complexity. The optimal complexity of $\mathcal{O}(n)$ can only be obtained for one-dimensional problems or special cases in higher dimensions. However, there exist sparse direct solvers, such as PARDISO [37], see also SCHENK AND GÄRTNER [166, 167], with complexities like $\mathcal{O}(n^{3/2})$ in three dimensions, and $\mathcal{O}(n \log^\alpha(n))$ in two dimensions. Other solvers worth mentioning are MUMPS (<http://graal.ens-lyon.fr/MUMPS>), UMFPACK (<http://www.cise.ufl.edu/research/sparse/umfpack/>), and SUPERLU (<http://www.cs.berkeley.edu/~demmel/SuperLU.html>).

Iterative solvers The most general iterative method is *Richardson's* method, where a successive application of the matrix (which can be performed in optimal complexity if the matrix is sparse) leads to an approximate solution of the system. The number of steps in order to obtain a certain precision is strongly depending on the spectral condition number κ of \mathbf{K} . For SPD systems, the *conjugate gradient* (CG) method accelerates the convergence: After k steps the error in the energy norm (induced by \mathbf{K}) decays at least by a factor

$$2 \left(\frac{\sqrt{\kappa} - 1}{\sqrt{\kappa} + 1} \right)^k,$$

In the non-symmetric case, methods with similar properties exist, named *Krylov methods*. However, we have seen that $\kappa(\mathbf{K}) \simeq h^{-2} \simeq n^{2/d}$ for a quasi-uniform mesh. In order to obtain better convergence we can seek for a preconditioner \mathbf{C} whose inverse can be applied in optimal complexity such that $\kappa(\mathbf{C}^{-1} \mathbf{K})$ is much smaller than $\kappa(\mathbf{K})$, ideally independent of N and h , or at least only weakly depending on N or h . We can then apply the same method to the preconditioned system

$$\mathbf{C}^{-1} \mathbf{K} \mathbf{u} = \mathbf{C}^{-1} \mathbf{f}.$$

For the CG method, the preconditioner \mathbf{C} must be SPD as well, then the method is still well-defined and can be seen as a CG method working with the inner product induced by the preconditioner. In that case we speak of the *preconditioned conjugate gradient* (PCG) method.

Solving the pure Neumann problem As discussed above, the stiffness matrix corresponding to the pure Neumann problem is not regular. However, many direct solvers are capable of factorizing such positive semi-definite matrices correctly. Alternatively, one can use one of the suggested regularizations, but taking care of the sparsity and the numerical stability. Using iterative solvers, one can make use of the fact that the application of any of the suggested regularizations $\tilde{\mathbf{K}}$ can be performed in optimal complexity.

1.5.2.4 The approximation error

The approximation error of the space $V^h(\Omega)$ is given as follows.

Lemma 1.27. *Let $\mathcal{T}^h(\Omega)$ be a geometrically conforming quasi-uniform triangulation, and assume that $u \in H^m(\Omega)$ for some $m \leq 2$. Then there exists a constant $C > 0$ depending on $\mathcal{T}^h(\Omega)$ such that*

$$\inf_{v^h \in V^h(\Omega)} \|u - v^h\|_{H^k(\Omega)} \leq C h^{m-k} |u|_{H^m(\Omega)} \quad \forall k \leq \min(m, 1).$$

The inequality also holds for real Sobolev indices m and k .

Proof. The proof uses a special interpolator, an affine map to a reference simplex, and the Bramble-Hilbert lemma, cf. BRENNER AND SCOTT [26, Sect. 4.4]. \square

1.5.2.5 The Scott-Zhang quasi-interpolation operator

The following lemma has been shown SCOTT AND ZHANG [170], see also BRENNER AND SCOTT [26].

Lemma 1.28. *For a family $\mathcal{T}^h(\Omega)$ of conforming and shape-regular triangulations of Ω , there exists a corresponding family of quasi-interpolation operators $\Pi^h : H^1(\Omega) \rightarrow V^h(\Omega)$ and a constant $C_{SZ} > 0$ depending only on the shape regularity constant of $\mathcal{T}^h(\Omega)$, such that*

$$\begin{aligned} (\Pi^h u_h)|_{\partial\Omega} &= u_h & \forall u_h \in V^h(\partial\Omega), \\ |\Pi^h u|_{H^1(\Omega)} &\leq C_{SZ} |u|_{H^1(\Omega)} & \forall u \in H^1(\Omega), \\ \|\Pi^h u\|_{L^2(\Omega)} &\leq C_{SZ} \|u\|_{L^2(\Omega)} & \forall u \in H^1(\Omega), \\ |u - \Pi^h u|_{H^\ell(\omega_\tau)} &\leq C_{SZ} h^{k-\ell} |u|_{H^k(\omega_\tau)} & \forall \tau \in \mathcal{T}^h(\Omega), \forall u \in H^k(\Omega), \forall 0 \leq \ell \leq k \leq 2, \end{aligned}$$

where ω_τ is the union of elements touching τ . The last estimate holds true even for real Sobolev indices k and ℓ .

Remark 1.29. The construction is somehow related to the quasi-interpolation operator introduced by CLÉMENT [36], which ensures the H^1 -continuity by averaging over volume patches. Scott and Zhang use a special basis which is dual to the nodal basis with respect to the L^2 -product on elements for nodes in the interior, and on element faces for nodes on the boundary.

Corollary 1.30 (Existence of a bounded discrete extension). *For a family $\mathcal{T}^h(\Omega)$ of conforming and shape-regular triangulations of Ω , there exists a corresponding family of bounded linear extension operators $\mathcal{E}^h : V^h(\partial\Omega) \rightarrow V^h(\Omega)$ such that*

$$|\mathcal{E}^h v_h|_{H^1(\Omega)}^2 \leq C_{SZ}^2 \langle S^{\text{int}} v_h, v_h \rangle \quad \forall v_h \in V^h(\partial\Omega).$$

with the constant $C_{SZ} > 0$ from Lemma 1.28

Proof. Let $\tilde{v} \in H^1(\Omega)$ be the harmonic extension of v_h such that $\langle S^{\text{int}} v_h, v_h \rangle = |\tilde{v}|_{H^1(\Omega)}^2$. Setting $\mathcal{E}^h v_h := \Pi^h \tilde{v}$ we obtain the desired statement. \square

Remark 1.31. An alternative proof of Corollary 1.30 is the following. The discrete trace theorem (cf. [184, Lemma 4.6]) states that for each function $v_h \in V^h(\partial\Omega)$ there exists a function $\tilde{v}_h \in V^h(\Omega)$

$$|\tilde{v}_h|_{H^1(\Omega_k)}^2 \leq C_t |v_h|_{H^{1/2}(\partial\Omega)}^2,$$

for a constant $C_t > 0$ depending only on the shape of Ω and the shape regularity constant of $\mathcal{T}^h(\Omega)$. The desired statement follows immediately since the norm induced by S^{int} and the $|\cdot|_{H^{1/2}(\partial\Omega)}$ -norm are equivalent. However, the constant in Corollary 1.30 is independent of the shape of Ω as well, which can be very irregular.

1.5.2.6 FEM approximation of the Steklov-Poincaré operator and the Newton potential

The Schur complement system Let \mathbf{K} and \mathbf{f} denote the full stiffness matrix and load vector corresponding to problem (1.72). We reorder and partition the stiffness matrix corresponding to interior DOFs (subscript I) and boundary DOFs (subscript B). We split the

load vector \mathbf{f} into two parts $\bar{\mathbf{f}}$ and \mathbf{t} . The part \mathbf{t} corresponds to the linear form $\int_{\partial\Omega} t \cdot ds$, where $t = \frac{\partial u}{\partial n}$ is the prescribed normal flux. The part $\bar{\mathbf{f}}$ corresponds to the linear form $\int_{\Omega} f \cdot dx$; we partition it into blocks $\bar{\mathbf{f}}_I$ and $\bar{\mathbf{f}}_B$ similarly to the stiffness matrix. The discrete FE equation reads

$$\begin{pmatrix} \mathbf{K}_{BB} & \mathbf{K}_{BI} \\ \mathbf{K}_{IB} & \mathbf{K}_{II} \end{pmatrix} \begin{pmatrix} \mathbf{u}_B \\ \mathbf{u}_I \end{pmatrix} = \begin{pmatrix} \bar{\mathbf{f}}_B + \mathbf{t} \\ \bar{\mathbf{f}}_I \end{pmatrix}.$$

We now eliminate the interior DOFs \mathbf{u}_I to obtain the Schur complement system

$$\mathbf{S} \mathbf{u}_B = \mathbf{N} \bar{\mathbf{f}} + \mathbf{t},$$

with

$$\mathbf{S} := \mathbf{K}_{BB} - \mathbf{K}_{BI}(\mathbf{K}_{II})^{-1}\mathbf{K}_{IB}, \quad (1.82)$$

$$\mathbf{N} := \left[\mathbf{I}_B \mid -\mathbf{K}_{BI}(\mathbf{K}_{II})^{-1} \right], \quad \mathbf{N} \bar{\mathbf{f}} = \bar{\mathbf{f}}_B - \mathbf{K}_{BI}(\mathbf{K}_{II})^{-1}\bar{\mathbf{f}}_I. \quad (1.83)$$

where \mathbf{I}_B is the identity with respect to the boundary DOFs. We can read off the discrete Dirichlet to Neumann map, $\mathbf{t} = \mathbf{S} \mathbf{u}_B - \mathbf{N} \bar{\mathbf{f}}$. Setting $\bar{\mathbf{f}} = 0$, which corresponds to the homogeneous problem, we find that $\mathbf{t} = \mathbf{S} \mathbf{u}_B$. For $\mathbf{u}_B = 0$, which corresponds to the homogeneous Dirichlet problem, we find that $\mathbf{t} = -\mathbf{N} \bar{\mathbf{f}}$.

A functional background to the discrete Schur complement system Due to Theorem 1.6, see also STEINBACH [174], we have

$$\langle S^{\text{int}} g, w \rangle = a(u_0 + \mathcal{E}g, \mathcal{E}w) \quad \forall g, w \in H^{1/2}(\partial\Omega), \quad (1.84)$$

where the operator \mathcal{E} is an arbitrary bounded extension operator, e. g., the one from Theorem 1.4, and the function $u_0 \in H_0^1(\Omega)$ is the unique solution of

$$a(u_0 + \mathcal{E}g, v) = 0 \quad \forall v \in H_0^1(\Omega). \quad (1.85)$$

Note, that this is also an alternative definition which generalizes the interior Steklov-Poincaré operator (i. e., the Neumann trace operator) for the case of more general coefficients. We define the operator

$$\begin{aligned} S_{\text{FEM}}^{\text{int}} &: H^{1/2}(\partial\Omega) \rightarrow H^{-1/2}(\partial\Omega), \\ \langle S_{\text{FEM}}^{\text{int}} g, w \rangle &= a(u_{0,h} + \mathcal{E}^h g, \mathcal{E}^h w) \quad \forall w \in H^{1/2}(\partial\Omega), \end{aligned} \quad (1.86)$$

where $\mathcal{E}^h := \Pi^h \mathcal{E}$ with the Scott-Zhang quasi-interpolation operator Π^h , and the function $u_{0,h} \in V_0^h(\Omega) := V^h(\Omega) \cap H_0^1(\Omega)$ is the unique solution of

$$a(u_{0,h} + \mathcal{E}^h g, v_h) = 0 \quad \forall v_h \in V_0^h(\Omega). \quad (1.87)$$

Apparently, the operator $S_{\text{FEM}}^{\text{int}}$ is symmetric and positive semidefinite. Combining the proof of STEINBACH [174, Theorem 3.5] with the approximation properties of the Scott-Zhang quasi-interpolation operator, one can show that the error $(S^{\text{int}} - S_{\text{FEM}}^{\text{int}})g$ is controlled by the approximation properties of the trial space $V^h(\Omega)$ and the Scott-Zhang quasi-interpolation operator Π^h for g sufficiently smooth. A careful investigation reveals that the Galerkin projection of $S_{\text{FEM}}^{\text{int}}$ to the space $V^h(\partial\Omega)$ is represented by the Schur complement matrix \mathbf{S}

from (1.82). Note that in general, since the approximation $S_{\text{FEM}}^{\text{int}}$ extends to Ω by discrete functions whereas S^{int} extends by H^1 -functions,

$$\langle S_{\text{FEM}}^{\text{int}} v_h, w_h \rangle \neq \langle S^{\text{int}} v_h, w_h \rangle \quad \text{for } v_h, w_h \in V^h(\partial\Omega).$$

With similar means one can show that the operator

$$N_{\text{FEM}} : V^h(\Omega)^* \rightarrow V^h(\partial\Omega)^* \quad (1.88)$$

corresponding to \mathbf{N} is a suitable approximation of the exact Newton potential N . For details see STEINBACH [174].

Minimization property of the Schur complement

Lemma 1.32. *The operator $S_{\text{FEM}}^{\text{int}}$ admits the minimizing property*

$$\langle S_{\text{FEM}}^{\text{int}} v_h, v_h \rangle = \min_{\substack{\tilde{v}_h \in V^h(\Omega) \\ \tilde{v}_h|_{\partial\Omega} = v_h}} a(\tilde{v}_h, \tilde{v}_h) \quad \forall v_h \in V^h(\partial\Omega). \quad (1.89)$$

Proof. Follows from the definition of \mathbf{S} and \mathbf{K} , and by simple linear algebra. \square

1.5.3 Boundary element method

The Galerkin boundary element method is a special Galerkin finite element method applied to boundary integral equations, cf. HSIAO AND WENDLAND [88]. For a comprehensive introduction we refer to the monographs by RJASANOW AND STEINBACH [158], SAUTER AND SCHWAB [164], and STEINBACH [175].

1.5.3.1 BEM approximation of S^{int} , S^{ext}

Recall our setting: Ω is a bounded domain with Lipschitz boundary Γ , and $\Omega^{\text{ext}} := \mathbb{R}^d \setminus \overline{\Omega}$. In order to get symmetric approximations of the Steklov-Poincaré operators S^{int} and S^{ext} using discretized boundary integral equations, we consider a triangulation $\mathcal{T}^h(\Gamma)$ of Γ . The leading role will be played by Calderón's system (1.53). We approximate the Dirichlet trace $\gamma_0^{\text{int}} u$ by a piecewise linear function $u_h \in V^h(\Gamma)$. The Neumann trace $\gamma_1^{\text{int}} u$ has two different kinds of approximations on which we will comment later on. One the one hand, we can approximate γ_1^{int} as a functional $t_h \in V^h(\Gamma)^* \subset H^{-1/2}(\Gamma)$, on the other hand, we can approximate it by a piecewise constant function $w_h \in Z^h \subset H^{-1/2}(\Gamma)$, where

$$Z^h(\Gamma) := \{z \in H^{-1/2}(\Gamma) : z|_{\tau} \in \mathcal{P}_0 \quad \forall \tau \in \mathcal{T}^h(\Gamma)\}. \quad (1.90)$$

Introducing a numbering of the nodes x_1, \dots, x_{n_N} in Γ^h , and the elements $\tau_1, \dots, \tau_{n_T}$ in $\mathcal{T}^h(\Gamma)$ we obtain bases for the two approximation spaces:

$$V^h(\Gamma) = \text{span}\{\varphi_i\}_{i=1}^{n_N}, \quad Z^h(\Gamma) = \text{span}\{\psi_k\}_{k=1}^{n_T}, \quad (1.91)$$

where φ_i is the nodal basis function being 1 at the i -th node and zero elsewhere, and ψ_k is 1 on the k -th element and zero elsewhere.

From (1.58) can conclude that

$$\begin{aligned} S^{\text{int}} g &= Dg + (\tfrac{1}{2}I + K^\top)w^{\text{int}}, \\ S^{\text{ext}} g &= Dg + (\tfrac{1}{2}I - K^\top)w^{\text{ext}}, \end{aligned} \quad (1.92)$$

where

$$\begin{aligned} \langle V w^{\text{int}}, z \rangle &= \langle (\tfrac{1}{2}I + K)g, z \rangle \quad \forall z \in H^{-1/2}(\Gamma), \\ \langle V w^{\text{ext}}, z \rangle &= \langle (\tfrac{1}{2}I - K)g, z \rangle \quad \forall z \in H^{-1/2}(\Gamma). \end{aligned} \quad (1.93)$$

The Galerkin projection of (1.93) to the space $Z^h(\Gamma)$ reads: Find $w_h^{\text{int}}, w_h^{\text{ext}} \in Z^h(\Gamma)$ such that

$$\begin{aligned} \langle V w_h^{\text{int}}, z_h \rangle &= \langle (\tfrac{1}{2}I + K)g, z_h \rangle \quad \forall z_h \in Z^h(\Gamma), \\ \langle V w_h^{\text{ext}}, z_h \rangle &= \langle (\tfrac{1}{2}I - K)g, z_h \rangle \quad \forall z_h \in Z^h(\Gamma). \end{aligned} \quad (1.94)$$

Replacing $w^{\text{int}}, w^{\text{ext}}$ in (1.92) by $w_h^{\text{int}}, w_h^{\text{ext}}$, respectively, we obtain the approximations $S_{\text{BEM}}^{\text{int}}, S_{\text{BEM}}^{\text{ext}} : H^{1/2}(\Gamma) \rightarrow H^{-1/2}(\Gamma)$ defined by

$$\begin{aligned} S_{\text{BEM}}^{\text{int}} g &= Dg + (\tfrac{1}{2}I + K^\top)w_h^{\text{int}}, \\ S_{\text{BEM}}^{\text{ext}} g &= Dg + (\tfrac{1}{2}I - K^\top)w_h^{\text{ext}}. \end{aligned} \quad (1.95)$$

According to STEINBACH [174] we have the quasi-optimal error estimate

$$\|(S^{\text{int}} - S_{\text{BEM}}^{\text{int}})g\|_{H^{-1/2}(\Gamma)} \leq c \inf_{z_h \in Z^h(\Gamma)} \|S^{\text{int}}g - z_h\|_{H^{-1/2}(\Gamma)} \quad \forall g \in H^{1/2}(\Gamma), \quad (1.96)$$

and the analogous estimate for S^{ext} . It states that the error is controlled by the approximation property of the trial space $Z^h(\Gamma)$. The Galerkin projections of $S_{\text{BEM}}^{\text{int}}, S_{\text{BEM}}^{\text{ext}}$ to the space $V^h(\Gamma)$ can be represented in matrix form by

$$\begin{aligned} \mathbf{S}^{\text{int}} &= \mathbf{D} + (\tfrac{1}{2}\mathbf{M}^\top + \mathbf{K}^\top)\mathbf{V}^{-1}(\tfrac{1}{2}\mathbf{M} + \mathbf{K}), \\ \mathbf{S}^{\text{ext}} &= \mathbf{D} + (\tfrac{1}{2}\mathbf{M}^\top - \mathbf{K}^\top)\mathbf{V}^{-1}(\tfrac{1}{2}\mathbf{M} - \mathbf{K}), \end{aligned} \quad (1.97)$$

with the boundary element matrices

$$\mathbf{D}_{ij} = \langle \varphi_j, D \varphi_i \rangle, \quad \mathbf{K}_{ik} = \langle \psi_k, K \varphi_i \rangle, \quad (1.98)$$

$$\mathbf{V}_{kl} = \langle \psi_l, V \psi_k \rangle, \quad \mathbf{M}_{ik} = \langle \psi_k, \varphi_i \rangle, \quad (1.99)$$

for $i, j = 1, \dots, n_N$, and $k, l = 1, \dots, n_T$. The approximations $S_{\text{BEM}}^{\text{int}}$ and $S_{\text{BEM}}^{\text{ext}}$ are self-adjoint and semi-elliptic, respectively, elliptic, as the original operators $S^{\text{int/ext}}$. In case of exact arithmetics we preserve the kernel of S^{int} ,

$$\ker S_{\text{BEM}}^{\text{int}} = \text{span}\{\mathbf{1}_\Gamma\}. \quad (1.100)$$

1.5.3.2 Data-sparse approximation and solvers for BEM systems

Except for the mass matrix \mathbf{M} , which is apparently sparse, all the boundary element matrices in (1.98) are dense (despite the fact that the basis functions have local support). This is because of the non-local operators involving the fundamental solution; for assembling the matrices, double integrals have to be evaluated. However, the fundamental solution $U^*(x, y)$ decays exponentially when moving away from the singularity at $x = y$.

The notion *fast boundary element methods* embraces techniques to design methods using this phenomenon in order to realize a fast (i. e., quasi-optimal) application of (approximate) BEM matrices, or even achieve data-sparse approximation of BEM matrices (i. e., quasi-optimal memory requirements). Only with fast BEM, quasi-optimal solvers of BEM systems become possible. For an overview we refer to STEINBACH [175] and RJASANOW AND STEINBACH [158] and the references therein. We mention the fast multipole method (ROKHLIN [159], CHENG, GREENGARD, AND ROKHLIN [33]), the panel clustering method (HACKBUSCH AND NOWAK [82]), wavelet approximations (SCHNEIDER [168]), and the adaptive cross approximation (ACA) (BEBENDORF [6]). The computational complexities and storage demands are typically $\mathcal{O}(N \log N)$ where N is the number of unknowns on the boundary.

The data structure for a data-sparse representation is called *hierarchical matrix* or \mathcal{H} -*matrix* using a hierarchy of low-rank approximations, where the maximum rank is bounded. The class of such matrices induces the so-called \mathcal{H} -*arithmetic*, cf. HACKBUSCH [79], HACKBUSCH AND KHOROMSKIJ [81], see also the recent monograph by BEBENDORF [8]. Within this arithmetic, one can compute an \mathcal{H} -*LU* factorization, cf. BEBENDORF [7], i. e., an approximate factorization of an \mathcal{H} -matrix, where the two factors are again \mathcal{H} -matrices. The factorization can also be done in a $\mathcal{O}(N \log N)$ -complexity, although it additionally depends on the maximum rank. We mention the two software packages AHMED (see <http://www.math.uni-leipzig.de/~bebendorf/AHMED.html> and BEBENDORF [8]), and Hlib (see <http://www.hlib.org> and BÖRM, GRASEDYCK, AND HACKBUSCH [14]).

1.5.3.3 BEM approximation of the Newton potential

A suitable BEM approximation of the Newton potential N can be found in STEINBACH [174]. In some cases volume triangulations can even be avoided; see, e. g., BERTOGLIO, HACKBUSCH, AND KHOROMSKIJ [10], KHOROMSKIJ [97, 98], OF, STEINBACH, AND URTHALER [140], and URTHALER [185]. In this work, however, we will use the boundary element method only on subdomains with vanishing sources.

1.6 Spectral estimates for approximate Steklov-Poincaré operators

Lemma 1.33. *The following spectral equivalence relations between the exact and approximated Steklov-Poincaré operators hold.*

$$\begin{aligned}
\langle S^{\text{int}} v_h, v_h \rangle &\leq \langle S_{\text{FEM}}^{\text{int}} v_h, v_h \rangle \leq C_{SZ}^2 \langle S^{\text{int}} v_h, v_h \rangle && \forall v_h \in V^h(\Gamma) \\
\frac{c_0}{c_K} \langle S^{\text{int}} v, v \rangle &\leq \langle S_{\text{BEM}}^{\text{int}} v, v \rangle \leq \langle S^{\text{int}} v, v \rangle && \forall v \in H^{1/2}(\Gamma) \\
&\langle S_{\text{BEM}}^{\text{ext}} v, v \rangle \leq \langle S^{\text{ext}} v, v \rangle && \forall v \in H^{1/2}(\Gamma) \\
\frac{c_0}{c_K} \langle S^{\text{ext}} v, v \rangle &\leq \langle S_{\text{BEM}}^{\text{ext}} v, v \rangle && \forall v \in H_*^{1/2}(\Gamma) \\
\frac{c_0}{c_K} \langle S^{\text{int}} v, v \rangle &\leq \langle S_{\text{BEM}}^{\text{ext}} v, v \rangle && \forall v \in H^{1/2}(\Gamma)
\end{aligned} \tag{1.101}$$

Additionally,

$$\begin{aligned}
\langle S^{\text{int}} v, v \rangle + \frac{1}{\text{diam } \Gamma} \|u\|_{L_2(\Gamma)}^2 &\leq C_{\text{ext}} \langle S_{\text{BEM}}^{\text{ext}} v, v \rangle && \forall v \in H^{1/2}(\Gamma), \\
\langle S^{\text{ext}} v, v \rangle &\leq C'_{\text{ext}} \langle S_{\text{BEM}}^{\text{ext}} v, v \rangle && \forall v \in H^{1/2}(\Gamma).
\end{aligned} \tag{1.102}$$

The constants c_0 , c_K , and C_{SZ} depend only on the shape of Γ and the shape regularity of the triangulation $\mathcal{T}^h(\Omega)$. In three dimensions, C_{ext} and C'_{ext} depend as well only on the shape of Γ .

Remark 1.34. In two dimensions, the constants C_{ext} and C'_{ext} additionally depend logarithmically on the diameter of Γ . Since we have to scale the domain anyway, we can fix the diameter, e. g., to $\text{diam } \Gamma = 1/2$.

Proof of Lemma 1.33. By (1.60) and (1.89), it becomes clear that

$$\langle S^{\text{int}} v_h, v_h \rangle \leq \langle S_{\text{FEM}}^{\text{int}} v_h, v_h \rangle \quad \forall v_h \in V^h(\Gamma).$$

The other direction follows from Lemma 1.32 and Lemma 1.30:

$$\langle S_{\text{FEM}}^{\text{int}} v_h, v_h \rangle \leq |\mathcal{E}^h v_h|_{H^1(\Omega)}^2 \leq C_{SZ}^2 \langle S^{\text{int}} v_h, v_h \rangle \quad \forall v_h \in V^h(\Gamma). \tag{1.103}$$

The following proof of the estimates concerning $S_{\text{BEM}}^{\text{int}}$, $S_{\text{BEM}}^{\text{ext}}$ follows the line in STEINBACH [174]. For the boundary element approximations $S_{\text{BEM}}^{\text{int}}$ of the continuous Steklov-Poincaré operator we can apply Lemma 1.19 choosing $Z^h \subset H^{-1/2}(\Gamma)$ as approximation space, $\langle V \cdot, \cdot \rangle$ as bilinear form, and $\langle (\frac{1}{2}I + K)v, \cdot \rangle$ as linear form to obtain that

$$\langle V w_h^{\text{int}}, w_h^{\text{int}} \rangle \leq \langle V w^{\text{int}}, w^{\text{int}} \rangle, \tag{1.104}$$

with the functions w^{int} , w_h^{int} from (1.93) and (1.94). Using the identities

$$\begin{aligned}
\langle S^{\text{int}} v, v \rangle &= \langle D v, v \rangle + \langle V w^{\text{int}}, w^{\text{int}} \rangle, \\
\langle S_{\text{BEM}}^{\text{int}} v, v \rangle &= \langle D v, v \rangle + \langle V w_h^{\text{int}}, w_h^{\text{int}} \rangle,
\end{aligned} \tag{1.105}$$

which follow from (1.57), the adjoint relation between K and K^\top , and the analogous arguments for the exterior operators S^{ext} and $S_{\text{BEM}}^{\text{ext}}$, we finally obtain

$$\langle S_{\text{BEM}}^{\text{int/ext}} v, v \rangle \leq \langle S^{\text{int/ext}} v, v \rangle \quad \forall v \in H^{1/2}(\Gamma).$$

For the opposite direction, we first obtain for $\tilde{v} \in H_*^{1/2}(\Gamma)$,

$$\begin{aligned} \langle S_{\text{BEM}}^{\text{int/ext}} \tilde{v}, \tilde{v} \rangle &= \langle D \tilde{v}, \tilde{v} \rangle + \langle V w_h, w_h \rangle \\ &\geq \langle D \tilde{v}, \tilde{v} \rangle \geq c_0 \langle V^{-1} \tilde{v}, \tilde{v} \rangle \geq \frac{c_0}{c_K} \langle S^{\text{int/ext}} \tilde{v}, \tilde{v} \rangle, \end{aligned} \quad (1.106)$$

where we have used the ellipticity of V , Lemma 1.23(v) and Lemma 1.25(i). Secondly, using the V^{-1} -orthogonal splitting $v = v_0 \mathbf{1}_\Gamma + \tilde{v}$ with $\tilde{v} \in H_*^{1/2}(\Gamma)$ and $v_0 \in \mathbb{R}$, see Lemma 1.25(iii), we get

$$\langle S_{\text{BEM}}^{\text{int/ext}} v, v \rangle \geq \langle D v, v \rangle = \langle D \tilde{v}, \tilde{v} \rangle \geq \frac{c_0}{c_K} \langle S^{\text{int}} \tilde{v}, \tilde{v} \rangle = \frac{c_0}{c_K} \langle S^{\text{int}} v, v \rangle.$$

This finishes the proof of the estimates (1.101).

Now, we prove the two estimates (1.102) of the $S_{\text{BEM}}^{\text{ext}}$ energy form from below by the S^{ext} form and a regularized S^{int} form on the whole space $H^{1/2}(\Gamma)$. In order to achieve this goal, we recall once again that

$$\langle S_{\text{BEM}}^{\text{ext}} v, v \rangle = \langle D v, v \rangle + \langle V w_h, w_h \rangle$$

with w_h defined by (1.94). We choose $w_0 \in \mathbb{R}$ by

$$w_0 = \frac{\langle (\frac{1}{2}I - K)v, \mathbf{1}_\Gamma \rangle}{\langle V \mathbf{1}_\Gamma, \mathbf{1}_\Gamma \rangle},$$

which is well-defined thanks to Assumption 1.22. Consequently, we get the relation

$$\langle V w_0 \mathbf{1}_\Gamma, \mathbf{1}_\Gamma \rangle = \langle (\frac{1}{2}I - K)v, \mathbf{1}_\Gamma \rangle$$

which is the Galerkin projection of equation (1.94) to the one-dimensional subspace

$$\text{span}\{\mathbf{1}_\Gamma\} \subset Z^h \subset H^{-1/2}(\Gamma).$$

Again, by Lemma 1.19 choosing $\text{span}\{\mathbf{1}_\Gamma\} \subset Z^h$ as approximation space, $\langle V \cdot, \cdot \rangle$ as bilinear form, and $\langle (\frac{1}{2}I - K)v, \cdot \rangle$ as linear form, we obtain

$$\langle V w_h, w_h \rangle \geq \langle V w_0 \mathbf{1}_\Gamma, w_0 \mathbf{1}_\Gamma \rangle = \frac{\langle (\frac{1}{2}I - K)v, \mathbf{1}_\Gamma \rangle^2}{\langle V \mathbf{1}_\Gamma, \mathbf{1}_\Gamma \rangle} = |\Psi(v)|^2. \quad (1.107)$$

with the linear functional $\Psi : H^{1/2}(\Gamma) \rightarrow \mathbb{R}$ defined by

$$\Psi(v) := \frac{\langle (\frac{1}{2}I - K)v, \mathbf{1}_\Gamma \rangle}{\langle V \mathbf{1}_\Gamma, \mathbf{1}_\Gamma \rangle^{1/2}} \quad \text{for } v \in H^{1/2}(\Gamma).$$

We observe that Ψ is bounded in the $H^{1/2}$ -norm and, most importantly, that the definition of Ψ is independent of the discretization parameter h . Furthermore, $|\Psi(v)|$ defines a semi-norm that becomes a norm on the constant functions, since for some $v_0 \in \mathbb{R}$ with $\Psi(v_0 \mathbf{1}_\Gamma) = 0$ we have

$$0 = \langle (\frac{1}{2}I - K)v_0 \mathbf{1}_\Gamma, \mathbf{1}_\Gamma \rangle = \langle v_0 \mathbf{1}_\Gamma, \mathbf{1}_\Gamma \rangle = v_0 \cdot |\Gamma|,$$

thus $v_0 = 0$. On the other hand, we obtain from (1.60) and (1.106) that

$$\langle Dv, v \rangle \geq \frac{c_0}{c_K} \langle S^{\text{int}} v, v \rangle = \frac{c_0}{c_K} \min_{\substack{\tilde{v} \in H^1(\Omega) \\ \tilde{v}|_\Gamma = v}} |\tilde{v}|_{H^1(\Omega)}^2. \quad (1.108)$$

Due to Theorem 1.7,

$$|u|_{H^1(\Omega)}^2 + |\Psi(u|_\Gamma)|^2 \simeq \|u\|_{H^1(\Omega)}^2 \simeq |u|_{H^1(\Omega)}^2 + \frac{1}{\text{diam } \Gamma} \|u|_\Gamma\|_{L_2(\Gamma)}^2,$$

where the scaling factor $1/\text{diam } \Gamma$ is obtained by dilation from a domain with unit diameter. Combining this result with (1.105), (1.107), and (1.108) we obtain

$$\begin{aligned} \langle S_{\text{BEM}}^{\text{ext}} v, v \rangle &= \langle Dv, v \rangle + \langle V w_h, w_h \rangle \geq \frac{c_0}{c_K} \min_{\substack{\tilde{v} \in H^1(\Omega) \\ \tilde{v}|_\Gamma = v}} \left\{ |\tilde{v}|_{H^1(\Omega)}^2 + |\Psi(v)|^2 \right\} \\ &\gtrsim \min_{\substack{\tilde{v} \in H^1(\Omega) \\ \tilde{v}|_\Gamma = v}} \left\{ |\tilde{v}|_{H^1(\Omega)}^2 + \frac{1}{\text{diam } \Gamma} \|v\|_{L_2(\Gamma)}^2 \right\} = \langle S^{\text{int}} v, v \rangle + \frac{1}{\text{diam } \Gamma} \|v\|_{L_2(\Gamma)}^2. \end{aligned}$$

In other words, there exists a constant $C_{\text{ext}} > 0$ such that

$$\langle S^{\text{int}} v, v \rangle + \frac{1}{\text{diam } \Gamma} \|v\|_{L_2(\Gamma)}^2 \leq C_{\text{ext}} \langle S_{\text{BEM}}^{\text{ext}} v, v \rangle. \quad (1.109)$$

The constant C_{ext} is independent of the discretization parameter h , and in three dimensions it is independent of $\text{diam } \Gamma$, i. e., it depends only on the shape of Ω . In two dimensions, the single layer potential V does not scale linearly due to the logarithmic term in the fundamental solution.

Finally, due to Lemma 1.25(iv) we have

$$\langle S^{\text{ext}} v, v \rangle \simeq \langle S^{\text{int}} v, v \rangle + \frac{\langle V^{-1}v, \mathbf{1}_\Gamma \rangle^2}{\langle V^{-1}\mathbf{1}_\Gamma, \mathbf{1}_\Gamma \rangle}.$$

Since $\Upsilon(v) := \langle V^{-1}v, \mathbf{1}_\Gamma \rangle / \|\mathbf{1}_\Gamma\|_{V^{-1}}$ is a bounded linear functional that reproduces the constant functions, we can apply Sobolev's norm theorem once again and using (1.109) we can conclude that

$$\langle S^{\text{ext}} v, v \rangle \leq C'_{\text{ext}} \langle S_{\text{BEM}}^{\text{ext}} v, v \rangle, \quad (1.110)$$

where C'_{ext} depends (at least in three dimensions) only on the shape of Ω .

This finishes the proof of Lemma 1.33. \square

Chapter 2

Hybrid one-level methods

This chapter deals with hybrid one-level tearing and interconnecting methods. The term “hybrid” refers to the coupling of finite elements and boundary elements. The term “one-level” refers to a special type of coarse space, which in case of the potential equation is spanned by piecewise constant functions.

We first introduce the concept of non-overlapping domain decomposition together with continuous and discrete variational skeleton formulations in Section 2.1. There we use the approximate Steklov-Poincaré operators from Section 1.5.2.6 and Section 1.5.3. The rest of the chapter is devoted to various one-level methods. In Section 2.2 we discuss two sub-classes of one-level FETI/BETI methods.

The first sub-class, which we call *standard one-level FETI/BETI methods*, was introduced by LANGER AND STEINBACH [118, 119] as a follow-up of a family of one-level FETI methods proposed and analyzed by KLAWONN AND WIDLUND [109], which builds upon works by RIXEN AND FARHAT [155, 156] and MANDEL AND TEZAUER [131]. These methods are completely analyzed, and our presentation basically follows [109, 118, 119] and the monograph by TOSELLI AND WIDLUND [184].

The second sub-class, which we call *all-floating FETI/BETI methods*, embraces hybrid methods which combine the *all-floating BETI methods*, introduced by OF [138, 139], and the *total FETI methods*, independently introduced by DOSTÁL, HORÁK, AND KUČERA [46]. Both approaches follow the same concept of additional Lagrange multipliers which enforce the Dirichlet boundary conditions. In this sense all subdomains are decoupled from the Dirichlet boundary, which we call *floating*. Although the all-floating methods are very close to the standard one-level methods, there are obviously some technical differences, such as the additional Lagrange multipliers and the larger coarse space. To the best of our knowledge the first rigorous condition number estimate for all-floating methods was given in PECHSTEIN [143].

The scope of Section 2.2 is to give a unified formulation and analysis of all these one-level methods, with the all-floating methods naturally included, to discuss implementation details, and to provide some numerical results. In Section 2.3, we finally discuss a special FETI method, called interface-concentrated FETI, which was introduced by BEUCHLER, EIBNER, AND LANGER [11], in particular we provide some numerical examples.

2.1 Variational skeleton formulations

2.1.1 Continuous skeleton formulations

Let $\Omega \subset \mathbb{R}^d$ ($d = 2$ or 3) be a bounded domain with Lipschitz boundary $\partial\Omega$ which consists of a Dirichlet boundary Γ_D , regarded as a relatively closed manifold, i. e., $\Gamma_D = \overline{\Gamma_D}$, and an open Neumann boundary Γ_N , such that $\partial\Omega = \Gamma_D \cup \Gamma_N$ and $\Gamma_D \cap \Gamma_N = \emptyset$. The outward unit normal vector to $\partial\Omega$ is denoted by n . We consider the following scalar elliptic model problem in its weak variational formulation: Find $u \in H^1(\Omega)$ with $u|_{\Gamma_D} = g_D$ such that

$$\int_{\Omega} \alpha \nabla u \cdot \nabla v \, dx = \int_{\Omega} f v \, dx + \int_{\Gamma_N} g_N v \, ds \quad \forall v \in H_D^1(\Omega), \quad (2.1)$$

where $H_D^1(\Omega) := \{v \in H^1(\Omega) : v|_{\Gamma_D} = 0\}$. For a simple presentation, assume that $f \in L^2(\Omega)$ and $g_N \in L^2(\Gamma_N)$ and that the coefficient α is piecewise constant. Let $\{\Omega_i\}_{i=1,\dots,s}$ be a non-overlapping partition of Ω into open subdomains Ω_i such that

$$\overline{\Omega} = \bigcup_{i=1}^s \overline{\Omega}_i, \quad \Omega_i \cap \Omega_j = \emptyset \quad \text{for } i \neq j, \quad (2.2)$$

and such that the coefficient is piecewise constant on the subdomains, i. e.,

$$\alpha|_{\Omega_i} = \alpha_i = \text{const} > 0 \quad \forall i = 1, \dots, s. \quad (2.3)$$

In the following we use the index set $\mathcal{I} := \{1, \dots, s\}$ as an abbreviation. We denote the subdomain boundaries by $\partial\Omega_i$, the corresponding outward unit normal vector by n_i , and we define the subdomain diameters $H_i := \text{diam } \Omega_i$. The following assumption ensures that the subdomains are Lipschitz, and that neighboring subdomains are of comparable size. In Section 2.2.4 we will additionally introduce stronger assumptions on the subdomain partition.

Assumption 2.1. *Each subdomain boundary is Lipschitz and the decomposition (2.2) fulfills*

$$H_i \leq C_{DD}^H H_j \quad \text{for } \partial\Omega_i \cap \partial\Omega_j \neq \emptyset,$$

with a uniformly bounded constant $C_{DD}^H > 0$.

We define the (pairwise) subdomain interfaces by

$$\Gamma_{ij} := (\partial\Omega_i \cap \partial\Omega_j) \setminus \Gamma_D \quad \text{for } i \neq j. \quad (2.4)$$

We exclude the Dirichlet boundary Γ_D from the interfaces because no coupling occurs there. Furthermore we define the *interface* Γ and the *skeleton* Γ_S by

$$\Gamma := \bigcup_{i \neq j} \Gamma_{ij}, \quad \Gamma_S := \bigcup_{i \in \mathcal{I}} \partial\Omega_i. \quad (2.5)$$

We additionally introduce the following topological sets generalizing a concept given in TOSELLI AND WIDLUND [184, Definition 4.1].

Definition 2.2. *In three dimensions, the skeleton Γ_S is the disjoint union of*

- subdomain faces, regarded as open and connected manifolds, which are shared by two subdomains or by one subdomain and the outer boundary $\partial\Omega$,
- subdomain edges, also regarded as open and connected, which are shared by at least two subdomains, such that the closure of all edges forms the boundaries of the faces,
- subdomain vertices, which are endpoints of edges.

In two dimensions, the subdomain edges are open and connected sets shared by two subdomains, or by one subdomain and the outer boundary $\partial\Omega$, and the vertices are the endpoints of the edges.

Notation. We denote faces, edges, and vertices that are part of the interface Γ and that are shared by at least two subdomains Ω_i and Ω_j generically by \mathcal{F}_{ij} , \mathcal{E}_{ij} , \mathcal{V}_{ij} , respectively. Note that the index pair (i, j) does not necessarily specify the face, edge, or vertex uniquely, and that, e. g., \mathcal{V}_{ij} can happen to be the same vertex as \mathcal{V}_{ik} for $k \neq j$. Faces, edges, and vertices on $\partial\Omega_i$ (possibly shared by Ω_i and the outer boundary) are denoted generically by \mathcal{F}_i , \mathcal{E}_i , and \mathcal{V}_i , respectively.

Remark 2.3. Our presentation slightly differs from the one in TOSELLI AND WIDLUND [184] because we will need to treat all-floating methods, which operate on the subdomain boundaries as well, not only on the interfaces.

Remark 2.4. With Assumption 2.1 being fulfilled, we can drop the assumption that the original domain Ω is Lipschitz, as long as the boundary of each subdomain remains Lipschitz. This might be advantageous in view of Figure 1.1, page 12. Note that of course the cut in the domain from Figure 1.1(left) must then be discretized on each subdomain separately without coupling conditions. Depending on the boundary conditions the solution may be discontinuous across that cut.

To be able to couple domain variational formulations and boundary integral equations, we need to make an additional assumption on the data. Let $\mathcal{I}_{\text{BEM}} \subset \mathcal{I}$ be a subset of indices such that

$$f|_{\Omega_i} = 0 \quad \forall i \in \mathcal{I}_{\text{BEM}}, \quad (2.6)$$

which makes it possible to use boundary elements on the corresponding subdomain boundaries only. See Remark 2.5 for more general assumptions. The remaining subdomains correspond to the index set $\mathcal{I}_{\text{FEM}} := \mathcal{I} \setminus \mathcal{I}_{\text{BEM}}$ and will be treated with the finite element method.

We can rewrite (2.1) as follows: Find $u \in H^1(\Omega)$ with $u|_{\Gamma_D} = g_D$ such that

$$\sum_{i \in \mathcal{I}} \alpha_i \int_{\Omega_i} \nabla u \cdot \nabla v \, dx = \int_{\Omega} f v \, dx + \int_{\Gamma_N} g_N v \, ds \quad \forall v \in H_D^1(\Omega). \quad (2.7)$$

Assume now for a moment that the Dirichlet trace of the solution u is known on the complete skeleton Γ_S . Then the conormal derivatives on the subdomains are given by the Dirichlet to Neumann map, i. e.,

$$t_i := \alpha_i \frac{\partial u}{\partial n_i} = S_i(u|_{\partial\Omega_i}) - N_i(f|_{\Omega_i}) \quad \forall i \in \mathcal{I}, \quad (2.8)$$

where $S_i = \alpha_i S_i^{\text{int}}$ is the interior Steklov-Poincaré operator on $\partial\Omega_i$, see Section 1.4.3, and $N_i : H^{-1}(\Omega_i) \rightarrow H^{1/2}(\partial\Omega_i)$, is the corresponding Newton potential on the subdomain Ω_i , see Section 1.4.4. In the present context, both operators scale with the coefficient α_i . In the following we simply write $S_i u$ for $S_i(u|_{\partial\Omega_i})$ and $N_i f$ for $N_i(f|_{\Omega_i})$ when the context allows to do so. By partial integration and a density argument, we find that the conormal derivatives have to fulfill the interface conditions

$$t_i + t_j = 0 \quad \text{on } \Gamma_{ij},$$

and the boundary conditions

$$t_i = g_N \quad \text{on } \partial\Omega_i \cap \Gamma_N.$$

We can summarize all these conditions in the weak *skeleton formulation*. Find $u \in H^{1/2}(\Gamma_S)$ with $u|_{\Gamma_D} = g_D$ such that

$$\sum_{i \in \mathcal{I}} \langle S_i u, v \rangle_{\partial\Omega_i} = \sum_{i \in \mathcal{I}} \langle f_i, v \rangle_{\partial\Omega_i} \quad \forall v \in H_D^{1/2}(\Gamma_S), \quad (2.9)$$

where $H_D^{1/2}(\Gamma_S) := \{v \in H^{1/2}(\Gamma_S) : v|_{\Gamma_D} = 0\}$ and the linear forms $f_i \in H^{-1/2}(\partial\Omega_i)$ are defined by

$$\langle f_i, v \rangle_{\partial\Omega_i} := \langle N_i f, v \rangle_{\partial\Omega_i} + \int_{\partial\Omega_i \cap \Gamma_N} g_N v \, ds \quad \text{for } v \in H^{1/2}(\partial\Omega_i). \quad (2.10)$$

Remark 2.5. We see that it is sufficient to assume that the coefficient $\alpha(\cdot)$ is in $L^\infty(\Omega_i)$ for $i \in \mathcal{I}_{\text{FEM}}$, uniformly positive, and sufficiently smooth such that the conormal derivatives on the subdomain boundaries $\partial\Omega_i$ are well-defined. In that case, we must use the general Steklov-Poincaré operator instead of $\alpha_i S_i$, and also the general Newton potential. We can also relax from $f \in L^2(\Omega)$ and $g_N \in L^2(\Gamma_N)$ to $f \in (H_D^1(\Omega))^*$ and $g_N \in H^{-1/2}(\Gamma_N)$ with the side condition that the restrictions of f to each subdomain Ω_i and of g_N to each part $\partial\Omega_i \cap \Gamma_N$ are well-defined. In the BEM subdomains, however, the coefficients must still be constant and the sources must vanish (unless suitable approximations of the Newton potentials are available, cf. Section 1.5.3).

With the usual homogenization technique, as described in Section 1.3.2, we can rewrite problem (2.9): Find $\tilde{u} \in H_D^{1/2}(\Gamma_S)$ such that

$$\sum_{i \in \mathcal{I}} \langle S_i \tilde{u}, v \rangle_{\partial\Omega_i} = \sum_{i \in \mathcal{I}} \langle f_i - S_i \tilde{g}_D, v \rangle_{\partial\Omega_i} \quad \forall v \in H_D^{1/2}(\Gamma_S), \quad (2.11)$$

where $\tilde{g}_D \in H^{1/2}(\Gamma_S)$ is an arbitrary extension of g_D from Γ_D to Γ_S , and the actual solution u is given by $u = \tilde{g}_D + \tilde{u}$. Both skeleton formulations (2.9) and (2.11) are equivalent to (2.7) in the sense that the solution $u \in H^{1/2}(\Gamma_S)$ of any of the skeleton formulations coincides with the trace of the solution u to the volume variational formulation (2.7) on Γ_S , in particular on all subdomain boundaries $\partial\Omega_i$. The values of the solution u in the subdomains Ω_i are then determined by purely local problems.

If the Dirichlet boundary is of positive surface measure, the symmetric bilinear form in (2.11) is elliptic on $H_D^{1/2}(\Gamma_S)$, which easily follows from the (semi-)ellipticity of the Steklov-Poincaré operators S_i , cf. Section 1.4.3 Hence, both skeleton problems (2.9) and (2.11) are well-posed.

2.1.2 Discrete skeleton formulations

Let $\mathcal{T}(\Gamma_S)$ be a conforming simplicial triangulation of the skeleton Γ_S . For $i \in \mathcal{I}$, let $\mathcal{T}(\partial\Omega_i)$ denote its restriction to the subdomain boundary $\partial\Omega_i$ with the local mesh parameter h_i . The local meshes $\mathcal{T}(\partial\Omega_i)$ are assumed to be shape-regular and quasi-uniform. As a consequence, $h_i \simeq h_j$ for neighboring subdomains Ω_i and Ω_j . On each FEM subdomain Ω_i , $i \in \mathcal{I}_{\text{FEM}}$, we extend the triangulation $\mathcal{T}(\partial\Omega_i)$ to a conforming, shape-regular, and quasi-uniform simplicial triangulation $\mathcal{T}(\Omega_i)$ of the subdomains Ω_i .

Notation. We denote by $\partial\Omega_i^h$ the set of nodes on $\partial\Omega_i$, and by Γ_S^h and Γ_{ij}^h the set of nodes on Γ_S and Γ_{ij} , respectively. Similarly, let \mathcal{F}_i^h and \mathcal{E}_i^h denote the set of nodes on the (open) face \mathcal{F}_i , respectively on the (open) edge \mathcal{E}_i . A typical node will be denoted by x^h .

Let $V^h(\Gamma_S)$ and $V^h(\partial\Omega_i)$ denote the spaces of continuous functions on Γ_S and $\partial\Omega_i$, respectively, which are piecewise linear on the elements of the triangulation. Let $V_D^h(\Gamma_S)$ and $V_D^h(\partial\Omega_i)$ denote the corresponding spaces which satisfy homogeneous Dirichlet boundary conditions on Γ_D . Based on these triangulations we discretize the derived skeleton formulations in two steps: First, we project the equations to the discrete spaces. Second, we approximate the Steklov-Poincaré operators S_i and the Newton potentials N_i by approximations $S_{i,h}$ and $N_{i,h}$, respectively. According to the notation from Section 1.5, we set

$$S_{i,h} := \begin{cases} \alpha_i S_{i,\text{BEM}}^{\text{int}} & \text{for } i \in \mathcal{I}_{\text{BEM}}, \\ \alpha_i S_{i,\text{FEM}}^{\text{int}} & \text{for } i \in \mathcal{I}_{\text{FEM}}. \end{cases} \quad (2.12)$$

$$N_{i,h} := \begin{cases} 0 & \text{for } i \in \mathcal{I}_{\text{BEM}}, \\ \alpha_i N_{i,\text{FEM}} & \text{for } i \in \mathcal{I}_{\text{FEM}}. \end{cases} \quad (2.13)$$

As we have seen there, these operators do in general not coincide with the Galerkin projections of S_i , N_i . Without loss of generality but for a simplified notation, assume that the boundary data g_D , \tilde{g}_D , and g_N are contained in the corresponding discrete spaces. Otherwise, we would have to project them as well.

Let $f_{i,h}$ denote the resulting approximations of the continuous linear forms f_i , replacing N_i by $N_{i,h}$. Then the approximation of (2.9) reads: Find $u \in V^h(\Gamma_S)$ with $u|_{\Gamma_D} = g_D$ such that

$$\sum_{i \in \mathcal{I}} \langle S_{i,h} u, v \rangle_{\partial\Omega_i} = \sum_{i \in \mathcal{I}} \langle f_{i,h}, v \rangle_{\partial\Omega_i} \quad \forall v \in V_D^h(\Gamma_S). \quad (2.14)$$

The approximation of (2.11) reads: Find $\tilde{u} \in V_D^h(\Gamma_S)$ such that

$$\sum_{i \in \mathcal{I}} \langle S_{i,h} \tilde{u}, v \rangle_{\partial\Omega_i} = \sum_{i \in \mathcal{I}} \langle f_{i,h} - S_{i,h} \tilde{g}_D, v \rangle_{\partial\Omega_i} \quad \forall v \in V_D^h(\Gamma_S), \quad (2.15)$$

As in the continuous case the bilinear form in (2.15) is symmetric and elliptic on $V_D^h(\Gamma_S)$. Therefore, the homogenized skeleton variational formulation (2.15) is equivalent to the minimization problem

$$\sum_{i \in \mathcal{I}} \left\{ \frac{1}{2} \langle S_{i,h} \tilde{u}, \tilde{u} \rangle_{\partial\Omega_i} - \langle f_{i,h} - S_{i,h} \tilde{g}_D, \tilde{u} \rangle_{\partial\Omega_i} \right\} \rightarrow \min_{\tilde{u} \in V_D^h(\Gamma_S)}. \quad (2.16)$$

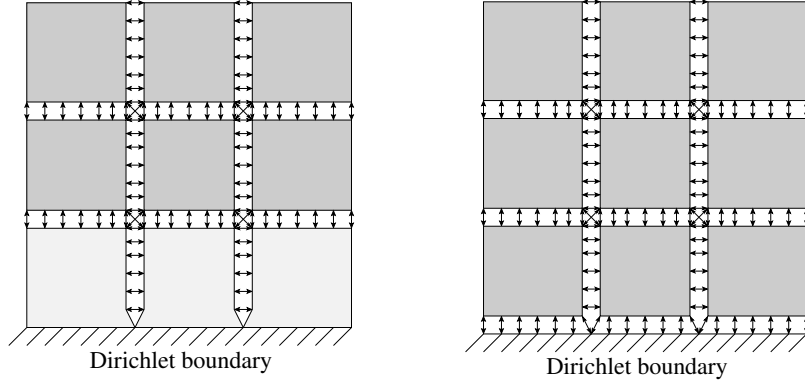


Figure 2.1: Illustration of two different one-level methods. *Left*: Standard one-level method. *Right*: All-floating method. Floating subdomains are dark-shaded.

A simple computation reveals that the non-homogenized problem (2.14) is equivalent to the minimization problem

$$\sum_{i \in \mathcal{I}} \left\{ \frac{1}{2} \langle S_{i,h} u, u \rangle_{\partial \Omega_i} - \langle f_{i,h}, u \rangle_{\partial \Omega_i} \right\} \rightarrow \min_{u \in V^h(\Gamma_S), u|_{\Gamma_D} = g_D} . \quad (2.17)$$

In the following two subsections we derive two different saddle point formulations using the tearing and interconnecting technique. The first formulation in Section 2.2.1 is derived from the homogenized minimization problem (2.16), and we refer to it by the term *standard one-level formulation*. The second one, the *all-floating formulation* treated in Section 2.2.2, is derived from the non-homogenized minimization problem (2.17).

Notation. Since the following methods are set up on the discrete level, we simplify our notation a bit and drop the subscript h in the approximate Steklov-Poincaré operators $S_{i,h}$ and in the right hand sides $f_{i,h}$ and write S_i, f_i .

2.2 Standard one-level and all-floating FETI/BETI methods

2.2.1 Formulation of standard one-level FETI/BETI methods

As mentioned before, our presentation follows Klawonn and Widlund [109], Langer and Steinbach [118, 119], and Toselli and Widlund [184, Sect. 6.3]. Our starting point is the homogenized minimization problem (2.16). To simplify the notation we assume only in this subsection on the standard one-level formulation that $g_D \equiv 0$. Otherwise we have to use $f_i - S_i \tilde{g}_D$ instead of f_i and \tilde{u} instead of u . We will not use such a homogenization in the all-floating methods in Section 2.2.2.

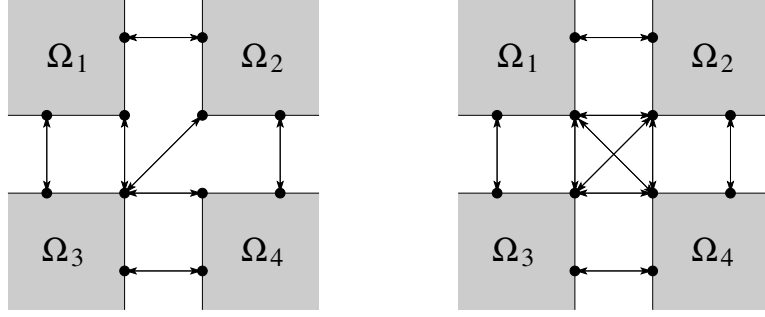


Figure 2.2: Sketch of non-redundant constraints (left) and fully redundant constraints (right) for a subdomain edge in three dimensions, or a subdomain vertex (cross point) in two dimensions sharing four subdomains.

2.2.1.1 Tearing and interconnecting

We introduce separate unknowns $u_i \in V_D^h(\partial\Omega_i)$ for u on the subdomains and define the working spaces

$$W_i := V_D^h(\partial\Omega_i) \quad \text{and} \quad W := \prod_{i \in \mathcal{I}} W_i. \quad (2.18)$$

Now we can compactly write

$$u := [u_i]_{i \in \mathcal{I}} \in W. \quad (2.19)$$

Functions in the product space W are typically discontinuous across subdomain interfaces. The continuity of the solution is enforced by constraints of the form

$$u_i(x^h) = u_j(x^h) \quad \text{for } x^h \in \Gamma_{ij}^h. \quad (2.20)$$

In this work, we restrict ourselves to fully redundant constraints, i. e., all possible constraints are used, cf. [184, Sect. 6.3.3]. They appear to be really advantageous in implementations due to the full symmetry, see Figure 2.2, right. In the non-redundant case (cf. [184, Sect. 6.3.2] and Figure 2.2, left) a minimal number of necessary constraints is used. For other variants, such as orthogonal constraints, see e. g. FRAGAKIS AND PAPADRAKAKIS [65, 66]. Introducing a jump operator $B = [B_i]_{i \in \mathcal{I}}$ we can write all the constraints (2.20) in the compact form

$$B u = 0, \quad \text{or equivalently,} \quad \sum_{i \in \mathcal{I}} B_i u_i = 0. \quad (2.21)$$

In the standard nodal basis the operators B and B_i can easily be represented by signed Boolean matrices, i. e., matrices with entries 0, 1 or -1 . To be a bit more precise we define the space of Lagrange multipliers

$$U := \mathbb{R}^m, \quad (2.22)$$

where m is the total number of constraints. In the following we continue our philosophy to keep track of “dual” (i. e., functional) and “primal” spaces, even if they might seem to be

the same in the discrete case. We choose the operator B to map into the space U^* of “dual” kind, as it *evaluates* the jump of u . Since the dual U^* can be identified with \mathbb{R}^m , the dual pairing in $U^* \times U$ is nothing else than the Euclidean inner product, i. e., $\langle \mu, \lambda \rangle = (\mu, \lambda)_{\ell^2}$ for $\lambda \in U$, $\mu \in U^*$.

Notation. The component of $\lambda \in U$ (respectively $\mu \in U^*$) which corresponds to the constraint $u_i(x^h) = u_j(x^h)$ at the node $x^h \in \Gamma_{ij}^h$ is denoted by $\lambda_{ij}(x^h)$ (respectively $\mu_{ij}(x^h)$).

We can now precisely define the jump operator $B : W \rightarrow U^*$ by

$$(Bw)_{ij}(x^h) = w_i(x^h) - w_j(x^h) \quad \text{for } x^h \in \Gamma_{ij}^h, \quad i > j, \quad (2.23)$$

where we have chosen a fixed (but in principle arbitrary) sign of the jump. Let $B_i : W_i \rightarrow U^*$ be defined by

$$(B_i w_i)_{jk}(x^h) = \begin{cases} w_i(x^h) & \text{if } i = j \\ -w_i(x^h) & \text{if } i = k \\ 0 & \text{else} \end{cases} \quad \text{for } x^h \in \Gamma_{jk}^h, \quad j > k. \quad (2.24)$$

By construction we have $\langle Bw, \lambda \rangle = \sum_{i \in \mathcal{I}} \langle B_i w_i, \lambda \rangle$ for all $\lambda \in U$. Apparently the compact form (2.21) of the constraints has to be read as an equation in U^* . For a comprehensive functional presentation of FETI type Lagrange multipliers we refer to BRENNER [23].

In what follows we will always regard the approximate Steklov-Poincaré operators S_i as operators mapping from W_i to W_i^* . In addition, we define $S : W \rightarrow W^*$ by

$$\langle Sw, v \rangle = \sum_{i \in \mathcal{I}} \langle S_i w_i, v_i \rangle \quad \text{for } w, v \in W, \quad (2.25)$$

in short $S := \text{diag}(S_i)$, and the linear form $f \in W^*$ by

$$\langle f, w \rangle := \sum_{i \in \mathcal{I}} \langle f_i, w_i \rangle \quad \text{for } w \in W, \quad (2.26)$$

in short $f := [f_i]_{i \in \mathcal{I}}$. With this notation we can write the minimization problem (2.16) equivalently as the constrained minimization problem

$$\frac{1}{2} \langle Su, u \rangle - \langle f, u \rangle \rightarrow \min_{u \in W, Bu=0}.$$

The corresponding saddle point problem reads as follows. Find $(u, \lambda) \in W \times U$:

$$\begin{pmatrix} S & B^\top \\ B & 0 \end{pmatrix} \begin{pmatrix} u \\ \lambda \end{pmatrix} = \begin{pmatrix} f \\ 0 \end{pmatrix}. \quad (2.27)$$

This problem is uniquely solvable (up to adding elements from $\ker B^\top$ to λ) if and only if

$$\ker S \cap \ker B = \{0\}, \quad (2.28)$$

cf. BREZZI AND FORTIN [29]. Condition (2.28) holds true whenever the Dirichlet boundary is non-empty. The solution u satisfies $Bu = 0$, i. e., it is continuous across the subdomain interfaces. We define the corresponding subspace of continuous functions by

$$\widehat{W} := \{w \in W : Bu = 0\}, \quad (2.29)$$

and point out that it can be identified with $V_D^h(\Gamma_S)$.

Remark 2.6. The saddle point formulation (2.27) can also be derived algebraically from the skeleton formulation without exploiting minimization problems. We show this alternative derivation because it gives more insight on the meaning of the Lagrange multipliers. Let

$$t_i := S_i u_i - f_i$$

denote the representation of the normal flux on the subdomain boundary $\partial\Omega_i$ in W_i^* . From the discrete skeleton formulation (2.14) we obtain that

$$\langle t, v \rangle = \sum_{i \in \mathcal{I}} \langle t_i, v_i \rangle_{\partial\Omega_i} = 0 \quad \forall v \in \widehat{W}. \quad (2.30)$$

We define the averaging operator $E : W \rightarrow \widehat{W} \subset W$ by the relation

$$(E w)_i(x^h) = \frac{1}{|\mathcal{N}_{x^h}|} \sum_{j \in \mathcal{N}_{x^h}} w_j(x^h) \quad \text{for } x^h \in \partial\Omega_i^h \setminus \Gamma_D, \quad w \in W, \quad (2.31)$$

where $\mathcal{N}_{x^h} := \{i \in \mathcal{I} : x^h \in \partial\Omega_i\}$, i. e., the index set of the subdomains sharing the node $x^h \in \Gamma_S^h$. Obviously, E is a projection onto the space \widehat{W} . Hence, we can represent v by $E w$ for some $w \in W$. Therefore, condition (2.30), which states that the fluxes are continuous, can be written as $\langle t, E w \rangle = 0$ or equivalently $\langle E^\top t, w \rangle = 0$. The complete set of equations for (u, t) reads

$$S u - t = f \quad \text{in } W^*, \quad (2.32)$$

$$B u = 0 \quad \text{in } U^*, \quad (2.33)$$

$$E^\top t = 0 \quad \text{in } W^*. \quad (2.34)$$

In order to get rid of condition (2.34) we represent the continuous flux t by $t = -B^\top \lambda$ for some Lagrange multiplier $\lambda \in U$. This is indeed possible because the condition $E^\top t = 0$ implies that t is in range B^\top . Condition (2.34) is now automatically satisfied because $B E = 0$ in U^* and consequently $E^\top B^\top = 0$ in W^* . Our set of equations transforms to

$$\begin{pmatrix} S & B^\top \\ B & 0 \end{pmatrix} \begin{pmatrix} u \\ \lambda \end{pmatrix} = \begin{pmatrix} f \\ 0 \end{pmatrix},$$

which is exactly (2.27). Under this perspective, the Lagrange multipliers themselves can be interpreted as normal fluxes. For such an interpretation in a mechanical context see RIXEN AND FARHAT [155, 156].

2.2.1.2 Singular local Neumann problems – A projection

In the usual theory of iterative substructuring methods, a *floating subdomain* is defined as a subdomain Ω_i whose boundary $\partial\Omega_i$ does not intersect the Dirichlet boundary Γ_D . In order to use this concept also for the all-floating methods in Section 2.2.2 and the FETI/BETI methods for unbounded domains in Chapter 3, we generalize the standard definition a bit.

Definition 2.7 (floating subdomain). *A subdomain Ω_i is by definition a floating subdomain if $S_i : W_i \rightarrow W_i^*$ is singular, otherwise it is a non-floating subdomain. We introduce the index set corresponding to the floating subdomains,*

$$\mathcal{I}_{\text{float}} := \{i \in \mathcal{I} : S_i \text{ is singular}\}.$$

In the case of our potential equation, the pure Neumann problem on a floating subdomain is uniquely solvable up to the constant function, and so

$$\begin{aligned} \ker S_i &= \text{span}\{\mathbf{1}_{\partial\Omega_i}\}, & \text{range } S_i &= \{v \in W_i^* : \langle v, \mathbf{1}_{\partial\Omega_i} \rangle = 0\} & \forall i \in \mathcal{I}_{\text{float}}, \\ \ker S_i &= \{0\}, & \text{range } S_i &= W_i & \forall i \notin \mathcal{I}_{\text{float}}. \end{aligned} \quad (2.35)$$

Consequently, a solution u in the first equation of (2.27) exists if and only if $f - B^\top \lambda \in \text{range } S$. This compatibility condition will lead to the introduction of a projection P . We introduce operators

$$R_i : \mathbb{R} \rightarrow W_i : \begin{cases} \xi_i \mapsto \xi_i \mathbf{1}_{\partial\Omega_i} & \text{for } i \in \mathcal{I}_{\text{float}}, \\ \xi_i \mapsto 0 & \text{else,} \end{cases} \quad (2.36)$$

such that $\text{range } R_i = \ker S_i$, and we define $R : Z \rightarrow \ker S$ by $R = \text{diag}(R_i)$ where

$$Z := \{\xi \in \mathbb{R}^s : \xi_i = 0 \quad \forall i \notin \mathcal{I}_{\text{float}}\}. \quad (2.37)$$

For $i \in \mathcal{I}_{\text{float}}$, let S_i^\dagger denote an arbitrary pseudoinverse of S_i and set $S_i^\dagger = S_i^{-1}$ for $i \notin \mathcal{I}_{\text{float}}$, as well as $S^\dagger := \text{diag}(S_i^\dagger)$. We will discuss later on how such pseudoinverses can be applied efficiently. With these considerations we obtain from (2.27) that

$$u_i = S_i^\dagger (f_i - B_i^\top \lambda) + R_i \xi_i, \quad (2.38)$$

for some $\xi \in Z$ under the compatibility condition

$$\begin{aligned} \langle f_i - B_i^\top \lambda, \mathbf{1}_{\partial\Omega_i} \rangle &= 0 & \forall i \in \mathcal{I}_{\text{float}}, \\ \text{or equivalently,} & & R_i^\top (f_i - B_i^\top \lambda) = 0 & \forall i \in \mathcal{I}. \end{aligned} \quad (2.39)$$

For a floating subdomain, the term $R_i \xi_i$ in (2.38) is the constant that we need to add in order to parameterize all possible solutions. For a non-floating subdomain Ω_i , the term $R_i \xi_i$ in (2.38) and the compatibility condition (2.39) are of course meaningless. Both could be dropped but we keep them to have a unified notation. With the abbreviations

$$F := B S^\dagger B^\top, \quad G := B R, \quad d := B S^\dagger f, \quad e := R^\top f, \quad (2.40)$$

condition (2.39) reads

$$e - G^\top \lambda = 0.$$

Using formula (2.38), the variable u can be expressed in terms of λ and ξ , and the continuity condition $B u = 0$ transforms to

$$d - F \lambda + G \xi = 0.$$

We can therefore reformulate problem (2.27) as follows. Find $(\lambda, \xi) \in U \times Z$ such that

$$\begin{pmatrix} F & -G \\ G^\top & 0 \end{pmatrix} \begin{pmatrix} \lambda \\ \xi \end{pmatrix} = \begin{pmatrix} d \\ e \end{pmatrix}. \quad (2.41)$$

Once solved, the solution u is given by (2.38). In order to satisfy the second equation (i. e., the compatibility condition), we introduce the projection $P : U \rightarrow \ker G^\top \subset U$,

$$P = I - Q G (G^\top Q G)^{-1} G^\top, \quad (2.42)$$

where the SPD operator $Q : U^* \rightarrow U$ is yet to be specified. For projections of this type see also Section 1.1.2. Note that $G^\top Q G$ is the Galerkin projection of $B^\top Q B$ onto $\ker S$. Because of (2.28), i. e., $\ker S \cap \ker B = \{0\}$, the operator G is injective. Hence, the operator $G^\top Q G$ is SPD as long as Q is SPD on $\text{range } G$. The operator P projects to the subspace

$$\begin{aligned} V &:= \{\lambda \in U : \langle Bz, \lambda \rangle = 0 \quad \forall z \in \ker S\} = \ker G^\top = \text{range } P \\ &= \{\lambda \in U : B^\top \lambda \in \text{range } S\}, \end{aligned} \quad (2.43)$$

which we call the space of *admissible Lagrange increments* following FARHAT, CHEN, AND MANDEL [58]. In case $f = 0$, this is the subspace of U where the compatibility condition (2.39) is fulfilled. In general, if we fix a particular $\lambda_0 \in U$ with $G^\top \lambda_0 = e$, the solution λ of (2.41) can be represented by $\lambda = \lambda_0 + \tilde{\lambda}$ for some $\tilde{\lambda} \in V$. In the following we use

$$\lambda_0 := Q G (G^\top Q G)^{-1} e. \quad (2.44)$$

In the spirit of Galerkin we can test the first equation in (2.41) with trial functions in V which yields the following problem: Find $\tilde{\lambda} \in V$ such that

$$P^\top F \tilde{\lambda} = P^\top (d - F \lambda_0). \quad (2.45)$$

The variable ξ has disappeared because $P^\top G = 0$. Once equation (2.45) is solved, the original variables λ and ξ can be recovered from the relations

$$\lambda = \lambda_0 + \tilde{\lambda} \quad \text{and} \quad \xi = (G^\top Q G)^{-1} G^\top Q (F \lambda - d), \quad (2.46)$$

where the second formula can be derived by testing the first equation in (2.41) with the remaining trial functions, i. e., applying $(I - P^\top)$ to it. For later purposes we define

$$V' := \{\mu \in U^* : \langle Bz, Q\mu \rangle = 0 \quad \forall z \in \ker S\} = \text{range } P^\top, \quad (2.47)$$

such that $P^\top : U^* \rightarrow V' \subset U^*$. It can be shown that V' is isomorphic to V .

The following lemma shows that problem (2.45) is in a certain sense SPD. Before, we define the spaces

$$\tilde{V} := V_{/\ker B^\top}, \quad \text{and} \quad \tilde{V}' := V' \cap \text{range } B. \quad (2.48)$$

The space \tilde{V} is the factor space of V with respect to $\ker B^\top$, where the redundancies in the Lagrange multipliers are unified, cf. TEZAUER [179, Sect. 3.1.4]. The following lemma would be straightforward if $\text{range } B = U$ and therefore $\tilde{V} = V$.

Lemma 2.8. *Let F and P be defined as above. Then the operator $P^\top F$ is SPD on the subspace \tilde{V} .*

Proof. First, from the definitions of F and P we see that $F\lambda$ and $P\lambda$ are invariant if we add elements from $\ker B^\top$ to λ , and that $P^\top F$ maps into $\text{range } B = (\ker B^\top)^\circ$. These considerations justify to work in the quotient factor. Secondly, we know from (2.43) that $B^\top \lambda \in \text{range } S$ for each $\lambda \in \tilde{V}$. Due to the fact that S^\dagger is SPD on $\text{range } S$, we obtain

$$\langle P^\top F \lambda, \lambda \rangle = \langle F \lambda, P \lambda \rangle = \langle F \lambda, \lambda \rangle = \langle S^\dagger B^\top \lambda, B^\top \lambda \rangle > 0 \quad \forall \lambda \in \tilde{V} \setminus \{0\},$$

which shows that $P^\top F$ is SPD on \tilde{V} . □

As a consequence of the above lemma, problem (2.45) can be solved using a preconditioned conjugate gradient subspace iteration. Of course, preconditioners accelerate the method. All FETI type preconditioners have the form

$$P M^{-1}, \quad (2.49)$$

where the operator $M^{-1} : U^* \rightarrow U$ is a suitable preconditioner for F . The projection P is necessary to keep the search directions in the space V . Since

$$\lambda \in V \implies P M^{-1} P^\top F \lambda = (P M^{-1} P^\top)(P^\top F P) \lambda,$$

the preconditioned operator is the product of two symmetric operators and can be analyzed in the usual framework. Once problem (2.45) is solved, the actual solution u can finally be recovered using formulae (2.46) and (2.38). Note that even if λ is only unique up to an element from $\ker B^\top$, the solution u is always unique. The crucial ingredients of the method are the choices of Q and M^{-1} above. If chosen in the right way the method will be (i) only weakly depending on the local problem size, (ii) robust with respect to the number s of subdomains, and (iii) robust with respect to the values of the coefficients α_i .

2.2.1.3 Preconditioning

In order to define a suitable preconditioner M^{-1} for F we first need to introduce some functions and operators, among them the weighted counting functions δ_j^\dagger which play an important role in balancing Neumann-Neumann methods, cf. TOSELLI AND WIDLUND [184, Section 6.2.1]. For each $j \in \mathcal{I}$ we define the function $\delta_j^\dagger \in V^h(\Gamma_S)$ by

$$\delta_j^\dagger(x^h) := \begin{cases} \frac{\alpha_j}{\sum_{k \in \mathcal{N}_{x^h}} \alpha_k} & \text{for } x^h \in \partial\Omega_j^h, \\ 0 & \text{for } x^h \in \Gamma_S^h \setminus \partial\Omega_j^h, \end{cases} \quad (2.50)$$

where $\mathcal{N}_{x^h} := \{i \in \mathcal{I} : x^h \in \partial\Omega_i\}$, i. e., the index set of the subdomains sharing the node $x^h \in \Gamma^h$. The union of all these functions provides a partition of unity on the skeleton. For each subdomain $i \in \mathcal{I}$ we define a diagonal scaling operator $D_i : U^* \rightarrow U$ by

$$(D_i \mu)_{ij}(x^h) := \delta_j^\dagger(x^h) \mu_{ij}(x^h) \quad \text{for } \mu \in U^*, \quad x^h \in \Gamma_{ij}^h, \quad (2.51)$$

where all other components are set to zero. We define the operator $B_D : W^* \rightarrow U$ by

$$B_D := \sum_{i \in \mathcal{I}} D_i B_i \mathcal{J}_{W_i}. \quad (2.52)$$

Here, \mathcal{J}_{W_i} denotes the Riesz isomorphism with respect to the Euclidean inner product in the standard nodal basis, i. e.,

$$\mathcal{J}_{W_i} : W_i^* \rightarrow W_i : f \mapsto \sum_{x^h \in \partial\Omega_i^h} \langle f, \varphi_{x^h} \rangle \varphi_{x^h}, \quad (2.53)$$

where φ_{x^h} is the basis function corresponding to the node $x^h \in \partial\Omega_i^h$. In matrix-vector notation, \mathcal{J}_{W_i} is the identity matrix and $B_D = [D_1 B_1 | \dots | D_s B_s]$. The preconditioner is now chosen to be

$$M^{-1} = B_D S B_D^\top. \quad (2.54)$$

Remark 2.9. For non-redundant Lagrange multipliers, the operator B_D reads

$$B_D = (B D^{-1} B^\top)^{-1} B D,$$

where $D : W^* \rightarrow W$ is a diagonal scaling operator similar to the D_i . For an efficient algorithmic construction of B_D see, e. g., OF [138]. In either case, redundant or non-redundant, the operator B_D^\top can be shown to be a pseudoinverse of B , such that $B B_D^\top B = B$ and $B_D B^\top B_D = B_D$, see MANDEL, DOHRMANN, AND TEZAUER [133] and Lemma 2.16 later on.

Remark 2.10. Each block S_i in S appearing in the preconditioner (2.54) may be replaced by the hypersingular operator on $\partial\Omega_i$ since it is spectrally equivalent to S_i , even for a FEM subdomain Ω_i . The resulting preconditioner is then called *scaled hypersingular BETI preconditioner*, cf. LANGER AND STEINBACH [118, 119].

2.2.1.4 The operator Q

According to KLAWONN AND WIDLUND [109], the linear operator $Q : U^* \rightarrow U$ is either set to M^{-1} or is chosen as a diagonal matrix. In the second case we set

$$(Q \mu)_{ij}(x^h) := \min(\alpha_i, \alpha_j) q_{ij}(x^h) \mu_{ij}(x^h) \quad \text{for } \mu \in U^*, \quad (2.55)$$

where $q_{ij}(x^h) = \min(q_i(x^h), q_j(x^h))$ and

$$q_i(x^h) := \left\{ \begin{array}{ll} (1 + \log(H_i/h_i)) \frac{h_i^2}{H_i} & \text{if } x^h \text{ lies on a face } \mathcal{F}_i \\ h_i & \text{if } x^h \text{ lies on an edge } \mathcal{E}_i \text{ or a vertex } \mathcal{V}_i \end{array} \right\} \quad \text{if } d = 3,$$

$$q_i(x^h) := \left\{ \begin{array}{ll} (1 + \log(H_i/h_i)) \frac{h_i}{H_i} & \text{if } x^h \text{ lies on an edge } \mathcal{E}_i \\ 1 & \text{if } x^h \text{ is a vertex } \mathcal{V}_i \end{array} \right\} \quad \text{if } d = 2. \quad (2.56)$$

Note that if $H_i \simeq H_j$ and $h_i \simeq h_j$ for neighboring subdomains Ω_i and Ω_j , then we have also $q_i(x^h) \simeq q_j(x^h)$. This diagonal choice of Q mimics the action of M^{-1} when restricted to range G , and it will be better understood in the proof of the condition number estimate. Nevertheless, in the following remark we inspect the structure of the operator $G^\top Q G$ which appears in the projections P and P^\top .

Remark 2.11. Let Q be chosen according to (2.55)–(2.56) and let \mathcal{G} denote the connectivity graph whose nodes correspond to the subdomains Ω_i with an edge between two nodes whenever the corresponding subdomains are neighboring, cf. Figure 2.3. Recall that $G = B R$ and that $R : Z \rightarrow \ker S$ with

$$Z = \{ \xi \in \mathbb{R}^s : \xi_i = 0 \quad \forall i \notin \mathcal{I}_{\text{float}} \}.$$

We can think of elements from Z as discrete functions on the nodes of \mathcal{G} which satisfy homogeneous boundary conditions at the nodes which correspond to the non-floating subdomains, cf. Figure 2.3. Using the definition of the jump operator B , we find that

$$\langle G^\top Q G y, z \rangle = \sum_{\substack{i \geq j \\ \Gamma_{ij} \neq \emptyset}} (y_i - y_j) \underbrace{\left\{ \min(\alpha_i, \alpha_j) \sum_{x^h \in \Gamma_{ij}^h} q_{ij}(x^h) \right\}}_{=: \mathcal{Q}_{ij}} (z_i - z_j) \quad \forall y, z \in Z.$$

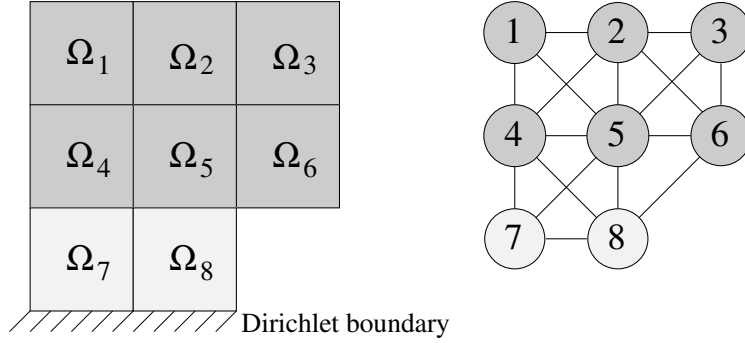


Figure 2.3: *Left:* Subdomains with Dirichlet boundary. *Right:* Corresponding connectivity graph \mathcal{G} .

This bilinear form corresponds to the (sparse) matrix induced by the graph Laplacian (see e. g., FIEDLER [64]) where we assign each edge between node i and j in \mathcal{G} the weight \mathcal{Q}_{ij} . Thus, $(G^\top Q G)^{-1}$ solves a discrete Laplace problem on the connectivity graph, which acts as a coarse problem for the FETI/BETI algorithm. Without this coarse problem, the method would for sure suffer from a dependency on the number of subdomains. Assume that in three dimensions each face \mathcal{F}_i covers $\mathcal{O}((H_i/h_i)^2)$ mesh nodes and each edge \mathcal{E}_i covers $\mathcal{O}(H_i/h_i)$ nodes. Then,

$$\mathcal{Q}_{ij} \simeq \begin{cases} \min(\alpha_i, \alpha_j) (1 + \log(H_i/h_i)) H_i & \text{if } \Omega_i \text{ and } \Omega_j \text{ share a subdomain face,} \\ \min(\alpha_i, \alpha_j) H_i & \text{if } \Omega_i \text{ and } \Omega_j \text{ share only a subdomain edge,} \\ \min(\alpha_i, \alpha_j) h_i & \text{if } \Omega_i \text{ and } \Omega_j \text{ share only a subdomain vertex.} \end{cases}$$

With the analogous assumptions in two dimensions we have

$$\mathcal{Q}_{ij} \simeq \begin{cases} \min(\alpha_i, \alpha_j) (1 + \log(H_i/h_i)) & \text{if } \Omega_i \text{ and } \Omega_j \text{ share a subdomain edge,} \\ \min(\alpha_i, \alpha_j) & \text{if } \Omega_i \text{ and } \Omega_j \text{ share only a subdomain vertex.} \end{cases}$$

We observe that vertex connections in three dimensions are weighted weaker than others, and that connections between subdomains with large coefficients are in general weighted stronger than others.

Remark 2.12. If the coefficients α_i are all equal, or only moderately varying, one can simplify the scaling operators D_i by replacing all the α_i by one. Then the functions δ_j^\dagger still form a partition of unity due to the node multiplicity involved. The scaling operator Q can then simply be chosen as the identity matrix.

2.2.1.5 Summary of the standard one-level FETI/BETI method

Let us summarize the standard one-level FETI/BETI algorithm. To solve system (2.41), we apply a projected preconditioned conjugate gradient method to the projected Lagrange multiplier system (2.45) with a special initial guess λ_0 given by (2.44). The actual solution u is then computed via the relations (2.46) and (2.38). In each step of the projected PCG method, the application of F essentially means solving local (regularized) Neumann problems, while the application of the preconditioner M^{-1} essentially means solving local

Dirichlet problems. The projection steps P and P^\top involve the solution of a coarse problem given by $G^\top Q G$. Implementation issues and the analysis of the method are treated in Section 2.2.3 and Section 2.2.4, respectively.

Remark 2.13. The name *one-level* method refers to the specific kind of coarse problem, not to the entire algorithm. On the contrary, *two-level* FETI methods were designed for biharmonic and shell problems (FARHAT, CHEN, MANDEL, AND ROUX [59], FARHAT AND MANDEL [54]) and, as we have already mentioned in the introduction, the dual-primal methods (FETI-DP, BETI-DP) end up with a completely different coarse problem.

2.2.2 Formulation of all-floating FETI/BETI methods

The starting point for the all-floating formulation is the non-homogenized minimization problem (2.17), i. e.,

$$\sum_{i \in \mathcal{I}} \left\{ \frac{1}{2} \langle S_i u, u \rangle_{\partial \Omega_i} - \langle f_i, u \rangle_{\partial \Omega_i} \right\} \rightarrow \min_{u \in V^h(\Gamma_S), u|_{\Gamma_D} = g_D} .$$

In contrast to the standard one-level formulation, we will not incorporate the Dirichlet conditions in the solution space but impose them as side conditions. Hence, we need new definitions of the working spaces and operators. Nevertheless, we use the same notation as in Section 2.2.1 because (i) there are only differences in details but not in the structure, (ii) the context should always be clear, and (iii) we will give uniform statements concerning both formulations later on. We define

$$W_i := V^h(\partial \Omega_i), \quad W := \prod_{i \in \mathcal{I}} W_i, \tag{2.57}$$

and we write

$$S_i : W_i \rightarrow W_i, \quad S : W \rightarrow W, \quad f_i \in W_i^*, \quad \text{and} \quad f \in W^* \tag{2.58}$$

for the corresponding Steklov-Poincaré operators and source functionals. As in the standard one-level formulation we introduce separate unknowns u_i for u and impose the continuity by the constraints

$$u_i(x^h) = u_j(x^h) \quad \text{for } x^h \in \Gamma_{ij}^h. \tag{2.59}$$

Additionally, we impose the (possibly inhomogeneous) Dirichlet boundary conditions by the constraints

$$u_i(x^h) = g_D(x^h) \quad \text{for } x^h \in \partial \Omega_i^h \cap \Gamma_D. \tag{2.60}$$

We define the space of Lagrange multipliers as $U := \mathbb{R}^m$, where m is the total number of constraints in (2.59) and (2.60). We can define a similar jump operator $B : W \rightarrow U^*$ as in Section 2.2.1 which evaluates additionally the jump on the Dirichlet interfaces $\partial \Omega_i \cap \Gamma_D$. For $\lambda \in U$ and $\mu \in U^*$ let again $\lambda_{ij}(x^h)$ and $\mu_{ij}(x^h)$ denote the components corresponding to the constraint (2.59) at the node $x^h \in \Gamma_{ij}^h$, respectively. Additionally, let $\lambda_{iD}(x^h)$ and

$\mu_{iD}(x^h)$ denote the components corresponding to the constraint (2.60) at the Dirichlet node $x^h \in \partial\Omega_i^h \cap \Gamma_D$. The operator $B : W \rightarrow U^*$ is defined by

$$\left\{ \begin{array}{ll} (Bw)_{ij}(x^h) = w_i(x^h) - w_j(x^h) & \text{for } x^h \in \Gamma_{ij}^h, \ i > j \\ (Bw)_{iD}(x^h) = w_i(x^h) & \text{for } x^h \in \partial\Omega_i^h \cap \Gamma_D \end{array} \right\} \quad \text{for } w \in W. \quad (2.61)$$

The operators $B_i : W_i \rightarrow U^*$ are defined accordingly such that $Bw = \sum_{i \in \mathcal{I}} B_i w_i$. We define $b \in U^*$ by

$$\left\{ \begin{array}{ll} b_{ij}(x^h) = 0 & \text{for } x^h \in \Gamma_{ij}^h, \\ b_{iD}(x^h) = g_D(x^h) & \text{for } x^h \in \partial\Omega_i^h \cap \Gamma_D. \end{array} \right. \quad (2.62)$$

In other words $b = B\tilde{g}_D$, where $(\tilde{g}_D)_i$ is the extension by zero of $g_D|_{\Gamma_D \cap \partial\Omega_i}$ to $\partial\Omega_i$ with respect to the nodal basis. We can summarize all the constraints in the compact form

$$Bu = b, \quad (2.63)$$

to be read as an equation in U^* . Note that

$$\widehat{W} := \{w \in W : Bw = 0\} \quad (2.64)$$

is the space of continuous functions which satisfy the homogeneous Dirichlet boundary conditions. Thus it coincides exactly with the corresponding space from the standard one-level formulation. Using the same tearing and interconnecting technique as in Section 2.2.1, we can derive the corresponding dual formulation: Find $(u, \lambda) \in W \times U$ such that

$$\begin{pmatrix} S & B^\top \\ B & 0 \end{pmatrix} \begin{pmatrix} u \\ \lambda \end{pmatrix} = \begin{pmatrix} f \\ b \end{pmatrix}. \quad (2.65)$$

Remark 2.14. As in the standard one-level formulation, the saddle point problem (2.65) can be derived directly from the skeleton formulation (2.14). We define the normal fluxes $t_i \in W_i^*$ by

$$t_i := S_i u_i - f_i,$$

and $t \in W^*$ by $\langle t, v \rangle := \sum_{i \in \mathcal{I}} \langle t_i, v_i \rangle_{\partial\Omega_i}$. As in Remark 2.6 we define the averaging operator $E : W \rightarrow \widehat{W} \subset W$ by

$$(Ew)_i(x^h) = \begin{cases} \frac{1}{|\mathcal{N}_{x^h}|} \sum_{j \in \mathcal{N}_{x^h}} w_j(x^h) & \text{for } x^h \in \partial\Omega_i^h \setminus \Gamma_D, \\ 0 & \text{for } x^h \in \partial\Omega_i^h \cap \Gamma_D, \end{cases} \quad (2.66)$$

for $w \in W$. Again, E is a projection onto \widehat{W} and it satisfies the identity $BE = 0$. Note that the space $V_D^h(\Gamma_S)$ can be identified with \widehat{W} and the skeleton formulation (2.14) yields the condition $\langle t, v \rangle = 0 \quad \forall v \in \widehat{W}$. Since each $v \in \widehat{W}$ can be represented by $E\tilde{v}$ for some $\tilde{v} \in W$, the complete set of equations reads

$$Su - t = f \quad \text{in } W^*, \quad Bu = b \quad \text{in } U^*, \quad E^\top t = 0 \quad \text{in } W^*.$$

The last condition can be eliminated introducing $\lambda \in U$ with $B^\top \lambda = -t$, which leads to problem (2.65).

Since the none of the local spaces W_i incorporates any Dirichlet boundary conditions, S_i always is singular, i. e.,

$$\ker S_i = \text{span}\{\mathbf{1}_{\partial\Omega_i}\}, \quad \text{range } S_i = \{v \in W_i^* : \langle v, \mathbf{1}_{\partial\Omega_i} \rangle = 0\} \quad \forall i \in \mathcal{I}. \quad (2.67)$$

Hence, all subdomains are floating in the sense of Definition 2.7. Also intuitively, imposing the Dirichlet boundary conditions by the Lagrange multipliers, all subdomains decouple from the Dirichlet boundary – they “float”, cf. Figure 2.1. For each $i \in \mathcal{I}$, define

$$R_i : \mathbb{R} \rightarrow W_i : \xi_i \mapsto \xi_i \mathbf{1}_{\partial\Omega_i}, \quad (2.68)$$

such that $R = \text{diag}(R_i) : \mathbb{R}^s \rightarrow \ker S$, and let S_i^\dagger be an arbitrary pseudoinverses of S_i . Analogously to Section 2.2.1, and with the abbreviations

$$F := B S^\dagger B^\top, \quad G := B R, \quad d := B S^\dagger f - b, \quad e := R^\top f, \quad (2.69)$$

(note that now d includes b) we arrive at the dual formulation

$$\begin{pmatrix} F & -G \\ G^\top & 0 \end{pmatrix} \begin{pmatrix} \lambda \\ \xi \end{pmatrix} = \begin{pmatrix} d \\ e \end{pmatrix}. \quad (2.70)$$

and the projected equation

$$P^\top F \tilde{\lambda} = P^\top (d - F \lambda_0), \quad (2.71)$$

where $P = I - Q G (G^\top Q G)^{-1} G^\top$ with $Q : U^* \rightarrow U$ specified below. The subspaces of admissible Lagrange increments read

$$\begin{aligned} V &:= \{\lambda \in U : \langle B z, \lambda \rangle = 0 \quad \forall z \in \ker S\} \\ &= \{\lambda \in U : \langle B_i^\top \lambda, \mathbf{1}_{\partial\Omega_i} \rangle = 0 \quad \forall i \in \mathcal{I}\}, \end{aligned} \quad (2.72)$$

$$V' := \{\mu \in U^* : \langle B z, Q \mu \rangle = 0 \quad \forall z \in \ker S\}. \quad (2.73)$$

Lemma 2.15. *The operator $P^\top F$ is SPD on the factor space $\tilde{V} = V_{/\ker B^\top}$.*

Proof. Analogously to Lemma 2.8. □

The preconditioner for $P^\top F$ is chosen to be $P M^{-1}$ with

$$M^{-1} := B_D S B_D^\top := \sum_{i \in \mathcal{I}} D_i B_i \mathcal{J}_{W_i} S_i \mathcal{J}_{W_i} B_i^\top D_i. \quad (2.74)$$

For the scaling operators $D_i : U^* \rightarrow U$ we can use the definition (2.51) from Section 2.2.1 and specify the additional values $(D_i \mu)_{iD}$ we need for the all-floating formulation. To summarize,

$$\left\{ \begin{array}{ll} (D_i \mu)_{ij}(x^h) := \delta_j^\dagger(x^h) \mu_{ij}(x^h) & \forall x^h \in \Gamma_{ij}^h \\ (D_i \mu)_{jD}(x^h) := \mu_{jD}(x^h) & \forall x^h \in \partial\Omega_j^h \cap \Gamma_D \end{array} \right\} \text{ for } \mu \in U^*, \quad (2.75)$$

with the weighted counting functions $\delta_j^\dagger(x^h)$ defined according to (2.50). Note that the factor in front of $\mu_{jD}(x^h)$ in the second line is 1 (although in general $\delta_j^\dagger(x^h) \neq 1$ for $x^h \in \partial\Omega_j^h \cap \Gamma_D$)

because the Dirichlet constraints are imposed locally on each subdomain. As in the standard one-level method, each block S_i in the preconditioner (2.74) may be replaced by the local hypersingular operator. Analogously to Section 2.2.1, the operator $Q : U^* \rightarrow U$ is either set to M^{-1} or chosen as

$$\left\{ \begin{array}{ll} (Q\mu)_{ij}(x^h) := \min(\alpha_i, \alpha_j) q_{ij}(x^h) \mu_{ij}(x^h) & \text{for } x^h \in \Gamma_{ij}^h, \\ (Q\mu)_{iD}(x^h) := \alpha_i q_i(x^h) \mu_{iD}(x^h) & \text{for } x^h \in \partial\Omega_i^h \cap \Gamma_D, \end{array} \right\} \quad \text{for } \mu \in U^*, \quad (2.76)$$

with $q_{ij}(x^h)$ and $q_i(x^h)$ defined as in the standard one-level formulation, i. e.,

$$q_i(x^h) := \left\{ \begin{array}{ll} (1 + \log(H_i/h_i)) \frac{h_i^2}{H_i} & \text{if } x^h \text{ lies on a face } \mathcal{F}_i \\ h_i & \text{if } x^h \text{ lies on an edge } \mathcal{E}_i \text{ or a vertex } \mathcal{V}_i \end{array} \right\} \quad \text{if } d = 3,$$

$$q_i(x^h) := \left\{ \begin{array}{ll} (1 + \log(H_i/h_i)) \frac{h_i}{H_i} & \text{if } x^h \text{ lies on an edge } \mathcal{E}_i \\ 1 & \text{if } x^h \text{ is a vertex } \mathcal{V}_i \end{array} \right\} \quad \text{if } d = 2,$$

$$q_{ij}(x^h) := \min(q_i(x^h), q_j(x^h)). \quad (2.77)$$

We see that structurally, the standard one-level and the all-floating methods do not differ from each other.

2.2.3 Implementation of one-level FETI/BETI methods

In this subsection we discuss implementation issues of the standard one-level and the all-floating FETI/BETI methods described above. The entire algorithm is displayed in Algorithm 1. The meaning of highlighted variables (boldface such as $\lambda^{(n)}$ and underlined such as $\underline{r}^{(n)}$) will be explained later on.

2.2.3.1 Mesh and topology information

In addition to the subdomain meshes and the usual coupling information, the algorithm needs the explicit information on the subdomain faces, edges, and vertices if Q is chosen in diagonal form according to (2.55)–(2.56) or (2.76)–(2.77). Either this topological information is provided together with a coarse mesh and updated during refinement, or it is generated from an already refined mesh by combinatorial means, see RHEINBACH [154, Sect. 3.3.3].

2.2.3.2 Implementation of the underlying operators

Jump operators. The operators B , B^\top , B_D and B_D^\top need not be stored but are encoded as routines which perform their application (matrix-by-vector multiplication).

Coarse space restriction/prolongation operators. Also the operators R and R^\top are not stored in matrix form but encoded directly.

Algorithm 1: Standard one-level / all-floating PCG FETI/BETI algorithm.

Input: f (and b for all-floating), ε , n_{\max}

Output: u

$$e = R^\top f$$

$$\underline{d} = B S^\dagger f \quad (\underline{d} = B S^\dagger f - b \quad \text{for all-floating})$$

$$\boldsymbol{\lambda}^{(0)} = Q G (G^\top Q G)^{-1} e$$

$$\underline{r}^{(0)} = P^\top (\underline{d} - F \boldsymbol{\lambda}^{(0)})$$

$$\mathbf{z}^{(0)} = P M^{-1} \underline{r}^{(0)}$$

$$\mathbf{s}^{(0)} = \mathbf{z}^{(0)}$$

$$\beta_0 = \langle \underline{r}^{(0)}, \mathbf{z}^{(0)} \rangle$$

$$n = 0$$

while $\beta_n \geq \beta_0 \cdot \varepsilon$ **and** $n < n_{\max}$ **do**

$$\underline{x}^{(n)} = P^\top F \mathbf{s}^{(n)}$$

$$\alpha_n = \langle \underline{x}^{(n)}, \mathbf{s}^{(n)} \rangle$$

$$\alpha = \beta_n / \alpha_n$$

$$\boldsymbol{\lambda}^{(n+1)} = \boldsymbol{\lambda}^{(n)} + \alpha \mathbf{s}^{(n)}$$

$$\underline{r}^{(n+1)} = \underline{r}^{(n)} - \alpha \underline{x}^{(n)}$$

$$\mathbf{z}^{(n+1)} = P M^{-1} \underline{r}^{(n+1)}$$

$$\beta_{n+1} = \langle \underline{r}^{(n+1)}, \mathbf{z}^{(n+1)} \rangle$$

$$\beta = \beta_{n+1} / \beta_n$$

$$\mathbf{s}^{(n+1)} = \mathbf{z}^{(n+1)} + \beta \mathbf{s}^{(n)}$$

$$n = n + 1$$

end

$$\xi = (G^\top Q G)^{-1} G^\top Q (F \boldsymbol{\lambda}^{(n)} - \underline{d})$$

$$u = S^\dagger (f - B^\top \boldsymbol{\lambda}^{(n)}) + R \xi$$

Local FEM Neumann problems. For a each $i \in \mathcal{I}_{\text{FEM}}$, the action $v_i = S_i^\dagger f_i$ for a given $f_i \in \text{range } S_i$ is performed as follows: Let \mathbf{v}_B and \mathbf{f}_B denote the vector representations of v_i and f_i , respectively, with respect to the standard nodal basis. Let \mathbf{K}_i denote the full FEM stiffness matrix on $\bar{\Omega}_i$ with respect to the same basis, grouped into DOFs on the subdomain boundary $\partial\Omega_i$ (subscript “B”) and DOFs in the interior of the subdomain Ω_i (subscript “I”), and \mathbf{S}_i the Schur complement of \mathbf{K}_i with respect to the interior DOFs, i. e.,

$$\mathbf{K}_i = \begin{pmatrix} \mathbf{K}_{BB}^{(i)} & \mathbf{K}_{BI}^{(i)} \\ \mathbf{K}_{IB}^{(i)} & \mathbf{K}_{II}^{(i)} \end{pmatrix}, \quad \mathbf{S}_i = \mathbf{K}_{BB}^{(i)} - \mathbf{K}_{BI}^{(i)} [\mathbf{K}_{II}^{(i)}]^{-1} \mathbf{K}_{IB}^{(i)}.$$

By definition, \mathbf{S}_i is the matrix representation of S_i . We search for some \mathbf{v}_B such that $\mathbf{S}_i \mathbf{v}_B = \mathbf{f}_B$. Introducing formally the auxiliary vector $\mathbf{v}_I = -[\mathbf{K}_{II}^{(i)}]^{-1} \mathbf{K}_{IB}^{(i)} \mathbf{v}_B$, we can rewrite the equation as

$$\begin{pmatrix} \mathbf{K}_{BB}^{(i)} & \mathbf{K}_{BI}^{(i)} \\ \mathbf{K}_{IB}^{(i)} & \mathbf{K}_{II}^{(i)} \end{pmatrix} \begin{pmatrix} \mathbf{v}_B \\ \mathbf{v}_I \end{pmatrix} = \begin{pmatrix} \mathbf{f}_B \\ \mathbf{0} \end{pmatrix},$$

which corresponds to solving a local problem with the full stiffness matrix \mathbf{K}_i . In case of a non-floating subdomain, some of the unknowns in \mathbf{v}_B are zero due to the definition of the space W_i , the corresponding rows and columns can be deleted, and the resulting matrix is SPD. For the floating subdomains, the solution $[\mathbf{v}_B^\top | \mathbf{v}_I^\top]^\top$ is unique only up to a constant. Both types of equations can be solved as discussed in Section 1.5.2. The factorizations of the corresponding matrices can be built and stored in the preprocessing phase.

Local BEM Neumann problems. For each $i \in \mathcal{I}_{\text{BEM}}$, the action $v_i = S_i^\dagger f_i$ for a given $f_i \in \text{range } S_i$ is performed as follows: Let \mathbf{v} and \mathbf{f} denote the vector representations of v_i and f_i , respectively, in the standard nodal basis. Let \mathbf{D}_i , \mathbf{K}_i , and \mathbf{V}_i denote the matrix representations of the hypersingular operator, the double layer potential, and the single layer potential, respectively, and let \mathbf{M}_i be the mass matrix from Section 1.5.3. Then $\mathbf{S}_i = \mathbf{D}_i + (\frac{1}{2}\mathbf{M}_i^\top + \mathbf{K}_i^\top) \mathbf{V}_i^{-1} (\frac{1}{2}\mathbf{M}_i + \mathbf{K}_i)$ is per construction the matrix representation of S_i . Instead of solving $\mathbf{S}_i \mathbf{v} = \mathbf{f}$, we formally introduce the auxiliary variable $\mathbf{t} = \mathbf{V}_i^{-1} (\frac{1}{2}\mathbf{M}_i + \mathbf{K}_i) \mathbf{v}$, and equivalently solve the saddle point problem

$$\begin{pmatrix} \mathbf{D}_i & \frac{1}{2}\mathbf{M}_i^\top + \mathbf{K}_i^\top \\ \frac{1}{2}\mathbf{M}_i + \mathbf{K}_i & -\mathbf{V}_i \end{pmatrix} \begin{pmatrix} \mathbf{v} \\ \mathbf{t} \end{pmatrix} = \begin{pmatrix} \mathbf{f} \\ \mathbf{0} \end{pmatrix},$$

which is a standard BEM problem corresponding to the local Neumann problem. If the subdomain Ω_i is floating, we can regularize the saddle point problem by regularizing the hypersingular operator \mathbf{D}_i similar as in the FEM case. As briefly described in Section 1.5.3 the matrices \mathbf{D}_i , \mathbf{K}_i , and \mathbf{V}_i can be approximated in data-sparse form using \mathcal{H} -matrices. Thus, also the matrix corresponding to the above, possibly regularized, saddle point problem is represented by an \mathcal{H} -matrix, and for each BEM subdomain its LU -factorization in the \mathcal{H} -arithmetic can be built and stored in quasi-optimal time and memory complexity in the preprocessing phase.

Local FEM Dirichlet problems. For each $i \in \mathcal{I}_{\text{FEM}}$, the action $f_i = S_i v_i$ for a given v_i is performed as follows: Let \mathbf{f}_B and \mathbf{v}_B denote the vector representations of f_i and v_i with

respect to the standard nodal basis, and let \mathbf{S}_i and \mathbf{K}_i be defined as above. Then, instead of forming the Schur complement and applying $\mathbf{f}_B = \mathbf{S}_i \mathbf{v}_B$ we solve the SPD system

$$\mathbf{K}_{II}^{(i)} \mathbf{v}_I = -\mathbf{K}_{IB}^{(i)} \mathbf{v}_B$$

for \mathbf{v}_I by a direct solver, and set $\mathbf{f}_B = \mathbf{K}_{BB}^{(i)} \mathbf{v}_B + \mathbf{K}_{BI}^{(i)} \mathbf{v}_I$. The factorization of $\mathbf{K}_{II}^{(i)}$ is also built and stored in the preprocessing phase.

Local BEM Dirichlet problems. For each $i \in \mathcal{I}_{\text{BEM}}$, the action of $f_i = S_i v_i$ for a given v_i is performed as follows: Let \mathbf{f} and \mathbf{v} denote the vector representations of f_i and v_i . Then we solve the SPD system

$$\mathbf{V}_i \mathbf{t} = \left(\frac{1}{2}\mathbf{M}_i + \mathbf{K}_i\right) \mathbf{v}$$

for \mathbf{t} , and set $\mathbf{f} = \mathbf{D}_i \mathbf{v} + \left(\frac{1}{2}\mathbf{M}_i^\top + \mathbf{K}_i^\top\right) \mathbf{t}$. An LU -factorization of \mathbf{V}_i in the \mathcal{H} -arithmetic can be built and stored in the preprocessing phase.

Operator F and preconditioner M^{-1} . Since $F = B S^\dagger B^\top$ and $M^{-1} = B_D S B_D^\top$ we see that the action of these operators mainly means solving local Dirichlet and Neumann problems as described above.

Coarse problem. Let \mathbf{G} and \mathbf{Q} denote the matrix representations of G and Q . As discussed in Remark 2.11, the matrix $\mathbf{G}^\top \mathbf{Q} \mathbf{G}$ is sparse and its sparsity pattern is determined by the connectivity graph of the subdomain partition where each floating subdomains is a node of that graph. Once $\mathbf{G}^\top \mathbf{Q} \mathbf{G}$ is assembled, its factorization (in the preprocessing phase) can be done very efficiently, as long as the number of subdomains is not very large. If we set $Q = M^{-1}$ an efficient assembly of $\mathbf{G}^\top \mathbf{Q} \mathbf{G}$ is tricky, and furthermore the extra actions of Q during the FETI/BETI algorithm involve the solution of extra local Dirichlet problems. Therefore, it is much more attractive to choose \mathbf{Q} as the diagonal matrix defined by (2.55)–(2.56) for standard one-level methods, or (2.76)–(2.77) for all-floating methods. In that case, the action of \mathbf{Q} and the assembly of $\mathbf{G}^\top \mathbf{Q} \mathbf{G}$ are of course cheap.

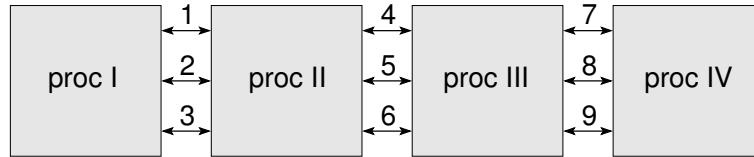
2.2.3.3 Stability with respect to redundancy

In Algorithm 1 we have highlighted the variables in the spaces U and U^* in the following way: The boldface variables $\boldsymbol{\lambda}^{(n)}$, $\mathbf{z}^{(n)}$, and $\mathbf{s}^{(n)}$ correspond to unknowns in V or $\lambda_0 + V$. The underlined variables $\underline{\mathbf{x}}^{(n)}$ and $\underline{\mathbf{r}}^{(n)}$ correspond to unknowns in $\tilde{V}' = V' \cap \text{range } B$. The key observations is that all operators applied to the boldface variables, such as F and B^\top , are invariant if we add elements from $\ker B^\top$, and each inner product of the form $\langle \underline{\mathbf{x}}^{(n)}, \mathbf{s}^{(n)} \rangle$ is invariant if we add terms from $\ker B^\top$ to $\mathbf{s}^{(n)}$ since $\underline{\mathbf{x}}^{(n)} \in \text{range } B$. Furthermore, all terms assigned to the underlined variables, such as $\underline{\mathbf{r}}^{(n)}$ really stay in $\tilde{V}' = V' \cap \text{range } B$. It can be shown by induction that the variables $\boldsymbol{\lambda}^{(n)}$, $\mathbf{z}^{(n)}$, and $\mathbf{s}^{(n)}$ are always sums of elements in $\text{range}(QB)$ and $\text{range } B_D$, i.e., sums of elements where the redundant parts are normalized. Therefore, no serious numerical stability problems will occur during the FETI/BETI iteration.

2.2.3.4 Parallelization

Algorithm 1 can easily be parallelized. In the simplest case each processor is responsible for one subdomain, but also the multi-subdomain case is possible. Each processor has to keep only the local mesh(es) with some information for communication. Such local meshes are either generated from a global mesh using a mesh partitioner such as METIS (see KARYPIS AND KUMAR [95, 96]). Alternatively, one can start from a geometric domain decomposition, mesh and distribute the skeleton Γ_S , and build the volume meshes in parallel.

The Lagrange parameters are global and have to be parallelized using the concept of *accumulated* and *distributed* vectors. We would like to briefly sketch this concept using a simple example. Below we see a sketch of a FETI method with nine Lagrange multipliers between four subdomains, each of them assigned to one processor. Due to the topology, two processors must handle six of the Lagrange multipliers, the others three of them.



The table below shows an accumulated and a distributed vector according to this setting: In the accumulated case, the entries of the vector of each processor match. In the distributed case, the entries of the local vectors must be summed up to the real value. For details we refer, e. g., to HAASE [77].

global index	accumulated				distributed				global vector
1	9	9	–	–	<u>5</u>	<u>4</u>	–	–	9
2	8	8	–	–	<u>3</u>	<u>5</u>	–	–	8
3	7	7	–	–	<u>6</u>	<u>1</u>	–	–	7
4	–	6	6	–	–	<u>3</u>	<u>3</u>	–	6
5	–	5	5	–	–	<u>3</u>	<u>2</u>	–	5
6	–	4	4	–	–	<u>3</u>	<u>1</u>	–	4
7	–	–	3	3	–	–	<u>1</u>	<u>2</u>	3
8	–	–	2	2	–	–	<u>-1</u>	<u>3</u>	2
9	–	–	1	1	–	–	<u>0</u>	<u>1</u>	1
processor	I	II	III	IV	I	II	III	IV	

The Lagrange variables in U and U^* in Algorithm 1 are encoded as accumulated and distributed vectors: The boldface variables, such as $\lambda^{(n)}$, correspond to accumulated vectors, whereas the underlined variables, such as $\underline{r}^{(n)}$, correspond to distributed vectors. The only communication is necessary for the evaluation of the inner products, the preconditioner, the projections, and the operations involving the coarse solver $(G^\top Q G)^{-1}$. For a more detailed discussion see OF [138]. If the data of the problem is kept locally as well, some extra communication is needed to provide the coefficient information for the weighted counting functions δ_j^\dagger .

2.2.3.5 Fast multipole and inexact BETI methods

We would like to mention, that the need of the assembling and the \mathcal{H} -LU factorization of the BEM matrices can be circumvented using special inexact formulations introduced by LANGER, OF, STEINBACH, AND ZULEHNER [122, 123], and which are related to an earlier work by KLAWONN AND WIDLUND [108]. There, the FETI/BETI system is rewritten as a two-fold saddle-point problem. For a pure BETI formulation it has the form

$$\begin{pmatrix} -V & \frac{1}{2}I + K & 0 \\ \frac{1}{2}I + K^\top & D & B^\top \\ 0 & B & \end{pmatrix} \begin{pmatrix} t \\ u \\ \lambda \end{pmatrix} = \begin{pmatrix} 0 \\ f \\ 0 \end{pmatrix}, \quad (2.78)$$

with the block operators $V = \text{diag}(V_i)$, $D = \text{diag}(D_i)$ (hyper singular operators), etc. Using standard preconditioners for the single layer potentials V_i and the Steklov-Poincaré operators S_i , and using the hypersingular BETI preconditioner, one can come up with an iterative method for the two-fold saddle-point problem which requires only the *application* of boundary element matrices, such as it is offered by the fast multipole method. The same technique can analogously be applied to hybrid FETI/BETI methods, as it is briefly discussed in LANGER AND PECHSTEIN [117].

2.2.4 Analysis of one-level FETI/BETI methods

In this subsection we show that the FETI/BETI methods described above are well-defined, and that the corresponding PCG subspace iteration is quasi-optimal. As discussed in Section 1.5.2.3, the convergence of the PCG method is determined by the condition number κ of the preconditioned system. In the case of one-level FETI/BETI we have to restrict this condition number to the subspace \tilde{V} . Following KLAWONN AND WIDLUND [109] we show that

$$\kappa \leq C \max_{i \in \mathcal{I}} (1 + \log(H_i/h_i))^2,$$

where the constant C is independent of H_i , h_i , the number of subdomains, and the values α_i of the coefficient. For a self-contained presentation we have included all the proofs in this work. Throughout the following analysis we extensively use the following (semi-)norms

$$|w_i|_{S_i} := \langle S_i w_i, w_i \rangle^{1/2}, \quad \text{for } w_i \in V^h(\partial\Omega_i), \quad (2.79)$$

$$|w|_S := \left(\sum_{i \in \mathcal{I}} |w_i|_{S_i}^2 \right)^{1/2} \quad \text{for } w \in \prod_{i \in \mathcal{I}} V^h(\partial\Omega_i). \quad (2.80)$$

2.2.4.1 Basic results on some of the FETI/BETI operators

First, we show that the projections P and P^\top are well-defined, and that the operator M^{-1} is SPD on $V' = \text{range } P^\top$. An important role is played by the projection operator

$$P_D := B_D^\top B, \quad (2.81)$$

whose properties are summarized in the following two lemmas. The result for standard one-level FETI methods was proved by KLAWONN AND WIDLUND [109], cf. [184].

Lemma 2.16. *The operator $P_D : W \rightarrow W$ defined in (2.81) satisfies the identities*

$$B M^{-1} B^\top = P_D^\top S P_D, \quad (2.82)$$

$$B P_D = B, \quad (2.83)$$

for both the standard one-level and the all-floating formulation. Furthermore, $E_D := I - P_D$ is a projection to the subspace \widehat{W} , and can be evaluated by

$$(E_D w)_i(x^h) := \begin{cases} \sum_{j \in \mathcal{N}_{x^h}} \delta_j^\dagger(x^h) w_j(x^h) & \text{for } x^h \in \partial\Omega_i^h \setminus \Gamma_D, \\ 0 & \text{for } x^h \in \partial\Omega_i^h \cap \Gamma_D. \end{cases} \quad (2.84)$$

In particular, $E_D w = w - P_D w$ satisfies the homogeneous Dirichlet boundary conditions on Γ_D , and $P_D w$ vanishes at all non-coupling Neumann nodes.

Proof. The identity $B M^{-1} B^\top = P_D^\top S P_D$ immediately follows from the definition of M^{-1} and P_D . From the definition of D_i , B_i , and B_D we find that for $v = B_D^\top \lambda$ we have

$$v_i(x^h) = \sum_{j \in \mathcal{N}_{x^h}} \pm \delta_j^\dagger(x^h) \lambda_{ij}(x^h) \quad \text{for } x^h \in \Gamma_{ij}^h,$$

$v_i(x^h) = \lambda_{iD}(x^h)$ for $x^h \in \partial\Omega_i^h \cap \Gamma_D$ in the all-floating case, and $v_i(x^h) = 0$ for non-coupling Neumann nodes $x^h \in (\partial\Omega_i^h \cap \Gamma_N) \setminus \Gamma$. Using the definition of the jump operator B and respecting the signs correctly, we obtain the formula

$$(P_D w)_i(x^h) = \begin{cases} \sum_{j \in \mathcal{N}_{x^h}} \delta_j^\dagger(x^h) (w_i(x^h) - w_j(x^h)) & \text{for } x \in \partial\Omega_i^h \setminus \Gamma_D, \\ w_i(x^h) & \text{for } x^h \in \partial\Omega_i^h \cap \Gamma_D. \end{cases} \quad (2.85)$$

It immediately implies that $P_D = I - E_D$ and therefore $B P_D = B - B E_D = B$. \square

Lemma 2.17. *For each $\mu \in \text{range } B$ we can find a function $w \in \text{range } P_D$ such that $\mu = B w$.*

Proof. Since $\mu \in \text{range } B$, we can find a function $\widehat{w} \in W$ with $\mu = B \widehat{w}$. By Lemma 2.16, $B P_D = B$. Hence, setting $w = P_D \widehat{w}$, we have $B w = B P_D \widehat{w} = B \widehat{w} = \mu$. \square

Remark 2.18. The weighted averaging operator E_D plays an important role in the theory of balancing Neumann-Neumann methods. If the coefficients α_i are all equal to one, we have $E_D = E$ with the operator E from Remark 2.6 for the standard one-level formulation, and Remark 2.14 for the all-floating formulation.

For the diagonal choices of Q according to (2.55)–(2.56) or (2.76)–(2.77), the operator Q is SPD per definition. Hence, $G^\top Q G$ is SPD, and therefore the projections P and P^\top are well-defined. As the following lemma shows, $G^\top Q G$ is also SPD for the choice $Q = M^{-1}$. We note that this issue has neither been discussed in [109] nor [184].

Lemma 2.19. *The operator $G^\top M^{-1} G$ is SPD, i. e.,*

$$\langle B z, M^{-1} B z \rangle > 0 \quad \forall z \in \ker S \setminus \{0\}.$$

Proof. From the definitions (2.54) and (2.74), we see that M^{-1} is positive semi-definite. To show the definiteness, assume that $\langle Bz, M^{-1}Bz \rangle = 0$ for some $z \in \ker S$. Due to identity (2.82) we obtain $|P_D z|_S^2 = 0$ which implies that $P_D z = z - E_D z \in \ker S$ and consequently, $E_D z \in \ker S$. However, $E_D z \in \ker B$ and $\ker S \cap \ker B = \{0\}$ imply that $E_D z = 0$. This means that the function z , which is piecewise constant on the subdomains, is continuous across the subdomain interfaces and vanishes on the Dirichlet boundary. Since the domain Ω is connected, there is no other possibility than $z = 0$, which shows the definiteness. \square

The next lemma follows [109] and shows that the preconditioner PM^{-1} is SPD on $\tilde{V}' = V' \cap \text{range } B$ for both choices of Q .

Lemma 2.20. *If Q is SPD on $\text{range } G$, then PM^{-1} is SPD on \tilde{V}' , i. e.,*

$$\langle \mu, M^{-1}\mu \rangle > 0 \quad \forall \mu \in \tilde{V}' \setminus \{0\}.$$

Proof. From the definitions (2.54) and (2.74), we see that M^{-1} is positive semi-definite. To show the definiteness on \tilde{V}' , we assume that

$$\langle \mu, M^{-1}\mu \rangle = 0 \quad \text{for some } \mu \in \tilde{V}'.$$

According to Lemma 2.17 we can find a function $w \in \text{range } P_D$ with $\mu = Bw$. Our assumption implies $\langle \mu, M^{-1}\mu \rangle = |P_D w|_S^2 = |w|_S^2 = 0$ and therefore $w \in \ker S$. From the definition of \tilde{V}' we conclude that

$$\underbrace{\langle Bw, Q \rangle}_{\in \tilde{V}'} \underbrace{Bw}_{\in \ker S} = 0.$$

Since Q is SPD on $\text{range } G = B(\ker S)$, we obtain that $\mu = Bw = 0$ which shows the definiteness. \square

2.2.4.2 The condition number estimate

Since we have seen that all operations in Algorithm 1 applied to elements in V are invariant if we add elements from $\ker B^\top$, we can identify all these elements using the factor space \tilde{V} . To be accurate in notation we introduce the operator $\Pi : V \rightarrow \tilde{V}$ which performs this identification. Lemma 2.8 and Lemma 2.15 show that the operator $P^\top F : \tilde{V} \rightarrow \tilde{V}'$ is SPD. From Lemma 2.20 we can conclude that the operator $\Pi P M^{-1} : \tilde{V}' \rightarrow \tilde{V}$ is SPD and has a well-defined SPD inverse

$$M : \tilde{V} \rightarrow \tilde{V}'. \tag{2.86}$$

The condition number of the preconditioned operator $\Pi P M^{-1} P^\top F : \tilde{V} \rightarrow \tilde{V}$ can be obtained by the Rayleigh quotient. We choose the inner product $\langle M \cdot, \cdot \rangle$ on the space \tilde{V} . If we have bounds $c_1, c_2 > 0$ such that

$$c_1 \leq \frac{\overbrace{\langle M \Pi P M^{-1} P^\top F \lambda, \lambda \rangle}^{=I}}{\langle M \lambda, \lambda \rangle} = \frac{\langle F \lambda, \lambda \rangle}{\langle M \lambda, \lambda \rangle} \leq c_2 \quad \forall \lambda \in \tilde{V}, \tag{2.87}$$

then $\kappa \leq c_2/c_1$.

The next two lemmas, proved in [109], characterize the operators F and M , and the space \tilde{V}' . Recall our convention that writing $\sup_{x \in X} \frac{a(x)}{b(x)}$ implicitly excludes those x from X with $a(x) = b(x) = 0$.

Lemma 2.21. *We have the identities*

$$\langle F \lambda, \lambda \rangle = \sup_{w \in W} \frac{\langle B w, \lambda \rangle^2}{|w|_S^2} \quad \forall \lambda \in \tilde{V}, \quad (2.88)$$

$$\langle M \lambda, \lambda \rangle = \sup_{\mu \in \tilde{V}'} \frac{\langle \mu, \lambda \rangle^2}{\langle \mu, M^{-1} \mu \rangle} \quad \forall \lambda \in \tilde{V}. \quad (2.89)$$

Proof. The second identity (2.89) follows from Lemma 1.1 and Lemma 2.17. For the first identity (2.88), recall that the pseudoinverse S^\dagger is SPD on $\text{range } S$ and that $B^\top \lambda \in \text{range } S$. Moreover, with $W_\perp := \text{range}(S^\dagger|_{\text{range } S})$ we have $W_\perp \oplus \ker S = W$. Finally, by Lemma 1.1,

$$\langle F \lambda, \lambda \rangle = \langle B^\top \lambda, S^\dagger B^\top \lambda \rangle = \sup_{w \in W_\perp} \frac{\langle B^\top \lambda, w \rangle^2}{|w|_S^2} = \sup_{\substack{w \in W_\perp \\ z \in \ker S}} \frac{\langle B(w+z), \lambda \rangle^2}{|w+z|_S^2} = \sup_{w \in W} \frac{\langle B^\top w, \lambda \rangle^2}{|w|_S^2},$$

where we have used that $\lambda \in V$. □

Lemma 2.22. *Let Q be SPD on $\text{range } G$ and symmetric positive semi-definite on U^* . Then, for any $w \in W$, there exists a unique $z_w \in \ker S$ such that $B(w+z_w) \in \tilde{V}'$. Moreover,*

$$z_w = \underset{z \in \ker S}{\text{argmin}} \|B(w+z)\|_Q, \quad \text{and} \quad \|B z_w\|_Q \leq \|B w\|_Q,$$

where $\|\mu\|_Q := \langle \mu, Q \mu \rangle^{1/2}$. The mapping $w \mapsto -z_w$ is a (linear) projection onto $\ker S = \text{range } R$ which is orthogonal with respect to the inner product induced by $B^\top Q B$.

Proof. Due to the definition of V' , the element z_w has to fulfill the equation

$$\langle Q B(w+z_w), B z \rangle = 0 \quad \forall z \in \ker S.$$

This is a Galerkin equation on the space $\ker S$, and equivalent to the above minimization problem because Q is SPD on $\text{range } G$. The solution z_w is explicitly given by

$$z_w = -R(G^\top Q G)^{-1} G^\top Q B w,$$

from which we see the linearity and the projection property. The minimizing property and the inequality follow from the Galerkin orthogonality. □

Until this point all the arguments were more or less algebraic and could be performed on the operator level. The key result for the FETI/BETI condition number bound, Lemma 2.27, however, needs deep insight in the structure of the underlying partial differential equation. Its statement

$$|P_D(w+z_w)|_S^2 \lesssim \max_{i \in \mathcal{I}} (1 + \log(H_i/h_i))^2 |w|_S^2 \quad \forall w \in W,$$

was proved by Klawonn and Widlund [109] for the standard one-level FETI case, building on a less general but pioneering proof by Mandel and Tezaur [131]. The standard one-level FETI/BETI case can be found in Langer and Steinbach [118, 119]. The general proof including the all-floating case will be given in Section 2.2.4.4. Before, we need some extra assumptions on the subdomain partition. The first assumption basically ensures that the subdomains are not very thin, cf. Toselli and Widlund [184, Assumption 4.3], Part 1, and it is stronger than Assumption 2.1.

Assumption 2.23. *Each subdomains is a union of a few simplices forming a bounded and connected Lipschitz domain. The simplices altogether form a coarse, shape-regular, and conforming triangulation \mathcal{T}_H of Ω . The number of simplices per subdomain is uniformly bounded.*

Remark 2.24. Assumption 2.23 is typical for iterative substructuring methods. It is of course very restrictive to assume that each subdomain is composed of a few simplices, in particular in view of mesh partitioning. Indeed, partitioning of unstructured meshes result in subdomains where one cannot even ensure that they are uniform Lipschitz. Recently, a new theory of domain decomposition methods for less regular subdomains was initiated by Dohrmann, Klawonn, and Widlund [44, 45] using in particular the theory of John domains (see Hajlasz [83] and the references therein). A complete analysis of FETI-DP methods in the plane is given by Klawonn, Rheinbach, and Widlund [113]. The three-dimensional case is still an open problem although there seem to be promising results [191]. We mention that one of the key tools for this theory is the Scott-Zhang quasi-interpolation operator, see Section 1.5.2.5. In this thesis we will stick to Assumption 2.23, also because we need uniform Lipschitz domains for the theory of boundary integral operators.

Assumption 2.23 implies that the number of subdomains sharing the same vertex, edge, or face is uniformly bounded, and the number of vertices, edges, and faces of a subdomain is uniformly bounded too.

The next assumption basically states that if a face intersects Γ_D the intersection has measure $\mathcal{O}(H_i^2)$ and is well-shaped, and if an edge intersects Γ_D the intersection has measure $\mathcal{O}(H_i)$ and is well-shaped too, see also [184, Assumption 4.3], Part 2. For simplicity, we introduce the following little bit stronger assumption.

Assumption 2.25. *The interface between the Dirichlet boundary Γ_D and the Neumann boundary Γ_N is aligned with the subdomain partition.*

With Definition 2.2 and Assumption 2.25, we find that $\Gamma_S \setminus (\Gamma \cup \Gamma_D)$ consists only of faces (edges in two dimensions) which are part of the Neumann boundary Γ_N .

The next assumption is only needed for the standard one-level method, and can be dropped in the all-floating case.

Assumption 2.26. *In case of the standard one-level formulation in three dimensions, we have to assume that the intersection of a subdomain boundary $\partial\Omega_i$ with the Dirichlet boundary Γ_D is either empty or at least a subdomain edge.*

For the following lemma and theorem, let all the assumptions from above be fulfilled, in particular Assumption 2.23, Assumption 2.25, and Assumption 2.26.

Lemma 2.27. *For the standard one-level or the all-floating method, let either Q be chosen according to (2.55)–(2.56), respectively (2.76)–(2.77), or let $Q = M^{-1}$. Then,*

$$|P_D(w + z_w)|_S^2 \leq C \max_{i \in \mathcal{I}} (1 + \log(H_i/h_i))^2 |w|_S^2 \quad \forall w \in W,$$

where $z_w \in \ker S$ is the unique element from Lemma 2.22 and the constant C is independent of H_i , h_i , the number of subdomains, and the values α_i of the coefficient.

Proof. Postponed to Section 2.2.4.4 □

With this lemma, we can formulate the main theorem on the condition number of the FETI/BETI algorithm, which is taken from [109].

Theorem 2.28. *For the standard one-level or the all-floating method, let either Q be chosen according to (2.55)–(2.56), respectively (2.76)–(2.77), or let $Q = M^{-1}$. Then we have the condition number bound*

$$\kappa \leq C \max_{i \in \mathcal{I}} (1 + \log(H_i/h_i))^2,$$

where the constant C is independent of H_i , h_i , the number of subdomains, and the values α_i of the coefficient.

Proof. With the previous considerations it suffices to show the upper and lower bound in (2.87).

Lower bound. Let $\mu \in \tilde{V}'$ be arbitrary. Due to Lemma 2.17 we can find a function $w \in \text{range } P_D$ with $Bw = \mu$. From Lemma 2.21 and Lemma 2.16 we obtain that

$$\langle F\lambda, \lambda \rangle \geq \frac{\langle Bw, \lambda \rangle^2}{|w|_S^2} = \frac{\langle \mu, \lambda \rangle^2}{|P_D w|_S^2} = \frac{\langle \mu, \lambda \rangle^2}{\langle Bw, M^{-1}Bw \rangle} = \frac{\langle \mu, \lambda \rangle^2}{\langle \mu, M^{-1}\mu \rangle} \quad \forall \lambda \in \tilde{V}. \quad (2.90)$$

Since $\mu \in \tilde{V}'$ was arbitrary, this implies the desired lower bound with $c_1 = 1$.

Upper bound. Let $\lambda \in \tilde{V}$ be arbitrary but fixed. According to Lemma 2.22, for each $w \in W$ there exists a unique $z_w \in \ker S$ with $B(w + z_w) \in \tilde{V}'$. It is also easy to see that the set $\{B(w + z_w) : w \in W\}$ is a non-trivial subset of \tilde{V}' . We obtain

$$\begin{aligned} \langle M\lambda, \lambda \rangle &\stackrel{\text{Lemma 2.21}}{=} \sup_{\mu \in \tilde{V}'} \frac{\langle \mu, \lambda \rangle^2}{\langle \mu, M^{-1}\mu \rangle} \\ &\stackrel{\text{smaller space}}{\geq} \sup_{w \in W} \frac{\langle B(w + z_w), \lambda \rangle^2}{\langle B(w + z_w), M^{-1}B(w + z_w) \rangle} \\ &\stackrel{z_w \in \ker S, \lambda \in \tilde{V}}{=} \sup_{w \in W} \frac{\langle Bw, \lambda \rangle^2}{|P_D(w + z_w)|_S^2} \\ &\stackrel{\text{Lemma 2.27}}{\geq} \frac{1}{C \max_{i \in \mathcal{I}} (1 + \log(H_i/h_i))^2} \sup_{w \in W} \frac{\langle Bw, \lambda \rangle^2}{|w|_S^2} \\ &\stackrel{\text{Lemma 2.21}}{=} \frac{1}{C \max_{i \in \mathcal{I}} (1 + \log(H_i/h_i))^2} \langle F\lambda, \lambda \rangle, \end{aligned}$$

which shows the desired upper bound with $c_2 = C \max_{i \in \mathcal{I}} (1 + \log(H_i/h_i))^2$. □

Remark 2.29. As shown in BRENNER [23], the condition number bound from Theorem 2.28 is sharp in two dimensions. Sharp bounds for the closely related Neumann-Neumann method in three dimensional can be found in BRENNER AND HE [25].

2.2.4.3 Technical tools

Recalling the characterization (2.85) of the P_D operator,

$$(P_D w)_i(x^h) = \begin{cases} \sum_{j \in \mathcal{N}_{x^h}} \delta_j^\dagger(x^h) (w_i(x^h) - w_j(x^h)) & \text{for } x \in \partial\Omega_i^h \setminus \Gamma_D, \\ w_i(x^h) & \text{for } x^h \in \partial\Omega_i^h \cap \Gamma_D, \end{cases}$$

we see that the operator delivers a weighted difference of w_i and neighboring functions w_j . Obviously, the set of neighboring functions changes if we move, e. g., from a subdomain face to a subdomain edge (see Definition 2.2). We can easily construct a function $u \in W$ such that $(P_D u)_i$ is supported only on an edge by choosing u discontinuous across the edge and continuous elsewhere. This observation suggests that we can estimate the face, edge, and vertex contributions of $P_D(w + z_z)$ separately without being too generous. Indeed, BRENNER AND HE [25] showed that the estimate in Theorem 2.28 is sharp. In order to separate the contributions we define the following cut-off functions, according to [184, Section 4.6].

Definition 2.30 (Finite element cut-off functions).

- For a vertex \mathcal{V}_i we define the function $\theta_{\mathcal{V}_i} \in V^h(\partial\Omega_i)$ as being 1 at the vertex \mathcal{V}_i , and zero on all other nodes.
- For an edge \mathcal{E}_i we define $\theta_{\mathcal{E}_i} \in V^h(\partial\Omega_i)$ as being 1 at the nodes on the (open) edge \mathcal{E}_i , and zero on all other nodes.
- For a face \mathcal{F}_i we define $\theta_{\mathcal{F}_i} \in V^h(\partial\Omega_i)$ as being 1 at the nodes on the (open) face \mathcal{F}_i , zero on all nodes.

Definition 2.31. Let I^h denote the nodal interpolator onto $V^h(\Omega_i)$ (resp. $V^h(\partial\Omega_i)$) which is continuous in the H^1 -seminorm (resp. $H^{1/2}$ -seminorm) and in the L^2 -norm for quadratic functions. See [184, Lemma 3.9].

Notation. We write \mathcal{X}_i generically for a face, edge, or vertex on $\partial\Omega_i$. By the expressions

$$\sum_{\mathcal{X}_i} I^h(\theta_{\mathcal{X}_i} w_i), \quad \sum_{\mathcal{X}_i \subset \Gamma} I^h(\theta_{\mathcal{X}_i} w_i), \quad \text{and} \quad \sum_{\mathcal{X}_i \subset \Gamma_D} I^h(\theta_{\mathcal{X}_i} w_i),$$

we mean that we sum over all faces, edges, and vertices on $\partial\Omega_i$, $\partial\Omega_i \cap \Gamma$, and $\partial\Omega_i \cap \Gamma_D$, respectively. In two dimensions, the faces are of course skipped.

The cut-off functions provide a partition of unity in the sense that

$$\sum_{\mathcal{X}_i} I^h(\theta_{\mathcal{X}_i} u) = u \quad \forall u \in V^h(\partial\Omega_i). \tag{2.91}$$

Definition 2.32 (discrete harmonic extension). For a function $u \in V^h(\partial\Omega_i)$ let $\mathcal{H}_i u \in V^h(\Omega_i)$ denote its discrete harmonic extension from $\partial\Omega_i$ to Ω_i such that

$$\mathcal{H}_i u = \underset{\substack{\tilde{u} \in V^h(\Omega_i) \\ \tilde{u}|_{\partial\Omega_i} = u}}{\operatorname{argmin}} |\tilde{u}|_{H^1(\Omega_i)}. \tag{2.92}$$

Due to the minimization property of the FEM Schur complement (Lemma 1.32) we have

$$|u|_{S_i}^2 = \alpha_i |\mathcal{H}_i u|_{H^1(\Omega_i)}^2 \quad \text{for } i \in \mathcal{I}_{\text{FEM}}. \quad (2.93)$$

In order to work with discrete harmonic extensions in the BEM domains as well, we introduce auxiliary quasi-uniform and shape-regular triangulations $\mathcal{T}(\Omega_i)$ with mesh parameter h_i for $i \in \mathcal{I}_{\text{BEM}}$. Due to the FEM-BEM equivalence from Lemma 1.33, we have

$$|u|_{S_i}^2 \simeq \alpha_i |\mathcal{H}_i u|_{H^1(\Omega_i)}^2 \quad \text{for } i \in \mathcal{I}_{\text{BEM}}. \quad (2.94)$$

Notation. To be short, we write $\mathcal{H}_i(\theta_{\mathcal{X}_i} u)$ for $\mathcal{H}_i(I^h(\theta_{\mathcal{X}_i} u))$.

Notation. In the sequel we use a scaled H^1 -norm defined by

$$\|u\|_{H^1(\Omega_i)}^2 = |u|_{H^1(\Omega_i)}^2 + \frac{1}{H_i^2} \|u\|_{L^2(\Omega_i)}^2, \quad (2.95)$$

which helps to keep track of the explicit dependency of the following estimates on the sub-domain diameters H_i .

The following two lemmas give several estimates on discrete spaces. The indicated references are to be understood as sources where the corresponding estimates can be found, but not necessarily the original sources.

Lemma 2.33. *In two dimensions, for all functions $u \in V^h(\Omega_i)$ we have*

- (i) $|\mathcal{H}_i(\theta_{\mathcal{V}_i} u)|_{H^1(\Omega_i)}^2 \lesssim |u(\mathcal{V}_i)|^2 \leq \|u\|_{L^\infty(\Omega_i)}^2$ *(trivially)*
- (ii) $\|u\|_{L^\infty(\Omega_i)}^2 \lesssim (1 + \log(H_i/h_i)) \|u\|_{H^1(\Omega_i)}^2$ *[184, Lemma 4.15]*
- (iii) $|\mathcal{H}_i(\theta_{\mathcal{E}_i} u)|_{H^1(\Omega_i)}^2 \lesssim (1 + \log(H_i/h_i))^2 \|u\|_{H^1(\Omega_i)}^2$,
- (iv) $|\mathcal{H}_i \theta_{\mathcal{E}_i}|_{H^1(\Omega_i)}^2 \lesssim (1 + \log(H_i/h_i))$.

For inequality (iii) we refer, e. g., to MANDEL AND BREZINA [129, Lemma 4.5] which provides (iv) as a byproduct. The first inequalities of that kind were probably given in BRAMBLE, PASCIAK, AND SCHATZ [19]. See BRENNER AND SUNG [28] for sharp estimates.

Lemma 2.34. *In three dimensions, for all functions $u \in V^h(\Omega_i)$ we have*

- (i) $|\mathcal{H}_i(\theta_{\mathcal{E}_i} u)|_{H^1(\Omega_i)}^2 \lesssim \|u\|_{L^2(\mathcal{E}_i)}^2$ *[184, Lemma 4.19]*
- (ii) $\|u\|_{L^2(\mathcal{E}_i)}^2 \lesssim (1 + \log(H_i/h_i)) \|u\|_{H^1(\Omega_i)}^2$ *[184, Lemma 4.16]*
- (iii) $|\mathcal{H}_i(\theta_{\mathcal{F}_i} u)|_{H^1(\Omega_i)}^2 \lesssim (1 + \log(H_i/h_i))^2 \|u\|_{H^1(\Omega_i)}^2$ *[184, Lemma 4.24]*
- (iv) $|\mathcal{H}_i \theta_{\mathcal{F}_i}|_{H^1(\Omega_i)}^2 \lesssim (1 + \log(H_i/h_i)) H_i$ *[184, Lemma 4.25]*

For a vertex \mathcal{V}_i in three dimensions, we see that $u(\mathcal{V}_i) \varphi_{\mathcal{V}_i}$ is a discrete extension of $I^h(\theta_{\mathcal{V}_i} u)$, where $\varphi_{\mathcal{V}_i}$ denotes the nodal finite element basis function corresponding to \mathcal{V}_i . Therefore, we obtain the trivial estimate

$$|\mathcal{H}_i(\theta_{\mathcal{V}_i} u)|_{H^1(\Omega_i)}^2 \lesssim h_i |u(\mathcal{V}_i)|^2 \leq \|u\|_{L^2(\mathcal{E}_i)}^2, \quad (2.96)$$

where \mathcal{E}_i is an edge with \mathcal{V}_i being one of its endpoints.

Remark 2.35. The face estimates in Lemma 2.34 are proved constructing a particular function $\vartheta_{\mathcal{F}_i} \in V^h(\Omega_i)$ which is an extension of $\theta_{\mathcal{F}_i}$ and which satisfies the same estimates. Similarly the edge estimates are proved using the function $\vartheta_{\mathcal{E}_i} \in V^h(\Omega_i)$ which equals 1 at all the nodes on the open edge \mathcal{E}_i , and zero elsewhere.

Corollary 2.36. *The cut-off functions from Definition 2.30 induce a stable decomposition in the sense that*

$$\sum_{\mathcal{X}_i} |\mathcal{H}_i(\theta_{\mathcal{X}_i} u)|_{H^1(\Omega_i)}^2 \lesssim (1 + \log(H_i/h_i))^2 \|u\|_{H^1(\Omega_i)}^2.$$

The constant hidden in “ \lesssim ” depends on the number of faces, edges, and vertices of Ω_i , which is due to our assumptions uniformly bounded by a relatively small number.

Proof. Directly follows from Lemma 2.34 and Lemma 2.33. □

The following lemma is kind of reverse to Corollary 2.36: The composition of cutted parts of a function is continuous in the energy norm.

Lemma 2.37. *For each $u \in V^h(\Omega_i)$ we have*

$$|\mathcal{H}_i u|_{H^1(\Omega_i)}^2 \lesssim \sum_{\mathcal{X}_i} |\mathcal{H}_i(\theta_{\mathcal{X}_i} u)|_{H^1(\Omega_i)}^2,$$

The constant hidden in “ \lesssim ” depends only on the number of faces, edges, and vertices of Ω_i .

Proof. With the partition of unity property (2.91) we see that $\sum_{\mathcal{X}_i} \mathcal{H}_i(\theta_{\mathcal{X}_i} u)$ is a discrete extension of u from $\partial\Omega_i$ to Ω_i . The minimization property (2.92) and the triangle inequality imply

$$|\mathcal{H}_i u|_{H^1(\Omega_i)}^2 \leq \left(\sum_{\mathcal{X}_i} |\mathcal{H}_i(\theta_{\mathcal{X}_i} u)|_{H^1(\Omega_i)} \right)^2.$$

Using the Cauchy-Schwarz inequality in the Euclidean space \mathbb{R}^m , where m is the number of faces, edges, and vertices of Ω_i , we obtain the desired statement. □

If a non-floating subdomain intersects the Dirichlet boundary Γ_D only in an edge (vertex in two dimensions), we cannot use a Friedrichs inequality, which we can if the intersection is a face. The following discrete Poincaré-Friedrichs inequality helps to overcome this problem in the discrete case.

Lemma 2.38 (Discrete Poincaré-Friedrichs inequality). *In two dimensions, let \mathcal{V}_i be a vertex of Ω_i . Then we have,*

$$\|u - u(\mathcal{V}_i)\|_{L^2(\Omega_i)}^2 \lesssim H_i^2 (1 + \log(H_i/h_i)) |u|_{H^1(\Omega_i)}^2 \quad \forall u \in V^h(\Omega_i).$$

In three dimensions, let \mathcal{E}_i be an edge of Ω_i . Then we have

$$\|u - \bar{u}^{\mathcal{E}_i}\|_{L^2(\Omega_i)}^2 \lesssim H_i^2 (1 + \log(H_i/h_i)) |u|_{H^1(\Omega_i)}^2 \quad \forall u \in V^h(\Omega_i),$$

with the edge average $\bar{u}^{\mathcal{E}_i} := \frac{1}{|\mathcal{E}_i|} \int_{\mathcal{E}_i} u \, ds$.

Proof. The statement in two dimensions is a direct consequence of Lemma 2.33,(i)–(ii). The three-dimensional case is proved using Lemma 2.34,(ii) and a Poincaré type inequality, see [184, Lemma 4.21]. \square

The last statement we need is that the discrete harmonic extensions from a face to its two adjacent subdomains are equivalent in the energy norm.

Lemma 2.39. *Let \mathcal{F}_{ij} be a face shared by Ω_i and Ω_j . Then,*

$$|\mathcal{H}_i(\theta_{\mathcal{F}_{ij}}u)|_{H^1(\Omega_i)}^2 \simeq |\mathcal{H}_j(\theta_{\mathcal{F}_{ij}}u)|_{H^1(\Omega_j)}^2 \quad \forall u \in V^h(\mathcal{F}_{ij}).$$

Proof. We present two techniques.

(i) One can use the discrete trace theorem (cf. [184, Lemma 4.6]) stating that

$$|\mathcal{H}_k(\theta_{\mathcal{F}_{ij}}u)|_{H^1(\Omega_k)}^2 \simeq |I^h(\theta_{\mathcal{F}_{ij}}u)|_{H^{1/2}(\partial\Omega_k)}^2 \quad \text{for } k = i, j.$$

The norm on the right hand side is equivalent to the $H_{00}^{1/2}$ -norm on the open face \mathcal{F}_{ij} for both $k = i$ and j and the equivalence constant depends only on the shapes of Ω_i and Ω_j because $H_i \simeq H_j$.

(ii) Let \mathcal{U}_{ij} denote the open union of Ω_i and Ω_j . Due to the extension theorem (cf. EVANS [53, Sect. 5.4]), there exists an operator $E_{ij} : H^1(\Omega_i) \rightarrow H^1(\mathcal{U}_{ij})$ with

$$(E_{ij}w)|_{\Omega_i} = w, \quad \text{and} \quad |E_{ij}w|_{H^1(\mathcal{U}_{ij})}^2 \lesssim |w|_{H^1(\Omega_i)}^2 \quad \forall w \in V^h(\Omega_i). \quad (2.97)$$

The hidden constant depends only on the shapes of Ω_i and \mathcal{U}_{ij} . As shown by SCOTT AND ZHANG [170], cf. Lemma 1.28, there exists a quasi-interpolation operator $\Pi^h : H^1(\mathcal{U}_{ij}) \rightarrow V^h(\mathcal{U}_{ij})$ with

$$\begin{aligned} (\Pi^h w)|_{\mathcal{F}_{ij}} &= w & \forall w \in V^h(\mathcal{U}_{ij}), \\ |\Pi^h w|_{H^1(\mathcal{U}_{ij})}^2 &\lesssim |w|_{H^1(\mathcal{U}_{ij})}^2 & \forall w \in H^1(\mathcal{U}_{ij}). \end{aligned} \quad (2.98)$$

The hidden constant depends only on the shapes regularity constant of $\mathcal{T}(\mathcal{U}_i)$. With these two operators we can conclude that for $\tilde{u}_i := \mathcal{H}_i(\theta_{\mathcal{F}_i}u)$, the function $(\Pi^h E_{ij}\tilde{u}_i)|_{\Omega_j}$ is an extension of $I^h(\theta_{\mathcal{F}_{ij}}u)$ from $V^h(\partial\Omega_j)$ to $V^h(\Omega_j)$. Finally, we can conclude from (2.97) and (2.98) that

$$|\mathcal{H}_j(\theta_{\mathcal{F}_{ij}}u)|_{H^1(\Omega_j)}^2 \lesssim |\Pi^h E_{ij}\tilde{u}_i|_{H^1(\Omega_j)}^2 \lesssim |E_{ij}\tilde{u}_i|_{H^1(\mathcal{U}_{ij})}^2 \lesssim |\tilde{u}_i|_{H^1(\Omega_i)}^2.$$

Switching the roles of i and j finishes the proof. \square

Remark 2.40. The norm $|\mathcal{H}_i(\theta_{\mathcal{F}_{ij}}u)|_{H^1(\Omega_i)}^2$ is a discrete realization of the $H_{00}^{1/2}$ -norm of u on the open face \mathcal{F}_{ij} .

2.2.4.4 The P_D -estimates

Applying the tools from the last subsection to $|(P_D w)_i|_{S_i}^2$ we will end up with terms in the scaled H^1 -norm,

$$\|\mathcal{H}_i w_i\|_{H^1(\Omega_i)}^2 = |\mathcal{H}_i w_i|_{H^1(\Omega_i)}^2 + \frac{1}{H_i^2} \|\mathcal{H}_i w_i\|_{L^2(\Omega_i)}^2.$$

In order to eliminate the L^2 -norms we would like to employ a Poincaré inequality on the floating subdomains: If the mean value of $\mathcal{H}_i w_i$ over the boundary $\partial\Omega_i$ vanishes, we have

$$\frac{1}{H_i^2} \|\mathcal{H}_i w_i\|_{L^2(\Omega_i)}^2 \leq \frac{1}{H_i^2} C_P^2 H_i^2 |\mathcal{H}_i w_i|_{H^1(\Omega_i)}^2 \lesssim |\mathcal{H}_i w_i|_{H^1(\Omega_i)}^2,$$

due to Corollary 1.10. The next lemma helps to make Poincaré's inequality applicable.

Lemma 2.41. *The following inequalities are equivalent.*

$$\begin{aligned} |P_D(w + z_w)|_S^2 &\leq C^* |w|_S^2 & \forall w \in W, \\ |P_D(w + z_w)|_S^2 &\leq C^* |w|_S^2 & \forall w \in W^\perp, \end{aligned}$$

where

$$W^\perp := \left\{ w \in W : \int_{\Omega_i} (\mathcal{H}_i w_i)(x) dx = 0 \quad \forall i \in \mathcal{I}_{\text{float}} \right\}.$$

Proof. Of course the first inequality implies the second one. Assume that the second inequality holds true, and let $w \in W$ be arbitrary but fixed. First, Lemma 2.22 states that the mapping $w \mapsto z_w$ is linear and that $z_y = -y$ for $y \in \ker S$. Therefore, $w + z_w = (w + y) + (z_{w+y})$ for any $y \in \ker S$. Secondly, $|w + y|_S^2 = |w|_S^2$ for any $y \in \ker S$. We can easily find an element $y_w \in \ker S$ such that $w + y_w \in W^\perp$ by setting

$$(y_w)_i := \frac{1}{|\Omega_i|} \int_{\Omega_i} (\mathcal{H}_i w_i)(x) dx \quad \text{for } i \in \mathcal{I}_{\text{float}}, \quad (y_w)_i := 0 \quad \text{for } i \notin \mathcal{I}_{\text{float}}.$$

Apparently, the above invariants directly imply the first inequality. □

Lemma 2.42. *We have*

$$|P_D w|_S^2 \lesssim \max_{i \in \mathcal{I}} (1 + \log(H_i/h_i))^2 |w|_S^2 \quad \forall w \in W^\perp.$$

Proof. We give the proof in three dimensions. The two-dimensional case works analogously. Let $w \in W^\perp$ and $i \in \mathcal{I}$ be fixed. Recall the characterization (2.85) of the P_D operator,

$$(P_D w)_i(x^h) = \begin{cases} \sum_{j \in \mathcal{N}_{x^h}} \delta_j^\dagger(x^h) (w_i(x^h) - w_j(x^h)) & \text{for } x \in \partial\Omega_i^h \setminus \Gamma_D, \\ w_i(x^h) & \text{for } x^h \in \partial\Omega_i^h \cap \Gamma_D, \end{cases}$$

which reveals that there is no contribution on non-coupling Neumann nodes. As noticed before, the index sets \mathcal{N}_{x^h} are invariant for $x^h \in \mathcal{X}_i$, which justifies to write $\mathcal{N}_{\mathcal{X}_i}$ for these sets. Using the BEM-FEM spectral equivalence (2.94) and Lemma 2.37 we obtain

$$\begin{aligned} |(P_D w)_i|_{S_i}^2 &\lesssim \alpha_i |\mathcal{H}_i(P_D w)_i|_{H^1(\Omega_i)}^2 \\ &\lesssim \underbrace{\alpha_i \sum_{\mathcal{X}_i \subset \Gamma} \left| \mathcal{H}_i \left\{ \theta_{\mathcal{X}_i} \sum_{j \in \mathcal{N}_{\mathcal{X}_i}} \delta_j^\dagger(w_i - w_j) \right\} \right|_{H^1(\Omega_i)}^2}_{=: \Upsilon_i} + \alpha_i \sum_{\mathcal{X}_i \subset \Gamma_D} |\mathcal{H}_i(\theta_{\mathcal{X}_i} w_i)|_{H^1(\Omega_i)}^2. \end{aligned} \quad (2.99)$$

Since the weighted counting functions δ_j^\dagger are invariant on the nodes on faces, edges, and vertices \mathcal{X}_i , we can write $\delta_j^\dagger|_{\mathcal{X}_i}$ for these constant values. Using the fact that each face, edge, and vertex is shared by a uniformly bounded number of subdomains, we obtain

$$\Upsilon_i \lesssim \sum_{\mathcal{X}_i \subset \Gamma} \sum_{j \in \mathcal{N}_{\mathcal{X}_i}} \alpha_i (\delta_j^\dagger|_{\mathcal{X}_i})^2 |\mathcal{H}_i(\theta_{\mathcal{X}_i}(w_i - w_j))|_{H^1(\Omega_i)}^2.$$

With the inequality

$$\alpha_i (\delta_j^\dagger(x^h))^2 \leq \min(\alpha_i, \alpha_j) \quad \forall x^h \in \Gamma_{ij}^h, \quad (2.100)$$

which can be proved by an elementary argument, we can conclude that

$$\Upsilon_i \lesssim \sum_{\mathcal{X}_i \subset \Gamma} \sum_{j \in \mathcal{N}_{\mathcal{X}_i}} \min(\alpha_i, \alpha_j) |\mathcal{H}_i(\theta_{\mathcal{X}_i}(w_i - w_j))|_{H^1(\Omega_i)}^2 \lesssim \sum_{\mathcal{X}_i \subset \Gamma} \sum_{j \in \mathcal{N}_{\mathcal{X}_i}} \alpha_j |\mathcal{H}_i(\theta_{\mathcal{X}_i} w_j)|_{H^1(\Omega_i)}^2.$$

Combining with (2.99) we obtain

$$|(P_D w)_i|_{S_i}^2 \lesssim \sum_{\mathcal{X}_i \subset \Gamma \cup \Gamma_D} \sum_{j \in \mathcal{N}_{\mathcal{X}_i}} \alpha_j |\mathcal{H}_i(\theta_{\mathcal{X}_i} w_j)|_{H^1(\Omega_i)}^2. \quad (2.101)$$

- For faces \mathcal{F}_i , Lemma 2.39 and Lemma 2.34(iii) gives

$$|\mathcal{H}_i(\theta_{\mathcal{F}_i} w_j)|_{H^1(\Omega_i)}^2 \lesssim |\mathcal{H}_j(\theta_{\mathcal{F}_i} w_j)|_{H^1(\Omega_j)}^2 \lesssim (1 + \log(H_j/h_j))^2 \|\mathcal{H}_j w_j\|_{H^1(\Omega_j)}^2 \quad \forall j \in \mathcal{N}_{\mathcal{F}_i}.$$

- For an edge \mathcal{E}_i , Lemma 2.34(i)–(ii) yields

$$|\mathcal{H}_i(\theta_{\mathcal{E}_i} w_j)|_{H^1(\Omega_i)}^2 \lesssim \|u\|_{L^2(\mathcal{E}_i)}^2 \lesssim (1 + \log(H_j/h_j)) \|w_j\|_{H^1(\Omega_j)}^2 \quad \forall j \in \mathcal{N}_{\mathcal{E}_i}.$$

- For a vertex \mathcal{V}_i we can find an edge \mathcal{E}_j for each $j \in \mathcal{N}_{\mathcal{V}_i}$ touching \mathcal{V}_i and obtain from (2.96) that

$$|\mathcal{H}_i(\theta_{\mathcal{V}_i} w_j)|_{H^1(\Omega_i)}^2 \lesssim \|u\|_{L^2(\mathcal{E}_j)}^2.$$

From here we can continue as in the edge case.

Summarizing, we have

$$|(P_D w)_i|_{S_i}^2 \lesssim \sum_{j \in \mathcal{N}_i} \alpha_j (1 + \log(H_j/h_j))^2 \|\mathcal{H}_j w_j\|_{H^1(\Omega_j)}^2, \quad (2.102)$$

where \mathcal{N}_i is the index set of subdomains which are neighbors of Ω_i . Since $w \in W^\perp$, we can use Poincaré's inequality on the floating subdomains to obtain

$$\|\mathcal{H}_j w_j\|_{H^1(\Omega_j)}^2 \lesssim |\mathcal{H}_j w_j|_{H^1(\Omega_j)}^2 \quad \forall j \in \mathcal{I}_{\text{float}}. \quad (2.103)$$

Note that the hidden constant is independent of H_i because we have used the scaled H^1 -norm due to (2.95).

All-floating formulation Since all subdomains are floating, we obtain from (2.102), (2.103), and the BEM-FEM spectral equivalence (2.94) that

$$|(P_D w)_i|_{S_i}^2 \lesssim \sum_{j \in \mathcal{N}_i} (1 + \log(H_j/h_j))^2 |w_j|_{S_j}^2. \quad (2.104)$$

Since the number of neighbors to each subdomain is uniformly bounded, the statement of Lemma 2.42 follows immediately.

Standard one-level formulation Here we need to investigate the non-floating subdomains. If a subdomain Ω_i shares a face with the Dirichlet boundary Γ_D , the Friedrichs inequality from Corollary 1.10 implies

$$\|\mathcal{H}_j w_j\|_{H^1(\Omega_j)}^2 \lesssim |\mathcal{H}_j w_j|_{H^1(\Omega_j)}^2.$$

Due to Assumption 2.26 the only case left is that a (non-floating) subdomain shares an edge \mathcal{E}_i with Γ_D . The discrete Poincaré-Friedrichs type inequality Lemma 2.38 yields

$$\|\mathcal{H}_j w_j\|_{H^1(\Omega_j)}^2 \lesssim (1 + \log(H_j/h_j)) |\mathcal{H}_j w_j|_{H^1(\Omega_j)}^2,$$

which would result in a total power of 3 in the logarithmic term compared to (2.104). To get rid of one power we need to enhance the estimates above, cf. KLAWONN AND WIDLUND [109]. First, note that in the standard one-level formulation, the second summand in (2.99) equals zero. Therefore,

$$|(P_D w)_i|_{S_i}^2 \lesssim \sum_{\mathcal{X}_i \subset \Gamma} \sum_{j \in \mathcal{N}_{\mathcal{X}_i}} |\mathcal{H}_i(\theta_{\mathcal{X}_i}(w_i - w_j))|_{H^1(\Omega_i)}^2. \quad (2.105)$$

We define the averages

$$\bar{w}_k := \frac{1}{|\Omega_k|} \int_{\Omega_k} (\mathcal{H}_k w_k)(x) dx \quad \text{for } k \in \mathcal{I}.$$

For a face \mathcal{F}_{ij} sharing Ω_i and Ω_j we have

$$\begin{aligned} & |\mathcal{H}_i(\theta_{\mathcal{F}_{ij}}(w_i - w_j))|_{H^1(\Omega_i)}^2 \\ & \lesssim |\mathcal{H}_i(\theta_{\mathcal{F}_{ij}}(w_i - \bar{w}_i))|_{H^1(\Omega_i)}^2 + |\bar{w}_i - \bar{w}_j|^2 |\mathcal{H}_i \theta_{\mathcal{F}_{ij}}|_{H^1(\Omega_i)}^2 + |\mathcal{H}_i(\theta_{\mathcal{F}_{ij}}(w_j - \bar{w}_j))|_{H^1(\Omega_i)}^2. \end{aligned}$$

The first term (and analogously the last term) can be estimated using Lemma 2.34(iii) and Poincaré's inequality:

$$\begin{aligned} |\mathcal{H}_i(\theta_{\mathcal{F}_{ij}}(w_i - \bar{w}_i))|_{H^1(\Omega_i)}^2 & \lesssim (1 + \log(H_i/h_i))^2 \|\mathcal{H}_i w_i - \bar{w}_i\|_{H^1(\Omega_i)}^2 \\ & \lesssim (1 + \log(H_i/h_i))^2 |\mathcal{H}_i w_i|_{H^1(\Omega_i)}^2. \end{aligned}$$

The second term can be bounded using Lemma 2.34(iv) and the Cauchy-Schwarz inequality:

$$\begin{aligned} |\bar{w}_i - \bar{w}_j|^2 |\mathcal{H}_i \theta_{\mathcal{F}_{ij}}|_{H^1(\Omega_i)}^2 & \lesssim (1 + \log(H_i/h_i)) \left\{ |\bar{w}_i|^2 + |\bar{w}_j|^2 \right\} \\ & \lesssim (1 + \log(H_i/h_i)) \left\{ \frac{1}{H_i^2} \|w_i\|_{L^2(\Omega_i)}^2 + \frac{1}{H_j^2} \|w_j\|_{L^2(\Omega_j)}^2 \right\}. \end{aligned}$$

Both L^2 -terms can be estimated in terms of the H^1 -seminorm using either the discrete Poincaré-Friedrichs inequality from Lemma 2.38 or Poincaré's inequality, resulting in a total factor of $(1 + \log(H_i/h_i))^2$. For edge and vertex terms, the estimates from above need not be modified, since they deliver only one power of the logarithmic term. This finishes the proof of Lemma 2.42. \square

Lemma 2.43. *If $Q = M^{-1}$, then*

$$|P_D z_w|_S^2 \leq |P_D w|_S^2.$$

Proof. Using identity (2.82), i. e., $P_D^\top S P_D = B^\top M^{-1} B = B^\top Q B$, and Lemma 2.22 we have $|P_D z_w|_S^2 = \|B z_w\|_Q^2 \leq \|B w\|_Q^2 = |P_D w|_S^2$. \square

Lemma 2.44. *If Q is chosen according to (2.55)–(2.56) or (2.76)–(2.77), then*

$$|P_D z_w|_S^2 \lesssim \max_{i \in \mathcal{I}} (1 + \log(H_i/h_i))^2 |w|_S^2 \quad \forall w \in W^\perp.$$

Proof. Again we give the proof in three dimensions. The two-dimensional case works analogously. Let $w \in W^\perp$ be fixed. Note that z_w is constant on the subdomains and vanishes on the non-floating subdomains. We denote the components by z_i . Using the same arguments as in the proof of Lemma 2.42 we obtain for each $i \in \mathcal{I}$,

$$\begin{aligned} & |(P_D z_w)_i|_{S_i}^2 && (2.106) \\ & \lesssim \sum_{\mathcal{X}_i \subset \Gamma} \sum_{j \in \mathcal{N}_{\mathcal{X}_i}} \min(\alpha_i, \alpha_j) |\mathcal{H}_i(\theta_{\mathcal{X}_i}(z_i - z_j))|_{H^1(\Omega_i)}^2 + \sum_{\mathcal{X}_i \subset \Gamma_D} \alpha_i |\mathcal{H}_i(\theta_{\mathcal{X}_i} z_i)|_{H^1(\Omega_i)}^2 \\ & = \sum_{\mathcal{X}_i \subset \Gamma} \sum_{j \in \mathcal{N}_{\mathcal{X}_i}} \min(\alpha_i, \alpha_j) |\mathcal{H}_i \theta_{\mathcal{X}_i}|_{H^1(\Omega_i)}^2 |z_i - z_j|^2 + \sum_{\mathcal{X}_i \subset \Gamma_D} \alpha_i |\mathcal{H}_i \theta_{\mathcal{X}_i}|_{H^1(\Omega_i)}^2 |z_i|^2. \end{aligned}$$

Lemma 2.34(i), (iv) and the trivial estimate (2.96) yield

$$\begin{aligned} |\mathcal{H}_i \theta_{\mathcal{F}_i}|_{H^1(\Omega_i)}^2 & \lesssim (1 + \log(H_i/h_i)) H_i, \\ |\mathcal{H}_i \theta_{\mathcal{E}_i}|_{H^1(\Omega_i)}^2 & \lesssim H_i, \\ |\mathcal{H}_i \theta_{\mathcal{V}_i}|_{H^1(\Omega_i)}^2 & \lesssim h_i. \end{aligned} \tag{2.107}$$

We interpret the terms $z_i - z_j$ as components of $B z_w$ (up to the sign). In the standard one-level case, the subdomains Ω_i touching the Dirichlet boundary are non-floating. Consequently, the second summand in (2.106) vanishes as $z_i = 0$ for $i \notin \mathcal{I}_{\text{float}}$. In the all-floating case, the z_i are components of $B z_w$ if the subdomain Ω_i touches the Dirichlet boundary. Using that each face \mathcal{F}_i contains $\mathcal{O}((H_i/h_i)^2)$ nodes, and each edge \mathcal{E}_i contains $\mathcal{O}(H_i/h_i)$ nodes, a coefficient comparison with the values of Q (see also Remark 2.11) reveals that

$$|(P_D z_w)_i|_{S_i}^2 \lesssim \|B z_w\|_Q^2 \leq \|B w\|_Q^2, \tag{2.108}$$

where in the last step we have used Lemma 2.22. The right choice for Q can in fact be read off from (2.106) and (2.107).

In order to bound $\|B w\|_Q^2$ in terms of $|w|_S^2$, we employ another splitting into face, edge, and vertex contributions.

- A face \mathcal{F}_{ij} contributes

$$\begin{aligned} & \sum_{x^h \in \mathcal{F}_{ij}^h} q_{ij}(x^h) |w_i(x^h) - w_j(x^h)|^2 \\ & \lesssim \min(\alpha_i, \alpha_j) (1 + \log(H_i/h_i)) \frac{1}{H_i} h_i^2 \underbrace{\sum_{x^h \in \mathcal{F}_{ij}^h} |w_i(x^h) - w_j(x^h)|^2}_{\simeq \|w_i - w_j\|_{L^2(\mathcal{F}_i)}^2} \\ & \lesssim \alpha_i (1 + \log(H_i/h_i)) \frac{1}{H_i} \|w_i\|_{L^2(\mathcal{F}_i)}^2 + \alpha_j (1 + \log(H_j/h_j)) \frac{1}{H_j} \|w_j\|_{L^2(\mathcal{F}_i)}^2. \end{aligned}$$

- Similarly, in the all-floating case, a face $\mathcal{F}_i \subset \Gamma_D$ contributes

$$\sum_{x^h \in \mathcal{F}_i^h} q_i(x^h) |w_i(x^h)|^2 \lesssim \alpha_i (1 + \log(H_i/h_i)) \frac{1}{H_i} \|w_i\|_{L^2(\mathcal{F}_i)}^2.$$

- An edge \mathcal{E}_{ij} contributes

$$\begin{aligned} & \sum_{x^h \in \mathcal{E}_{ij}^h} q_{ij}(x^h) |w_i(x^h) - w_j(x^h)|^2 \lesssim \min(\alpha_i, \alpha_j) h_i \sum_{x^h \in \mathcal{E}_{ij}^h} |w_i(x^h) - w_j(x^h)|^2 \\ & \lesssim \min(\alpha_i, \alpha_j) \|w_i - w_j\|_{L^2(\mathcal{E}_i)}^2 \lesssim \alpha_i \|w_i\|_{L^2(\mathcal{E}_i)}^2 + \alpha_j \|w_j\|_{L^2(\mathcal{E}_i)}^2. \end{aligned}$$

- Similarly, in the all-floating case, an edge $\mathcal{E}_i \subset \Gamma_D$ contributes

$$\sum_{x^h \in \mathcal{E}_i^h} q_i(x^h) |w_i(x^h)|^2 \lesssim \alpha_i \|w_i\|_{L^2(\mathcal{E}_i)}^2.$$

- The contribution from a vertex \mathcal{V}_{ij} can be bounded as follows,

$$\begin{aligned} q_{ij}(\mathcal{V}_{ij}^h) |w_i(\mathcal{V}_{ij}) - w_j(\mathcal{V}_{ij})|^2 & \lesssim \min(\alpha_i, \alpha_j) h_i |w_i(\mathcal{V}_{ij}) - w_j(\mathcal{V}_{ij})|^2 \\ & \lesssim \alpha_i \|w_i\|_{L^2(\mathcal{E}_i)}^2 + \alpha_j \|w_j\|_{L^2(\mathcal{E}_j)}^2, \end{aligned}$$

where the edges \mathcal{E}_i and \mathcal{E}_j are chosen such that they touch \mathcal{V}_{ij} .

- Similarly, in the all-floating case, the contribution from a vertex $\mathcal{V}_i \subset \Gamma_D$ can be bounded by

$$q_i(\mathcal{V}_i^h) |w_i(\mathcal{V}_i)|^2 \lesssim \alpha_i h_i |w_i(\mathcal{V}_i)|^2 \lesssim \alpha_i \|w_j\|_{L^2(\mathcal{E}_i)}^2,$$

for an edge \mathcal{E}_i touching \mathcal{V}_i .

Summarizing, we obtain

$$\|Bw\|_Q^2 \lesssim \sum_{i \in \mathcal{I}} \sum_{j \in \mathcal{N}_i} \alpha_j (1 + \log(H_j/h_j)) \left\{ \frac{1}{H_j} \|w_j\|_{L^2(\partial\Omega_j)}^2 + \sum_{\mathcal{E}_j} \|w_j\|_{L^2(\mathcal{E}_j)}^2 \right\}. \quad (2.109)$$

Using Corollary 1.12, the term $\frac{1}{H_j} \|w_j\|_{L^2(\partial\Omega_j)}^2$ is bounded by $\|\mathcal{H}_j w_j\|_{H^1(\Omega_j)}^2$. With the help of Lemma 2.34(ii) we can bound the edge terms,

$$\|w_j\|_{L^2(\mathcal{E}_j)}^2 \lesssim (1 + \log(H_j/h_j)) \|\mathcal{H}_j w_j\|_{H^1(\Omega_j)}^2.$$

With the discrete Poincaré-Friedrichs inequality, and combining (2.108) and (2.109) we obtain

$$|P_D z_w|_S^2 \lesssim \sum_{i \in \mathcal{I}} \sum_{j \in \mathcal{N}_i} \alpha_j (1 + \log(H_j/h_j))^2 |\mathcal{H}_j w_j|_{H^1(\Omega_j)}^2 \lesssim \max_{i \in \mathcal{I}} (1 + \log(H_i/h_i))^2 |w|_S^2,$$

where in the last step we have used the BEM-FEM spectral equivalence (2.94). This finishes the proof of Lemma 2.44. \square

Combining Lemma 2.42, Lemma 2.43, and Lemma 2.44 immediately implies the statement of Lemma 2.27.

Remark 2.45. If the coefficients are all equal (or at least only moderately varying) and $Q = I$, the statement of Lemma 2.44 holds still true, cf. KLAWONN AND WIDLUND [108]. We see this from a slight modification of the above proof. The only crucial point is that if two subdomains Ω_i, Ω_j share an edge or a vertex but not a face, the term $|z_i - z_j|^2$ can be simply estimated by the sum of terms $|z_k - z_\ell|^2$ where Ω_k and Ω_ℓ share a face. Note that here we really use that the coefficients are all equal. This way all terms can be estimated by face contributions of Bz . The rest of the proof is then mainly identical.

2.2.5 Numerical results

In this section we present some numerical results for one-level FETI/BETI methods for a two-dimensional linear model problem with coefficient jumps. The main implementation was done in C^{++} . The FEM stiffness matrices and the coarse matrix were factorized using PARDISO [37, 166, 167]. For the boundary element method we have used Olaf Steinbach's Fortran package OSTBEM [176]. The condition numbers are estimated using the Lanczos method, where we used a code fragment by Eero Vainikko. For the visualization we use GMV (see <http://www-xdiv.lanl.gov/XCM/gmv/GMVHome.html>). Mainly interested in verifying the theoretical results of this chapter, we have not used any data-sparse approximation of the boundary element matrices.

Note that detailed computational results for FETI methods are found in RHEINBACH [153]; for numerical results on all-floating BETI methods see OF [138, 139].

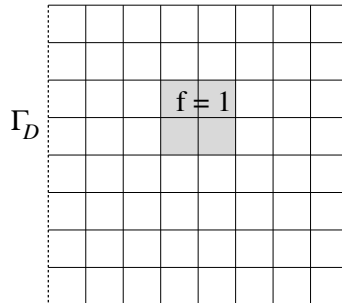


Figure 2.4: Example 2.1: Unit square.

Example 2.1: Unit square, homogeneous coefficient We consider the unit square $\Omega = (0, 1)^2$, subdivided into 64 equal-sized square-shaped subdomains, with homogeneous Dirichlet boundary conditions on the left side Γ_D , and homogeneous Neumann boundary conditions on the rest of $\partial\Omega$. The source term f is chosen to be zero except for the four shaded subdomains in Figure 2.4, and the coefficient α is set uniformly to one.

Table 2.1 and Table 2.2 show the results for FETI and FETI/BETI, respectively. There, the column entitled ‘‘Lagr. mult.’’ indicates number of Lagrange multipliers (additional multipliers enforcing the Dirichlet boundary conditions in the all-floating method are not counted). For simplicity, H denotes the height/width of the subdomain. In the columns entitled ‘‘PCG’’ we give the number of PCG steps needed to get a reduction of $\varepsilon = 10^{-8}$ in the residual, and the columns entitled ‘‘cond.’’ show the estimated condition number using the Lanczos method. We see that the condition numbers of the preconditioned systems behaves as predicted by the theory. From the first column in the two tables one can observe the reduction in the global DOFs when using the boundary element method. In Table 2.3 we demonstrate the scalability, i. e., the robustness with respect to the number of subdomains.

global DOFs	Lagr. mult.	local DOFs	H/h	std. one-level		all-floating	
				PCG	cond.	PCG	cond.
289	406	9	2	9	1.67	8	1.40
1 089	630	25	4	11	2.20	10	1.88
4 225	1 078	81	8	13	2.97	12	2.43
16 641	1 974	289	16	16	3.92	14	3.15
66 049	3 766	1 089	32	18	5.05	16	4.05
263 169	7 350	4 225	64	21	6.33	18	5.12
1 050 625	14 518	16 641	128	23	7.77	19	6.36
4 198 403	28 854	66 049	256	24	9.38	21	7.76
16 785 409	57 526	263 169	512	25	11.15	23	9.33

Table 2.1: Example 2.1: Standard one-level vs. all-floating FETI method; 64 subdomains.

global DOFs	Lagr. mult.	FEM loc. DOFs	BEM loc. DOFs	H/h	std. one-level		all-floating	
					PCG	cond.	PCG	cond.
229	406	9	8	2	9	1.65	9	1.64
549	630	25	16	4	10	1.91	9	1.67
1 285	1 078	81	32	8	13	2.58	11	2.08
3 141	1 974	289	64	16	15	3.44	13	2.72
8 389	3 766	1 089	128	32	18	4.48	16	3.54
25 029	7 350	4 225	256	64	20	5.68	18	4.54
82 885	14 518	16 641	512	128	23	7.03	20	5.71
296 901	28 854	66 049	1024	256	24	8.55	22	7.05
1 118 149	57 526	263 169	2048	512	25	10.24	23	8.55

Table 2.2: Example 2.1: Standard one-level vs. all-floating FETI/BETI method; 64 subdomains (60 BEM, 4 FEM).

number of subdomains	global DOFs	std. one-level		all-floating	
		PCG	cond.	PCG	cond.
64	66 049	18	5.049	16	4.045
256	263 169	18	5.055	16	4.064
1024	591 361	18	5.055	16	4.064
4096	1 050 625	18	5.053	15	4.057

Table 2.3: Example 2.1: Standard one-level vs. all-floating FETI method; fixed ratio $H/h = 32$; fixed number 1089 of local FEM DOFs, varying number of subdomains.

Example 2.2: Unit square, heterogeneous coefficient In this example we consider the unit square $(0, 1)^2$ with the same partitioning as before, but we choose the coefficient α and the source f according to Figure 2.5, left. The Dirichlet boundary conditions read

$$u(x_1, x_2) = 8x_2(1 - 8x_2) \quad \text{for } (x_1, x_2) \in \Gamma_D,$$

and on the rest of $\partial\Omega$ we impose homogeneous Neumann boundary conditions.

Table 2.4 and Table 2.5 show the number of PCG steps and the estimated condition number for the standard one-level and all-floating FETI and FETI/BETI method, respectively. In the second case, the BEM subdomains are exactly those where $f = 0$. The numbers in the tables demonstrate the robustness with respect to the heterogeneous coefficient, which would not be the case without the careful scalings in D_i and Q . Figure 2.5, right displays the solution u to the problem. We see that a large coefficient results in a relatively flat solution.

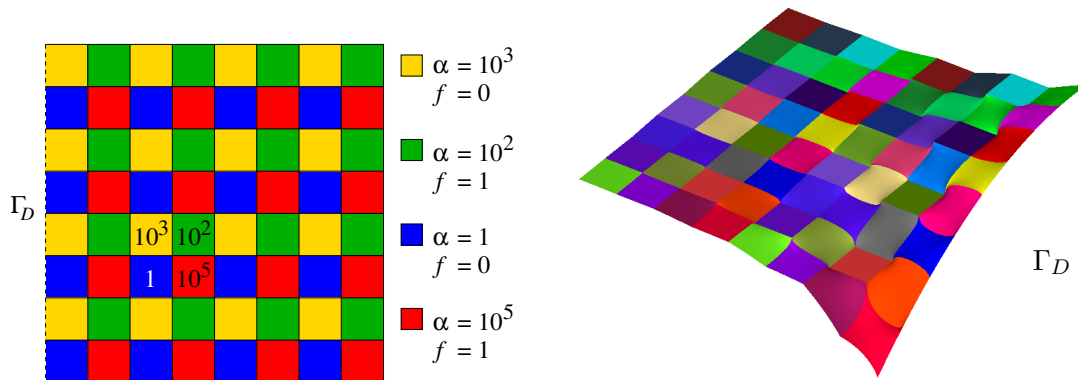


Figure 2.5: *Left*: Setting in Example 2.2: Piecewise constant coefficient distribution, Dirichlet boundary, source distribution. *Right*: Visualization of the solution u via the graph $(x_1, x_2, u(x_1, x_2))$; different colors indicate different subdomains.

global DOFs	local DOFs	H/h	std. one-level		all-floating	
			PCG	cond.	PCG	cond.
289	9	2	10	2.23	8	1.54
1 089	25	4	11	2.69	11	2.12
4 225	81	8	13	3.18	13	2.90
16 641	289	16	15	3.84	15	3.84
66 049	1 089	32	17	4.91	17	4.91
263 169	4 255	64	19	6.10	19	6.10
1 050 625	16 641	128	21	7.42	22	7.43
4 198 401	66 049	256	23	8.91	24	8.88
16 785 409	263 169	512	26	10.60	25	10.47

Table 2.4: Example 2.2: Standard one-level vs. all-floating FETI for jumping coefficients.

global DOFs	FEM loc. DOFs	BEM loc. DOFs	H/h	std. one-level		all-floating	
				PCG	cond.	PCG	cond.
257	9	8	2	7	1.68	7	1.64
801	25	16	4	10	2.24	9	2.24
2 657	81	32	8	11	3.09	12	3.09
9 441	289	64	16	13	4.08	13	4.08
35 297	1 089	128	32	14	5.21	15	5.21
136 161	4 255	256	64	16	6.46	17	6.46
534 497	16 641	512	128	17	7.83	18	7.83
2 117 601	66 049	1024	256	18	9.33	20	9.33
8 429 537	263 169	2048	512	19	10.96	21	10.96

Table 2.5: Example 2.2: Standard one-level vs. all-floating FETI/BETI for jumping coefficients; 32 FEM, 32 BEM subdomains.

The above results and the ones that follow were carried out on the RICAM computer `thebrain` which offers four dual-core Intel Xeon processors at 3.40 GHz (in total 8 processors), 16 MB processor cache and 64 GB RAM in total.

2.2.6 A reformulation of the FETI/BETI PCG algorithm

In this subsection we present a slightly different approach to the analysis of the FETI/BETI methods discussed before which uses a (formal) reformulation of Algorithm 1. In our reformulation we get rid of the auxiliary Lagrange variables in U and U^* via a transformation to variables in W^* and W . This is *not* in order to enhance the FETI/BETI algorithm, but to gain more insight into the algorithm. In particular we will see that the Lagrange multipliers are just auxiliary variables which parameterize the flux, and that the actual FETI/BETI method happens between Dirichlet and Neumann data on the interface.

With the notation from Algorithm 1 we introduce new variables

$$\begin{aligned}\mathbf{t}^{(n)} &:= B^\top \boldsymbol{\lambda}^{(n)}, \\ \mathbf{s}^{(n)} &:= B^\top \mathbf{s}^{(n)}, \\ \mathbf{z}^{(n)} &:= B^\top \mathbf{z}^{(n)},\end{aligned}\tag{2.110}$$

in $\text{range } B^\top \subset W^*$ and choose $\underline{\mathbf{r}}^{(n)}, \underline{\mathbf{x}}^{(n)} \in W$ such that

$$\begin{aligned}\underline{\mathbf{r}}^{(n)} &= B \underline{\mathbf{r}}^{(n)}, \\ \underline{\mathbf{x}}^{(n)} &= B \underline{\mathbf{x}}^{(n)}.\end{aligned}\tag{2.111}$$

Note, that $\mathbf{t}^{(n)}$ is an element from W^* and not a vector. In order to reformulate Algorithm 1 in terms of the new variables, we define the operators

$$P_W := I - R(G^\top Q G)^{-1} G^\top Q B,\tag{2.112}$$

$$P_W^\top := I - B^\top Q G (G^\top Q G)^{-1} R^\top,\tag{2.113}$$

which imply the relations

$$B^\top P = P_W^\top B^\top, \quad P^\top B = B P_W, \quad S P_W = S,\tag{2.114}$$

Recall that

$$b = B \tilde{g}_D\tag{2.115}$$

for the all-floating methods. The resulting reformulation is displayed in Algorithm 2 for the all-floating case. To obtain the standard one-level FETI/BETI algorithm, we formally have to set $\tilde{g}_D = 0$. We point out that the Lagrange multipliers are now hidden in the operators P_D and P_W .

A short investigation reveals that $P_W : W \rightarrow W$ and $P_W^\top : W^* \rightarrow W^*$ are projections satisfying

$$\text{range } P_W = (\ker S)^\perp_{B^\top Q B} = \{w \in W : \langle B^\top Q B w, z \rangle = 0 \quad \forall z \in \ker S\},\tag{2.116}$$

$$\text{range } P_W^\top = \text{range } S = \ker R^\top.\tag{2.117}$$

The projection $I - P_W$ onto $\ker S = \text{range } R$ is $B^\top Q B$ -orthogonal. From the proof of Lemma 2.22 we see that

$$P_W w = w + z_w.$$

Furthermore, we have the following invariants in Algorithm 1 (left column) and in Algorithm 2 (right column) which can easily be shown by induction.

$$\begin{aligned}f - B^\top \boldsymbol{\lambda}^{(n)} &\in \text{range } S, & f - \mathbf{t}^{(n)} &\in \text{range } P_W^\top = \text{range } S, \\ \boldsymbol{\lambda}^{(n)} - \boldsymbol{\lambda}^{(0)} &\in \text{range } P = V, & \mathbf{t}^{(n)} - \mathbf{t}^{(0)} &\in \text{range } P_W^\top \cap \text{range } B^\top, \\ & & \mathbf{t}^{(n)} &\in \text{range } B^\top, \\ \mathbf{z}^{(n)}, \mathbf{s}^{(n)} &\in \text{range } P, & \mathbf{z}^{(n)}, \mathbf{s}^{(n)} &\in \text{range } P_W^\top \cap \text{range } B^\top, \\ \underline{\mathbf{x}}^{(n)}, \underline{\mathbf{r}}^{(n)} &\in \text{range } P^\top \cap \text{range } B = \tilde{V}', & \underline{\mathbf{x}}^{(n)}, \underline{\mathbf{r}}^{(n)} &\in \text{range } P_W, \\ \underline{\mathbf{r}}^{(n)} &= P^\top (d - F \boldsymbol{\lambda}^{(n)}), & \underline{\mathbf{r}}^{(n)} &= P_W S^\dagger [(f - \mathbf{r}^{(n)}) - \tilde{g}_D].\end{aligned}\tag{2.118}$$

Algorithm 2: Reformulated all-floating FETI/BETI algorithm.

Input: f (and b for all-floating), ε , n_{\max}

Output: u

$$\mathbf{t}^{(0)} = (I - P_W^\top) f$$

$$\underline{\mathbf{r}}^{(0)} = P_W [S^\dagger (f - \mathbf{t}^{(0)}) - \tilde{g}_D] = P_W (S^\dagger P_W^\top f - \tilde{g}_D)$$

$$\mathbf{z}^{(0)} = P_W^\top P_D^\top S P_D \underline{\mathbf{r}}^{(0)}$$

$$\mathbf{s}^{(0)} = \mathbf{z}^{(0)}$$

$$\beta_0 = \langle \underline{\mathbf{r}}^{(0)}, \mathbf{z}^{(0)} \rangle$$

$$n = 0$$

while $\beta_n \geq \beta_0 \cdot \varepsilon$ **and** $n < n_{\max}$ **do**

$$\underline{\mathbf{x}}^{(n)} = P_W S^\dagger \mathbf{s}^{(n)}$$

$$\alpha_n = \langle \underline{\mathbf{x}}^{(n)}, \mathbf{s}^{(n)} \rangle$$

$$\alpha = \beta_n / \alpha_n$$

$$\mathbf{t}^{(n+1)} = \mathbf{t}^{(n)} + \alpha \mathbf{s}^{(n)}$$

$$\underline{\mathbf{r}}^{(n+1)} = \underline{\mathbf{r}}^{(n)} - \alpha \underline{\mathbf{x}}^{(n)}$$

$$\mathbf{z}^{(n+1)} = P_W^\top P_D^\top S P_D \underline{\mathbf{r}}^{(n)}$$

$$\beta_{n+1} = \langle \underline{\mathbf{r}}^{(n+1)}, \mathbf{z}^{(n+1)} \rangle$$

$$\beta = \beta_{n+1} / \beta_n$$

$$\mathbf{s}^{(n+1)} = \mathbf{z}^{(n+1)} + \beta \mathbf{s}^{(n)}$$

$$n = n + 1$$

end

$$\left. \begin{aligned} \xi &= (G^\top Q G)^{-1} G^\top Q B [S^\dagger (\mathbf{t}^{(n)} - f) + \tilde{g}_D] \\ u &= S^\dagger (f - \mathbf{t}^{(n)}) + R \xi \end{aligned} \right\} u = P_W [S^\dagger (f - \mathbf{t}^{(n)}) - \tilde{g}_D] + \tilde{g}_D$$

From the last line above, we see that if the algorithm terminates after n steps, we have

$$u = \underline{r}^{(n)} + \tilde{g}_D. \quad (2.119)$$

We summarize that there are two kinds of main variables in Algorithm 2:

- The variables $\mathbf{t}^{(n)}$, $\mathbf{z}^{(n)}$, and $\mathbf{s}^{(n)} \in \text{range } B^\top \subset W^*$ are *continuous normal fluxes* because $E^\top \mathbf{t} = 0$, see Remark 2.6 and Remark 2.14. The expressions $f - \mathbf{t}^{(n)}$, $\mathbf{t}^{(n)} - \mathbf{t}^{(0)}$, $\mathbf{z}^{(n)}$, and $\mathbf{s}^{(n)}$ stay in the subspace $\text{range } P_W^\top = \text{range } S$. The block pseudoinverse S^\dagger is only applied to these expressions.
- The variables $\underline{r}^{(n)}$ and $\underline{x}^{(n)}$ are *projected, discontinuous Dirichlet traces* in the subspace $\text{range } P_W \subset W$. Note that the space of continuous functions \widehat{W} is a subspace of $\text{range } P_W$. Since $(I - P_W)\underline{r}^{(n)} = 0$ and $(I - P_W)\underline{x}^{(n)} = 0$, we can call $\underline{r}^{(n)}$ and $\underline{x}^{(n)}$ *partially continuous* as their projections to the coarse space $\ker S$ are continuous.

The inner product used in the PCG is nothing but the duality pairing $\langle \cdot, \cdot \rangle_{W^* \times W}$.

Assume that we have exact arithmetics and that the original FETI/BETI algorithm terminates after n steps such that $\beta_n = 0$. This implies $\langle M^{-1}\underline{r}^{(n)}, \underline{r}^{(n)} \rangle = 0$. Since M^{-1} is SPD on \tilde{V}' , we can conclude that $r^{(n)} = P^\top(d - F\boldsymbol{\lambda}^{(n)}) = 0$. The resulting solution u is continuous and satisfies the given Dirichlet boundary conditions because

$$Bu = BP_W^\top S^\dagger [(B^\top \boldsymbol{\lambda}^{(n)} - f) + \tilde{g}_D] + B\tilde{g}_D = \underbrace{P^\top (F\boldsymbol{\lambda}^{(n)} - d)}_{=-r^{(n)}=0} + b = b, \quad (2.120)$$

where we have used the identity (2.115). The continuous solution u satisfies the skeleton equation (2.14) because

$$\begin{aligned} E^\top (f - Su) &= E^\top f - E^\top S S^\dagger (f - B^\top \boldsymbol{\lambda}^{(n)}) - SR\xi \\ &= E^\top f - E^\top (f - B^\top \boldsymbol{\lambda}^{(n)}) = E^\top B^\top \boldsymbol{\lambda}^{(n)} = 0. \end{aligned} \quad (2.121)$$

Here, we have used the fact that $f - B^\top \boldsymbol{\lambda}^{(n)} \in \text{range } S$, and the identities $SR = 0$ and $E^\top B^\top = 0$, see also Remark 2.6 and Remark 2.14.

These properties can also be seen from the reformulated FETI/BETI algorithm. If it terminates after n steps with exact arithmetics and $\varepsilon = 0$, we have β_n which implies that

$$|P_D \underline{r}^{(n)}|_S^2 = 0. \quad (2.122)$$

Lemma 2.46. *For each $w \in \text{range } P_W$, we have $P_D w \in \text{range } P_W$.*

Proof. Let $w \in \text{range } P_W = (\ker S)^\perp_{B^\top Q B}$ be fixed, then we have

$$\langle Bw, QBz \rangle = 0 \quad \forall z \in \ker S.$$

By Lemma 2.16 we have $BP_D = B$ and can conclude that

$$\langle BP_D w, QBz \rangle = 0 \quad \forall z \in \ker S,$$

which proves that $P_D w \in \text{range } P_W$. □

Using Lemma 2.46 and the fact that S is SPD on $\text{range } P_W = (\ker S)^{\perp_{B^\top Q B}}$, equation (2.122) implies

$$P_D \underline{r}^{(n)} = 0.$$

Using the identity (2.119) ($u = \underline{r}^{(n)} + \tilde{g}_D$) and Lemma 2.16 ($B P_D = B$) we obtain

$$B u = B \underline{r}^{(n)} + B \tilde{g}_D = B \underbrace{P_D \underline{r}^{(n)}}_{=0} + b = b, \quad (2.123)$$

showing that the solution u is continuous across Γ and satisfies the correct Dirichlet boundary conditions on Γ_D . The skeleton equation (2.14) is satisfied since

$$\begin{aligned} E^\top (f - S u) &= E^\top f - E^\top S \left\{ P_W [S^\dagger (f - \mathbf{t}^{(n)}) - \tilde{g}_D] + \tilde{g}_D \right\} \\ &= E^\top f - E^\top \underbrace{S P_W}_{=S} S^\dagger (f - \mathbf{t}^{(n)}) + E^\top \underbrace{S P_W}_{=S} \tilde{g}_D - E^\top S \tilde{g}_D \\ &= E^\top f - E^\top \underbrace{S S^\dagger (f - \mathbf{t}^{(n)})}_{=f - \mathbf{t}^{(n)}} = E^\top \mathbf{t}^{(n)} = 0. \end{aligned} \quad (2.124)$$

Here, $S S^\dagger (f - \mathbf{t}^{(n)}) = f - \mathbf{t}^{(n)}$ because $f - \mathbf{t}^{(n)} \in \text{range } S$, and in the last step we have used that $\mathbf{t}^{(n)} \in \text{range } B^\top$.

Remark 2.47. This above discussion reveals the role of the residual, here for simplicity for the standard one-level method. Since $\langle M^{-1} \underline{r}^{(n)}, \underline{r}^{(n)} \rangle = |P_D \underline{r}^{(n)}|_S^2$, and since after n steps we set $u = \underline{r}^{(n)}$, we have

$$\langle M^{-1} \underline{r}^{(n)}, \underline{r}^{(n)} \rangle = |u - E_D u|_S^2. \quad (2.125)$$

This means, by controlling the energy norm of the residual $\underline{r}^{(n)}$, we control the error between the discontinuous approximation u and its average $E_D u$ in the energy norm.

Next, we show that Algorithm 2 is a well-defined projected PCG method. We define

$$\begin{aligned} \mathcal{W}' &:= \text{range } P_W^\top \cap \text{range } B^\top = \text{range } S \cap \text{range } B^\top, \\ \mathcal{W} &:= \{w \in \text{range } P_W : S w \in \text{range } B^\top\}. \end{aligned} \quad (2.126)$$

Lemma 2.48. For each $w \in \mathcal{W}$,

$$\langle S w, \hat{w} \rangle = 0 \quad \forall \hat{w} \in \widehat{W}$$

holds. In particular we have $\langle S w, E_D w \rangle = 0$.

Proof. Since $\text{range } B^\top = (\ker B)^\circ$ and $\ker B = \widehat{W}$, the definition of \mathcal{W} immediately implies $\langle S w, \hat{w} \rangle = 0$. \square

Lemma 2.49. Algorithm 2 is a projected PCG method with the operator

$$P_W S^\dagger : \mathcal{W}' \rightarrow \mathcal{W},$$

and with the preconditioner

$$P_W^\top P_D^\top S P_D : \mathcal{W} \rightarrow \mathcal{W}'.$$

The condition number of the preconditioned system is bounded by c_2/c_1 where

$$c_1 |w|_S^2 \leq |P_D w|_S^2 \leq c_2 |w|_S^2 \quad \forall w \in \mathcal{W}. \quad (2.127)$$

Since Algorithm 2 is just a reformulation of Algorithm 1, this implies the condition number bound

$$\kappa \leq c_2/c_1,$$

where κ is the condition number of the preconditioned FETI/BETI system $P M^{-1} P^\top F$ on the space \tilde{V} .

Proof. First we see that $P_W S^\dagger : \text{range } P_W^\top \rightarrow P_W$ is SPD and its inverse is

$$S : \text{range } P_W \rightarrow \text{range } P_W^\top = \text{range } S.$$

By the definition of \mathcal{W}' and \mathcal{W} , we have that $P_W S^\dagger$ maps \mathcal{W}' into \mathcal{W} . The preconditioner

$$P_W^\top P_D^\top S P_D : \text{range } P_W \rightarrow \text{range } P_W^\top$$

is positive semidefinite. Since $P_W^\top(\text{range } B^\top) \subset \text{range } B^\top$ and $\text{range } P_D^\top \subset \text{range } B^\top$, we find that

$$P_W^\top P_D^\top S P_D : \mathcal{W} \rightarrow \mathcal{W}'.$$

Moreover it is definite on \mathcal{W} : Suppose that $\langle S P_D w, P_D w \rangle = 0$ for some $w \in \mathcal{W}$. Since S is SPD on $\text{range } P_W$ and $P_D w \in \text{range } P_W$, we can conclude that $P_D w = 0$. Lemma 2.48 and Lemma 2.16 ($I = E_D + P_D$) imply

$$0 = \langle S w, E_D w \rangle = \langle S E_D w, E_D w \rangle.$$

Since $\ker S \cap \ker B = \{0\}$ and $E_D w \in \ker B$ we can conclude that $E_D w = 0$. Hence,

$$w = P_D w + E_D w = 0,$$

which shows the definiteness. The condition number of the preconditioned operator

$$P_W^\top P_D^\top S P_D P_W S^\dagger : \mathcal{W}' \rightarrow \mathcal{W}'$$

can be determined using the Rayleigh quotient in the inner product $\langle \cdot, P_W S^\dagger \cdot \rangle$:

$$\frac{\langle \overbrace{P_W^\top P_D^\top S P_D}^{=:w} \overbrace{P_W S^\dagger t}^{=:w}, \overbrace{P_W S^\dagger t}^{=:w} \rangle}{\langle \underbrace{t}_{=:P_W^\top S w}, \underbrace{P_W S^\dagger t}_{=:w} \rangle} = \frac{\langle P_D^\top S P_D w, w \rangle}{\langle S w, w \rangle}, \quad (2.128)$$

where $t \in \mathcal{W}'$ and $w \in \mathcal{W}$. To bound the Rayleigh quotient from above and from below, we have to show that

$$c_1 |w|_S^2 \leq |P_D w|_S^2 \leq c_2 |w|_S^2 \quad \forall w \in \mathcal{W}. \quad (2.129)$$

□

The upper bound in (2.127) has been shown already in Lemma 2.27. For the lower bound we use Lemma 2.16 ($I = E_D + P_D$), Lemma 2.48, and the Cauchy-Schwarz inequality with respect to the positive semi-definite inner product $\langle S \cdot, \cdot \rangle$ to obtain

$$|w|_S^2 = \langle S w, w \rangle = \underbrace{\langle S w, E_D w \rangle}_{=0} + \langle S w, P_D w \rangle \leq |w|_S |P_D w|_S.$$

This implies the desired lower bound with $c_1 = 1$.

2.3 Interface-concentrated FETI methods

In this section we briefly describe a variant of FETI introduced by BEUCHLER, EIBNER, AND LANGER [11] using interface-concentrated meshes and a special high-order finite element method, called *boundary-concentrated* FEM, which was originally introduced by KHOROMSKIJ AND MELENK [100]. The main idea thereof is that singularities at the boundary can be well approximated using linear finite elements, whereas the smooth solution in the interior can be well approximated by high-order polynomials on larger elements. With this technique the local number of DOFs on each subdomain Ω_i can be reduced to $\mathcal{O}((H_i/h_i)^{d-1})$ where h_i is the mesh size on the subdomain boundary, i. e., one gets the same complexity as in the boundary element method. The usual condition number estimate of the corresponding FETI methods and hybrid FETI/BETI methods remain valid.

2.3.1 Boundary-concentrated FEM

In this subsection we briefly introduce the concept of the boundary-concentrated FEM. For details see the original paper by KHOROMSKIJ AND MELENK [100] and the doctoral dissertation by EIBNER [50]. For local error analysis and efficient solvers we refer also to KHOROMSKIJ AND MELENK [99] and EIBNER AND MELENK [51, 52].

Let $\Omega \in \mathbb{R}^d$ (with $d = 2$ or 3) be a bounded domain with Lipschitz boundary $\partial\Omega$ and let $\mathcal{T}(\Omega)$ be a conforming, shape-regular, and simplicial triangulation of Ω . Each element τ is the image of the reference simplex $\hat{\tau}$ under the affine linear map $F_\tau : \hat{\tau} \rightarrow \tau$.

Definition 2.50 (geometric mesh). *A triangulation $\mathcal{T}(\Omega)$ is called a geometric mesh with boundary mesh size $h > 0$ if there exist constants $c_1, c_2 > 0$ such that for all $\tau \in \mathcal{T}(\Omega)$,*

- (i) if $\bar{\tau} \cap \partial\Omega \neq \emptyset$ then $h \leq h_\tau \leq c_2 h$, and
- (ii) if $\bar{\tau} \cap \partial\Omega = \emptyset$ then $c_1 \inf_{x \in \tau} \text{dist}(x, \partial\Omega) \leq h_\tau \leq c_2 \sup_{x \in \tau} \text{dist}(x, \partial\Omega)$.

Note that the corresponding boundary mesh $\mathcal{T}(\partial\Omega)$ is quasi-uniform with mesh size h .

Next, we define an hp -FEM space on the geometric mesh. To each element $\tau \in \mathcal{T}(\Omega)$, we associate a polynomial degree $p_\tau \in \mathbb{N}$ and collect these p_τ in the *polynomial degree vector* $\mathbf{p} := (p_\tau)_{\tau \in \mathcal{T}(\Omega)}$.

Definition 2.51 (linear degree vector). *Let $\mathcal{T}(\Omega)$ be a geometric mesh with boundary mesh size h and let \mathbf{p} be a polynomial degree vector. We call \mathbf{p} a linear degree vector with slope $\alpha > 0$ if there exist constants $c_1, c_2 > 0$ such that*

$$1 + c_1 \alpha \log \frac{h_\tau}{h} \leq p_\tau \leq 1 + c_2 \alpha \log \frac{h_\tau}{h}.$$

In practical applications, one usually sets $\alpha = 1$. In particular, the polynomial degree equals one in the elements touching the boundary.

Furthermore, for each edge e and face f of the triangulation we define

$$\begin{aligned} p_e &:= \min\{p_\tau : e \text{ is an edge of the element } \tau\}, \\ p_f &:= \min\{p_\tau : f \text{ is a face of the element } \tau\}, \end{aligned} \tag{2.130}$$

respectively. For each element τ we collect all the degrees corresponding to τ in a vector

$$\mathbf{p}_\tau := (p_\tau, \{p_e\}_{e: \text{edge of } \tau}, \{p_f\}_{f: \text{face of } \tau}). \quad (2.131)$$

The hp -FEM spaces $V^{hp}(\Omega)$ and $V_0^{hp}(\Omega)$ are defined by

$$\begin{aligned} V^{hp}(\Omega) &:= \{v \in H^1(\Omega) : v \circ F_\tau \in \mathcal{P}_{\mathbf{p}_\tau}(\hat{\tau}) \quad \forall \tau \in \mathcal{T}(\Omega)\}, \\ V_0^{hp}(\Omega) &:= V^{hp}(\Omega) \cap H_0^1(\Omega). \end{aligned} \quad (2.132)$$

where $\mathcal{P}_{\mathbf{p}_\tau}$ is the space of polynomials on the reference simplex $\hat{\tau}$ with the polynomial degrees on the elements, edges, and faces are given according to \mathbf{p}_τ .

Due to [100, Proposition 2.7], there exists a constant $C > 0$ depending on the shape-regularity constant of $\mathcal{T}(\Omega)$ and on the constants in Definition 2.50 and Definition 2.51 such that

$$\begin{aligned} \sum_{\tau \in \mathcal{T}(\Omega)} 1 &\leq C (H/h)^{(d-1)}, & \dim V^{hp}(\Omega) &\leq C (H/h)^{(d-1)}, \\ \max_{\tau \in \mathcal{T}(\Omega)} p_\tau &\leq C (1 + \log(H/h)), \end{aligned} \quad (2.133)$$

where $H = \text{diam } \Omega$. In particular there are as many elements in $\mathcal{T}(\Omega)$ and DOFs in $V^{hp}(\Omega)$, as there are elements on the boundary $\partial\Omega$, and the maximal polynomial degree grows only logarithmically with the number of elements on the boundary.

In case that the coefficients and the right hand side of the PDE are sufficiently smooth (analytic), the discretization error of the boundary concentrated FEM is of the same order of magnitude as the discretization error of a low-order FEM on a quasi-uniform triangulation \mathcal{T}^h of Ω . Due to BEUCHLER, EIBNER, AND LANGER [11, Theorem 3.13], the Schur complement of the hp -stiffness matrix is spectrally equivalent to the Schur complement of the stiffness matrix of the quasi-uniform FEM.

A finite element basis for the space $V^{hp}(\Omega)$ is given by a hierarchical basis using vertex-based, edge-based, cell-based, and (in three dimensions) face-based basis functions, cf. KARNIADAKIS AND SHERWIN [94]. The term ‘‘hierarchical’’ means that for increasing polynomial degree new basis functions are added to the basis, whereas the other ones remain unchanged. This is not the case for basis functions related to the Gauss-Lobatto points as used in spectral element methods; see, e. g., KARNIADAKIS AND SHERWIN [94], TOSELLI AND WIDLUND [184, Sect. 7].

2.3.2 Interface-concentrated FETI

Consider a partition of a domain Ω into subdomains. We can now use the boundary-concentrated FEM *on each subdomain*. The resulting global mesh is then *interface-concentrated*, cf. Figure 2.6. If the polynomial degree on those elements touching the subdomain boundaries is one, we immediately obtain the interface-concentrated FETI (IC-FETI) method from the standard low-order FETI method by just replacing the low-order stiffness matrices by the hp -BC-FEM stiffness matrices with respect to the hierarchical basis. Thanks to the spectral equivalence of the corresponding Schur complement matrices, the analysis is straightforward, and the condition number bound reads

$$\kappa \leq C \max_{i \in \mathcal{I}} (1 + \log(H_i/h_i))^2,$$

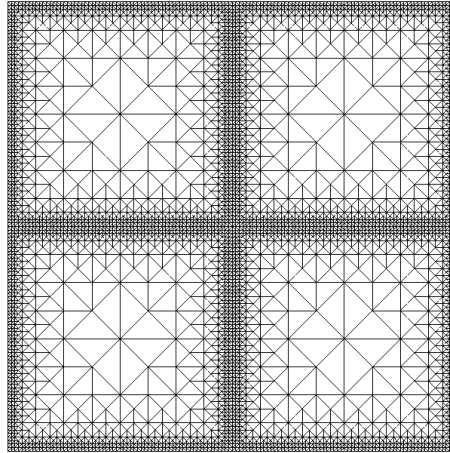


Figure 2.6: Example for an interface concentrated mesh for a partition of the unit square into four subdomains.

where h_i is the mesh size of the subdomain boundary $\partial\Omega_i$, and the constant $C > 0$ is independent of H_i , h_i , the polynomial degrees \mathbf{p}_i , the number s of subdomains, and the values of the coefficients α_i (provided that there are constant on each subdomain).

2.3.3 Numerical results

In this subsection, we would like to briefly demonstrate the reduction of DOFs using IC-FETI and also IC-FETI/BETI. The following results were obtained using some code fragments by Tino Eibner and parts of the open source code NetGen/NGSolve by Joachim Schöberl (see <http://www.hpfem.jku.at>) for the generation of the high-order element stiffness matrices and for visualization. For similar results see also LANGER AND PECHSTEIN [117].

Example 2.3 In this example we have chosen a model problem related to magnetic field computations, as we will discuss in Chapter 6. The coefficient and the source distribution on the square $(0, 0.1)^2$ are displayed in Figure 2.7, left. We impose homogeneous Dirichlet boundary conditions on the whole of $\partial\Omega$.

Table 2.6 shows the number of global DOFs, the number of PCG iterations and the condition numbers for FETI, IC-FETI and IC-FETI/BETI. In the latter case we use BEM on all of the “air” subdomains. The largest polynomial degree used for the interface-concentrated methods is displayed in column “ p_{\max} ”. We see that the number of PCG iterations and the condition numbers of all the three methods are comparable. The number of global DOFs is however significantly reduced using the interface-concentrated methods. In the last row, the low-order approximation results in 1 050 625 DOFs per subdomain, and the corresponding local matrices could not be factored in memory. This reduction also takes place using BETI, but interface-concentrated methods can be used for non-vanishing source terms and, more importantly, also for non-constant coefficients. Figure 2.7, right displays a detail of the mesh and the solution u in the vicinity of a material corner.

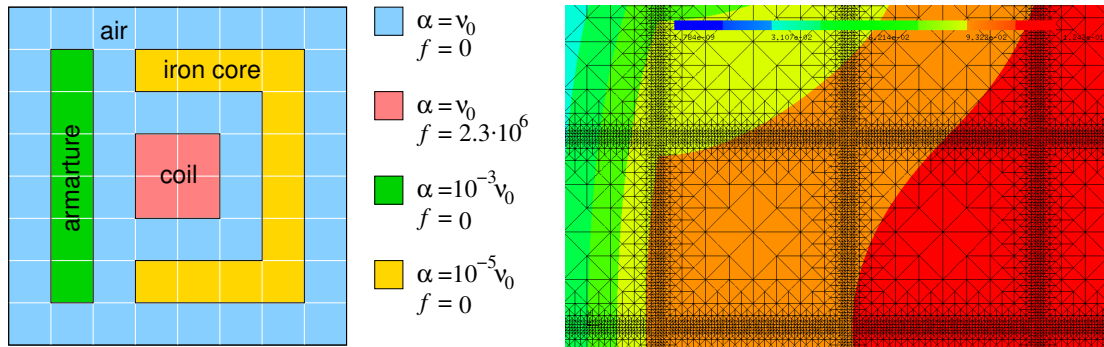


Figure 2.7: Example 2.3: *Left*: Model valve problem. Here, $\nu_0 = 10^7/(4\pi)$. *Right*: Zoom into the mesh, with solution u (visualization by NGSolve).

global DOFs			H/h	PCG			cond.			p_{\max}
289	289	247	2	8	8	9	1.61	1.75	1.77	1
1 089	1 089	711	4	9	10	11	2.13	2.40	2.23	1
4 225	3 969	2 079	8	11	12	14	2.85	3.24	3.08	1
16 641	13 313	6 047	16	13	15	17	3.73	4.24	4.08	2
66 049	42 497	17 591	32	15	17	19	4.77	5.40	5.23	3
263 169	121 875	47 895	64	17	18	21	5.96	6.72	6.54	4
1 050 625	315 649	120 559	128	18	20	23	7.31	8.19	8.00	5
4 198 401	755 969	284 015	256	19	21	25	8.82	9.81	9.62	6
16 785 409	1 710 593	636 359	512	21	22	27	11.40	11.60	11.39	7
67 125 249	3 718 657	1 375 015	1024	—	23	30	—	13.54	13.31	8

Table 2.6: Example 2.3: Comparison between FETI, IC-FETI, and coupled IC-FETI/BETI.

Chapter 3

One-level methods for unbounded domains

In this chapter we extend the methods and theory from Chapter 2 to a specific class of problems in unbounded domains. We add an unbounded exterior subdomain (similar to Ω^{ext} from Section 1.4) to our potential equation and prescribe a radiation condition for $u(x)$ as $|x|$ goes to infinity. The treatment of other problem classes concerning unbounded domains, such as half-spaces, with FETI/BETI methods is probably possible but not scope of this thesis. In Section 3.1 we introduce a precise description of our model problem and the corresponding variational skeleton formulation. Section 3.2 discusses a generalization of standard one-level as well as all-floating FETI/BETI methods for this model problem, which has been published in PECHSTEIN [143, 144].

It might seem that such generalizations are straightforward as the exterior part can be modeled simply by the exterior Steklov-Poincaré operator from Section 1.4.3. However, some of the properties of the bounded case apparently fail to hold in the general unbounded case. In the bounded case, a shape-regular subdomain partition implies that each subdomain has a finite number of neighboring subdomain, and that the diameters of two neighboring subdomains are comparable. In the unbounded case such an assumption is very limiting. Actually, we are looking for a method that works for the case where the number of neighbors of the exterior subdomain can be large, and where the boundary of the exterior subdomain can be very large in comparison to the interior subdomains. A straightforward analysis of FETI/BETI methods would lead to a condition number estimate which is not anymore robust with respect to the number of neighbors and sizes of the subdomains. In the course of this chapter we derive tools which allows for an analysis with explicit estimates.

In the case that in addition to the radiation condition no further Dirichlet boundary conditions are given, we obtain the same type of estimate as in the bounded case, i. e., $\kappa \leq C(1 + \log(H/h))^2$. The method is robust with respect to the above described possibly large parameters under reasonable assumptions. The case of interior Dirichlet boundary conditions is more subtle. One of our crucial tools is the so-called *extension indicator* which relates the Dirichlet boundary and the boundary of the exterior subdomain. We are able to give a condition number estimate for one-level FETI/BETI methods in terms of the extension indicator, and we show how to bound that indicator in terms of a few accessible geometric parameters. The reason for such a subtle condition number bound is the lack of coarse space components corresponding to the exterior subdomain.

3.1 Model problem and skeleton formulation

3.1.1 Continuous formulation

Let $\Omega \subset \mathbb{R}^d$ (with $d = 2$ or 3) be an unbounded domain which can be decomposed into finitely many bounded Lipschitz domains and an unbounded part Ω_0 whose complement is bounded and Lipschitz. Furthermore, let the bounded part $\Omega \setminus \Omega_0$ be Lipschitz too. Let the coefficient α and the source f satisfy

$$\alpha|_{\Omega_0} = \alpha_0 = \text{const} > 0, \quad \text{and} \quad f|_{\Omega_0} = 0. \quad (3.1)$$

With our assumptions it is possible that Ω has no boundary at all ($\Omega = \mathbb{R}^d$), and it is also possible that its boundary $\partial\Omega$ consists of more than one connected component. We assume that each such connected component of $\partial\Omega$ is Lipschitz, and we denote the corresponding outward unit normal vector by n . As in Chapter 2, $\partial\Omega$ decomposes into a Dirichlet boundary Γ_D (regarded as relatively closed) and an open Neumann boundary Γ_N which are disjoint to each other. Of course also these parts may be empty or may consist of more than one component. Note, that we can allow the boundary $\partial\Omega$ to touch $\partial\Omega_0$. For an illustration of such different configurations see Figure 3.1.

Our model problem reads as follows. Find the weak solution $u \in H_{\text{loc}}^1(\Omega)$ to

$$-\text{div} [\alpha \nabla u] = f \quad \text{in } \Omega, \quad (3.2)$$

$$u = g_D \quad \text{on } \Gamma_D, \quad (3.3)$$

$$\alpha \frac{\partial u}{\partial n} = g_N \quad \text{on } \Gamma_N, \quad (3.4)$$

with the radiation condition (1.49) from Section 1.4.1, which is equivalent to

$$u(x) = \begin{cases} b \log |x| + \mathcal{O}(|x|^{-1}) & \text{for } d = 2, \\ \mathcal{O}(|x|^{-1}) & \text{for } d = 3, \end{cases}$$

as $|x| \rightarrow \infty$, for some $b \in \mathbb{R}$ (see Lemma 1.21). Note that even if Γ_D is empty, the problem is still well-posed, because the radiation condition acts like a Dirichlet boundary condition at infinity. Since we will model the equation in Ω_0 using the exterior Steklov-Poincaré operator, we call Ω_0 the *exterior part*.

We consider a non-overlapping partition $\{\Omega_i\}_{i=0,\dots,s}$ of Ω into open subdomains such that

$$\bar{\Omega} = \bigcup_{i=0}^s \bar{\Omega}_i, \quad \Omega_i \cap \Omega_j = \emptyset \quad \text{for } i \neq j,$$

where Ω_0 is the exterior part from above. The subdomain boundaries are denoted by $\partial\Omega_i$ (hence, $\partial\Omega_0$ is the interface between the exterior part and the rest), and n_i is the outward unit normal vector to $\partial\Omega_i$. In particular, n_0 points inside $\Omega \setminus \Omega_0$ (similar to n^{ext} introduced in Section 1.3.1.2). We define $H_i := \text{diam } \Omega_i$ for $i \neq 0$, and set

$$H_0 := \text{diam } \Omega_0^c, \quad (3.5)$$

where $\Omega_0^c := \mathbb{R}^d \setminus \bar{\Omega}_0$. Due to our assumption, H_0 is finite, but it can happen that $H_0 \gg H_i$ for some $i \neq 0$. Similarly to Chapter 2, we will heavily work with the index set

$$\mathcal{I} := \{0, \dots, s\}, \quad (3.6)$$

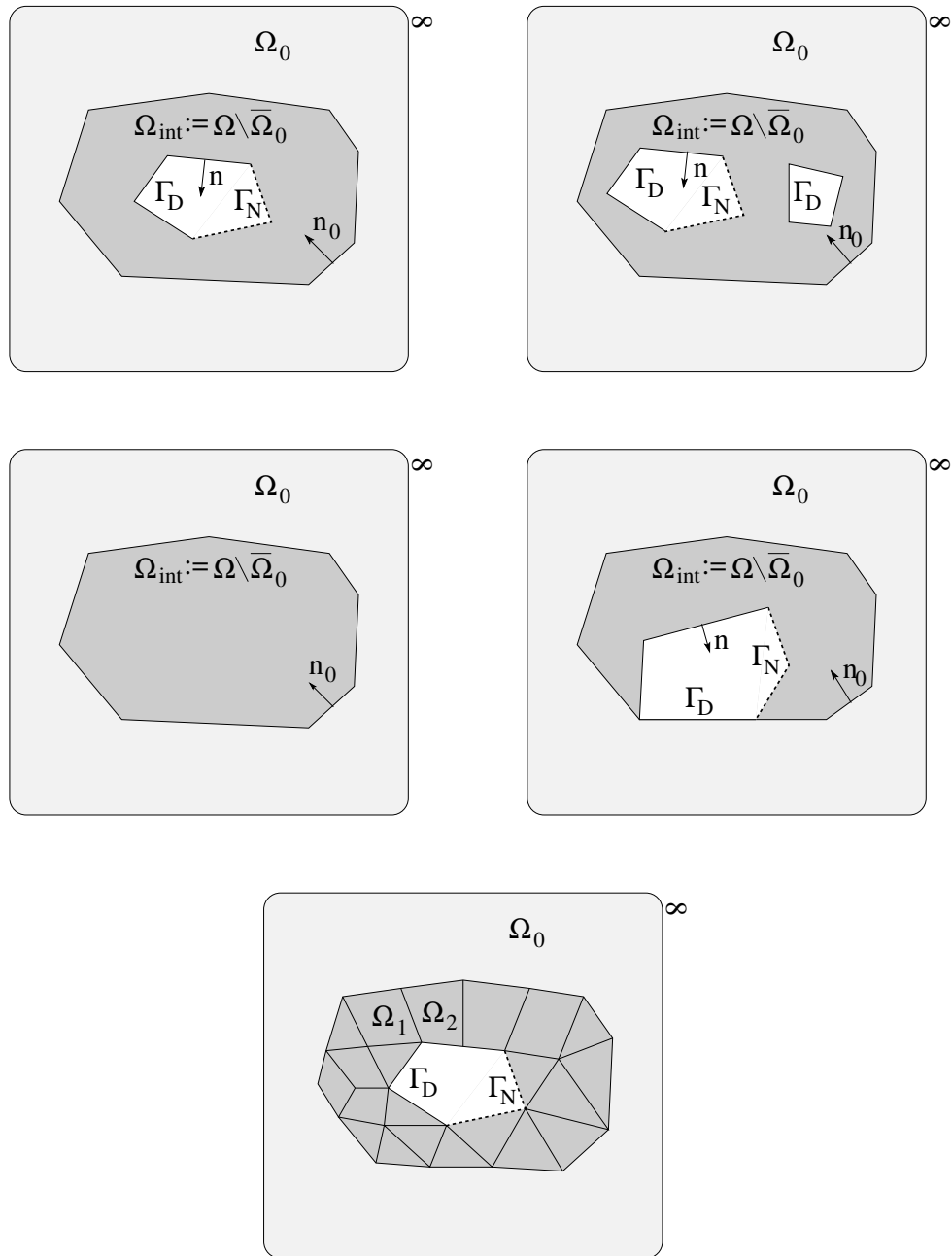


Figure 3.1: Illustrations of the configuration of the unbounded setting. The grey region is the domain Ω , the white region is excluded from Ω . Illustrated are the exterior part Ω_0 , the Dirichlet boundary Γ_D , the Neumann boundary Γ_N , and the outward unit normal vector n to $\partial\Omega$. *Upper left:* Configuration with a connected boundary $\partial\Omega$. *Upper right:* Configuration with a boundary $\partial\Omega$ consisting of two connected components. *Middle left:* Configuration with no boundary, $\partial\Omega = \emptyset$. *Middle right:* Configuration with a Dirichlet boundary Γ_D that touches $\partial\Omega_0$. *Lower:* Subdomain partition for the first configuration.

and consider subsets $\mathcal{I}_{\text{FEM}} \subset \mathcal{I}$ and $\mathcal{I}_{\text{BEM}} = \mathcal{I} \setminus \mathcal{I}_{\text{FEM}}$ such that $0 \in \mathcal{I}_{\text{BEM}}$. Finally, we define the *interior part* Ω_{int} and the index set of the *interior subdomains* by

$$\Omega_{\text{int}} := \Omega \setminus \bar{\Omega}_0, \quad \mathcal{I}_{\text{int}} := \mathcal{I} \setminus \{0\}, \quad (3.7)$$

such that $\bar{\Omega}_{\text{int}} = \bigcup_{i \in \mathcal{I}_{\text{int}}} \bar{\Omega}_i$. In the following, we make assumptions on the data and on the subdomain partition similar to those in Chapter 2. We consider constant coefficients on the all subdomains,

$$\alpha_{|\Omega_i} = \alpha_i = \text{const} > 0 \quad \forall i \in \mathcal{I}, \quad (3.8)$$

and assume that $f \in L^2(\Omega)$, $g_D \in H^{1/2}(\Gamma_D)$, and $g_N \in L^2(\Gamma_N)$. The source f must vanish in all BEM subdomains, i. e.,

$$f|_{\Omega_i} = 0 \quad \forall i \in \mathcal{I}_{\text{BEM}}. \quad (3.9)$$

Remark 3.1. Note that as in Chapter 2 we can relax the assumptions on the coefficients α , the source function f , and the prescribed Neumann trace g_N . We can also relax the assumption that the bounded part Ω_{int} is Lipschitz to a certain extent, cf. Remark 2.4.

The following assumption is almost identical to Assumption 2.23 but it concerns only the interior subdomains.

Assumption 3.2. *The interior subdomains Ω_i , $i \in \mathcal{I}_{\text{int}}$ are bounded and connected Lipschitz domains, each one formed by a few simplices. The simplices altogether form a coarse, shape-regular, and conforming triangulation \mathcal{T}_H of Ω_{int} . The number of simplices per subdomain is uniformly bounded.*

The shape-regularity from Assumption 3.2 implies the existence of a uniformly bounded constant $C_{\text{DD}}^H > 0$ such that

$$\partial\Omega_i \cap \partial\Omega_j \neq \emptyset \quad \implies \quad H_i \leq C_{\text{DD}}^H H_j \quad \forall i, j \in \mathcal{I}_{\text{int}}.$$

Concerning the exterior part, we need to make the following assumption.

Assumption 3.3. *The coarse triangulation of Ω_{int} can be extended to a shape-regular, conforming triangulation of an auxiliary domain $\Omega' \subset \Omega$ such that Ω_{int} is compactly contained in Ω' .*

For an illustration see Figure 3.2, which shows that there exist configurations which fulfill Assumption 3.2 but violate Assumption 3.3 in the sense that the shape regularity constant is very large. In case that Ω_0 is well-shaped, Assumption 3.3 poses no real restriction.

As in the bounded case we can define the subdomain interfaces Γ_{ij} , the interface Γ , and the skeleton Γ_S by

$$\Gamma_{ij} := (\partial\Omega_i \cap \partial\Omega_j) \setminus \Gamma_D, \quad \Gamma := \bigcup_{i \neq j} \Gamma_{ij}, \quad \Gamma_S := \bigcup_{i \in \mathcal{I}} \partial\Omega_i. \quad (3.10)$$

Similarly we can define faces, edges, and vertices according to Definition 2.2. Assumption 3.2 implies that the number of subdomains sharing the same vertex, edge, or face is uniformly

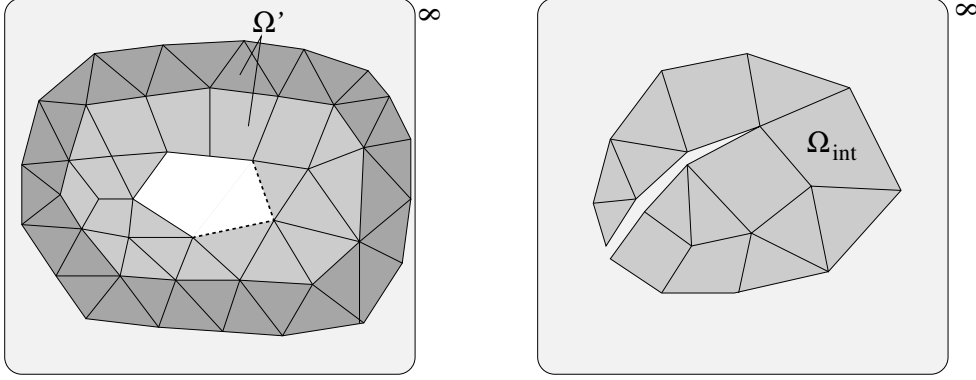


Figure 3.2: *Left:* Illustration of the extended triangulation of the auxiliary domain Ω' in Assumption 3.3 for the example in Figure 3.1 (light grey: Ω_{int} , dark grey: $\Omega' \setminus \Omega_{\text{int}}$). *Right:* Different configuration with small geometric angle.

bounded, and the number of vertices, edges, and faces of each *interior* subdomain is uniformly bounded too. On the contrary, the number of faces, edges, and vertices of the *exterior* part Ω_0 can be very large.

Analogously to Section 2.1, we can introduce the conormal derivatives t_i of the solution u on the subdomain boundaries, given in terms of Steklov-Poincaré operators and Newton potentials. In order to model the equation in Ω_0 correctly, we have to use $\alpha_0 S_0^{\text{ext}}$ as Steklov-Poincaré operator. From the transmission and boundary conditions on t_i , we can derive a continuous skeleton formulation. Since S_0^{ext} is elliptic (due to the radiation condition), this problem is well-posed even if the Dirichlet boundary Γ_D is empty.

3.1.2 Discrete formulation

We introduce triangulations of the subdomain boundaries and the FEM subdomains as in Section 2.1. Let $\mathcal{T}^h(\Gamma_S)$ be a shape-regular triangulation of Γ_S . For each $i \in \mathcal{I}_{\text{FEM}}$ let $\mathcal{T}^h(\Omega_i)$ be a quasi-uniform and shape-regular triangulation of Ω_i with mesh parameter h_i which matches with $\mathcal{T}^h(\Gamma_S)$. For each $i \in \mathcal{I}_{\text{BEM}}$ let the restriction $\mathcal{T}^h(\partial\Omega_i)$ of $\mathcal{T}^h(\Gamma_S)$ to $\partial\Omega_i$ be a quasi-uniform and shape-regular triangulation of $\partial\Omega_i$ of mesh parameter h_i . In particular, the restriction $\mathcal{T}^h(\partial\Omega_0)$ of $\mathcal{T}^h(\Gamma_S)$ to $\partial\Omega_0$ is assumed to be quasi-uniform with mesh parameter h_0 , and $h_0 \simeq h_i$ if the subdomain Ω_i touches $\partial\Omega_0$. We define the approximations

$$S_i := \begin{cases} \alpha_0 S_{0,\text{BEM}}^{\text{ext}} & \text{for } i = 0, \\ \alpha_i S_{i,\text{BEM}}^{\text{int}} & \text{for } i \in \mathcal{I}_{\text{BEM}} \setminus \{0\}, \\ \alpha_i S_{i,\text{FEM}}^{\text{int}} & \text{for } i \in \mathcal{I}_{\text{FEM}}. \end{cases} \quad (3.11)$$

and the functionals f_i by

$$\begin{aligned} \langle f_i, v \rangle_{\partial\Omega_i} &= \alpha_i \langle N_{i,\text{FEM}} f, v \rangle_{\partial\Omega_i} + \int_{\partial\Omega_i \cap \Gamma_N} g_N v \, ds & \text{for } v \in V^h(\partial\Omega_i), i \in \mathcal{I}_{\text{FEM}}, \\ \langle f_i, v \rangle_{\partial\Omega_i} &= \int_{\partial\Omega_i \cap \Gamma_N} g_N v \, ds & \text{for } v \in V^h(\partial\Omega_i), i \in \mathcal{I}_{\text{BEM}}. \end{aligned} \quad (3.12)$$

Since we will work in the discrete setting only, we omit the subscript h . We assume again that g_D and g_N are contained in the corresponding discrete spaces. Finally, the discrete skeleton formulation reads: Find $u \in V^h(\Gamma_S)$ with $u|_{\Gamma_D} = g_D$ such that

$$\sum_{i \in \mathcal{I}} \langle S_i u, v \rangle_{\partial\Omega_i} = \sum_{i \in \mathcal{I}} \langle f_i, v \rangle_{\partial\Omega_i} \quad \forall v \in V_D^h(\Gamma_S), \quad (3.13)$$

where $V_D^h(\Gamma_S) = \{v \in V^h(\Gamma_S) : v|_{\Gamma_D} = 0\}$. Recall, that by Lemma 1.33,

$$\langle S_0 u, u \rangle \simeq \alpha_0 \left\{ |u|_{H^{1/2}(\partial\Omega_0)}^2 + \frac{1}{H_0} \|u\|_{L^2(\partial\Omega_0)}^2 \right\}. \quad (3.14)$$

3.2 Difficulties in the case of unbounded domains

As outlined in the beginning of this chapter, we face two crucial difficulties that are not present in the bounded case.

- The number of neighbors of Ω_0 can be arbitrary.
- The diameter H_0 can be very large compared to the diameter H_i of a neighboring subdomain.

However, we are looking for a method that is robust with respect to the possibly large number of neighbors of Ω_0 , and with respect to the ratio

$$\max_{i \in \mathcal{N}_0} \frac{H_0}{H_i},$$

where \mathcal{N}_0 is the index set of neighboring subdomains of Ω_0 . As our discussion will show, this is in some cases possible. We give explicit estimates of the condition number in terms of geometric parameters such as H_i , H_0 , h_i , and the so-called *extension indicator* $\gamma_h(\Omega_0, \Omega_{\text{int}}, \Gamma_D)$. In special cases, this indicator can be estimated again in terms of H_0 , h_i , and a shape parameter η which will be introduced later on. It will turn out that if the Dirichlet boundary Γ_D is empty or sufficiently separated from $\partial\Omega_0$, we get perfect robustness with respect to the ratio $\max_{i \in \mathcal{N}_0} H_0/H_i$.

3.3 Formulation of FETI/BETI methods in unbounded domains

The following two assumptions are just the same as in the bounded case.

Assumption 3.4. *The interface between the Dirichlet boundary Γ_D and the Neumann boundary Γ_N is aligned with the subdomain partition.*

Assumption 3.5. *In case of the standard one-level formulation in three dimensions, we have to assume that the intersection of a subdomain boundary $\partial\Omega_i$ and the Dirichlet boundary Γ_D is either empty or at least a subdomain edge.*

We can set up the standard one-level and the all-floating method *analogously* to Section 2.2. The exterior part Ω_0 is just an additional subdomain with a special Steklov-Poincaré operator. Only the following issues are of crucial importance.

- (i) Ω_0 is always a *non-floating* subdomain because the operator S_0 is regular, see (3.14), even in the case of an all-floating method (cf. Definition 2.7 on page 55).
- (ii) If the Dirichlet boundary Γ_D touches $\partial\Omega_0$, we do always incorporate the corresponding Dirichlet conditions into the space W_0 , even in the case of an all-floating method. As a consequence we have no Lagrange multipliers of the form λ_{0D} and we always have

$$W_0 := V_D^h(\partial\Omega_0) = \{w \in V^h(\partial\Omega_0) : w|_{\Gamma_D} = 0\}. \quad (3.15)$$

- (iii) We need to adapt the operator Q slightly.
- (iv) If we are in two dimensions, the coordinates must be scaled such that $H_0 = \frac{1}{2}$ for theoretical reasons, cf. Lemma 1.33, page 44. Doing so, all interior diameters H_i stay below 1, such that the local single layer potentials remain elliptic.

Everything else is analogous to Section 2.2. Convention (ii) is needed for technical reasons and it forces us to add the following assumption.

Assumption 3.6. *In case of the all-floating formulation in three dimensions, we have to assume that the intersection of the Dirichlet boundary Γ_D with $\partial\Omega_0$ is either empty or at least a subdomain edge.*

Remark 3.7. Similarly as outlined in Remark 2.10, the block S_0 appearing in the preconditioner $M^{-1} = B_D S B_D^T$ may be replaced by a suitable regularization \tilde{D}_0 of the hypersingular operator on $\partial\Omega_0$, for instance defined by

$$\langle \tilde{D}_0 v, w \rangle = \langle D_0 v, w \rangle + \frac{1}{H_0^d} \int_{\partial\Omega_0} v ds \int_{\partial\Omega_0} w ds.$$

The operator Q is either set to M^{-1} (which is however not recommended) or defined by

$$(Q\mu)_{ij}(x^h) := \min(\alpha_i, \alpha_j) q_{ij}(x^h) \mu_{ij}(x^h) \quad \text{for } \mu \in U^*, \quad (3.16)$$

$$\begin{aligned} q_{0i}(x^h) &:= q_{i0}(x^h) := q_i(x^h), \\ q_{ij}(x^h) &:= \min(q_i(x^h), q_j(x^h)) \quad \text{for } i, j \neq 0, \end{aligned} \quad (3.17)$$

$$q_i(x^h) := \left\{ \begin{array}{ll} (1 + \log(H_i/h_i)) \frac{h_i^2}{H_i} & \text{if } x^h \text{ lies on a face } \mathcal{F}_i \\ h_i & \text{if } x^h \text{ lies on an edge } \mathcal{E}_i \text{ or a vertex } \mathcal{V}_i \end{array} \right\} \quad \text{if } d = 3,$$

$$q_i(x^h) := \left\{ \begin{array}{ll} (1 + \log(H_i/h_i)) \frac{h_i}{H_i} & \text{if } x^h \text{ lies on an edge } \mathcal{E}_i \\ 1 & \text{if } x^h \text{ is a vertex } \mathcal{V}_i \end{array} \right\} \quad \text{if } d = 2. \quad (3.18)$$

For the all-floating method, we additionally set

$$(Q\mu)_{iD}(x^h) := \alpha_i q_i(x^h) \mu_{iD}(x^h) \quad \text{for } x^h \in \partial\Omega_i^h \cap \Gamma_D \quad \text{for } \mu \in U^*, \quad (3.19)$$

where $i \neq 0$. Note that by this construction, the possibly large diameter H_0 never occurs in the entries of Q . Alternatively, we could have also used the diameters of the faces and edges instead of the subdomain diameters H_i .

3.4 Condition number estimates for FETI/BETI methods in unbounded domains

3.4.1 The extension indicator

It turns out that in the case of Dirichlet boundary conditions, cf. Figure 3.1, the condition number depends on a geometric parameter, the *extension indicator*, which is associated to the Dirichlet boundary Γ_D and the outer boundary $\partial\Omega_0$. In this subsection we define this indicator and give bounds in terms of more accessible parameters.

First of all, we need a technical assumption and some definitions.

Assumption 3.8. *There exists an auxiliary triangulation $\tilde{\mathcal{T}}^h(\Omega_{\text{int}})$ of the interior part Ω_{int} which is shape-regular and quasi-uniform with mesh parameter h_0 , which matches with the triangulation $\mathcal{T}^h(\partial\Omega_0)$, and which resolves Γ_D .*

Note that $\tilde{\mathcal{T}}^h(\Omega_{\text{int}})$ does not need to match with the existing triangulations on the interface Γ and on the FEM subdomains. We will transfer between the different meshes using the Scott-Zhang quasi-interpolation operator.

Remark 3.9. Assumption 3.8 holds unless the interior part Ω_{int} or the Dirichlet boundary Γ_D exhibit fine geometric details that cannot be resolved using the mesh parameter h_0 , in other words, h_0 needs to be small enough. We will comment on a remedy in Remark 3.17.

We fix a triangulation $\tilde{\mathcal{T}}^h(\Omega_{\text{int}})$ which fulfills the requirements of Assumption 3.8 and denote the finite element space associated to it by $\tilde{V}^h(\Omega_{\text{int}})$. For a discrete function $w_0 \in V_D^h(\partial\Omega_0)$, the discrete harmonic extension $\tilde{\mathcal{H}}^{\text{int}} w_0 \in \tilde{V}^h(\Omega_{\text{int}})$ is defined by

$$\tilde{\mathcal{H}}^{\text{int}} w_0 := \operatorname{argmin} \{ |v|_{H^1(\Omega_{\text{int}})} : v \in \tilde{V}^h(\Omega_{\text{int}}), v|_{\partial\Omega_0} = w_0 \}. \quad (3.20)$$

We define a second discrete extension that satisfies homogeneous Dirichlet boundary conditions on Γ_D .

Definition 3.10 (Restricted discrete harmonic extension). *For a function $w_0 \in V_D^h(\partial\Omega_0)$, the restricted discrete harmonic extension $\tilde{\mathcal{H}}_D^{\text{int}} w_0 \in \tilde{V}^h(\Omega_{\text{int}})$ is defined by*

$$\tilde{\mathcal{H}}_D^{\text{int}} w_0 := \operatorname{argmin} \{ |v|_{H^1(\Omega_{\text{int}})} : v \in \tilde{V}^h(\Omega_{\text{int}}), v|_{\partial\Omega_0} = w_0, v|_{\Gamma_D} = 0 \}.$$

The following indicator measures the ratio of the two different extensions in suitable energy norms.

Definition 3.11 (Extension indicator). *We call*

$$\gamma_h(\Omega_0, \Omega_{\text{int}}, \Gamma_D) := \sup_{w_0 \in V_D^h(\partial\Omega_0)} \frac{|\tilde{\mathcal{H}}_D^{\text{int}} w_0|_{H^1(\Omega_{\text{int}})}^2}{|\tilde{\mathcal{H}}^{\text{int}} w_0|_{H^1(\Omega_{\text{int}})}^2 + \frac{1}{H_0} \|w_0\|_{L^2(\partial\Omega_0)}^2}.$$

the extension indicator. The subscript h indicates the dependence on $\tilde{\mathcal{T}}^h(\Omega_{\text{int}})$.

Note that

$$\Gamma_D = \emptyset \quad \text{or} \quad \Gamma_D \subset \partial\Omega_0 \quad \implies \quad \gamma_h(\Omega_0, \Omega_{\text{int}}, \Gamma_D) \leq 1, \quad (3.21)$$

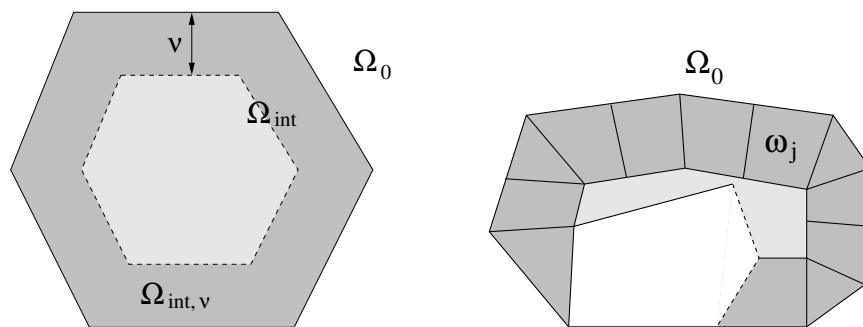


Figure 3.3: Illustration of the boundary layer $\Omega_{\text{int},\nu}$ from Definition 3.12 for two different configurations. Dark grey: $\Omega_{\text{int},\nu}$; light grey: $\Omega_{\text{int}} \setminus \Omega_{\text{int},\nu}$. Right: Illustration of the partition property, see Definition 3.13.

because then, the two extensions, $\tilde{\mathcal{H}}^{\text{int}} w_0$ and $\tilde{\mathcal{H}}_D^{\text{int}} w_0$ coincide. In all other cases, the extension indicator can be bounded in terms of a shape parameter η which is specified in the sequel. The following concept of boundary layers and shape parameters is borrowed from a work by GRAHAM, LECHNER, AND SCHEICHL [75] on overlapping Schwarz methods and slightly adapted for our purposes.

Definition 3.12 (Boundary layer). *A subset $\Omega_{\text{int},\nu}$ of Ω_{int} is called boundary layer of Ω_{int} with parameter ν if it fulfills*

$$\forall x \in \Omega_{\text{int},\nu} : \text{dist}(x, \partial\Omega_0) < 2\nu, \quad \forall x \in \partial\Omega_0 : B_{x,\nu} \cap \Omega_{\text{int}} \subset \Omega_{\text{int},\nu},$$

where $B_{x,\nu}$ is the open ball with center x and radius ν .

Note that in the above definition, we use the distance of points $x \in \Omega_{\text{int}}$ from the outer boundary $\partial\Omega_0$, and not the boundary $\partial\Omega_{\text{int}}$ of the interior part, which are not necessarily the same, cf. Figure 3.3.

Definition 3.13 (Partition property). *A boundary layer $\Omega_{\text{int},\nu}$ fulfills the partition property if it can be partitioned into finitely many non-overlapping patches $\{\omega_j\}_{j \in \mathcal{J}}$ such that the following holds.*

- (i) *Each patch ω_j consists of a union of a few simplices with $\text{diam } \omega_j \simeq \nu$ and the number of simplices per patch is uniformly bounded.*
- (ii) *The union of all the simplices forms a quasi-uniform, shape-regular coarse triangulation of $\Omega_{\text{int},\nu}$.*
- (iii) *For each $j \in \mathcal{J}$, the intersection $\gamma_j := \partial\omega_j \cap \partial\Omega_0$ is the closure of a union of faces (edges in two dimensions) of the simplices of the coarse triangulation, and in particular, $\text{diam}(\gamma_j) \simeq \nu$.*
- (iv) *The patches are aligned with the auxiliary triangulation $\tilde{\mathcal{T}}^h(\Omega_{\text{int}})$.*

For an illustration see Figure 3.3, right. Since the auxiliary triangulation $\tilde{\mathcal{T}}^h(\Omega_{\text{int}})$ can be chosen almost arbitrarily, the requirement that the patches are aligned with $\tilde{\mathcal{T}}^h(\Omega_{\text{int}})$

poses no real restriction concerning the interfaces between the patches. The patches must however resolve the interior part of $\partial\Omega_{\text{int},\nu}$, that is why we allow a distance up to 2ν in Definition 3.12.

Definition 3.14 (Shape parameter η). *The shape parameter $\eta > 0$ is the largest number such that a boundary layer $\Omega_{\text{int},\eta}$ of Ω_{int} exists which fulfills the partition property.*

By this construction we have for sure that $\eta \geq H_i$ for $i \in \mathcal{N}_0$. If the boundary $\partial\Omega_0$ stays fixed, or if it is sufficiently regular in the sense that it can be represented by a small number of straight-sided faces (edges), we have

$$\eta \simeq \text{dist}(\Gamma_D \setminus \partial\Omega_0, \partial\Omega_0) \quad \text{if} \quad \text{dist}(\Gamma_D \setminus \partial\Omega_0, \partial\Omega_0) > 0, \quad (3.22)$$

see also Remark 3.18 at the end of this subsection. In case the Dirichlet boundary Γ_D touches $\partial\Omega_0$, there exists a shape parameter $\eta > 0$ in the sense of Definition 3.14 as long as there exists at least one interior subdomain, for an illustration see Figure 3.3, right.

The following theorem gives bounds of the extension indicator for different classes of geometric configurations.

Theorem 3.15. *Let the extension indicator $\gamma_h(\Omega_0, \Omega_{\text{int}}, \Gamma_D)$ and the shape parameter $\eta > 0$ be defined according to Definition 3.11 and Definition 3.14. Then the following estimates hold.*

- (i) If Γ_D is empty or if $\Gamma_D \subset \partial\Omega_0$ then $\gamma_h(\Omega_0, \Omega_{\text{int}}, \Gamma_D) \leq 1$,
- (ii) if $\Gamma_D \setminus \partial\Omega_0$ is separated from $\partial\Omega_0$ then $\gamma_h(\Omega_0, \Omega_{\text{int}}, \Gamma_D) \lesssim \frac{H_0}{\eta}$,
- (iii) otherwise, $\gamma_h(\Omega_0, \Omega_{\text{int}}, \Gamma_D) \lesssim \frac{H_0}{\eta} (1 + \log(\eta/h_0))^2$.

Note that *Part (i)* is trivial due to Definition 3.11. Before we give the proofs of *Part (ii)* and *Part (iii)* we need the following lemma which is related to a partition of unity function used for overlapping Schwarz methods, cf. TOSELLI AND WIDLUND [184, Lemma 3.4].

Lemma 3.16. *Assume that $\Gamma_D \setminus \partial\Omega_0$ is separated from $\partial\Omega_0$ (Case (ii) of Theorem 3.15). Then there exists a discrete cut-off function $\chi \in \tilde{V}^h(\Omega_{\text{int}})$ which fulfills*

- (i) $\chi(x) \in [0, 1] \quad \forall x \in \overline{\Omega}_{\text{int}}$,
- (ii) $\chi|_{\partial\Omega_0} = 1$, and χ vanishes entirely on $\Omega_{\text{int}} \setminus \Omega_{\text{int},\eta}$, in particular on $\Gamma_D \setminus \partial\Omega_0$,
- (iii) $\|\nabla\chi\|_{L^\infty(\Omega_{\text{int}})} \lesssim 1/\eta$,

where η is the shape parameter and $\Omega_{\text{int},\eta}$ the boundary layer according to Definition 3.14.

Proof. We construct a particular cut-off function χ . First, we define the continuous function

$$\chi_0(x) := \left\{ \begin{array}{ll} 1 - \frac{\text{dist}(x, \partial\Omega_0)}{\eta} & \text{if } \text{dist}(x, \partial\Omega_0) \leq \eta, \\ 0 & \text{otherwise,} \end{array} \right\} \quad \text{for } x \in \Omega_{\text{int}}.$$

A simple inspection shows that this function is well-defined, continuous, and that $\nabla\chi_0 \in L^\infty(\Omega_{\text{int}})$. We define $\chi \in \tilde{V}^h(\Omega_{\text{int}})$ by the nodal interpolation of χ_0 . Both functions obviously fulfill the properties (i)–(iii). \square

Proof of Theorem 3.15, Part (ii): In this proof we estimate the energy of a particular extension that matches the Dirichlet boundary conditions using the cut-off function $\chi \in \tilde{V}^h(\Omega_{\text{int}})$ from Lemma 3.16. Our argumentation follows the line of GRAHAM, LECHNER, AND SCHEICHL [75, Lemma 3.3 and Theorem 4.3], where instead of χ , a continuous partition of unity function with respect to an overlapping subdomain partition is used.

Let $w_0 \in V_D^h(\partial\Omega_0)$ be fixed and let $\tilde{w} := \tilde{\mathcal{H}}^{\text{int}} w_0 \in \tilde{V}^h(\Omega_{\text{int}})$ denote its discrete harmonic extension. Recall that $\Omega_{\text{int},\eta}$ is partitioned into finitely many shape-regular patches ω_j , $j \in \mathcal{J}$. Let \tilde{I}^h denote the nodal interpolator with respect to the triangulation $\tilde{\mathcal{T}}^h(\Omega_{\text{int}})$. Because of Lemma 3.16(ii), the function $\tilde{I}^h(\chi \tilde{w})$ is an extension of w_0 from $\partial\Omega_0$ to $\tilde{V}^h(\Omega_{\text{int}})$ and it vanishes on Γ_D and on $\Omega_{\text{int}} \setminus \Omega_{\text{int},\eta}$. By Definition 3.10 of the restricted discrete harmonic extension, the H^1 -continuity of \tilde{I}^h , and Lemma 3.16 we obtain

$$\begin{aligned} |\tilde{\mathcal{H}}_D^{\text{int}} w_0|_{H^1(\Omega_{\text{int}})}^2 &\leq |\tilde{I}^h(\chi \tilde{w})|_{H^1(\Omega_{\text{int}})}^2 = |\tilde{I}^h(\chi \tilde{w})|_{H^1(\Omega_{\text{int},\eta})}^2 \\ &\lesssim \int_{\Omega_{\text{int},\eta}} |\nabla(\chi(x) \tilde{w}(x))|^2 dx \\ &\lesssim \int_{\Omega_{\text{int},\eta}} |\nabla\chi(x)|^2 |\tilde{w}(x)|^2 + |\chi(x)|^2 |\nabla\tilde{w}(x)|^2 dx \quad (3.23) \\ &\lesssim \|\nabla\chi\|_{L^\infty(\Omega_{\text{int}})}^2 \|\tilde{w}\|_{L^2(\Omega_{\text{int},\eta})}^2 + |\tilde{w}|_{H^1(\Omega_{\text{int},\eta})}^2 \\ &\lesssim \sum_{j \in \mathcal{J}} \left\{ \frac{1}{\eta^2} \|\tilde{w}\|_{L^2(\omega_j)}^2 + |\tilde{w}|_{H^1(\omega_j)}^2 \right\}. \end{aligned}$$

By Theorem 1.7 (see also TOSELLI AND WIDLUND [184, Corollary A.15]), whose application is justified by Definition 3.13(iii), we conclude that

$$\frac{1}{\eta^2} \|\tilde{w}\|_{L^2(\omega_j)}^2 \lesssim |\tilde{w}|_{H^1(\omega_j)}^2 + \frac{1}{\eta} \|\tilde{w}\|_{L^2(\partial\omega_j \cap \partial\Omega_0)}^2. \quad (3.24)$$

Finally, since the union of the patches forms the boundary layer $\Omega_{\text{int},\eta} \subset \Omega_{\text{int}}$ and using the fact that $H_0 \geq \eta$, we can conclude from (3.23) and (3.24) that

$$\begin{aligned} |\tilde{\mathcal{H}}_D^{\text{int}} w_0|_{H^1(\Omega_{\text{int}})}^2 &\lesssim |\tilde{w}|_{H^1(\Omega_{\text{int}})}^2 + \frac{1}{\eta} \|\tilde{w}\|_{L^2(\partial\Omega_0)}^2 \\ &\lesssim \frac{H_0}{\eta} \left\{ |\tilde{\mathcal{H}}_D^{\text{int}} w_0|_{H^1(\Omega_{\text{int}})}^2 + \frac{1}{H_0} \|w_0\|_{L^2(\partial\Omega_0)}^2 \right\}, \end{aligned}$$

which proves Part (ii) of Theorem 3.15. \square

Proof of Theorem 3.15, Part (iii): In this case, Γ_D touches $\partial\Omega_0$. We cannot use the cut-off function from Lemma 3.16 anymore. However, due to Definition 3.14 we still have the partition $\{\omega_j\}_{j \in \mathcal{J}}$ of the boundary layer $\Omega_{\text{int},\eta}$, where the shape-regular patches ω_j have a diameter proportional to the shape parameter η . The partition defines *patch* faces, edges, and vertices analogous to Definition 2.2 (page 48) considering a patch as a subdomain. For a patch ω_j , we denote by

- \mathbf{f}_j the *patch face*,
- \mathbf{e}_j (generically) a *patch edge*,
- \mathbf{v}_j (generically) a *patch vertex*,

of ω_j which is part of the boundary $\partial\Omega_0$ (in two dimension we have of course no faces). The interior patch faces, edges, and vertices are not considered. Using the auxiliary triangulation $\tilde{\mathcal{T}}^h(\Omega_{\text{int}})$ we can define the cut-off functions $\vartheta_{\mathbf{f}_j}$, $\vartheta_{\mathbf{e}_j}$, and $\vartheta_{\mathbf{v}_j} \in \tilde{V}^h(\Omega_{\text{int}})$, according to Definition 2.30 (page 75) and Remark 2.35 (page 77), see also TOSELLI AND WIDLUND [184, Sect. 4.6]. Each such function is supported in only a few patches, and the supports of all these functions overlap finitely many times. For a patch face, edge, or vertex of ω_j which is part of the boundary $\partial\Omega_0$ we generically write \mathbf{x}_j , similar to the notation on page 75. For a fixed function $w \in V_D^h(\partial\Omega_0)$ we denote its discrete harmonic extension by $\tilde{w} := \tilde{\mathcal{H}}^{\text{int}} w \in \tilde{V}^h(\Omega_{\text{int}})$. We define another function

$$\hat{w} := \sum_{\mathbf{x}_j} \tilde{I}^h(\vartheta_{\mathbf{x}_j} \tilde{w}),$$

where the sum runs over all the patch faces, edges, and vertices of the partition which are part of the boundary $\partial\Omega_0$. Using Remark 2.35 and Definition 3.14, it is not hard to see that (i) the function \hat{w} is an element of $\tilde{V}^h(\Omega_{\text{int}})$, (ii) the function \hat{w} is a discrete extension of w , and (iii) the function \hat{w} vanishes on Γ_D . Using Definition 3.10, the finite overlap of the supports of the functions $\vartheta_{\mathbf{x}_j}$, TOSELLI AND WIDLUND [184, Lemma 4.15, Lemma 4.19, and Lemma 4.24] (see also Lemma 2.33 and Lemma 2.34), and Theorem 1.7, we obtain

$$\begin{aligned} |\tilde{\mathcal{H}}_D^{\text{int}} w_0|_{H^1(\Omega_{\text{int}})}^2 &\leq |\hat{w}|_{H^1(\Omega_{\text{int}})}^2 \lesssim \sum_{\mathbf{x}_j} |I^h(\vartheta_{\mathbf{x}_j} \tilde{w})|_{H^1(\text{supp}(\vartheta_{\mathbf{x}_j}))}^2 \\ &\lesssim \sum_{j \in \mathcal{J}} (1 + \log(\eta/h_0))^2 \left\{ |\tilde{w}|_{H^1(\omega_j)}^2 + \frac{1}{\eta^2} \|\tilde{w}\|_{L^2(\omega_j)}^2 \right\} \\ &\lesssim \sum_{j \in \mathcal{J}} (1 + \log(\eta/h_0))^2 \left\{ |\tilde{w}|_{H^1(\omega_j)}^2 + \frac{1}{\eta} \|\tilde{w}\|_{L^2(\partial\omega_j \cap \partial\Omega_0)}^2 \right\} \\ &\leq (1 + \log(\eta/h_0))^2 \left\{ |\tilde{w}|_{H^1(\Omega_{\text{int}})}^2 + \frac{1}{\eta} \|\tilde{w}\|_{L^2(\partial\Omega_0)}^2 \right\} \\ &\leq (1 + \log(\eta/h_0))^2 \frac{H_0}{\eta} \left\{ |\tilde{\mathcal{H}}^{\text{int}} w_0|_{H^1(\Omega_{\text{int}})}^2 + \frac{1}{H_0} \|w_0\|_{L^2(\partial\Omega_0)}^2 \right\}, \end{aligned}$$

which concludes the proof of Theorem 3.15, Part (iii). \square

We finish this subsection with two remarks on possible extensions of Theorem 3.15.

Remark 3.17. In case Assumption 3.8 is violated (i. e., h_0 cannot resolve fine details in Ω_{int} or Γ_D) the theory being presented in this section may still be useful. One needs to replace Ω_{int} and Γ_D in Definition 3.11 by suitable sets $\tilde{\Omega}_{\text{int}}$ and $\tilde{\Gamma}_D$, respectively, such that $\tilde{\Omega}_{\text{int}}$ excludes the fine details, and $\tilde{\Gamma}_D$ is chosen such that any function $w \in V^h(\tilde{\Omega}_{\text{int}})$ with $w|_{\tilde{\Gamma}_D} = 0$ can be extended by zero to Ω_{int} where this extension vanishes on Γ_D .

Remark 3.18. If the outer boundary $\partial\Omega_0$ has many faces, it can happen that $\eta \simeq H_i$ for $i \in \mathcal{N}_0$ because $\partial\Omega_0$ is too “rough” in the sense that it cannot be represented by a small number of straight faces. Using the theory from [45] and [113] concerning domain decomposition methods for less regular subdomains (at least in two dimensions), we may relax the partition property from Definition 3.13 such that the patches can be chosen less regular. For many cases this may result in a larger shape parameter η , and therefore better bounds in Theorem 3.15. However, this issue is only important if one is interested in asymptotic bounds that remain robust when changing the outer boundary $\partial\Omega_0$. Note also, that the constants in our bounds depend in any case on the shapes of the subdomains.

3.4.2 Main result

As discussed in Section 2.2.4, most arguments in the analysis of one-level FETI/BETI methods are algebraic except for the estimate of the P_D -operator. This is indeed true for the present case. The following lemma gives such P_D -estimates. Recall the space

$$W^\perp := \left\{ w \in W : \int_{\Omega_i} \mathcal{H}_i w_i dx = 0 \quad \forall i \in \mathcal{I}_{\text{float}} \right\}. \quad (3.25)$$

Lemma 3.19. *Let $w \in W^\perp$ be arbitrary but fixed and let $z_w \in \ker S$ be the unique element from Lemma 2.22. Then for $Q = M^{-1}$ or Q chosen according to (3.16)–(3.19), the estimates*

$$\begin{aligned} |P_D(w + z_w)|_S^2 &\leq C \max_{j \in \mathcal{N}_0} \frac{H_0}{H_j} \max_{i \in \mathcal{I}_{\text{int}}} (1 + \log(H_i/h_i))^2 |w|_S^2, \\ |P_D(w + z_w)|_S^2 &\leq C \gamma_h(\Omega_0, \Omega_{\text{int}}, \Gamma_D) \max_{j \in \mathcal{I}} \frac{\alpha_j}{\alpha_0} \max_{i \in \mathcal{I}_{\text{int}}} (1 + \log(H_i/h_i))^2 |w|_S^2, \end{aligned}$$

hold, where $\gamma_h(\Omega_0, \Omega_{\text{int}}, \Gamma_D)$ is the extension indicator according to Definition 3.11, and the constant $C > 0$ is independent of H_i , h_i , the number of subdomains, the number of neighbors of the exterior part Ω_0 , and the coefficients α_i .

Proof. Postponed to Section 3.4.4. □

The above lemma immediately implies our main result of the current section.

Theorem 3.20. *For $Q = M^{-1}$ or Q chosen according to (3.16)–(3.19), the one-level and the all-floating FETI/BETI methods for unbounded domains defined in this section satisfy the condition number estimates*

$$\begin{aligned} \kappa &\leq C \max_{j \in \mathcal{N}_0} \frac{H_0}{H_j} \max_{i \in \mathcal{I}_{\text{int}}} (1 + \log(H_i/h_i))^2, \\ \kappa &\leq C \gamma_h(\Omega_0, \Omega_{\text{int}}, \Gamma_D) \max_{j \in \mathcal{I}} \frac{\alpha_j}{\alpha_0} \max_{i \in \mathcal{I}_{\text{int}}} (1 + \log(H_i/h_i))^2, \end{aligned}$$

where $\gamma_h(\Omega_0, \Omega_{\text{int}}, \Gamma_D)$ is the extension indicator according to Definition 3.11, and the constant $C > 0$ is independent of H_i , h_i , the number of subdomains, the number of neighbors of the exterior part Ω_0 , and the coefficients α_i .

Proof. The proof is identical to the proof of Theorem 2.28 in Section 2.2.4 replacing Lemma 2.27 by Lemma 3.19. □

Remark 3.21. Note that under the condition $\alpha_0 \gtrsim \alpha_i$ for all $i \in \mathcal{I}_{\text{int}}$, we have

$$\max_{j \in \mathcal{I}} \frac{\alpha_j}{\alpha_0} \simeq 1.$$

If additionally, the Dirichlet boundary Γ_D is empty, or separated from $\partial\Omega_0$ with a shape parameter η being proportional to H_0 , we get the quasi-optimal bound

$$\kappa \leq C \max_{i \in \mathcal{I}_{\text{int}}} (1 + \log(H_i/h_i))^2,$$

according to Theorem 3.15. This is the same (sharp) estimate that we obtained in the bounded case, cf. Theorem 2.28.

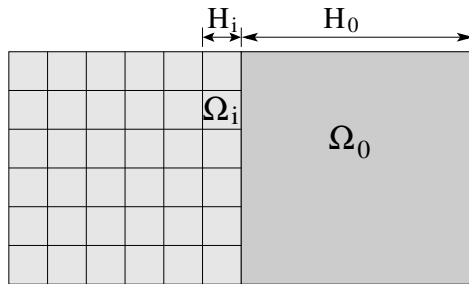


Figure 3.4: Illustration of Remark 3.22.

Remark 3.22. The fact that the quasi-optimal condition number estimate does not hold in general is not so surprising: Since Ω_0 is a non-floating subdomain there is no direct coarse space component concerning S_0 . However, S_0 is regular, which is similar to the case that we have an equation of the type

$$-\alpha_0 \Delta u + \frac{\alpha_0}{H_0^2} u = 0 \quad \text{in } \Omega_0,$$

with a bounded domain Ω_0 as sketched in Figure 3.4. As pointed out by FARHAT, CHEN, AND MANDEL [58], differential operators of the form $-\operatorname{div}[\alpha \nabla u] + \beta u$ (which occur mostly in connection with time-dependent problems) require a different projection (and therefore a different method) to guarantee robustness with respect to the number of subdomains. See also TOSELLI AND KLAWONN [182] for related electromagnetic problems.

The result of Theorem 3.20, however, shows that the coarse space built from the interior subdomains is strong enough to serve for the exterior part as well, as long as the interior coefficients are not essentially larger than α_0 , and as long as there is enough (geometric) space in Ω_{int} in the neighborhood of $\partial\Omega_0$. We note close similarities to the theory of overlapping Schwarz methods; in particular the shape parameter η acts like the overlap parameter, cf. TOSELLI AND WIDLUND [184, Sect. 3] and GRAHAM, LECHNER, AND SCHEICHL [75].

Remark 3.23. We point out that the following tools and proofs might also be useful for the bounded case, e. g., to give precise estimates for the case that a large region of homogeneous material is handled by one single BEM subdomain with smaller neighboring subdomains, cf. Figure 3.5.

3.4.3 Additional technical tools

Before we come to the proof of Lemma 3.19, we need a few additional technical tools. As in Chapter 2 we restrict ourselves to the three-dimensional case, since the two-dimensional case can be derived from it. First, we need some constructions and a lemma which allows to estimate split and composed functions in the energy-norm induced by the exterior Steklov-Poincaré operator S_0 .

Construction 3.24. Using the coarse triangulation of the auxiliary domain Ω' , see Assumption 3.3, we can find for each face \mathcal{F}_0 an auxiliary subdomain $\Omega'_{\mathcal{F}_0} \subset \Omega' \setminus \overline{\Omega}_{\text{int}}$ consisting of a few simplices, such that \mathcal{F}_0 is shared by an interior subdomain and the auxiliary subdomain $\Omega'_{\mathcal{F}_0}$. Similarly, for each edge \mathcal{E}_0 (and respectively each vertex \mathcal{V}_0), we can find auxiliary

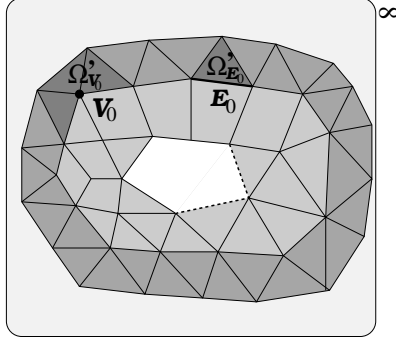


Figure 3.5: Illustration of the auxiliary subdomains $\Omega'_{\mathcal{E}_0}$, and $\Omega'_{\mathcal{V}_0}$ from Construction 3.24 for a two-dimensional configuration.

subdomains $\Omega'_{\mathcal{E}_0}$ (respectively $\Omega'_{\mathcal{V}_0}$) such that all the simplices from the coarse triangulation that touch \mathcal{E}_0 (respectively \mathcal{V}_0) are contained in $\Omega'_{\mathcal{E}_0}$ (respectively $\Omega'_{\mathcal{V}_0}$). This construction can be done such that the auxiliary subdomains have diameters proportional to the diameters of the interior subdomains which share the corresponding face, edge, or vertex. For an illustration see Figure 3.5.

Construction 3.25. We introduce an auxiliary triangulation $\mathcal{T}^h(\Omega' \setminus \overline{\Omega}_{\text{int}})$ which is conforming, shape-regular, and quasi-uniform with shape parameter h_0 and which matches with $\mathcal{T}^h(\partial\Omega_0)$ and with the coarse triangulation of Ω' . We denote the corresponding finite element space by $V^h(\Omega' \setminus \overline{\Omega}_{\text{int}})$ and the local restrictions of that space to $\Omega'_{\mathcal{X}_0}$ by $V^h(\Omega'_{\mathcal{X}_0})$. Analogously to Definition 2.30 (page 75) and Remark 2.35 (page 77) we define the cut-off functions $\vartheta'_{\mathcal{F}_0} \in V^h(\Omega'_{\mathcal{F}_0})$, $\vartheta'_{\mathcal{E}_0} \in V^h(\Omega'_{\mathcal{E}_0})$, and $\vartheta'_{\mathcal{V}_0} \in V^h(\Omega'_{\mathcal{V}_0})$. Finally, we denote the discrete harmonic extension of a function $w \in V^h(\mathcal{F}_0)$ to $V^h(\Omega'_{\mathcal{F}_0})$ by $\mathcal{H}'_{\mathcal{F}_0} w$ such that

$$\mathcal{H}'_{\mathcal{F}_0} w = \operatorname{argmin} \{ |\tilde{w}|_{H^1(\Omega'_{\mathcal{F}_0})} : \tilde{w} \in V^h(\Omega'_{\mathcal{F}_0}), \tilde{w}|_{\overline{\mathcal{F}_0}} = w \}. \quad (3.26)$$

Lemma 3.26. For all $w \in V^h(\partial\Omega_0)$, and any extension \tilde{w} of w from $\partial\Omega_0$ to $V^h(\Omega' \setminus \overline{\Omega}_{\text{int}})$, we have

$$(i) \quad |w|_{S_0}^2 \lesssim \sum_{\mathcal{X}_0} \alpha_0 |I^h(\vartheta'_{\mathcal{X}_0} \tilde{w})|_{H^1(\Omega'_{\mathcal{X}_0})}^2,$$

$$(ii) \quad \sum_{\mathcal{F}_0} \alpha_0 |\mathcal{H}'_{\mathcal{F}_0} w|_{H^1(\Omega'_{\mathcal{F}_0})}^2 \lesssim |w|_{S_0}^2.$$

Proof. Part (i): Let $w \in V^h(\partial\Omega_0)$ be fixed. By Construction 3.24, the function

$$\psi = \sum_{\mathcal{X}_0} I^h(\vartheta'_{\mathcal{X}_0} \tilde{w})$$

is an extension of w from $\partial\Omega_0$ to $H_*^1(\Omega_0)$ because it vanishes outside of $\Omega' \setminus \overline{\Omega}_{\text{int}}$. Using

relation (1.62) from page 32 we obtain

$$\begin{aligned} |w|_{S_0}^2 &\leq \alpha_0 \min_{\substack{u \in H_*^1(\Omega_0) \\ u|_{\partial\Omega_0} = w}} \int_{\Omega_0} |\nabla u|^2 dx \\ &\leq \alpha_0 \int_{\Omega_0} \left| \nabla \left(\sum_{\mathcal{X}_0} I^h(\vartheta'_{\mathcal{X}_0} \tilde{w}) \right) \right|^2 dx \lesssim \sum_{\mathcal{X}_0} \alpha_0 |I^h(\vartheta'_{\mathcal{X}_0} \tilde{w})|_{H^1(\Omega'_{\mathcal{X}_0})}^2, \end{aligned}$$

where in the last step we have used that the supports of the cut-off functions $\vartheta_{\mathcal{X}_0}$ have finite overlap.

Part (ii): First we show

$$\sum_{\mathcal{F}_0} |\mathcal{H}'_{\mathcal{F}_0} w|_{H^1(\Omega'_{\mathcal{F}_0})}^2 \lesssim |w|_{S_{0,\text{FEM}}^{\text{int}}}^2, \quad (3.27)$$

where $S_{0,\text{FEM}}^{\text{int}}$ is the Steklov-Poincaré FEM-approximation using an auxiliary triangulation $\tilde{\mathcal{T}}^h(\Omega \setminus \bar{\Omega}_0)$ of $\Omega \setminus \bar{\Omega}_0$ which is shape-regular and quasi-uniform with mesh parameter h_0 . Let \hat{w} denote the discrete harmonic extension of w from $\partial\Omega_0$ to $V^h(\Omega \setminus \bar{\Omega}_0)$ such that

$$|w|_{S_{0,\text{FEM}}^{\text{int}}}^2 = |\hat{w}|_{H^1(\Omega \setminus \Omega_0)}^2.$$

Let now \mathcal{F}_0 be a face shared by the interior subdomain Ω_i and the auxiliary subdomain $\Omega'_{\mathcal{F}_0}$. Using Lemma 2.39 (see page 78) we can conclude that

$$|\mathcal{H}'_{\mathcal{F}_0} w|_{H^1(\Omega'_{\mathcal{F}_0})} \lesssim |\mathcal{H}_i w|_{H^1(\Omega_i)} \leq |\hat{w}|_{H^1(\Omega_i)}^2,$$

which immediately implies (3.27) by summing over the faces. Using Lemma 1.33 we obtain

$$\sum_{\mathcal{F}_0} |\mathcal{H}'_{\mathcal{F}_0} w|_{H^1(\Omega'_{\mathcal{F}_0})}^2 \lesssim |w|_{S_{0,\text{FEM}}^{\text{int}}}^2 \lesssim |w|_{S_{0,\text{BEM}}^{\text{ext}}}^2,$$

which shows the desired statement. \square

Remark 3.27. We can read Lemma 3.26(ii) as

$$\sum_{\mathcal{F}_0} \alpha_0 |\mathcal{H}'_{\mathcal{F}_0} w|_{H^{1/2}(\mathcal{F}_0)}^2 \lesssim |w|_{S_0}^2 \simeq \alpha_0 \left\{ |w|_{H^{1/2}(\partial\Omega_0)}^2 + \frac{1}{H_0} \|w\|_{L^2(\partial\Omega_0)}^2 \right\}.$$

Assume that the function $w \in V^h(\partial\Omega_0)$ vanishes on the boundaries of all faces \mathcal{F}_0 , then Lemma 3.26(i) can be read as

$$|w|_{S_0}^2 \lesssim \sum_{\mathcal{F}_0} \alpha_0 |w|_{H_0^{1/2}(\mathcal{F}_0)}^2.$$

Under this viewpoint, our theory of one-level methods for unbounded domains is strongly connected to the theory of iterative substructuring and additive Schwarz methods for the BEM, see, e. g., the works by AINSWORTH AND GUO [2], HEUER [85], HEUER AND STEPHAN [86, 87], STEPHAN AND TRAN [178], and VON PETERSDORFF [188].

Lemma 3.28. *For all $w \in W$ and for all $i \in \mathcal{I}_{\text{int}}$, we have*

$$\begin{aligned} |(P_D w)_i|_{S_i}^2 &\lesssim \sum_{\mathcal{X}_i \cap \Gamma} \sum_{j \in \mathcal{N}_{\mathcal{X}_i}} \min(\alpha_i, \alpha_j) |I^h(\vartheta_{\mathcal{X}_i}(w_i - w_j))|_{H^1(\Omega_i)}^2 + \sum_{\mathcal{X}_i \cap \Gamma_D} \alpha_i |I^h(\vartheta_{\mathcal{X}_i} w_i)|_{H^1(\Omega_i)}^2, \\ |(P_D w)_0|_{S_0}^2 &\lesssim \sum_{\mathcal{X}_0 \cap \Gamma} \sum_{j \in \mathcal{N}_{\mathcal{X}_0}} \min(\alpha_0, \alpha_j) |I^h(\vartheta'_{\mathcal{X}_0}(w_0 - w_j))|_{H^1(\Omega'_{\mathcal{X}_0})}^2 + \sum_{\mathcal{X}_0 \cap \Gamma_D} \alpha_0 |I^h(\vartheta_{\mathcal{X}_0} w_0)|_{H^1(\Omega'_{\mathcal{X}_0})}^2. \end{aligned}$$

Proof. Reusing Lemma 2.16 we can show that in the current unbounded case, the operator P_D is characterized by

$$(P_D w)_i(x^h) = \begin{cases} \sum_{j \in \mathcal{N}_{x^h}} \delta_j^\dagger(x^h) (w_i(x^h) - w_j(x^h)) & \text{for } x^h \in \partial\Omega_i^h \setminus \Gamma_D, \\ w_i(x^h) & \text{for } x^h \in \partial\Omega_i^h \cap \Gamma_D. \end{cases} \quad (3.28)$$

Using the proof in Section 2.2.4.4, Lemma 2.39, and Lemma 3.26(i), we obtain for $i \in \mathcal{I}_{\text{int}}$,

$$\begin{aligned} |(P_D w)_i|_{S_i}^2 &\lesssim \sum_{\mathcal{X}_i \cap \Gamma} \alpha_i \left| \sum_{j \in \mathcal{N}_{\mathcal{X}_i}} I^h(\delta_j^\dagger \vartheta_{\mathcal{X}_i}(w_i - w_j)) \right|_{H^1(\Omega_i)}^2 + \sum_{\mathcal{X}_i \cap \Gamma_D} \alpha_i |I^h(\vartheta_{\mathcal{X}_i} w_i)|_{H^1(\Omega_i)}^2, \\ |(P_D w)_0|_{S_0}^2 &\lesssim \sum_{\mathcal{X}_0} \alpha_0 \left| \sum_{j \in \mathcal{N}_{\mathcal{X}_0}} I^h(\delta_j^\dagger \vartheta'_{\mathcal{X}_0}(w_0 - w_j)) \right|_{H^1(\Omega'_{\mathcal{X}_0})}^2 + \sum_{\mathcal{X}_0 \cap \Gamma_D} \alpha_0 |I^h(\vartheta_{\mathcal{X}_0} w_0)|_{H^1(\Omega'_{\mathcal{X}_0})}^2. \end{aligned}$$

Using the fact that δ_j^\dagger is constant on the inner nodes of each edge and face, and using the elementary inequality (2.100) from page 80, we obtain the desired statement. \square

3.4.4 The P_D estimates – Proof of Lemma 3.19

Let $w \in W^\perp$ be arbitrary. We introduce the projection that selects the component of $w_0 \in V_D^h(\partial\Omega_0)$, i. e.,

$$\Pi_0 w := [w_0, 0, \dots, 0]. \quad (3.29)$$

In the following we write $w = \Pi_0 w + \tilde{w}$ where $\tilde{w} = (I - \Pi_0)w$, i. e., $\tilde{w}_0 = 0$. Lemma 2.22 assures that z_w depends linearly on w . Hence, $z_w = z_{(\Pi_0 w)} + z_{\tilde{w}}$, which implies

$$|P_D(w + z_w)|_S^2 \lesssim |P_D(\tilde{w} + z_{\tilde{w}})|_S^2 + |P_D(\Pi_0 w + z_{(\Pi_0 w)})|_S^2. \quad (3.30)$$

Using the fact that $\tilde{w}_0 = 0$, and using Lemma 3.28 and the proof of Lemma 2.27 from Section 2.2.4.4, one can show that

$$|P_D(\tilde{w} + z_{\tilde{w}})|_S^2 \lesssim \max_{i \in \mathcal{I}_{\text{int}}} (1 + \log(H_i/h_i))^2 |\tilde{w}|_S^2, \quad (3.31)$$

which bounds the first summand in (3.30). For the second summand we prove the following estimates.

Claim 1. For all $w \in W$,

$$|P_D(\Pi_0 w + z_{(\Pi_0 w)})|_S^2 \leq C \max_{j \in \mathcal{N}_0} \frac{H_0}{H_j} \max_{i \in \mathcal{I}_{\text{int}}} (1 + \log(H_i/h_i))^2 |w_0|_{S_0}^2.$$

Claim 2. For all $w \in W$,

$$|P_D(\Pi_0 w + z_{(\Pi_0 w)})|_S^2 \leq C \gamma_h(\Omega_0, \Omega_{\text{int}}, \Gamma_D) \max_{j \in \mathcal{I}} \frac{\alpha_j}{\alpha_0} \max_{i \in \mathcal{I}_{\text{int}}} (1 + \log(H_i/h_i))^2 |w_0|_{S_0}^2.$$

Proof of Claim 1 for the case $Q = M^{-1}$. First, the identity $P_D^\top S P_D = B^\top M^{-1} B = B^\top Q B$ (see Lemma 2.16, page 70) and Lemma 2.22 (page 72) imply

$$\begin{aligned} |P_D(\Pi_0 w + z_{(\Pi_0 w)})|_S^2 &= \|B(\Pi_0 w + z_{(\Pi_0 w)})\|_Q^2 \\ &= \min_{z \in \ker S} \|B(\Pi_0 w + z)\|_Q^2 \leq \|B(\Pi_0 w)\|_Q^2 = |P_D(\Pi_0 w)|_S^2. \end{aligned} \quad (3.32)$$

Secondly, we apply Lemma 3.28. Due to the fact that $\Pi_0 w$ has only a non-trivial zero-component, we get only contributions from faces, edges, and vertices \mathcal{X}_{j_0} shared by Ω_0 and one of its neighboring subdomains Ω_j . There are no contributions from the Dirichlet boundary, because $(w_0)|_{\Gamma_D} = 0$ due to (3.15).

$$\begin{aligned} |P_D(\Pi_0 w)|_S^2 &\lesssim \sum_{\mathcal{X}_{j_0}} \min(\alpha_0, \alpha_j) |I^h(\vartheta'_{\mathcal{X}_{j_0}} w_0)|_{H^1(\Omega'_{\mathcal{X}_{j_0}})}^2 \\ &\quad + \sum_{\mathcal{X}_{j_0}} \min(\alpha_0, \alpha_j) |I^h(\vartheta_{\mathcal{X}_{j_0}} w_0)|_{H^1(\Omega_j)}^2. \end{aligned} \quad (3.33)$$

We can simply estimate $\min(\alpha_0, \alpha_j)$ from above by α_0 . By Lemma 2.39 and Lemma 2.34 we obtain

$$\begin{aligned} &|I^h(\vartheta'_{\mathcal{X}_{j_0}} w_0)|_{H^1(\Omega'_{\mathcal{X}_{j_0}})}^2 + |I^h(\vartheta_{\mathcal{X}_{j_0}} w_0)|_{H^1(\Omega_j)}^2 \\ &\lesssim (1 + \log(H_j/h_j))^2 \left\{ |\mathcal{H}'_{\mathcal{X}_{j_0}} w_0|_{H^1(\Omega'_{\mathcal{X}_{j_0}})}^2 + \frac{1}{H_j} \|w_0\|_{L^2(\mathcal{F}_{0k})}^2 \right\}, \end{aligned} \quad (3.34)$$

where \mathcal{F}_{0k} is chosen such that \mathcal{X}_{j_0} touches it. Combining (3.33), (3.34), and Lemma 3.26(ii), we obtain

$$\begin{aligned} |P_D(\Pi_0 w)|_S^2 &\lesssim \max_{j \in \mathcal{N}_0} (1 + \log(H_j/h_j))^2 \left\{ |w_0|_{S_0}^2 + \sum_{\mathcal{F}_{0k}} \frac{\alpha_0}{H_k} \|w_0\|_{L^2(\mathcal{F}_{0k})}^2 \right\} \\ &\lesssim \max_{j \in \mathcal{N}_0} (1 + \log(H_j/h_j))^2 \max_{k \in \mathcal{N}_0} \frac{H_0}{H_k} \left\{ |w_0|_{S_0}^2 + \frac{\alpha_0}{H_0} \|w_0\|_{L^2(\partial\Omega_0)}^2 \right\}. \end{aligned}$$

Using Lemma 1.33, the L^2 -term in the last line can be bounded from above by $|w_0|_{S_0}^2$. Combining the last result with (3.32) proves Claim 1 for the case $Q = M^{-1}$. \square

Proof of Claim 1 for Q chosen according to (3.16)–(3.19). We start with the elementary estimate

$$|P_D(\Pi_0 w + z_{(\Pi_0 w)})|_S^2 \lesssim |P_D(\Pi_0 w)|_S^2 + |P_D z_{(\Pi_0 w)}|_S^2. \quad (3.35)$$

As shown in the above proof of Claim 1 (for $Q = M^{-1}$),

$$|P_D(\Pi_0 w)|_S^2 \lesssim \max_{j \in \mathcal{N}_0} (1 + \log(H_j/h_j))^2 \max_{k \in \mathcal{N}_0} \frac{H_0}{H_k} |w_0|_{S_0}^2, \quad (3.36)$$

which bounds the first term in (3.35). For the second term, let z_i denote the (constant) components of $z_{(\Pi_0 w)}$. Since Ω_0 is a non-floating subdomain, $z_0 = 0$. Lemma 3.28, Lemma 2.34

and a comparison with the entries of Q yield

$$\begin{aligned} |P_D z_{(\Pi_0 w)}|_S^2 &\lesssim \sum_{i \in \mathcal{I}_{\text{int}}} \sum_{\mathcal{X}_{j_i}} \min(\alpha_i, \alpha_j) |\vartheta_{\mathcal{X}_{j_i}}(z_i - z_j)|_{H^1(\Omega_i)}^2 + \sum_{\mathcal{X}_i \cap \Gamma_D} \alpha_i |\vartheta_{\mathcal{X}_i} z_i|_{H^1(\Omega_i)}^2 \\ &\quad + \sum_{\mathcal{X}_{j_0} \cap \Gamma} \min(\alpha_0, \alpha_j) |\vartheta_{\mathcal{X}_{j_0}}(z_0 - z_j)|_{H^1(\Omega'_{\mathcal{X}_{j_0}})}^2 \\ &\lesssim \|B z_{(\Pi_0 w)}\|_Q^2. \end{aligned}$$

The above estimate holds for both the standard and the all-floating formulation, see the proof of Lemma 2.44, page 82ff. Using Lemma 2.22 and the same technique as in the proof of Lemma 2.44 we obtain

$$\begin{aligned} |P_D z_{(\Pi_0 w)}|_S^2 &\lesssim \|B z_{(\Pi_0 w)}\|_Q^2 \leq \|B(\Pi_0 w)\|_Q^2 \\ &\lesssim \sum_{\mathcal{F}_{0j}} \alpha_0 (1 + \log(H_j/h_j)) \frac{1}{H_j} \|w_0\|_{L^2(\mathcal{F}_{0j})}^2 + \sum_{\mathcal{E}_{0k}} \alpha_0 \|w_0\|_{L^2(\mathcal{E}_{0k})}^2. \end{aligned}$$

Using Lemma 2.34(ii), one can show that

$$\|w_0\|_{L^2(\mathcal{E}_{0k})}^2 \lesssim (1 + \log(H_j/h_j)) \left\{ |\mathcal{H}'_{\mathcal{F}_j} w_0|_{H^1(\Omega'_{\mathcal{F}_j})}^2 + \frac{1}{H_j} \|w_0\|_{L^2(\mathcal{F}_j)}^2 \right\}$$

if the face \mathcal{F}_j touches the edge \mathcal{E}_{0k} . Combining the last two estimates, Lemma 3.26(ii), and Lemma 1.33 we finally obtain

$$\begin{aligned} |P_D z_{(\Pi_0 w)}|_S^2 &\lesssim \max_{k \in \mathcal{N}_k} (1 + \log(H_k/h_k)) \left\{ \max_{i \in \mathcal{N}_0} \frac{\alpha_0}{H_i} \|w_0\|_{L^2(\partial\Omega_0)}^2 + \sum_{\mathcal{F}_{0j}} \alpha_0 |\mathcal{H}'_{\mathcal{F}_j} w_0|_{H^1(\Omega'_{\mathcal{F}_j})}^2 \right\} \\ &\lesssim \max_{k \in \mathcal{N}_k} (1 + \log(H_k/h_k)) \max_{i \in \mathcal{N}_0} \frac{H_0}{H_i} |w_0|_{S_0}^2, \end{aligned}$$

which proves Claim 1 for the diagonal choice of Q . \square

Proof of Claim 2 for the case $Q = M^{-1}$. We show

$$|P_D(\Pi_0 w + z_{(\Pi_0 w)})|_S^2 \leq C \gamma_h(\Omega_0, \Omega_{\text{int}}, \Gamma_D) \max_{j \in \mathcal{I}} \frac{\alpha_j}{\alpha_0} \max_{i \in \mathcal{I}_{\text{int}}} (1 + \log(H_i/h_i))^2 |w_0|_{S_0}^2.$$

As shown in the proof of Claim 1 for the case $Q = M^{-1}$,

$$|P_D(\Pi_0 w + z_{(\Pi_0 w)})|_S^2 = \min_{z \in \ker S} |P_D(\Pi_0 w + z)|_S^2. \quad (3.37)$$

We construct a special element $\tilde{z} \in \ker S$ to bound this minimum from above:

$$\tilde{z}_i := \begin{cases} \frac{1}{|\Omega_i|} \int_{\Omega_i} \Pi_i^h \tilde{\mathcal{H}}_D^{\text{int}} w_0 dx & \text{if } i \in \mathcal{I}_{\text{float}}, \\ 0 & \text{else,} \end{cases} \quad (3.38)$$

where $\tilde{\mathcal{H}}_D^{\text{int}} w_0 \in \tilde{V}^h(\Omega_{\text{int}})$ is the restricted discrete harmonic extension according to Definition 3.10, and Π_i^h is the Scott-Zhang quasi-interpolation operator corresponding to the

triangulation $\mathcal{T}^h(\Omega_i)$ which preserves the boundary values on Γ_{i0} (if this set is non-empty). With the abbreviation $y := \Pi_0 w + \tilde{z}$, Lemma 3.28 yields

$$\begin{aligned} |P_D(\Pi_0 w + \tilde{z})|_S^2 &\lesssim \underbrace{\sum_{\mathcal{X}_{j0}} \min(\alpha_0, \alpha_j) |I^h(\vartheta'_{\mathcal{X}_{j0}}(w_0 - \tilde{z}_j))|_{H^1(\Omega'_{\mathcal{X}_{j0}})}^2}_{=: \varphi_1} \\ &+ \sum_{i \in \mathcal{I}_{\text{int}}} \left\{ \underbrace{\sum_{\mathcal{X}_{ij}} \min(\alpha_i, \alpha_j) |I^h(\vartheta_{\mathcal{X}_{ij}}(y_i - y_j))|_{H^1(\Omega_i)}^2}_{=: \varphi_2} + \underbrace{\sum_{\mathcal{X}_i \cap \Gamma_D} \alpha_i |I^h(\vartheta_{\mathcal{X}_i} y_i)|_{H^1(\Omega_i)}^2}_{=: \varphi_3} \right\}. \end{aligned} \quad (3.39)$$

Note, that we have no contributions from $\partial\Omega_0 \cap \Gamma_D$ because w_0 vanishes there. For the contributions in φ_1 we first note that the function $\Pi_j^h \tilde{\mathcal{H}}_D^{\text{int}} w_0$ is an extension of w_0 from \mathcal{X}_{j0} to $V^h(\Omega_j)$. This follows mainly from the properties of the Scott-Zhang quasi-interpolation operator. Using the face extension Lemma 2.39 (page 78) and the discrete estimates from Lemma 2.34 (page 76) we obtain

$$\begin{aligned} &|I^h(\vartheta'_{\mathcal{X}_{j0}}(w_0 - \tilde{z}_j))|_{H^1(\Omega'_{\mathcal{X}_{j0}})}^2 \\ &\lesssim (1 + \log(H_j/h_j))^2 \left\{ |\Pi_j^h \tilde{\mathcal{H}}_D^{\text{int}} w_0|_{H^1(\Omega_j)}^2 + \frac{1}{H_j^2} \|\Pi_j^h \tilde{\mathcal{H}}_D^{\text{int}} w_0 - \tilde{z}_j\|_{L^2(\Omega_j)}^2 \right\}. \end{aligned} \quad (3.40)$$

If Ω_i is a floating subdomain, we can eliminate the L^2 -term using the definition of \tilde{z}_j and Poincaré's inequality. If Ω_i is non-floating, $\tilde{z}_j = 0$, but Assumption 3.5 and Assumption 3.6 assure that the intersection $\partial\Omega_i \cap \Gamma_D$ is at least an edge of $\partial\Omega_i$. By the discrete Poincaré-Friedrichs inequality (Lemma 2.38, page 77), we conclude that

$$\frac{1}{H_j^2} \|\Pi_j^h \tilde{\mathcal{H}}_D^{\text{int}} w_0\|_{L^2(\Omega_j)}^2 \lesssim (1 + \log(H_j/h_j)) |\Pi_j^h \tilde{\mathcal{H}}_D^{\text{int}} w_0|_{H^1(\Omega_j)}^2.$$

Using a similar trick as in the proof of Lemma 2.42 (see the part *standard one-level formulation*), we can avoid getting three powers of the logarithmic factor. Combining these results with Lemma 1.28 (page 39) we obtain

$$|I^h(\vartheta'_{\mathcal{X}_{j0}}(w_0 - \tilde{z}_j))|_{H^1(\Omega'_{\mathcal{X}_{j0}})}^2 \lesssim (1 + \log(H_j/h_j))^2 |\tilde{\mathcal{H}}_D^{\text{int}} w_0|_{H^1(\Omega_j)}^2, \quad (3.41)$$

and thus,

$$\varphi_1 \lesssim \alpha_0 \sum_{j \in \mathcal{N}_0} (1 + \log(H_j/h_j))^2 |\tilde{\mathcal{H}}_D^{\text{int}} w_0|_{H^1(\Omega_j)}^2. \quad (3.42)$$

In order to bound φ_2 , assume that $i \in \mathcal{I}_{\text{int}}$ and let \mathcal{X}_{ij} be a face, edge, or vertex shared by Ω_i and Ω_j . If $j = 0$ the corresponding terms can be bounded using the same ideas as above. Otherwise, Lemma 2.34 yields

$$\begin{aligned} |I^h(\vartheta_{\mathcal{X}_{ij}}(y_i - y_j))|_{H^1(\Omega_i)}^2 &= |I^h(\vartheta_{\mathcal{X}_{ij}}(\tilde{z}_i - \tilde{z}_j))|_{H^1(\Omega_i)}^2 \\ &\lesssim (1 + \log(H_j/h_j)) H_j |\tilde{z}_i - \tilde{z}_j|^2. \end{aligned} \quad (3.43)$$

Let $\mathcal{U}_{ij} \subset \Omega_{\text{int}}$ be a suitably shaped connected domain containing Ω_i and Ω_j such that $\text{diam} \mathcal{U}_{ij} \simeq H_i \simeq H_j$. Furthermore, let Π_{ij}^h denote the Scott-Zhang quasi-interpolation operator on \mathcal{U}_{ij} whose restrictions to Ω_i and Ω_j coincide with Π_i^h and Π_j^h , respectively.

If $i, j \in \mathcal{I}_{\text{float}}$, the Bramble-Hilbert lemma (Lemma 1.13) and the continuity of Π_{ij}^h yield

$$H_j |\tilde{z}_i - \tilde{z}_j|^2 \lesssim |\Pi_{ij}^h \tilde{\mathcal{H}}_D^{\text{int}} w_0|_{H^1(\mathcal{U}_{ij})}^2 \lesssim |\tilde{\mathcal{H}}_D^{\text{int}} w_0|_{H^1(\mathcal{U}_{ij})}^2. \quad (3.44)$$

The case $i \in \mathcal{I}_{\text{float}}$ and $j \notin \mathcal{I}_{\text{float}}$ can only happen in the standard formulation. Note that then, $\tilde{z}_j = 0$ and $\tilde{\mathcal{H}}_D^{\text{int}} w_0$ vanishes at least on an edge of Ω_j (cf. Assumption 3.5). With the definition of

$$\hat{z}_j := \frac{1}{|\Omega_j|} \int_{\Omega_j} \Pi_j^h \tilde{\mathcal{H}}_D^{\text{int}} w_0 \, dx,$$

we obtain the following estimate by similar arguments,

$$\begin{aligned} H_j |\tilde{z}_i - \tilde{z}_j|^2 &\lesssim H_j |\tilde{z}_i - \hat{z}_j|^2 + H_j |\hat{z}_j|^2 \\ &\lesssim |\Pi_{ij}^h \tilde{\mathcal{H}}_D^{\text{int}} w_0|_{H^1(\mathcal{U}_{ij})}^2 + \frac{1}{H_j^2} \|\Pi_j^h \tilde{\mathcal{H}}_D^{\text{int}} w_0\|_{L^2(\Omega_j)}^2 \\ &\lesssim |\tilde{\mathcal{H}}_D^{\text{int}} w_0|_{H^1(\mathcal{U}_{ij})}^2 + \frac{1}{H_j^2} \|\tilde{\mathcal{H}}_D^{\text{int}} w_0\|_{L^2(\Omega_j)}^2 \\ &\lesssim (1 + \log(H_i/h_i)) |\tilde{\mathcal{H}}_D^{\text{int}} w_0|_{H^1(\mathcal{U}_{ij})}^2. \end{aligned} \quad (3.45)$$

Here, we have used the same Bramble-Hilbert argument as before, the Cauchy-Schwarz inequality, the continuity of the Scott-Zhang quasi-interpolation operator, the fact that $H_i \simeq H_j$ and $|\Omega_j| \simeq H_j^3$, and the discrete Poincaré-Friedrichs inequality. With the previous considerations, i. e., combining (3.43), (3.44), and (3.45), and using the fact that the auxiliary domains \mathcal{U}_{ij} have finite overlap, we can conclude that

$$\begin{aligned} \varphi_2 &\lesssim \sum_{i \in \mathcal{I}_{\text{int}}} \sum_{j \in \mathcal{N}_i} \min(\alpha_i, \alpha_j) (1 + \log(H_j/h_j)) |\tilde{\mathcal{H}}_D^{\text{int}} w_0|_{H^1(\mathcal{U}_{ij})}^2 \\ &\lesssim \max_{k \in \mathcal{I}} \frac{\alpha_k}{\alpha_0} \max_{j \in \mathcal{I}_{\text{int}}} (1 + \log(H_j/h_j))^2 \alpha_0 |\tilde{\mathcal{H}}_D^{\text{int}} w_0|_{H^1(\Omega_{\text{int}})}^2, \end{aligned} \quad (3.46)$$

where $\mathcal{U}_{i0} := \Omega_i$.

In case of the standard formulation, $\varphi_3 = 0$. For the all-floating formulation we can use Lemma 2.34 to show

$$\begin{aligned} \varphi_3 &= \sum_{\mathcal{X}_i \cap \Gamma_D} \alpha_i |I^h(\vartheta_{\mathcal{X}_i} \tilde{z}_i)|_{H^1(\Omega_i)}^2 \lesssim \sum_{i \in \mathcal{I}_{\text{int}} \setminus \mathcal{I}_{\text{float}}} (1 + \log(H_i/h_i)) \alpha_i H_i |\tilde{z}_i|^2 \\ &\lesssim \sum_{i \in \mathcal{I}_{\text{int}} \setminus \mathcal{I}_{\text{float}}} (1 + \log(H_i/h_i)) \frac{\alpha_i}{H_i^2} \|\Pi_i^h \tilde{\mathcal{H}}_D^{\text{int}} w_0\|_{L^2(\Omega_i)}^2 \\ &\lesssim \sum_{i \in \mathcal{I}_{\text{int}} \setminus \mathcal{I}_{\text{float}}} (1 + \log(H_i/h_i))^2 \alpha_i |\tilde{\mathcal{H}}_D^{\text{int}} w_0|_{H^1(\Omega_i)}^2, \end{aligned}$$

where in the last steps we have used the Cauchy-Schwarz inequality, Lemma 1.28, and the discrete Poincaré-Friedrichs inequality, which is justified because $\tilde{\mathcal{H}}_D^{\text{int}} w_0$ vanishes on Γ_D . We see that φ_3 is absorbed in the bound (3.46).

Combining the estimates for φ_1 , φ_2 , and φ_3 , and using the definition of the extension indicator, we obtain

$$\begin{aligned} |P_D(\Pi_0 w + \tilde{z})|_S^2 &\lesssim \max_{k \in \mathcal{I}} \frac{\alpha_k}{\alpha_0} \max_{j \in \mathcal{I}_{\text{int}}} (1 + \log(H_j/h_j))^2 \alpha_0 |\tilde{\mathcal{H}}_D^{\text{int}} w_0|_{H^1(\Omega_{\text{int}})}^2 \\ &\lesssim \gamma_h(\Omega_0, \Omega_{\text{int}}, \Gamma_D) \max_{k \in \mathcal{I}} \frac{\alpha_k}{\alpha_0} \max_{j \in \mathcal{I}_{\text{int}}} (1 + \log(H_j/h_j))^2 \alpha_0 \left\{ |\tilde{\mathcal{H}}_D^{\text{int}} w_0|_{H^1(\Omega_{\text{int}})}^2 + \frac{1}{H_0} \|w_0\|_{L^2(\partial\Omega_0)}^2 \right\}. \end{aligned}$$

Combining this result with (3.37) and Lemma 1.33 we can conclude that

$$|P_D(\Pi_0 w + z_{\Pi_0 w})|_S^2 \lesssim \gamma_h(\Omega_0, \Omega_{\text{int}}, \Gamma_D) \max_{k \in \mathcal{I}} \frac{\alpha_k}{\alpha_0} \max_{j \in \mathcal{I}_{\text{int}}} (1 + \log(H_j/h_j))^2 |w_0|_{S_0}^2,$$

which proves Claim 2 for the case $Q = M^{-1}$.

Proof of Claim 2 for Q chosen according to (3.16)–(3.19). With the special $\tilde{z} \in \ker S$ defined in the last proof, we obtain by the triangle inequality that

$$|P_D(\Pi_0 w + z_{\Pi_0 w})|_S^2 \lesssim |P_D(\Pi_0 w + \tilde{z})|_S^2 + |P_D(\tilde{z} - z_{\Pi_0 w})|_S^2. \quad (3.47)$$

The first term can be bounded using the proof of Claim 2 for $Q = M^{-1}$. For the second term we perform the usual splitting into face, edge, and vertex terms, and bound these local contributions, just as in the proof of Claim 1 for the diagonal choice of Q . Exploiting the careful choice of Q , the sum of all these local estimates can be bounded by $\|B(\tilde{z} - z_{\Pi_0 w})\|_Q^2$. By another application of the triangle inequality and Lemma 2.22, we obtain

$$\begin{aligned} |P_D(\Pi_0 w + z_{\Pi_0 w})|_S^2 &\lesssim \|B(\tilde{z} - z_{\Pi_0 w})\|_Q^2 \lesssim \|B(\Pi_0 w - \tilde{z})\|_Q^2 + \|B(\Pi_0 w - z_{\Pi_0 w})\|_Q^2 \\ &= \|B(\Pi_0 w - \tilde{z})\|_Q^2 + \min_{z \in \ker S} \|B(\Pi_0 w - z)\|_Q^2 \lesssim \|B(\Pi_0 w - \tilde{z})\|_Q^2. \end{aligned} \quad (3.48)$$

Similar to previous proofs we consider the contributions of $\|B(\Pi_0 w - \tilde{z})\|_Q^2$ from face, edge, and vertex separately. For a face, edge, or vertex \mathcal{X}_{0i} , the contributions can be bounded by

$$\min(\alpha_0, \alpha_i) (1 + \log(H_i/h_i)) \frac{1}{H_i^2} \|\tilde{z}_i - \Pi_i^h \tilde{\mathcal{H}}_D^{\text{int}} w_0\|_{L^2(\Omega_i)}^2.$$

If $i \notin \mathcal{I}_{\text{float}}$, then Ω_i has at least an edge in common with Γ_D and $\tilde{z}_i = 0$, thus we can use the discrete Poincaré-Friedrichs inequality and the H^1 -stability of the Scott-Zhang quasi-interpolation operator to bound the L^2 -term by the H^1 -norm of $\tilde{\mathcal{H}}_D^{\text{int}} w_0$ times another logarithmic factor. If $i \in \mathcal{I}_{\text{float}}$, \tilde{z}_i is the average of $\Pi_i^h \tilde{\mathcal{H}}_D^{\text{int}} w_0$ on Ω_i , thus we can apply Poincaré's inequality in order to get the same bound, i. e.,

$$\min(\alpha_0, \alpha_i) (1 + \log(H_i/h_i))^2 |\tilde{\mathcal{H}}_D^{\text{int}} w_0|_{H^1(\Omega_i)}^2.$$

The contribution from a face, edge, or vertex \mathcal{X}_{ij} with $i, j \neq 0$ can be bounded by

$$\min(\alpha_i, \alpha_j) (1 + \log(H_i/h_i)) H_i |\tilde{z}_i - \tilde{z}_j|^2.$$

Using estimates (3.44) and (3.45), we obtain the bound

$$\left(\max_{k \in \mathcal{I}} \frac{\alpha_k}{\alpha_0} \right) (1 + \log(H_i/h_i)) \alpha_0 |\tilde{\mathcal{H}}_D^{\text{int}} w_0|_{H^1(\mathcal{U}_{ij})}^2.$$

For the all-floating formulation we additionally have to investigate the contributions from faces, edges, and vertices \mathcal{X}_i on the Dirichlet boundary. Note that since w_0 vanishes on Γ_D , there is no contribution if $i = 0$. For $i \neq 0$, the contribution can be bounded by

$$\alpha_i (1 + \log(H_i/h_i)) H_i |\tilde{z}_i|^2 \lesssim \alpha_i (1 + \log(H_i/h_i)) \frac{1}{H_i^2} \|\Pi_i^h \tilde{\mathcal{H}}_D^{\text{int}} w_0\|_{L^2(\Omega_i)}^2.$$

Due to the finite overlap of all these local estimates, we finally obtain

$$\|B(\Pi_0 w + \tilde{z})\|_Q^2 \lesssim \left(\max_{k \in \mathcal{I}} \frac{\alpha_k}{\alpha_0} \right) \max_{i \in \mathcal{I}_{\text{int}}} (1 + \log(H_i/h_i)) \alpha_0 |\tilde{\mathcal{H}}_D^{\text{int}} w_0|_{H^1(\Omega_{\text{int}})}^2.$$

Combining this result with (3.47) and (3.48) we can continue in the analogous way to the proof of Claim 2 for $Q = M^{-1}$. In the end, we get the desired estimate

$$|P_D(\Pi_0 w + z_{\Pi_0 w})|_S^2 \lesssim \gamma_h(\Omega_0, \Omega_{\text{int}}, \Gamma_D) \max_{k \in \mathcal{I}} \frac{\alpha_k}{\alpha_0} \max_{i \in \mathcal{I}_{\text{int}}} (1 + \log(H_i/h_i))^2 |w_0|_{S_0}^2,$$

which finishes the proof of Claim 2.

3.5 Numerical results

In the following, we give some results on one-level BETI methods for two-dimensional unbounded domains. We consider three different geometric configurations. First, we choose Ω_{int} to be the unit square, second, ring-shaped as in Figure 3.6 (left), and last, C-shaped as in Figure 3.6 (middle). In our examples we vary the subdomain partition of Ω_{int} , where we use simply quadrilaterals as subdomains, and we vary the discretization parameters, $h_i = h_0 = h$. Tables 3.1–3.3 display the number of PCG iterations and the condition numbers (estimated by the Lanczos method) for the three geometric configurations. In the tables, we have used the notation $H/h = \max_{i \in \mathcal{I}} H_i/h_i$ and $H_0/H_F = \max_{i \in \mathcal{N}_0} H_0/H_i$. In the computations we have considered the heterogeneous coefficient distribution shown in Figure 3.6, right. Choosing the homogeneous coefficient distribution $\alpha_i \equiv 1$ results in almost the same behavior. In our implementation, which builds upon OSTBEM [176], we have used the diagonal choice of Q according to (3.16)–(3.19), and the PCG iteration was stopped when the relative error (measured in the energy norm) went below $\varepsilon = 10^{-8}$.

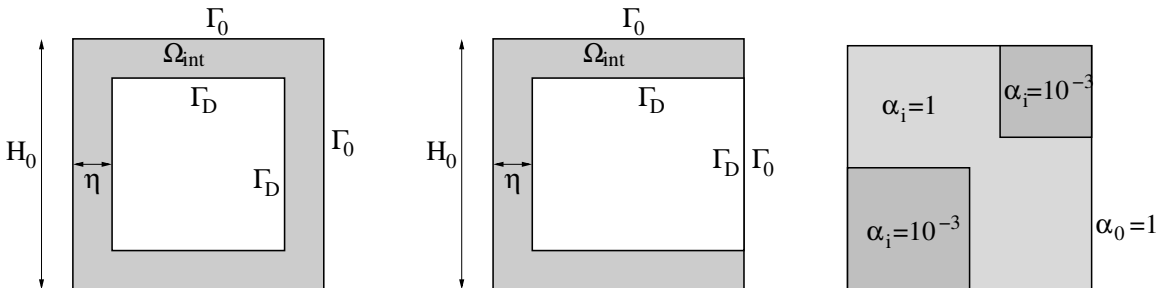


Figure 3.6: Sketch of the geometries for Table 3.2 (left) and Table 3.3 (middle). Right: Coefficient distribution with jumps.

Example 3.1 We choose Ω to be a square plus its exterior domain, where the square is subdivided into the interior subdomains. Thus, we expect the quasi-optimal bound $C \max_{i \in \mathcal{I}_{\text{int}}} (1 + \log(H_i/h_i))^2$ which is reflected by the condition numbers displayed in Table 3.1. We mention that the case $H_0/H_F = 96$ corresponds to 1297 subdomains. The slightly growing numbers as the ratio H_0/H_F increases are probably due to pre-asymptotic effects.

H_0/H_F	$H/h = 2$		4		8		16		32		64	
6	9	1.6	10	2.0	12	2.6	14	3.5	16	4.4	18	5.6
12	9	1.8	11	2.5	14	3.3	16	4.3	18	5.5	20	6.8
24	10	2.1	12	2.9	14	3.9	17	5.2	18	6.5	20	7.9
48	10	2.4	12	3.4	15	4.6	18	6.0	20	7.5	—	—
96	11	2.6	13	3.8	16	5.1	18	6.6	—	—	—	—

Table 3.1: Number of PCG iterations and *condition numbers* for a unit square plus its exterior without any interior boundary conditions.

Example 3.2 Here, we choose the geometry shown in Figure 3.6, left, where the grey region is subdivided into subdomains. As we see the Dirichlet boundary is separated from $\partial\Omega_0$ by a distance η , which implies the condition number bound

$$\kappa \leq C \frac{H_0}{\eta} \max_{i \in \mathcal{I}_{\text{int}}} (1 + \log(H_i/h_i))^2.$$

Indeed we observe a non-negligible growth in the estimated condition numbers in Table 3.2 compared to Table 3.1 when we vary the ratio H_0/η .

H_0/H_F	$H/h = 2$		4		8		16		32		64		
$H_0/\eta = 6$	6	11	2.3	13	4.1	15	6.4	18	9.3	20	12.7	21	16.7
	12	12	3.3	15	5.7	17	9.0	21	13.1	24	18.0	28	23.9
	24	13	3.1	15	5.0	17	7.9	21	11.7	24	16.3	27	21.7
	48	12	3.3	15	5.0	18	7.7	21	11.4	24	15.8	—	—
	96	13	3.5	15	5.1	18	7.6	21	11.2	—	—	—	—
H_0/H_F	$H/h = 2$		4		8		16		32				
$H_0/\eta = 24$	24	13	4.6	16	7.2	20	11.8	23	15.1	25	18.4		
	48	15	7.0	20	13.1	22	18.1	25	23.4	27	28.8		
	96	17	10.6	20	16.0	24	21.7	28	27.7	—	—		
	192	17	12.1	21	17.8	24	23.8	—	—	—	—		
H_0/H_F	$H/h = 2$		4		8		16						
$H_0/\eta = 96$	96	18	19.1	23	31.5	28	43.8	33	56.1				
	192	23	31.6	30	49.6	35	68.7	—	—				
	384	27	40.7	33	61.9	—	—	—	—				

Table 3.2: Number of PCG iterations and *condition numbers* for a unit square with Dirichlet conditions on a “hole” (cf. Figure 3.6, left) with distance η from Γ_0 .

Example 3.3 For the example shown in Figure 3.6, middle, and Table 3.3, we have proved the same bound with an additional logarithmic factor. However, we do not observe this behavior in our calculations: the condition numbers are actually better than predicted, and effectively a bit less than those in Table 3.2. This is no contradiction to our theory

since we have proved (asymptotic) upper bounds only. The numbers of PCG iterations are comparable to those in Table 3.2 and they show the efficiency of the proposed one-level BETI preconditioner.

H_0/H_F	$H/h = 2$	4	8	16	32	64	
$H_0/\eta = 6$	6	11 2.3	13 4.1	16 6.4	18 9.3	21 12.7	23 16.7
	12	12 3.3	15 5.7	18 9.0	21 13.1	24 18.0	26 23.9
	24	13 3.1	15 5.1	17 8.0	21 11.7	25 16.3	27 21.7
	48	13 3.3	15 5.1	18 7.8	21 11.4	24 15.8	— —
	96	13 3.5	16 5.2	19 7.6	22 11.2	— —	— —
H_0/H_F	$H/h = 2$	4	8	16	32		
$H_0/\eta = 24$	24	13 5.0	17 7.8	19 10.7	22 13.7	25 16.8	
	48	16 7.6	19 11.8	22 16.4	24 21.2	28 26.1	
	96	16 9.6	21 14.5	24 19.7	28 25.1	— —	
	192	18 10.9	21 16.2	25 21.6	— —	— —	
H_0/H_F	$H/h = 2$	4	8	16			
$H_0/\eta = 96$	96	20 17.1	25 28.1	28 39.1	32 50.0		
	192	24 28.1	30 44.2	35 61.2	— —		
	384	27 36.3	33 55.2	— —	— —		

Table 3.3: Number of PCG iterations and *condition numbers* for a unit square with Dirichlet conditions on a rectangular outline touching Γ_0 , see Figure 3.6, middle.

Choosing a heterogeneous coefficient distribution with very small interior coefficients $\alpha_i \ll \alpha_0$ (10^{-3} , 10^{-5}) leads to better condition numbers. This might be due the fact that the solution is relatively flat in Ω_0 and so the problem gets more similar to a Dirichlet problem on the bounded domain Ω_{int} .

3.6 Implementation issues

As outlined before, the principal differences to FETI/BETI methods for the bounded case are

- (i) the possibly large number of neighbors to $\partial\Omega_0$, and
- (ii) the possibly large number of DOFs in $V^h(\partial\Omega_0)$ compared to the other subdomains.

Issue (i) means that in practice, the processor which handles the exterior subdomain has to communicate with a lot of other processors. Issue (ii) implies that we might have no *load balancing*. In order to address these problems we can go for the following strategies.

Buffering We introduce several layers of “buffer” subdomains in between the original interior subdomains and the exterior subdomain Ω_0 , cf. Figure 3.7. This way we can reduce the number of neighbors to Ω_0 . If the problem setting permits, we can make the mesh on $\partial\Omega_0$ coarser such that we regain load balancing. However, this strategy is somehow against the principle of using a boundary element approximation for the exterior subdomain instead of introducing a large layer (as the buffering layer) with Dirichlet boundary conditions on the outer boundary.

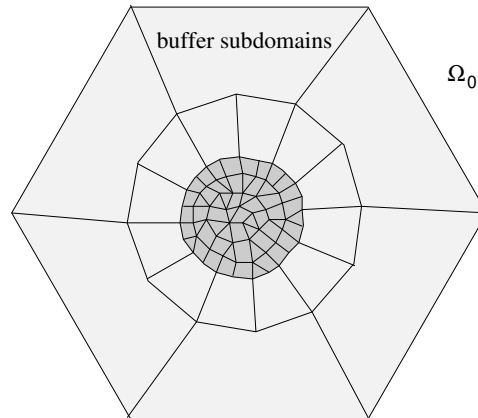


Figure 3.7: Illustration of the buffering strategy. Original interior subdomains in dark grey, buffering subdomains in light gray.

Sub-parallelization It would be more favorable if the computational work corresponding to the exterior subdomain Ω_0 could be further distributed. In this context we would like to briefly discuss a possible procedure. The two bottlenecks in the method are the application of S_0 in the preconditioner M^{-1} and the application of S_0^{-1} in the operator F .

According to Remark 3.7, we can replace the block S_0 appearing in the preconditioner M^{-1} by the regularized hypersingular operators \tilde{D}_0 . A close inspection of the underlying proofs reveals that S in the preconditioner can be replaced by any operator S_M which satisfies

$$|w|_S^2 \leq C_1 |w|_{S_M}^2, \quad \text{and} \quad |P_D|_{S_M}^2 \leq C_2 |w|_S^2.$$

Then the condition number bound is given by $C_1 C_2$. For example, we can use $S_M := (S_{M,0}, S_1, \dots, S_s)$ where $S_{M,0}$ is a parallelizable preconditioner, e. g., a suitable wirebasket type preconditioner, see TOSELLI AND WIDLUND [184, Sect. 5.4.2] and the references therein.

In order to sub-parallelize the action of S_0^{-1} we can move to the inexact method, cf. Section 2.2.3.5. Assume for the time being that we are in the pure BETI case. The system to solve has the form

$$\begin{pmatrix} -V & \frac{1}{2}I + K & 0 \\ \frac{1}{2}I + K^\top & D & B^\top P \\ 0 & P^\top B & 0 \end{pmatrix} \begin{pmatrix} t \\ u \\ \lambda \end{pmatrix} = \begin{pmatrix} 0 \\ f \\ 0 \end{pmatrix}.$$

Having at hand

- (i) parallel applications of the boundary element matrices V_0 , K_0 , M_0 , and D_0 ,
- (ii) parallel preconditioners for V_0 and S_0 , and
- (iii) a sub-parallelized BETI preconditioner (e. g., of wirebasket type as described above),

we can perform the inexact BETI method with a quasi-optimal load balancing. Here, there is some space left for future research, although many BEM parallelization techniques can be found in the literature, see, e. g., BOERM AND BENDORAITYTE [13], BEBENDORF AND KRIEMANN [9], CHEW ET AL. [34]. We remark that if $\partial\Omega_0$ is a circle or a sphere, the Steklov-Poincaré operator can be realized very efficiently using the fast Fourier transform, see, e. g., RJASANOW [157].

Chapter 4

Dual-primal methods

Dual-primal FETI (FETI-DP) methods were first introduced by FARHAT, LESOINNE, LE TALLEC, PIERSON, AND RIXEN [63]. Their idea was to keep the unknowns at the subdomain vertices “primal”, i. e., do not break the continuity there. This way, after an elimination of these unknowns, the resulting subdomain operators are always invertible. The elimination step of the primal unknowns can be seen as a coarse problem. A first analysis for the two-dimensional case was given by MANDEL AND TEZAUER [132], which showed that the method of this type equipped with a Dirichlet preconditioner leads to the condition number bound $C(1 + \log(H/h))^2$, the same as for one-level FETI methods. Algorithms for the three-dimensional case were contributed by FARHAT, LESOINNE, AND PIERSON [61], see also the doctoral dissertation by PIERSON [149], and finally by KLAWONN, WIDLUND, AND DRYJA [111] where a rigorous analysis of the three-dimensional case can be found. See also BRENNER [24] and BRENNER AND HE [25] for sharp estimates. It turned out that in three dimensions, primal vertex constraints result in a poor condition number. A polylogarithmic bound can be obtained by additionally imposing edge and/or face average constraints. A comprehensive description of various FETI-DP algorithms and their analysis is contained in the monograph by TOSELLI AND WIDLUND [184].

The dual-primal BETI (BETI-DP) methods were introduced in LANGER, POHOAȚĂ, AND STEINBACH [121], however, without giving any analysis and without much discussion on an efficient implementation for large-scale problems. It is clear from Chapter 2 that the condition number bound will again be $C(1 + \log(H/h))^2$ for the BETI-DP and hybrid dual-primal methods, due to the spectral equivalence of the BEM and FEM approximations of the Steklov-Poincaré operator. Nevertheless, it is at first glance unclear if difficulties will arise in case of an unbounded domain.

Section 4.1 gives the formulation of hybrid FETI/BETI-DP methods, where the unbounded case is included. A condition number bound is proved in Section 4.2. It will turn out that, in contrast to Chapter 3, we get the quasi-optimal bound also for the unbounded case since the coarse space directly incorporates the exterior problem. However, assembling the coarse matrix is much more costly as compared to our proposed one-level method. This is because many exterior problems need to be solved, leading to a non-optimal computational complexity. We discuss implementation issues and possible future extensions for both one-level and dual-primal methods in Section 4.3. We note that parts of this chapter rely on results published in PECHSTEIN [143, 145].

4.1 Formulation of FETI/BETI-DP methods

In the sequel, we consider the weak formulation of the potential equation

$$-\operatorname{div}[\alpha_i \nabla u] = f \quad \text{in } \Omega_i, \quad i \in \mathcal{I},$$

cf. Chapter 2 and Chapter 3, where we treat the bounded ($0 \notin \mathcal{I}$) and the unbounded case ($0 \in \mathcal{I}$) in one and the same formulation. We assume that either $0 \in \mathcal{I}$ and the radiation condition (1.49) is fulfilled, or we have a Dirichlet boundary Γ_D of positive surface measure. We take the same assumptions on the coefficient, the source, and the Neumann data as we did in the previous chapters, and without loss of generality, we assume homogeneous Dirichlet boundary conditions, i. e., $g_D \equiv 0$. In what follows, we will restrict ourselves mostly to the three-dimensional case. Note, however, that in contrast to the methods before, we can allow that the Dirichlet boundary touches a subdomain only in a vertex, even if this subdomain is the exterior domain. As in Section 2.2 and Chapter 3, we start from the discrete skeleton formulation, see, e. g., (3.13), which is equivalent to the minimization problem

$$\sum_{i \in \mathcal{I}} \left[\frac{1}{2} \langle S_i u, u \rangle_{\partial \Omega_i} - \langle f_i, u \rangle_{\partial \Omega_i} \right] \rightarrow \min_{u \in V_D^h(\Gamma_S)}. \quad (4.1)$$

There again, S_i denotes the discrete Steklov-Poincaré operator, obtained by FEM or BEM, depending on the subdomain. As in the formulation of standard one-level methods, we use the definitions

$$W_i := V_D^h(\Gamma_i) \quad \text{and} \quad W := \prod_{i \in \mathcal{I}} W_i, \quad (4.2)$$

and we consider the Steklov-Poincaré operators S_i as mappings from W_i to W_i^* . Similarly, we set $S = \operatorname{diag}(S_i) : W \rightarrow W^*$ and $f = [f_i]_{i \in \mathcal{I}} \in W^*$.

4.1.1 Dual-primal spaces

In dual-primal methods, one works with subspaces $\widetilde{W} \subset W$, for which sufficiently many constraints are enforced such that the block operator S is SPD when restricted to \widetilde{W} , cf. TOSELLI AND WIDLUND [184, Sect. 6.4]. Such spaces are constructed as follows. We choose a *primal space* $\widehat{W}_\Pi \subset V_D^h(\Gamma_S)$ and a *dual subspace* $\widehat{W}_\Delta \subset \widetilde{W}$ such that

$$\widetilde{W} = \widehat{W}_\Pi \oplus \widehat{W}_\Delta.$$

Note that for simplicity, we identify functions from $V_D^h(\Gamma_S)$ with the corresponding continuous functions in the product space W . We denote the component of the product space \widehat{W}_Δ which corresponds to the i -th subdomain by $\widetilde{W}_{\Delta,i}$. According to KLAWONN, WIDLUND, AND DRYJA [111] we display several choices of the space \widetilde{W} . The first one, Algorithm A, is illustrated in Figure 4.1.

Algorithm A. The primal subspace \widehat{W}_Π is spanned by the nodal basis functions $\theta_{\mathcal{V}_{ij}} \in V_D^h(\Gamma_S)$, where \mathcal{V}_{ij} runs over all the subdomain vertices on the interface. The local subspace $\widetilde{W}_{\Delta,i}$ is defined as the subspace of W_i with its elements vanishing on the subdomain vertices, i. e.,

$$\widetilde{W}_{\Delta,i} := \{w_i \in W_i : w_i(\mathcal{V}_{ij}) = 0 \quad \forall \mathcal{V}_{ij}\}.$$

Thus, \widetilde{W} is the subspace of W of functions being continuous at the subdomain vertices.

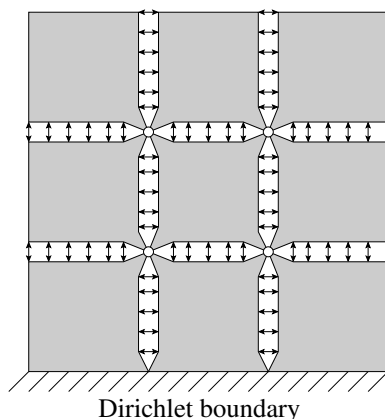


Figure 4.1: Illustration of the dual-primal space in Algorithm A. The “o” indicate the primal DOFs.

Algorithm B. The primal subspace \widehat{W}_Π is spanned by the nodal basis functions $\theta_{\mathcal{V}_{ij}} \in V_D^h(\Gamma_S)$, for all subdomain vertices on the interface, and the cut-off functions $\theta_{\mathcal{E}_{ij}}, \theta_{\mathcal{F}_{ij}} \in V_D^h(\Gamma_S)$, for subdomain edges and faces on the interface. The local subspace $\widetilde{W}_{\Delta,i}$ is defined as the subspace of W_i where the values at the subdomain vertices vanish, together with the averages

$$\overline{w}_i^{\mathcal{E}_{ij}} := \frac{1}{|\mathcal{E}_{ij}|} \int_{\mathcal{E}_{ij}} w_i(x) ds_x, \quad \overline{w}_i^{\mathcal{F}_{ij}} := \frac{1}{|\mathcal{F}_{ij}|} \int_{\mathcal{F}_{ij}} w_i(x) ds_x,$$

i. e.,

$$\widetilde{W}_{\Delta,i} := \{w_i \in W_i : w_i(\mathcal{V}_{ij}) = 0, \overline{w}_i^{\mathcal{E}_{ij}} = 0, \overline{w}_i^{\mathcal{F}_{ij}} = 0 \quad \forall \mathcal{V}_{ij}, \mathcal{E}_{ij}, \mathcal{F}_{ij}\}.$$

Thus, \widetilde{W} is the subspace of W of functions being continuous at the subdomain vertices and with continuous edge and face averages.

Algorithm C. The primal subspace \widehat{W}_Π is spanned by the nodal basis functions $\theta_{\mathcal{V}_{ij}} \in V_D^h(\Gamma_S)$ for all interface subdomain vertices, and the cut-off functions $\theta_{\mathcal{E}_{ij}} \in V_D^h(\Gamma_S)$, for all interface subdomain edges. The local subspace $\widetilde{W}_{\Delta,i}$ is defined as the subspace of W_i where the values at the subdomain vertices vanish, together with the edge averages, i. e.,

$$\widetilde{W}_{\Delta,i} := \{w_i \in W_i : w_i(\mathcal{V}_{ij}) = 0, \overline{w}_i^{\mathcal{E}_{ij}} = 0 \quad \forall \mathcal{V}_{ij}, \mathcal{E}_{ij}\}.$$

Thus, \widetilde{W} is the subspace of W of functions being continuous at the subdomain vertices and with continuous edge averages.

Note, that Algorithm A works well in two dimensions only, see also FARHAT, LESOINNE, LE TALLEC, PIERSON, AND RIXEN [63] and MANDEL AND TEZAUER [132] for some numerical experiments on such FETI-DP methods. Its poor behavior in three dimensions relates to the fact that there is no comparable discrete Poincaré-Friedrichs inequality to Lemma 2.38 for functions vanishing at single vertices, at least not with a logarithmic factor. On the contrary, Algorithms B and C will lead to a polylogarithmic bound for the condition number. We will briefly sketch another algorithm (Algorithm D) at the end of Section 4.2 after the proof of the condition number bound.

4.1.2 The actual dual-primal methods

Depending on the choice of the spaces \widetilde{W}_Δ and \widehat{W}_Π , we define the Schur complement operator $\widetilde{S} : \widetilde{W}_\Delta \rightarrow \widetilde{W}_\Delta^*$ by

$$\widetilde{S} := S_\Delta - S_{\Delta\Pi} S_\Pi^{-1} S_{\Pi\Delta}, \quad (4.3)$$

where the block operators $S_\Delta : \widetilde{W}_\Delta \rightarrow \widetilde{W}_\Delta^*$, $S_{\Pi\Delta} : \widehat{W}_\Pi \rightarrow \widetilde{W}_\Delta^*$, $S_{\Delta\Pi} : \widetilde{W}_\Delta \rightarrow \widehat{W}_\Pi^*$ and $S_\Pi : \widehat{W}_\Pi \rightarrow \widehat{W}_\Pi^*$ satisfy the relations

$$\begin{aligned} \langle S_\Delta v_\Delta, w_\Delta \rangle &= \langle S v_\Delta, w_\Delta \rangle & \forall v_\Delta, w_\Delta \in \widetilde{W}_\Delta, \\ \langle S_{\Delta\Pi} v_\Delta, w_\Pi \rangle &= \langle S_{\Pi\Delta} w_\Pi, v_\Delta \rangle = \langle S v_\Delta, w_\Pi \rangle & \forall v_\Delta \in \widetilde{W}_\Delta, \forall w_\Pi \in \widehat{W}_\Pi, \\ \langle S_\Pi v_\Pi, w_\Pi \rangle &= \langle S v_\Pi, w_\Pi \rangle & \forall v_\Pi, w_\Pi \in \widehat{W}_\Pi. \end{aligned}$$

Due to the nature of the space \widetilde{W}_Δ , the operator S_Δ can be written in the form $\text{diag}(S_{\Delta,i})$. It is important to note that in particular for Algorithms A–C, the operators S_Π and S_Δ are SPD. The latter is true because on each subdomain Ω_i , at least one vertex DOFs is fixed to zero, thus $\ker S_{\Delta,i} = \{0\}$. Moreover, we have the minimizing property

$$\langle \widetilde{S} w_\Delta, w_\Delta \rangle = \min_{w_\Pi \in \widehat{W}_\Pi} \langle S(w_\Delta + w_\Pi), w_\Delta + w_\Pi \rangle. \quad (4.4)$$

Furthermore, we define the functional

$$\widetilde{f} := f_\Delta - S_{\Delta\Pi} S_\Pi^{-1} f_\Pi \quad \text{in } \widetilde{W}_\Delta^*, \quad (4.5)$$

where f_Δ and f_Π are the projections of f onto the corresponding subspaces. The continuity constraints on the interface are incorporated using fully redundant Lagrange multipliers, but (in contrast to one-level methods) only for the degrees of freedom in \widetilde{W}_Δ . In particular, for Algorithms A–C, there are no Lagrange multipliers corresponding to subdomain vertices. We denote the space of these Lagrange multipliers by U_Δ and define the corresponding jump operators $B_{\Delta,i}^{(i)} : \widetilde{W}_{\Delta,i} \rightarrow U_\Delta^*$ and $B_\Delta : \widetilde{W}_\Delta \rightarrow U_\Delta^*$ analogously to Chapter 2. Since functions from \widehat{W}_Π are continuous, we will occasionally extend the domain of definition of B_Δ to the full space \widetilde{W} . As in Chapter 2, we restrict ourselves to fully redundant constraints. Note, that the continuous edge averages in Algorithms B and C already create some redundancy, cf. [184, Sect. 6.4.2]. With these definitions, we arrive at the following minimization problem,

$$\sum_{i \in \mathcal{I}} \left[\frac{1}{2} \langle \widetilde{S} u_\Delta, u_\Delta \rangle - \langle \widetilde{f}, u_\Delta \rangle \right] \rightarrow \min_{\substack{u_\Delta \in \widetilde{W}_\Delta \\ B_\Delta u_\Delta = 0}}. \quad (4.6)$$

This problem is equivalent to (4.1). Suppose we have the solution u_Δ to (4.6), then the solution to (4.1) is given by $u = u_\Delta + u_\Pi$ with $u_\Pi = S_\Pi^{-1}(f_\Pi - S_{\Pi\Delta} u_\Delta)$. The above minimization problem is equivalent to the following saddle point problem: Find $(u_\Delta, \lambda) \in \widetilde{W}_\Delta \times U_\Delta$ such that

$$\begin{pmatrix} \widetilde{S} & B_\Delta^\top \\ B_\Delta & 0 \end{pmatrix} \begin{pmatrix} u_\Delta \\ \lambda \end{pmatrix} = \begin{pmatrix} \widetilde{f} \\ 0 \end{pmatrix},$$

where the Lagrange parameters λ are unique up to $\ker B_\Delta^\top$. It can be shown that \tilde{S} is SPD on \widetilde{W}_Δ , cf. [184, Lemma 6.33], and thus its inverse \tilde{S}^{-1} exists. We define the operator $F : U_\Delta \rightarrow U_\Delta^*$ and the functional $d \in U_\Delta^*$ by

$$F := B_\Delta \tilde{S}^{-1} B_\Delta^\top \quad \text{and} \quad d := B_\Delta \tilde{S}^{-1} \tilde{f}.$$

Then, the above saddle point problem reduces to find $\lambda \in U_\Delta$ such that

$$F \lambda = d. \quad (4.7)$$

Similar to Chapter 2 we see that F is SPD (and invariant) on the factor space $V := (U_\Delta)_{/\ker B_\Delta^\top}$, and maps to $V' := U_\Delta^* \cap \text{range } B_\Delta$. Hence, λ can be obtained by a PCG iteration on V . A suitable preconditioner M^{-1} is introduced in the next paragraph. By the same arguments as in Chapter 2, we do not have to care about any contributions from $\ker B_\Delta^\top$ in the Lagrange multipliers during the PCG algorithm. As a main difference to the one-level method discussed in Chapter 2 and Section 2.2, no projection P appears, instead we need the coarse solve S_Π^{-1} in every PCG step when applying \tilde{S}^{-1} , cf. formula (4.3).

Analogously to Section 2.2.1 we introduce the scaled jump operator $B_{D,\Delta} : \widetilde{W}_\Delta^* \rightarrow U$. Let δ_j^\dagger denote the weighted counting functions (see equation (2.50) in Chapter 2). For each $i \in \mathcal{I}$, define the operators $D_i : U_\Delta^* \rightarrow U_\Delta$ by

$$(D_i \mu)_{ij}(x^h) := \delta_j^\dagger(x^h) \mu_{ij}(x^h) \quad \text{for } \mu \in U_\Delta^*, \quad x^h \in \Gamma_{ij}^h, \quad (4.8)$$

where all other components are set to zero. Finally, we set

$$B_{D,\Delta} := \sum_{i \in \mathcal{I}} D_i B_\Delta^{(i)} \mathcal{J}_{W_{\Delta,i}},$$

where $\mathcal{J}_{W_{\Delta,i}} : W_{\Delta,i}^* \rightarrow W_{\Delta,i}$ is the Riesz isomorphism with respect to the Euclidean inner product, cf. Chapter 2.53. Note that, when using the standard nodal basis, $\mathcal{J}_{W_{\Delta,i}}$ corresponds to the identity matrix. According to [111, 184], the preconditioner is defined by

$$M^{-1} = B_{D,\Delta} S_\Delta B_{D,\Delta}^\top.$$

As we have seen before, $S_\Delta = \text{diag}(S_{\Delta,i})$ with the operators $S_{\Delta,i} : \widetilde{W}_{\Delta,i} \rightarrow \widetilde{W}_{\Delta,i}^*$ defined by the projections of S_i to the corresponding spaces. Consequently, the application of S_Δ is purely local and the application of M^{-1} can easily be parallelized. For the BEM subdomains (including the exterior one), the operator $S_{\Delta,i}$ in the preconditioner may be replaced by the Galerkin projection of the hypersingular operator $D_{\Delta,i} : W_{\Delta,i} \rightarrow W_{\Delta,i}^*$, cf. LANGER, POHOATĂ, AND STEINBACH [121].

As the next section will show, the system $M^{-1}F \lambda = M^{-1}d$ satisfies the same condition number bound as that of the one-level FETI/BETI methods in the bounded case. For unbounded domains, it satisfies in general a better bound than the one-level method.

4.2 Condition number bounds for dual-primal methods

In the sequel we elaborate a characterization of the dual-primal preconditioner M^{-1} in terms of the projection

$$P_\Delta := B_{D,\Delta}^\top B_\Delta,$$

so that $B_\Delta^\top M^{-1} B_\Delta = P_\Delta^\top S_\Delta P_\Delta$, similar to Section 2.2.1.3.

Lemma 4.1. *Let the spaces \widehat{W}_Π and \widetilde{W}_Δ be defined according to Algorithm A, B or C. Then, for all $w_\Delta \in \widetilde{W}_\Delta$,*

$$(P_\Delta w_\Delta)_i(x^h) = \begin{cases} \sum_{j \in \mathcal{N}_{x^h}} \delta_j^\dagger(x^h) (w_{\Delta,i}(x^h) - w_{\Delta,j}(x^h)) & \text{for } x^h \in \partial\Omega_i^h \setminus \Gamma_D, \\ w_{\Delta,i}(x^h) = 0 & \text{for } x^h \in \partial\Omega_i^h \cap \Gamma_D. \end{cases}$$

In particular, $P_\Delta w_\Delta$ vanishes at all non-coupling Neumann nodes. Furthermore, $P_\Delta w \in \widetilde{W}_\Delta$ for any $w \in \widetilde{W}$, and $B_\Delta P_\Delta = B_\Delta$.

Proof. The proof is in most parts analogous to the proof of Lemma 2.16, see also Klawonn, Widlund, and Dryja [111]. The only difference is that there are no Lagrange multipliers corresponding to subdomain vertices; however, the values of w_Δ vanish there anyway. \square

It can be shown that the operator $F : V \rightarrow V'$ is invertible. Let $\Pi : U_\Delta \rightarrow V$ the ℓ^2 -projection that fixes the $\ker B_\Delta^\top$ component of a Lagrange multiplier and embeds the result in the factor space $V = U_{\Delta/\ker B_\Delta^\top}$. Then one can show that the mapping $\Pi M^{-1} : V' \rightarrow V$ is invertible. For a detailed proof for many different choices of the spaces \widetilde{W}_Δ and \widehat{W}_Π we refer to Toselli and Widlund [184, Lemma 6.33]. Similar to our discussion in Section 2.2.4.2, the solution u obtained by the dual primal PCG algorithm does not change when we omit the projection Π ; only the Lagrange multipliers λ differ by a term from $\ker B_\Delta^\top$.

Next we state a stability estimate similar to Lemma 2.27 and Lemma 3.19.

Lemma 4.2. *Let \widetilde{W}_Δ be defined according to Algorithm B or Algorithm C. Then,*

$$|P_\Delta w_\Delta|_{S_\Delta}^2 \leq C \max_{i \in \mathcal{I}_{\text{int}}} (1 + \log(H_i/h_i))^2 |w_\Delta|_{\widetilde{S}}^2 \quad \forall w_\Delta \in \widetilde{W}_\Delta,$$

where $\mathcal{I}_{\text{int}} = \mathcal{I} \setminus \{0\}$ and the constant $C > 0$ is independent of h_i , H_i , the values of α_i , the number of subdomains, and the number of neighbors of Ω_0 . In particular, the estimate does not depend on H_0 .

Proof. The proof follows the line of Klawonn, Widlund, and Dryja [111], see also Toselli and Widlund [184, Sect. 6.4.3]. Only a few of the arguments need to be adapted to the unbounded case. For the sake of completeness, we display the whole proof for the three-dimensional case. A proof for the case of Algorithm A in two dimensions can then be derived relatively easily.

Let $w_\Delta \in \widetilde{W}_\Delta$ be arbitrary and let $w_\Pi \in \widehat{W}_\Pi$ denote the minimizing function, such that we have $|w_\Delta|_{\widetilde{S}} = |w|_S$, with $w = w_\Delta + w_\Pi$, see equation (4.4). Since w_Π is continuous across the subdomain interfaces and vanishes on Γ_D , we obtain by Lemma 4.1 that $P_\Delta w = P_\Delta w_\Delta$. Moreover, recall that $P_\Delta w \in \widetilde{W}_\Delta$, and that S_Δ is identical to S on the subspace \widetilde{W}_Δ . With these considerations it suffices to show that

$$|P_\Delta w|_S^2 \leq C \max_{i \in \mathcal{I}_{\text{int}}} (1 + \log(H/h))^2 |w|_S^2 \quad \forall w \in \widetilde{W}. \quad (4.9)$$

As in previous proofs we split $|(P_\Delta w)_i|_{S_i}^2$ into edge and face contributions. For the algorithms considered, we do neither get any vertex contributions nor contributions from the Dirichlet boundary Γ_D because $P_\Delta w \in \widetilde{W}_\Delta$. For convenience we introduce the notation \mathcal{Y}_{ij} referring

to edges and faces on the interface Γ_{ij} . Analogous to the analysis of one-level methods we can show that for $i \neq 0$,

$$\begin{aligned} |(P_\Delta w)_i|_{S_i}^2 &= \left| \sum_{\mathcal{Y}_{ij}} I^h(\delta_j^\dagger \theta_{\mathcal{Y}_{ij}}(w_i - w_j)) \right|_{S_i}^2 \\ &\lesssim \sum_{\mathcal{Y}_{ij}} \underbrace{\alpha_i (\delta_j^\dagger)^2}_{\leq \min(\alpha_i, \alpha_j)} \left| \mathcal{H}_i(\theta_{\mathcal{Y}_{ij}}(w_i - w_j)) \right|_{H^1(\Omega_i)}^2. \end{aligned} \quad (4.10)$$

By similar arguments and the help of Lemma 3.26(i) and Lemma 2.39,

$$|(P_\Delta w)_0|_{S_0}^2 \lesssim \sum_{\mathcal{Y}_{0j}} \min(\alpha_0, \alpha_j) \left| \mathcal{H}_j(\theta_{\mathcal{Y}_{0j}}(w_0 - w_j)) \right|_{H^1(\Omega_j)}^2. \quad (4.11)$$

Face contributions Let the face \mathcal{F}_{ij} be fixed with $i \in \mathcal{I}$ and $j \neq 0$. By Lemma 2.34 and Lemma 2.39, the contributions from the face \mathcal{F}_{ij} of (4.10) and (4.11) are bounded by

$$\begin{aligned} &\min(\alpha_i, \alpha_j) \left| \mathcal{H}_j(\theta_{\mathcal{F}_{ij}}(w_i - w_j)) \right|_{H^1(\Omega_j)}^2 \\ &= \min(\alpha_i, \alpha_j) \left| \mathcal{H}_j[\theta_{\mathcal{F}_{ij}}((w_i - \overline{w}_i^{\mathcal{F}_{ij}}) - (w_j - \overline{w}_j^{\mathcal{F}_{ij}}) + (\overline{w}_i^{\mathcal{F}_{ij}} - \overline{w}_j^{\mathcal{F}_{ij}}))] \right|_{H^1(\Omega_j)}^2 \\ &\lesssim (1 + \log(H_j/h_j))^2 \min(\alpha_i, \alpha_j) \left\{ |\mathcal{H}_j(w_i - w_j)|_{H^1(\Omega_j)}^2 + \right. \\ &\quad \left. + \frac{1}{H_j} \|(w_i - \overline{w}_i^{\mathcal{F}_{ij}}) - (w_j - \overline{w}_j^{\mathcal{F}_{ij}})\|_{L^2(\mathcal{F}_{ij})}^2 \right\} + \min(\alpha_i, \alpha_j) |\overline{w}_i^{\mathcal{F}_{ij}} - \overline{w}_j^{\mathcal{F}_{ij}}|^2 |\mathcal{H}_j \theta_{\mathcal{F}_{ij}}|_{H^1(\Omega_j)}^2. \end{aligned} \quad (4.12)$$

In case of Algorithm B, we have continuous face averages by the definition of the space \widetilde{W} , i. e., $\overline{w}_i^{\mathcal{F}_{ij}} = \overline{w}_j^{\mathcal{F}_{ij}}$, and so the last term vanishes. For the remaining L^2 -term we use a Poincaré-Friedrichs type inequality (based on Theorem 1.7) to finally obtain the bound

$$C (1 + \log(H_j/h_j))^2 \left\{ \alpha_i |\mathcal{H}_i w_i|_{H^1(\Omega_i)}^2 + \alpha_j |\mathcal{H}_j w_j|_{H^1(\Omega_j)}^2 \right\},$$

of the face contribution for the case $i \neq 0$. If $i = 0$, we have to replace the term $|\mathcal{H}_i w_i|_{H^1(\Omega_i)}^2$ by $|\mathcal{H}'_{\mathcal{F}_{0j}} w_0|_{H^1(\Omega'_{\mathcal{F}_{0j}})}$, i. e., the extension of w_0 from the face \mathcal{F}_{0j} to auxiliary subdomain $\Omega'_{\mathcal{F}_{0j}}$, cf. Section 3.4.3.

For Algorithm C, Lemma 2.34(iv) yields

$$|\mathcal{H}_j \theta_F|_{H^1(\Omega_j)}^2 \lesssim (1 + \log(H_j/h_j)) H_j. \quad (4.13)$$

We choose an edge $\mathcal{E}_{ij} \subset \partial \mathcal{F}_{ij}$ and obtain

$$\begin{aligned} |\overline{w}_i^{\mathcal{F}_{ij}} - \overline{w}_j^{\mathcal{F}_{ij}}|^2 &\lesssim |\overline{w}_i^{\mathcal{F}_{ij}} - \overline{w}_i^{\mathcal{E}_{ij}}|^2 + |\overline{w}_j^{\mathcal{F}_{ij}} - \overline{w}_j^{\mathcal{E}_{ij}}|^2 \\ &= \left| \overline{(w_i - \overline{w}_i^{\mathcal{F}_{ij}})}^{\mathcal{E}_{ij}} \right|^2 + \left| \overline{(w_j - \overline{w}_j^{\mathcal{F}_{ij}})}^{\mathcal{E}_{ij}} \right|^2 \end{aligned} \quad (4.14)$$

because $\overline{w}_i^{\mathcal{E}_{ij}} = \overline{w}_j^{\mathcal{E}_{ij}}$ due to the definition of \widetilde{W} . Using the definition of the edge average, the Cauchy-Schwarz inequality and Lemma 2.34(ii), we obtain

$$\begin{aligned} \left| \overline{(w_j - \overline{w}_j^{\mathcal{F}_{ij}})}^{\mathcal{E}_{ij}} \right|^2 &\lesssim \frac{1}{H_j} \|w_j - \overline{w}_j^{\mathcal{F}_{ij}}\|_{L^2(\mathcal{E}_{ij})}^2 \\ &\lesssim \frac{1}{H_j} (1 + \log(H_j/h_j)) \left\{ |\mathcal{H}_j w_j|_{H^1(\Omega_j)}^2 + \frac{1}{H_j} \|w_j - \overline{w}_j^{\mathcal{F}_{ij}}\|_{L^2(\mathcal{F}_{ij})}^2 \right\}. \end{aligned} \quad (4.15)$$

An analogous estimate holds for the first term in (4.14). Combining (4.12)–(4.15) and using again a Poincaré-Friedrichs type inequality, we are finally able to bound the face contribution (4.12) from above by

$$C (1 + \log(H_j/h_j))^2 \left\{ \alpha_i |\mathcal{H}_i w_i|_{H^1(\Omega_i)}^2 + \alpha_j |\mathcal{H}_j w_j|_{H^1(\Omega_j)}^2 \right\},$$

where again, if $i = 0$, we need to replace $|\mathcal{H}_i w_i|_{H^1(\Omega_i)}^2$ by $|\mathcal{H}'_{\mathcal{F}_{0j}} w_0|_{H^1(\Omega'_{\mathcal{F}_{0j}})}^2$.

Edge contributions We fix an edge \mathcal{E}_{ij} with $i \in \mathcal{I}$ and $j \neq 0$. Using Lemma 2.34(i) and the face that for both Algorithms B and C, $\overline{w_i^{\mathcal{E}_{ij}}} = \overline{w_j^{\mathcal{E}_{ij}}}$, the contributions in (4.10) and (4.11) from the edge \mathcal{E}_{ij} can be bounded by

$$\begin{aligned} & \min(\alpha_i, \alpha_j) \left\| \mathcal{H}_j(\theta_{\mathcal{E}_{ij}}(w_i - w_j)) \right\|_{H^1(\Omega_j)}^2 \\ & \lesssim \min(\alpha_i, \alpha_j) \|w_i - w_j\|_{L^2(\mathcal{E}_{ij})}^2 \\ & = \min(\alpha_i, \alpha_j) \left\| (w_i - \overline{w_i^{\mathcal{E}_{ij}}}) - (w_j - \overline{w_j^{\mathcal{E}_{ij}}}) \right\|_{L^2(\mathcal{E}_{ij})}^2 \\ & = \min(\alpha_i, \alpha_j) \left\| \left[(w_i - \overline{w_i^{\mathcal{F}_i})} - \overline{(w_i - \overline{w_i^{\mathcal{F}_i})}^{\mathcal{E}_{ij}})} \right] + \left[(w_j - \overline{w_j^{\mathcal{F}_j})} - \overline{(w_j - \overline{w_j^{\mathcal{F}_j})}^{\mathcal{E}_{ij}})} \right] \right\|_{L^2(\mathcal{E}_{ij})}^2, \end{aligned}$$

where the faces \mathcal{F}_i and \mathcal{F}_j are chosen such that $\mathcal{E}_{ij} \subset \partial\mathcal{F}_i \cap \partial\mathcal{F}_j$. By the Cauchy-Schwarz inequality, we see that

$$\left\| \overline{(w_i - \overline{w_i^{\mathcal{F}_i})}^{\mathcal{E}_{ij}}} \right\|_{L^2(\mathcal{E}_{ij})}^2 \lesssim \|w_i - \overline{w_i^{\mathcal{F}_i}}\|_{L^2(\mathcal{E}_{ij})}^2.$$

If $i \neq 0$, Lemma 2.34(ii) and a Poincaré-Friedrichs type inequality yield

$$\begin{aligned} & \min(\alpha_i, \alpha_j) \left\| \mathcal{H}_j(\theta_{\mathcal{E}_{ij}}(w_i - w_j)) \right\|_{H^1(\Omega_j)}^2 \\ & \lesssim \alpha_i \|w_i - \overline{w_i^{\mathcal{F}_i}}\|_{L^2(\mathcal{E}_{ij})}^2 + \alpha_j \|w_j - \overline{w_j^{\mathcal{F}_j}}\|_{L^2(\mathcal{E}_{ij})}^2 \\ & \lesssim (1 + \log(H_j/h_j)) \left\{ \alpha_i \left[|\mathcal{H}_i w_i|_{H^1(\Omega_i)}^2 + \frac{1}{H_j} \|w_i - \overline{w_i^{\mathcal{F}_i}}\|_{L^2(\mathcal{F}_i)}^2 \right] + \right. \\ & \quad \left. + \alpha_j \left[|\mathcal{H}_j w_j|_{H^1(\Omega_j)}^2 + \frac{1}{H_j} \|w_j - \overline{w_j^{\mathcal{F}_j}}\|_{L^2(\mathcal{F}_j)}^2 \right] \right\} \\ & \lesssim (1 + \log(H_j/h_j)) \left\{ \alpha_i |\mathcal{H}_i w_i|_{H^1(\Omega_i)}^2 + \alpha_j |\mathcal{H}_j w_j|_{H^1(\Omega_j)}^2 \right\}. \end{aligned}$$

For the case $i = 0$, we obtain the bound

$$C (1 + \log(H_j/h_j)) \left\{ \alpha_0 |\mathcal{H}'_0 w_0|_{H^1(\Omega'_{\mathcal{F}_i})}^2 + \alpha_j |\mathcal{H}_j w_j|_{H^1(\Omega_j)}^2 \right\}.$$

Since each edge and face is shared only by a finite number of subdomains, we obtain

$$|P_\Delta w|_{\mathcal{S}}^2 \lesssim \max_{j \in \mathcal{I}_{\text{int}}} (1 + \log(H_j/h_j))^2 \left\{ \left[\sum_{i \in \mathcal{I}_{\text{int}}} \alpha_i |\mathcal{H}_i w_i|_{H^1(\Omega_i)}^2 \right] + \sum_{\mathcal{F}_{0j}} \alpha_0 |\mathcal{H}'_j w_0|_{H^1(\Omega'_{\mathcal{F}_{0j}})}^2 \right\}.$$

Using the equivalence relations of the Steklov-Poincaré operators and Lemma 3.26(ii), we obtain the desired result,

$$|P_\Delta w|_{\mathcal{S}}^2 \lesssim \max_{j \in \mathcal{I}_{\text{int}}} (1 + \log(H_j/h_j))^2 \sum_{i \in \mathcal{I}} |w_i|_{\mathcal{S}_i}^2 \quad \forall w \in \widetilde{W}.$$

which concludes the proof of Lemma 4.2. \square

The estimate of the P_D operator directly leads to the main theorem.

Theorem 4.3. *Let the spaces \widetilde{W}_Π and \widetilde{W}_Δ be defined according to Algorithm B or C. Then the dual-primal preconditioner fulfills the following condition number estimate,*

$$\kappa(M^{-1}F) \leq C \max_{i \in \mathcal{I}_{\text{int}}} (1 + \log(H_i/h_i))^2,$$

which is to be understood in the factor space modulo $\ker B_\Delta^\top$. The constant C is independent from H_i , h_i , the values α_i , and the number of subdomains. If $0 \in \mathcal{I}$, the entire bound is independent of H_0 and the number of neighbors of Ω_0 .

Proof. For completeness, we display the proof which can be found in Klawonn et al. [111]. The crucial estimate is of course that from Lemma 4.2. From previous considerations we know that the inverse $M : V \rightarrow V'$ of ΠM^{-1} exists. Hence, it suffices to show

$$\langle M\lambda, \lambda \rangle \leq \langle F\lambda, \lambda \rangle \leq C \max_{i \in \mathcal{I}_{\text{int}}} (1 + \log(H_i/h_i))^2 \langle M\lambda, \lambda \rangle \quad \forall \lambda \in V. \quad (4.16)$$

Lower bound. Due to Lemma 1.1,

$$\langle F\lambda, \lambda \rangle = \sup_{v_\Delta \in \widetilde{W}_\Delta} \frac{\langle \lambda, B_\Delta v_\Delta \rangle^2}{|v_\Delta|_{\widetilde{S}}^2}, \quad \langle M\lambda, \lambda \rangle = \sup_{\mu \in V'} \frac{\langle \lambda, \mu \rangle^2}{\langle M^{-1}\mu, \mu \rangle}.$$

For an arbitrary $\mu \in V'$ there exists a function $w_\Delta \in \widetilde{W}_\Delta$ with $\mu = B_\Delta w_\Delta$. Recall from Lemma 4.1 that $B_\Delta P_\Delta = B_\Delta$ and $\text{range } P_\Delta \subset \widetilde{W}_\Delta$. Since the minimizing property (4.4) implies $|u_\Delta|_{\widetilde{S}} \leq |u_\Delta|_{S_\Delta}$ for all $u_\Delta \in \widetilde{W}_\Delta$, we can conclude that

$$\langle F\lambda, \lambda \rangle \geq \frac{\langle \lambda, B_\Delta P_\Delta w_\Delta \rangle^2}{|P_\Delta w_\Delta|_{\widetilde{S}}^2} \geq \frac{\langle \lambda, B_\Delta w_\Delta \rangle^2}{|P_\Delta w_\Delta|_{S_\Delta}^2} = \frac{\langle \lambda, \mu \rangle^2}{\langle M^{-1}\mu, \mu \rangle}.$$

Choosing $\mu = M\lambda$ we arrive at the lower bound in (4.16).

Upper bound. Combining the estimates from before with Lemma 4.1, and Lemma 4.2, we can conclude that for all $\lambda \in V$,

$$\begin{aligned} \langle F\lambda, \lambda \rangle &= \sup_{v_\Delta \in \widetilde{W}_\Delta} \frac{\langle \lambda, B_\Delta v_\Delta \rangle^2}{|v_\Delta|_{\widetilde{S}}^2} \\ &\stackrel{\text{Lemma 4.2}}{\lesssim} \max_{i \in \mathcal{I}_{\text{int}}} (1 + \log(H_i/h_i))^2 \sup_{v_\Delta \in \widetilde{W}_\Delta} \frac{\langle \lambda, B_\Delta v_\Delta \rangle^2}{|P_\Delta v_\Delta|_{\widetilde{S}}^2} \\ &\stackrel{\text{Lemma 4.1}}{\lesssim} \max_{i \in \mathcal{I}_{\text{int}}} (1 + \log(H_i/h_i))^2 \sup_{v_\Delta \in \widetilde{W}_\Delta} \frac{\langle \lambda, B_\Delta v_\Delta \rangle^2}{\langle M^{-1}B_\Delta v_\Delta, B_\Delta v_\Delta \rangle} \\ &\stackrel{V' = U_\Delta^* \cap \text{range } B_\Delta}{\lesssim} \max_{i \in \mathcal{I}_{\text{int}}} (1 + \log(H_i/h_i))^2 \sup_{\mu \in V'} \frac{\langle \lambda, \mu \rangle^2}{\langle M^{-1}\mu, \mu \rangle}. \end{aligned}$$

By Lemma 1.1 we arrive at the upper bound in (4.16). \square

Remark 4.4. 1. In two dimensions, Algorithm A gives the same condition number estimate, also in presence of an unbounded subdomain. The proof of such an estimate requires no new ideas and is therefore skipped.

2. It was shown in BRENNER [24] that for bounded domains, the estimate in Theorem 4.3 is sharp in two dimensions. For sharp bounds of related three-dimensional non-overlapping DD methods see BRENNER AND HE [25].
3. We see that in contrast to the one-level methods, the analysis for dual-primal methods with unbounded domains is much simpler, because the L^2 -terms on the faces of the exterior domain Ω_0 can immediately be eliminated using the continuity properties of the space \widetilde{W} . Moreover, we do not need any restrictions on the coefficients or on the boundary conditions. This means the coarse spaces W_{Π} of the dual-primal methods are more powerful than the coarse spaces of the one-level methods. In the next section, we discuss drawbacks of this coarse space.

The number of DOFs of the coarse spaces from Algorithms B and C can be very large in comparison to the coarse space from the one-level methods. The following algorithm proposed by KLOWONN, WIDLUND, AND DRYJA [111] addresses this issue. In the unbounded case, it is possible to show the polylogarithmic bound from Theorem 4.3 also for this algorithm by combining the previously presented ideas and the proof in [111].

Algorithm D. In order to get a small number of primal DOFs, we select only a few primal edges and vertices, while at the same time assuring that each local problem is well-posed, and that the overall dual-primal system is well-conditioned. We sketch this selection algorithm in brief. For each face, at least one edge must be designated as primal. For all pairs of subdomains Ω_i, Ω_j which share an edge but not a face, or share a vertex but not an edge, a so-called *acceptable edge path* must exist. Such a path is a sequence of subdomains $\Omega_i, \Omega_k, \dots, \Omega_j$, linked through primal edges, where the coefficients assigned to the subdomains in between are effectively not smaller than $\min(\alpha_i, \alpha_j)$. This means, in the case of jumping coefficients, some of the vertices and edges must additionally be designated primal in order to achieve this property. For details, see, e. g., TOSELLI AND WIDLUND [184, pp. 171ff].

4.3 Implementation issues of dual-primal methods

In this section, we would like to give a few remarks on the implementation of the previously discussed hybrid dual-primal methods. First, we briefly describe how the operators are actually realized. There, much of the material is taken from the doctoral dissertation by RHEINBACH [154] where a detailed description of FETI-DP methods can be found, see also KLOWONN AND RHEINBACH [105]. Last, we compare the dual-primal methods to the one-level methods from Chapter 2 and Chapter 3. In particular we discuss how effective each of them performs in the unbounded case.

4.3.1 Handling of edge and face constraints

For the implementation of methods for three-dimensional problems, one needs to handle the edge and possibly face average constraints, cf. Algorithms B and C. We briefly discuss two approaches, which are well-described in RHEINBACH [154, Sect. 3.3.1f],

Change of basis. We first restrict ourselves to Algorithm C. Let the subdomain Ω_i be fixed and let $x^h \in \partial\Omega_i^h$ be an interior node of the edge \mathcal{E}_{ij} . In a first step we replace the nodal

basis function φ_{x^h} by the cut-off function $\theta_{\mathcal{E}_{ij}}$.¹ The remaining nodal basis functions φ_{y^h} for nodes y^h in the interior of the edge are orthogonalized such that $\int_{\mathcal{E}_{ij}} \varphi_{y^h} ds = 0$. We perform analogously for every edge. Doing so, the functions $\varphi_{\mathcal{V}_{ij}}, \theta_{\mathcal{E}_{ij}}$ form a basis of $\widehat{W}_{\Pi,i}$, i. e., the space \widehat{W}_{Π} restricted to $\partial\Omega_i$, whereas the remaining basis functions span $\widetilde{W}_{\Delta,i}$. The analogous recipe can be applied for Algorithm B. For a FEM subdomain, the stiffness matrices, load vectors, and boundary element matrices with respect to the new basis can be calculated via a standard basis transformation. Elements in $W_{i,\Delta}$ can then easily be represented by constraining their DOFs with respect to the vertex-, edge-, and possibly face-based basis functions to zero. It is clear that this approach will affect the sparsity of the stiffness matrix, at least for Algorithm B in three dimensions.

Local Lagrange multipliers. The basis transformation is carried out as before, but we can circumvent forming the matrices with respect to the new basis. For a FEM subdomain Ω_i , let \mathbf{K}_i and \mathbf{f}_i denote the (full) stiffness matrix and load vector with respect to the original basis, and let $\widehat{\mathbf{K}}_i$ and $\widehat{\mathbf{f}}_i$ be the stiffness matrix and load vector with respect to the new basis. Furthermore, let $\widehat{\mathbf{K}}_{RR}^{(i)}$ and $\widehat{\mathbf{f}}_R^{(i)}$ denote the blocks without the primal DOFs (here we assume that the primal DOFs are indexed at the very end). A system of the form

$$\widehat{\mathbf{K}}_{RR}^{(i)} \widehat{\mathbf{u}}_R^{(i)} = \widehat{\mathbf{f}}_R^{(i)} \quad (4.17)$$

is then solved by the constrained system

$$\begin{pmatrix} \mathbf{K}_i & \mathbf{C}_i^\top \\ \mathbf{C}_i & 0 \end{pmatrix} \begin{pmatrix} \mathbf{u}_i \\ \mu_i \end{pmatrix} = \begin{pmatrix} \mathbf{T}_i^{-\top} \begin{pmatrix} \widehat{\mathbf{f}}_{i,R} \\ 0 \end{pmatrix} \\ 0 \end{pmatrix}. \quad (4.18)$$

Here, \mathbf{T}_i denotes the transformation from the new basis to the standard nodal basis and \mathbf{C}_i is the matrix which constrains \mathbf{u}_i (which is given in the original basis) such that $u_i \in \widetilde{W}_{i,\Delta}$. The solution to the original system (4.17) is finally given by

$$\widehat{\mathbf{u}}_R^{(i)} = (\mathbf{I}_R^{(i)} \mid 0) \mathbf{T}_i^{-1} \mathbf{u}_i.$$

This means, instead of an SPD system with a possibly non-sparse stiffness matrix $\widehat{\mathbf{K}}_{RR}^{(i)}$, we can solve a saddle point system with the original sparse stiffness matrix and with the local Lagrange multiplier μ_i . The same technique can be applied also for the BEM subdomains, as we will demonstrate below.

4.3.2 Realization of the operators

Realization of $S_{\Delta,i}$ on a FEM subdomain. First, we partition the full stiffness matrix $\widehat{\mathbf{K}}_i$ into blocks

$$\widehat{\mathbf{K}}_i = \begin{pmatrix} \widehat{\mathbf{K}}_{\Delta\Delta}^{(i)} & \widehat{\mathbf{K}}_{\Delta I}^{(i)} & \widehat{\mathbf{K}}_{\Delta\Pi}^{(i)} \\ \widehat{\mathbf{K}}_{I\Delta}^{(i)} & \widehat{\mathbf{K}}_{II}^{(i)} & \widehat{\mathbf{K}}_{I\Pi}^{(i)} \\ \widehat{\mathbf{K}}_{\Pi\Delta}^{(i)} & \widehat{\mathbf{K}}_{\Pi I}^{(i)} & \widehat{\mathbf{K}}_{\Pi\Pi}^{(i)} \end{pmatrix}.$$

¹In the finite element context, this means effectively that we replace φ_{x^h} by $\vartheta_{\mathcal{E}_{ij}}$, see Remark 2.35.

Here, the subscript I refers to the DOFs corresponding to nodes in the interior of the subdomain, whereas Δ and Π refer to the dual and primal DOFs, respectively, which can be associated to nodes, vertices, edges, or faces on the boundary $\partial\Omega_i$. The matrix representation of $S_{\Delta,i}$ is then given by

$$\widehat{\mathbf{S}}_{\Delta\Delta,i} = \widehat{\mathbf{K}}_{\Delta\Delta}^{(i)} - \widehat{\mathbf{K}}_{\Delta I}^{(i)} [\widehat{\mathbf{K}}_{II}^{(i)}]^{-1} \widehat{\mathbf{K}}_{I\Delta}^{(i)}.$$

Note, that for the basis transformation described above, $\widehat{\mathbf{K}}_{II}^{(i)} = \mathbf{K}_{II}^{(i)}$. Therefore, up to the basis transformation, the application of $S_{\Delta,i}$ is performed by solving a Dirichlet problem, analogously to Section 2.2.3.

Realization of $S_{\Delta,i}$ on a BEM subdomain. Let \mathbf{T}_i denote the basis transformation on W_i which transforms from the new basis to the old basis. By \mathbf{D}_i , \mathbf{M}_i , \mathbf{K}_i and \mathbf{V}_i we denote the usual boundary integral matrices with respect to the standard bases. Furthermore, let $\widehat{\mathbf{D}}_i$, $\widehat{\mathbf{M}}_i$, and $\widehat{\mathbf{K}}_i$ denote the matrix representation with respect to the new basis for the space $V^h(\partial\Omega_i)$, whereas the basis for $Z^h(\partial\Omega_i)$ remains unchanged. The Steklov-Poincaré operator S_i has also two representations, \mathbf{S}_i and $\widehat{\mathbf{S}}_i$ with

$$\widehat{\mathbf{S}}_i = \begin{pmatrix} \widehat{\mathbf{S}}_{\Delta\Delta}^{(i)} & \widehat{\mathbf{S}}_{\Delta\Pi}^{(i)} \\ \widehat{\mathbf{S}}_{\Pi\Delta}^{(i)} & \widehat{\mathbf{S}}_{\Pi\Pi}^{(i)} \end{pmatrix}.$$

In order to compute $\widehat{\mathbf{f}}_{\Delta}^{(i)} = \widehat{\mathbf{S}}_{\Delta\Delta}^{(i)} \widehat{\mathbf{v}}_{\Delta}^{(i)}$, we can solve $\mathbf{t}_i = \mathbf{V}_i^{-1} (\frac{1}{2} \widehat{\mathbf{M}}_{\Delta}^{(i)} + \widehat{\mathbf{K}}_{\Delta}^{(i)}) \mathbf{v}_{\Delta}^{(i)}$ and set

$$\widehat{\mathbf{f}}_{\Delta}^{(i)} = \widehat{\mathbf{D}}_{\Delta\Delta}^{(i)} \widehat{\mathbf{v}}_{\Delta}^{(i)} + (\frac{1}{2} [\widehat{\mathbf{M}}_{\Delta}^{(i)}]^\top + [\widehat{\mathbf{K}}_{\Delta}^{(i)}]^\top) \mathbf{t}_i.$$

Up to the basis transformation, this is the same procedure as described in Section 2.2.3.

Realization of $S_{\Delta,i}^{-1}$ for a FEM subdomain. In order to compute $\widehat{\mathbf{v}}_{\Delta}^{(i)} = [\widehat{\mathbf{S}}_{\Delta\Delta}^{(i)}]^{-1} \widehat{\mathbf{g}}_{\Delta}^{(i)}$, we can solve

$$\begin{pmatrix} \widehat{\mathbf{K}}_{\Delta\Delta}^{(i)} & \widehat{\mathbf{K}}_{\Delta I}^{(i)} \\ \widehat{\mathbf{K}}_{I\Delta}^{(i)} & \widehat{\mathbf{K}}_{II}^{(i)} \end{pmatrix} \begin{pmatrix} \widehat{\mathbf{v}}_{\Delta}^{(i)} \\ \widehat{\mathbf{v}}_I^{(i)} \end{pmatrix} = \begin{pmatrix} \widehat{\mathbf{g}}_{\Delta}^{(i)} \\ 0 \end{pmatrix},$$

which is of the form (4.17).

Realization of $S_{\Delta,i}^{-1}$ for a BEM subdomain. Instead of computing $\widehat{\mathbf{v}}_{\Delta}^{(i)} = [\widehat{\mathbf{S}}_{\Delta\Delta}^{(i)}]^{-1} \widehat{\mathbf{g}}_{\Delta}^{(i)}$, we can solve the saddle point system

$$\begin{pmatrix} \widehat{\mathbf{D}}_{\Delta\Delta}^{(i)} & \frac{1}{2} [\widehat{\mathbf{M}}_{\Delta}^{(i)}]^\top + [\widehat{\mathbf{K}}_{\Delta}^{(i)}]^\top \\ \frac{1}{2} \widehat{\mathbf{M}}_{\Delta}^{(i)} + \widehat{\mathbf{K}}_{\Delta}^{(i)} & -\mathbf{V}_i \end{pmatrix} \begin{pmatrix} \widehat{\mathbf{v}}_{\Delta}^{(i)} \\ \mathbf{t}_i \end{pmatrix} = \begin{pmatrix} \widehat{\mathbf{g}}_{\Delta}^{(i)} \\ 0 \end{pmatrix}. \quad (4.19)$$

If one wishes to use the original matrices, one can instead solve the modified system

$$\begin{pmatrix} \mathbf{D}_i & \frac{1}{2} \mathbf{M}_i^\top + \mathbf{K}_i^\top & \mathbf{C}_i^\top \\ \frac{1}{2} \mathbf{M}_i + \mathbf{K}_i & -\mathbf{V}_i & 0 \\ \mathbf{C}_i & 0 & 0 \end{pmatrix} \begin{pmatrix} \mathbf{v}_i \\ \mathbf{t}_i \\ \mu_i \end{pmatrix} = \begin{pmatrix} \mathbf{T}_i^{-\top} \begin{pmatrix} \widehat{\mathbf{g}}_{\Delta}^{(i)} \\ 0 \end{pmatrix} \\ 0 \\ 0 \end{pmatrix}, \quad (4.20)$$

where \mathbf{C}_i is the matrix with respect to the standard nodal basis which constrains the respective function to be in $\widetilde{W}_{i,\Delta}$, and set $\widehat{\mathbf{v}}_{\Delta}^{(i)} = (\mathbf{I}_{\Delta}^{(i)} | 0) \mathbf{T}_i^{-1} \mathbf{v}_i$.

Realization of \tilde{S}^{-1} . Computing $v_\Delta = \tilde{S}^{-1}g_\Delta$ is equivalent to solving

$$\begin{pmatrix} S_\Delta & S_{\Delta\Pi} \\ S_{\Pi\Delta} & S_\Pi \end{pmatrix} \begin{pmatrix} v_\Delta \\ v_\Pi \end{pmatrix} = \begin{pmatrix} g_\Delta \\ 0 \end{pmatrix}. \quad (4.21)$$

We use the block factorization

$$\begin{pmatrix} S_\Delta & S_{\Delta\Pi} \\ S_{\Pi\Delta} & S_\Pi \end{pmatrix}^{-1} = \begin{pmatrix} I_\Delta & -S_\Delta^{-1}S_{\Delta\Pi} \\ 0 & I_\Pi \end{pmatrix} \begin{pmatrix} S_\Delta^{-1} & 0 \\ 0 & \tilde{S}_\Pi^{-1} \end{pmatrix} \begin{pmatrix} I_\Delta & 0 \\ -S_{\Pi\Delta}S_\Delta^{-1} & I_\Pi \end{pmatrix}, \quad (4.22)$$

with

$$\tilde{S}_\Pi := S_\Pi - S_{\Pi\Delta}S_\Delta^{-1}S_{\Delta\Pi}.$$

Let $\tilde{\mathbf{S}}_{\text{III}}$ denote the matrix representing \tilde{S}_Π with respect to the new basis. We first describe how to assemble $\tilde{\mathbf{S}}_{\text{III}}$ from local contributions $\tilde{\mathbf{S}}_{\text{III}}^{(i)}$. For each FEM subdomain Ω_i , we find that

$$\tilde{\mathbf{S}}_{\text{III}}^{(i)} = \hat{\mathbf{K}}_{\text{III}}^{(i)} - \hat{\mathbf{K}}_{\text{IR}}^{(i)} [\hat{\mathbf{K}}_{\text{RR}}^{(i)}]^{-1} \hat{\mathbf{K}}_{\text{RI}}^{(i)},$$

i. e., the entries can be obtained by solving one Dirichlet problem for each local primal DOF, cf. (4.17). For a BEM subdomain the corresponding entries can be obtained using the identity

$$\tilde{\mathbf{S}}_{\text{III}}^{(i)} = \hat{\mathbf{D}}_{\text{III}}^{(i)} + (\frac{1}{2}[\hat{\mathbf{M}}_\Pi^{(i)}]^\top + [\hat{\mathbf{K}}_\Pi^{(i)}]^\top) \mathbf{V}_i^{-1} \left\{ (\frac{1}{2}\hat{\mathbf{M}}_\Pi^{(i)} + \hat{\mathbf{K}}_\Pi^{(i)}) - (\frac{1}{2}\hat{\mathbf{M}}_\Delta^{(i)} + \hat{\mathbf{K}}_\Delta^{(i)}) [\hat{\mathbf{S}}_{\Delta\Delta}^{(i)}]^{-1} \hat{\mathbf{S}}_{\Delta\Pi}^{(i)} \right\},$$

from which we see that the action can be performed solving two systems with the single layer potential, and one saddle point system of the form (4.19) or (4.20). As soon as the matrix $\tilde{\mathbf{S}}_{\text{III}}$ has been assembled, its factorization can be performed and stored. Under the condition that the number of local primal DOFs is uniformly bounded, it can be shown that the matrix $\tilde{\mathbf{S}}_{\text{III}}$ is sparse, as the coarse matrix $\mathbf{G}^\top \mathbf{Q} \mathbf{G}$ occurring in the one-level methods. We will return to that issue in Section 4.3.3.

Looking back to (4.22) we see that the application of \tilde{S}^{-1} reduces essentially to applications of $S_{i,\Delta}^{-1}$ and \tilde{S}_Π^{-1} . Further simplifications by exploiting the Schur complement structure are possible, for FETI methods see RHEINBACH [154].

Representation of $d = \tilde{S}^{-1}\tilde{f}$. Instead of forming and factorizing a matrix representing S_Π to obtain \tilde{f} according to (4.5), we find that $v_\Delta = \tilde{S}^{-1}\tilde{f}$ is equivalent to solving

$$\begin{pmatrix} S_\Delta & S_{\Delta\Pi} \\ S_{\Pi\Delta} & S_\Pi \end{pmatrix} \begin{pmatrix} v_\Delta \\ v_\Pi \end{pmatrix} = \begin{pmatrix} f_\Delta \\ f_\Pi \end{pmatrix}, \quad (4.23)$$

i. e., we can use the block factorization from above.

Computing u from λ . The realizations of F , M^{-1} , and d are now clear. Let λ denote the solution to (4.7) after the PCG iteration has been stopped. The solution u we are looking for is then obtained as follows. We solve (4.23) replacing f_Δ by $f_\Delta - B_\Delta^\top \lambda$ and set $u = \begin{pmatrix} v_\Delta \\ v_\Pi \end{pmatrix}$.

For the FEM subdomains, the interior values $\mathbf{u}_I^{(i)}$ are provided as a byproduct, for details see RHEINBACH [154].

In order to obtain an efficient algorithm, all the BEM matrices need to be approximated by data-sparse matrices, and all corresponding BEM systems need to be efficiently solved, e. g., using \mathcal{H} -LU factorization, cf. BEBENDORF [7, 8].

4.3.3 Comparison of dual-primal and one-level methods

4.3.3.1 The bounded case

A fine comparison of FETI-DP and the standard one-level FETI methods can be found in TOSELLI AND WIDLUND [184, Sect. 6.4.1]. In the following, we compare the dual primal methods to the one-level methods, including the all-floating methods.

- Dual-primal algorithms do not require the characterization of the kernels of the Steklov-Poincaré operators in practice. All-floating methods need such a characterization but without incorporation of (possibly complicated) boundary conditions.
- In three dimensions, the dual-primal methods require the handling of edge and possibly face constraints via a change of basis, which is not needed at all in case of the one-level methods. In order to be competitive with the one-level methods in view of the size of the coarse problem, dual-primal methods require a careful choice of the primal DOFs, such as Algorithm D.
- The same dual-primal algorithms and codes can be applied to problems with and without non-trivial local kernels, e. g., differential operators with zero-order terms. According to Remark 3.22, in such cases, one-level methods need a non-trivial adaption.
- Dual-primal methods do not require the construction of a scaling matrix Q which appears in the coarse solver of one-level methods. The dual-primal coarse solver is determined just by the FEM or BEM system matrices and the primal DOFs.
- As a possible drawback of one-level methods, the initial guess λ_0 of the underlying projected PCG methods needs to be fixed somehow, since the condition $G^\top \lambda_0 = e$ must hold. This initial guess can however be far away from the solution λ . In contrast, an arbitrary initial guess λ_0 can be employed for dual-primal methods.

4.3.3.2 The unbounded case

We have seen that the coarse space of dual-primal methods for unbounded domains is more powerful than that of the one-level methods. However, this goes along with a possibly high computational cost. If the number of primal DOFs $n_{\Pi,0}$ on $\partial\Omega_0$ stays small, the algorithm will work fine. If $n_{\Pi,0}$ grows, however, alone the assembling of the coarse matrix representing \tilde{S}_Π involves at least $n_{\Pi,0}$ solves of the single layer potential on $\partial\Omega_0$. Note that even for the carefully selecting Algorithm D, $n_{\Pi,0}$ is at least as big as the number of faces on $\partial\Omega_0$. In other words, a large number $n_{\Pi,0}$ goes along with a large number of neighbors of $\partial\Omega_0$. This, in turn, implies that the coarse matrix \tilde{S}_Π loses its sparsity. It might be that this problem can be solved using an \mathcal{H} -matrix approximation of \tilde{S}_Π . Note that such a fill-in phenomenon cannot happen in case of the one-level methods, since the Steklov-Poincaré operator S_0 does not at all contribute to the coarse matrix $G^\top Q G$. When being parallelized, both the one-level and the dual-primal methods can suffer from the lack of load balancing if the number of DOFs on $\partial\Omega_0$ is large. The buffer strategy outlined in Section 3.6 can be used to cope with this problem. To summarize, the one-level method can be used unless the predicted condition number due to Theorem 3.20, Theorem 3.15 is getting very large, either because of a relatively small coefficient α_0 or a relatively small shape parameter η . In such cases, the dual-primal method might be of greater advantage.

Chapter 5

Multiscale coefficients

In this chapter, we would like to discuss FETI methods for problems with highly heterogeneous (multiscale) coefficients, i. e., coefficients which do not only jump across material interfaces resolved by the subdomain partitioning, but which can have large jumps or large variation on the fine scale.

To the best of our knowledge, all the present analyses of FETI methods assume that the coefficient α is piecewise constant with respect to the subdomain partitioning (or at least only moderately varying in each subdomain). It has already been observed numerically by several authors (see Klawonn and Rheinbach [107], Langer and Pechstein [116], and Rixen and Farhat [155, 156]) that a simple generalization of the scaling employed by Klawonn and Widlund [109] (cf. Section 2.2.1.3) leads to robustness of the FETI method even in this case. However, a theoretical justification for this kind of robustness has been still lacking. In this chapter we give an analysis which was first published in Pechstein and Scheichl [147]. It shows that the condition number of the preconditioned system depends only on the variation of the coefficient in the vicinity of the subdomain interfaces. More precisely, if we fix a boundary layer of width η in each subdomain such that $\alpha(x) \leq C_\eta \alpha(y)$ for all x, y in each subdomain boundary layer, the condition number bound reads $C_\eta (H/\eta)^2$. Under stronger assumptions, the quadratic dependence on H/η can be relaxed to a linear one. Our result is a generalization of that by Klawonn and Widlund [109] (cf. Theorem 2.28) and it shows that FETI methods can still be very robust if the coefficient varies a lot in the interior of each subdomain. The same statement holds for FETI-DP methods.

Our theoretical findings for the one-level methods are confirmed in numerical experiments. These also show that our bound is not always sharp when the coefficient varies strongly near subdomain interfaces. In practice FETI methods often seem to be robust even in this case, in particular when the variation along the interface is smooth or when the coefficient jumps only in a few places. The analysis in this case is much harder and will be the focus of future investigations.

In Section 5.1 we briefly discuss the multiscale elliptic model problem. Section 5.2 embraces the formulation of one-level FETI methods for this problem, where we adapt and generalize the one-level methods from Chapter 2. The main robustness results are contained in Section 5.3. The proof of these results is given in Section 5.4, where we also introduce some technical tools needed for the analysis, in particular generalized Poincaré, Friedrichs, and discrete Sobolev type inequalities for boundary layers. Finally, we give numerical results in Section 5.5.

5.1 Problem formulation of multiscale elliptic PDEs

As discussed in the introduction, highly heterogeneous (multiscale) coefficients arise, e. g., in the simulation of complicated layered media or heterogeneous (e. g., porous) media. Large but smooth variation of coefficients can appear in the setting of nonlinear problems. In the following we consider the scalar elliptic model problem

$$\begin{aligned} -\operatorname{div}(\alpha \nabla u) &= f && \text{in } \Omega, \\ u &= 0 && \text{on } \Gamma_D, \\ \alpha \frac{\partial u}{\partial n} &= g_N && \text{on } \Gamma_N, \end{aligned} \tag{5.1}$$

on a bounded domain Ω in \mathbb{R}^2 or \mathbb{R}^3 where Γ_D is a relatively closed part of $\partial\Omega$ of positive surface measure and $\Gamma_N = \partial\Omega \setminus \Gamma_D$. For the sake of simplicity, we consider only homogeneous Dirichlet boundary conditions on Γ_D , and we assume that $g_N \in L^2(\Gamma_N)$ and $f \in L^2(\Omega)$.

Unlike in Chapter 2, the coefficient $\alpha(\cdot)$ may vary over many orders of magnitude in an unstructured way on Ω . Concerning the discretization we consider a family of shape-regular, geometrically conforming meshes $\mathcal{T}^h(\Omega)$ resolving Γ_D and Γ_N . We need the following assumption on the regularity of the coefficient $\alpha(\cdot)$.

Assumption 5.1. *The coefficient $\alpha(\cdot)$ is assumed to be in $L^\infty(\Omega)$, uniformly strictly positive, and constant in the elements of the triangulation $\mathcal{T}^h(\Omega)$.*

Under this assumption, the bilinear form associated to (5.1) is elliptic on $H_D^1(\Omega)$ and bounded on $H^1(\Omega)$ according to Lemma 1.15. Hence, Theorem 1.16 (Lax-Milgram) guarantees the existence of a unique solution. The assumption that the coefficient is constant on each element is not essential when working with linear finite elements, because

$$\int_{\tau} \alpha(x) \nabla u(x) \cdot \nabla v(x) dx = \left(\int_{\tau} \alpha(x) dx \right) \nabla u|_{\tau} \cdot \nabla v|_{\tau}, \quad \forall u, v \in \mathcal{P}_1(\tau), \forall \tau \in \mathcal{T}^h(\Omega),$$

cf. GRAHAM, LECHNER, AND SCHEICHL [75].

The discrete variational problem reads: Find $u_h \in V_D^h(\Omega)$ such that

$$\int_{\Omega} \alpha \nabla u_h \cdot \nabla v_h dx = \int_{\Omega} f v_h dx + \int_{\Gamma_N} g_N v_h ds \quad \forall v_h \in V_D^h(\Omega), \tag{5.2}$$

where $V^h(\Omega)$, $V_D^h(\Omega)$ are defined according to (1.5.2). The global system of finite element equations reads

$$\tilde{\mathbf{K}} \tilde{\mathbf{u}} = \tilde{\mathbf{f}}. \tag{5.3}$$

It is easily shown that the condition number $\kappa(\tilde{\mathbf{K}})$ fulfills the bound

$$\kappa(\tilde{\mathbf{K}}) \leq C \sup_{x,y \in \Omega} \frac{\alpha(x)}{\alpha(y)} h^{-2}, \tag{5.4}$$

for the case of a globally quasi-uniform mesh. As outlined before we are interested in iterative solvers which are not only robust with respect to the factor h^{-2} , but also with respect to the coefficient variation.

5.2 Formulation of FETI methods for multiscale PDEs

First we briefly recall some of the notations and assumptions from Chapter 2. Let $\{\Omega_i\}_{i \in \mathcal{I}}$ be a shape-regular subdomain partition of Ω , and let the global mesh $\mathcal{T}^h(\Omega)$ be chosen such that it resolves the subdomain interfaces. For each subdomain Ω_i , the restriction $\mathcal{T}^h(\Omega_i)$ of $\mathcal{T}^h(\Omega)$ to Ω_i is assumed to be quasi-uniform with mesh size h_i . In particular, we have $H_i \simeq H_j$ and $h_i \simeq h_j$ for neighboring subdomains Ω_i, Ω_j . As in previous sections we assume that the boundary parts Γ_D and Γ_N are unions of faces, edges, and vertices of the subdomain partition, cf. Assumption 2.25.

In principle, the derivation of standard one-level and all-floating methods for problem (5.1) is performed analogously to Chapter 2, where we carefully generalize for the case of the non-constant coefficients. Note that for the standard one-level formulation we need Assumption 2.26, which states that in three dimensions, $\partial\Omega_i \cap \Gamma_D$ is either empty or at least an edge. We define the local spaces

$$\begin{aligned} W^h(\Omega_i) &:= V_D^h(\Omega_i), \quad W_i := V_D^h(\partial\Omega_i) \quad \text{for a standard one-level method,} \\ W^h(\Omega_i) &:= V^h(\Omega_i), \quad W_i := V^h(\partial\Omega_i) \quad \text{for an all-floating method,} \end{aligned} \quad (5.5)$$

and the product space $W := \prod_{i \in \mathcal{I}} W_i$. On each subdomain Ω_i , let $\mathbf{K}^{(i)}$ and $\mathbf{f}^{(i)}$ denote the stiffness matrix and the load vector with respect to the space $W^h(\Omega_i)$. By $S_i : W_i \rightarrow W_i^*$ and $f_i \in W_i^*$ we denote the discrete Steklov-Poincaré operator and the discrete Newton potential which correspond to the matrix/vector representations

$$\mathbf{S}_i = \mathbf{K}_{BB}^{(i)} - \mathbf{K}_{BI}^{(i)} [\mathbf{K}_{II}^{(i)}]^{-1} \mathbf{K}_{IB}^{(i)}, \quad \mathbf{N}_i \mathbf{f}^{(i)} = \mathbf{f}_B^{(i)} - \mathbf{K}_{BI}^{(i)} [\mathbf{K}_{II}^{(i)}]^{-1} \mathbf{f}_I^{(i)},$$

respectively, where the subscript I indicates interior DOFs, and the subscript B indicates the (free) DOFs associated to nodes on $\partial\Omega_i^h$. Apparently, $\ker S_i = \{\mathbf{1}_{\partial\Omega_i}\}$ in case of the all-floating formulation, and otherwise, $\ker S_i = \{0\}$ if and only if $\partial\Omega_i \cap \Gamma_D \neq \emptyset$. Finally, we set $S := \text{diag}(S_i) : W \rightarrow W^*$ and $f := [f_i]_{i \in \mathcal{I}}$.

Analogously to Chapter 2 we introduce suitable jump operators $B_i : W_i \rightarrow U^*$ and $B : W \rightarrow U^*$ with the Lagrange multiplier space U , the (pseudo)inverses $S_i^\dagger : W_i^* \rightarrow W_i$, $S^\dagger = \text{diag}(S_i^\dagger)$, the operators R_i with range $R_i = \ker S_i$ and $R : Z \rightarrow W$ defined according to (2.36)–(2.37), $G = BR$, and the projection $P = I - QG(G^\top QG)^{-1}G^\top$ where the SPD operator $Q : U^* \rightarrow U$ is yet to be specified. With $F = BS^\dagger B^\top$ and $d = BS^\dagger f$, we obtain the equation

$$P^\top F \tilde{\lambda} = P^\top (d - F \lambda_0) \quad \forall \tilde{\lambda} \in V, \quad (5.6)$$

where $\lambda_0 = QG(G^\top QG)^{-1}R^\top f$ and $V = \{\lambda \in U : \langle B^\top \lambda, z \rangle = 0 \quad \forall z \in \ker S\}$.

Remark 5.2. (i) In case of the all-floating formulation for non-homogeneous Dirichlet problems we have to use $d = BS^\dagger f - b$ where $b \in U^*$ contains the Dirichlet values, cf. Section 2.2.2.

(ii) If we view the operators B_i as mappings from $W^h(\Omega_i)$ to U^* and let $f_i \in W^h(\Omega_i)^*$ correspond to the load vectors $\mathbf{f}^{(i)}$, we can equivalently use

$$F = \sum_{i \in \mathcal{I}} B_i K_i^\dagger B_i^\top, \quad d = \sum_{i \in \mathcal{I}} B_i K_i^\dagger f_i,$$

where on the floating subdomains, the pseudoinverse $K_i^\dagger : W^h(\Omega_i)^* \rightarrow W^h(\Omega_i)$ can be realized using a suitable regularization of the stiffness matrix $\mathbf{K}^{(i)}$, see also Section 1.5.2. With $\lambda = \lambda_0 + \tilde{\lambda}$ and with R_i mapping to the constant functions in $W^h(\Omega_i)$, the solution u to the original problem is given by

$$u_i = K_i^\dagger (f_i - B_i^\top \lambda) + R_i (G^\top Q G)^{-1} G^\top Q (F \lambda - d).$$

5.2.1 Different scaling operators and preconditioners

In Chapter 2 we have used the constant values $\alpha_i = \alpha|_{\Omega_i} = \text{const}$ in the scaling matrices D_i and Q . However, the entries of D_i and Q are associated to entries of Lagrange multipliers and therefore to nodes x^h . In order to generalize such scalings for multiscale coefficients we can either use

- (i) constant values, such as the upper and lower bound of $\alpha(\cdot)$ on each subdomain,
- (ii) some nodal evaluations of the varying coefficient $\alpha(\cdot)$, or
- (iii) some evaluations of the coefficient on a part of the subdomain (such as maximum, minimum, or average).

Ad (i). Assumption 5.1 allows to define

$$\bar{\alpha}_i := \max_{\tau \in \mathcal{T}^h(\Omega_i)} \alpha|_\tau, \quad \underline{\alpha}_i := \min_{\tau \in \mathcal{T}^h(\Omega_i)} \alpha|_\tau > 0. \quad (5.7)$$

Ad (ii). We define for each node $x^h \in \partial\Omega_i^h$ the open nodal subdomain patch $\omega^i(x^h) \subset \Omega_i$ by the relation

$$\overline{\omega^i(x^h)} = \bigcup \{ \bar{\tau} : \tau \in \mathcal{T}^h(\Omega_i), x^h \in \bar{\tau} \}, \quad (5.8)$$

i. e., the patch of elements in Ω_i around x^h (cf. Figure 5.1, left). Using these patches, we can define the following nodal evaluations of α ,

$$\left. \begin{aligned} \hat{\alpha}_i^{\max}(x^h) &:= \max_{y \in \omega^i(x^h)} \alpha(y) \\ \hat{\alpha}_i^{\min}(x^h) &:= \min_{y \in \omega^i(x^h)} \alpha(y) \\ \hat{\alpha}_i^{\text{mean}}(x^h) &:= \frac{1}{|\omega^i(x^h)|} \int_{\omega^i(x^h)} \alpha(y) dy \end{aligned} \right\} \quad \text{for } x^h \in \partial\Omega_i^h, \quad (5.9)$$

Ad (iii). The following variant is mainly needed for theoretical purposes. Here, we reuse the concept of a *boundary layer* introduced in Section 3.4.1, and we will use the maximum of the coefficient on this boundary layer for scaling.

Definition 5.3 (Boundary layer). *A subset Ω_{i,η_i} of Ω_i is called boundary layer of Ω_i with parameter $\eta_i > 0$ if it fulfills*

$$\forall x \in \Omega_{i,\eta_i} : \text{dist}(x, \partial\Omega_i) < 2\eta_i \quad \text{and} \quad \forall x \in \partial\Omega_i : B_{x,\eta_i} \cap \Omega_i \subset \Omega_{i,\eta_i},$$

where B_{x,η_i} is the open ball with center x and radius η_i .

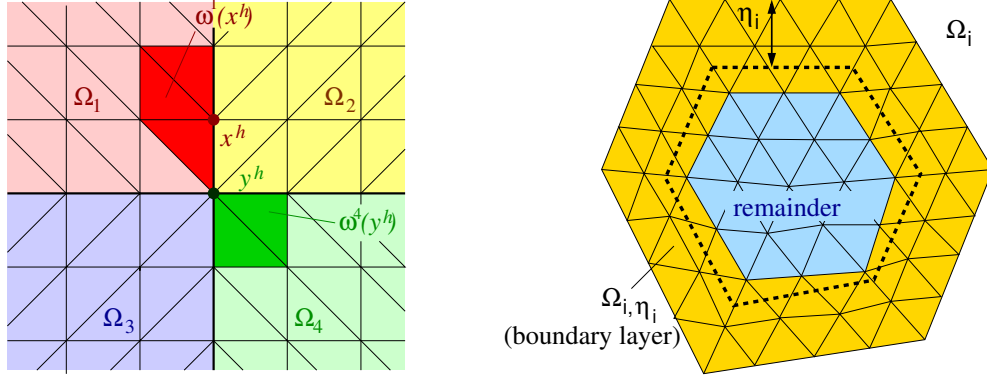


Figure 5.1: *Left:* Subdomain node patches $\omega^1(x^h)$, $\omega^4(y^h)$ corresponding to the nodes x^h and y^h , cf. (5.8). *Right:* Boundary layer Ω_{i,η_i} of the subdomain Ω_i , cf. Definition 5.3.

For the rest of this chapter we assume that we have fixed parameters η_i and boundary layers Ω_{i,η_i} which are the union of elements of the triangulations $\mathcal{T}^h(\Omega_i)$, cf. Figure 5.1, right. We set

$$\bar{\alpha}_i^{\eta_i} := \max_{x \in \Omega_{i,\eta_i}} \alpha(x), \quad \underline{\alpha}_i^{\eta_i} := \min_{x \in \Omega_{i,\eta_i}} \alpha(x) > 0. \quad (5.10)$$

Remark 5.4. It is important to note that the ratio $\bar{\alpha}_i^{\eta_i} / \underline{\alpha}_i^{\eta_i}$ neither depends on inter-subdomain coefficient jumps nor on the values of $\alpha(\cdot)$ in the interior regions $\Omega_i \setminus \Omega_{i,\eta_i}$. The coefficients $\alpha(\cdot)$ may have arbitrary large jumps across the subdomain interfaces and arbitrary but positive values in the subdomain interiors.

In order to define the scaling operators D_i and Q we choose the functions $\hat{\alpha}_i \in V^h(\partial\Omega_i)$ from the set $\{\bar{\alpha}_i, \underline{\alpha}_i, \hat{\alpha}_i^{\max}, \hat{\alpha}_i^{\min}, \hat{\alpha}_i^{\text{mean}}, \bar{\alpha}_i^{\eta_i}, \underline{\alpha}_i^{\eta_i}\}$, and define the weighted counting functions

$$\hat{\delta}_j^\dagger(x^h) := \begin{cases} \frac{\hat{\alpha}_j(x^h)}{\sum_{k \in \mathcal{N}_{x^h}} \hat{\alpha}_k(x^h)} & \text{for } x^h \in \partial\Omega_j^h, \\ 0 & \text{for } x^h \in \Gamma_S^h \setminus \partial\Omega_j^h. \end{cases} \quad (5.11)$$

We can now define $D_i : U^* \rightarrow U$ by

$$\begin{aligned} (D_i \mu)_{ij}(x^h) &:= \hat{\delta}_j^\dagger(x^h) \mu_{ij}(x^h) & \forall x^h \in \Gamma_{ij}^h, \\ (D_i \mu)_{jD}(x^h) &:= \mu_{jD}(x^h) & \forall x^h \in \partial\Omega_j^h \cap \Gamma_D, \end{aligned} \quad (5.12)$$

for $\mu \in U^*$, where the second line has to be dropped in case of a standard one-level FETI method. In three dimensions, the scaling operator $Q : U^* \rightarrow U$ is defined by

$$\begin{aligned} (Q \mu)_{ij}(x^h) &:= \min(\hat{\alpha}_i(x^h), \hat{\alpha}_j(x^h)) q_{ij}(x^h) \mu_{ij}(x^h) & \text{for } x^h \in \Gamma_{ij}^h, \\ (Q \mu)_{iD}(x^h) &:= \hat{\alpha}_i(x^h) q_i(x^h) \mu_{iD}(x^h) & \text{for } x^h \in \partial\Omega_i^h \cap \Gamma_D, \end{aligned} \quad (5.13)$$

for $\mu \in U^*$, where $q_{ij}(x^h)$ and $q_i(x^h)$ are defined according to (2.56) and (2.77), and the second line is dropped for standard one-level FETI methods.

Note that we will use the parameters $\bar{\alpha}_i^{\eta_i}$, $\underline{\alpha}_i^{\eta_i}$ mostly for theoretical purposes. In practice $\hat{\alpha}_i^{\max}$ is a much more convenient choice. Nevertheless, if α is constant on each boundary layer, we have

$$\bar{\alpha}_i^{\eta_i} = \hat{\alpha}_i^{\max}(x^h) \quad \forall x^h \in \partial\Omega_i^h.$$

The preconditioner finally reads

$$M^{-1} = B_D S B_D^\top = \sum_{i \in \mathcal{I}} D_i B_i \mathcal{J}_{W_i} S_i \mathcal{J}_{W_i}^\top B_i^\top D_i. \quad (5.14)$$

Remark 5.5. When substituting the coefficient $\hat{\alpha}_i(x^h)$ in (5.11) by the entry of the stiffness matrix $\mathbf{K}^{(i)}$ corresponding to the basis function $\varphi_{x^h}^{(i)}$, the scaling operators D_i are exactly those proposed by RIXEN AND FARHAT [155, 156], known as *superlumped smoothing*.

As we know from Chapter 2, each step of the FETI PCG algorithm needs the solution of a Dirichlet problem, a regularized Neumann problem, and the coarse problem given by the operator $G^\top Q G$. In what follows, we assume that all these problems can be handled by direct solvers, which means that their condition numbers (which will usually be large due to the coefficient variation) do not affect the solves.

5.3 Robustness analysis

5.3.1 A straightforward condition number bound

First, we would like to clarify the efficiency of the constant weights $\bar{\alpha}_i$, $\underline{\alpha}_i$, from which we do not expect robustness in general. The following lemma (which can essentially be found in LANGER AND PECHSTEIN [116, Proposition 2.2]) states that constant weights result in a linear factor of the maximal subdomain variation in the condition number bound.

Lemma 5.6. *Let $\hat{\alpha}_i = \bar{\alpha}_i$ for all $i \in \mathcal{I}$ and let the operators D_i and Q be defined according to (5.11)–(5.13). Then the condition number κ of the preconditioned FETI system (standard one-level or all-floating) satisfies the bound*

$$\kappa \leq C \left\{ \max_{i \in \mathcal{I}} \max_{x, y \in \Omega_i} \frac{\alpha(x)}{\alpha(y)} \right\} \max_{j \in \mathcal{I}} (1 + \log(H_j/h_j))^2,$$

with $C > 0$ independent of H_i , h_i , $\alpha(\cdot)$, and the number of subdomains. The statement remains valid if we choose $\hat{\alpha}_i = \bar{\alpha}_i^\beta \underline{\alpha}_i^{1-\beta}$ with some global exponent $\beta \in [0, 1]$.

Proof. A careful inspection of the analysis from Chapter 2 reveals that we only need to bound $|P_D(w + z_w)|_S$ in terms of $|w|_S$ for all $w \in W$. Let $\bar{S}_i, \underline{S}_i : W_i \rightarrow W_i^*$ denote the Steklov-Poincaré operators corresponding to the bilinear forms

$$\bar{a}_i(u, v) := \bar{\alpha}_i \int_{\Omega_i} \nabla u \cdot \nabla v \, dx, \quad \underline{a}_i(u, v) := \underline{\alpha}_i \int_{\Omega_i} \nabla u \cdot \nabla v \, dx,$$

respectively, where $u, v \in W^h(\Omega_i)$. Furthermore, we set $\bar{S} = \text{diag}(\bar{S}_i)$ and $\underline{S} = \text{diag}(\underline{S}_i)$. By the minimizing property of the FEM Schur complement, cf. Lemma 1.32, we easily obtain

$$|w_i|_{\underline{S}_i}^2 \leq |w_i|_{\bar{S}_i}^2 \leq |w_i|_{\underline{S}_i}^2 = \frac{\bar{\alpha}_i}{\underline{\alpha}_i} |w_i|_{\underline{S}_i}^2 \quad \forall w_i \in W_i.$$

We see that the weights in D_i and Q are exactly those of the method from Chapter 2 for the bilinear form $\bar{\alpha}_i(u, v)$. Reusing Lemma 2.27 we obtain

$$\begin{aligned} |P_D(w + z_w)|_S^2 &\leq |P_D(w + z_w)|_S^2 \leq \max_{j \in \mathcal{I}} C(1 + \log(H_j/h_j)) |w|_S^2 \\ &\leq \max_{j \in \mathcal{I}} C(1 + \log(H_j/h_j)) \max_{i \in \mathcal{I}} \frac{\bar{\alpha}_i}{\underline{\alpha}_i} |w|_S^2, \end{aligned}$$

for all $w \in W$. The proof for the case $\beta \neq 1$ follows immediately, for details see [116]. \square

5.3.2 New coefficient-robust condition number bounds

In this section we analyze the proposed FETI method with the weights $\hat{\alpha}_i = \bar{\alpha}_i^{\eta_i}$. We give a condition number bound which is independent of the values of α in the interior $\Omega_i \setminus \Omega_{i, \eta_i}$ of each subdomain Ω_i , but which depends on the variation of α in the boundary layers and on the ratios H_i/η_i .

Assumption 5.7. *For each $i \in \mathcal{I}$ let Ω_{i, η_i} be a boundary layer with parameter $\eta_i > 0$ such that*

$$\underline{\alpha}_i^{\eta_i} \leq \alpha(x) \leq \bar{\alpha}_i^{\eta_i} \quad \forall x \in \Omega_{i, \eta_i},$$

and assume that $\eta_i \simeq \eta_j$ for neighboring subdomains Ω_i, Ω_j .

Before we state our main result, we need a few regularity assumptions on the subdomains and the boundary layers.

Definition 5.8 (Regular domain). *For $d = 2$ or 3 , we call a domain $D \subset \mathbb{R}^d$ regular if it is bounded, contractible, and Lipschitz, and if it can be decomposed into a conforming coarse mesh of shape-regular triangles (tetrahedra). Whenever considering a family of regular domains, such as partitions into subdomains, we implicitly assume that the number of simplices forming an individual subdomain is uniformly bounded.*

Definition 5.9 (Shape parameter). *We define the shape parameter of a regular domain D by*

$$\rho(D) := \min_{1 \leq i \leq s} \rho(T_i),$$

where $\{T_i\}_{1 \leq i \leq s}$ are the simplices according to Definition 5.8 and $\rho(T_i)$ is the diameter of the largest ball contained in \bar{T}_i .

As in Chapter 2 we assume that the subdomains are regular domains with

$$\rho(\Omega_i) \simeq H_i \quad \text{and} \quad H_i \simeq H_j \quad \text{for } \partial\Omega_i \cap \partial\Omega_j \neq \emptyset.$$

cf. Assumption 2.1 and Assumption 2.23. The following assumption concerning the boundary layers Ω_{i, η_i} is very similar to the *partition property* from Definition 3.13.

Assumption 5.10. *Assume that for each $i \in \mathcal{I}$, the boundary layer Ω_{i, η_i} is a union of elements of the triangulation $\mathcal{T}^h(\Omega_i)$ and that it can be covered by finitely many patches $\{\omega_j^{(i)}\}_{j \in \mathcal{J}^{(i)}}$ such that the following assumptions hold.*

- (i) *The patches $\{\omega_j^{(i)}\}_{j \in \mathcal{J}^{(i)}}$ form a family of regular domains in the sense of Definition 5.8 with $\text{diam } \omega_j^{(i)} \simeq \eta_i$, such that the number of simplices per patch is uniformly bounded.*

- (ii) The patches have finite overlap, i. e., the number of patches sharing a point $y \in \Omega_{i,\eta_i}$ is uniformly bounded.
- (iii) For each $j \in \mathcal{J}^{(i)}$, the intersection $\gamma_j^{(i)} := \partial\omega_j^{(i)} \cap \partial\Omega_i$ is the closure of a union of faces (edges in two dimensions) of the simplices forming the patch. Furthermore in three dimensions, for any edge \mathcal{E}_i of Ω_i , the intersection $\partial\omega_j^{(i)} \cap \mathcal{E}_i$ is a union of edges of the simplices forming the patch $\omega_j^{(i)}$.
- (iv) For two neighboring patches $\omega_j^{(i)}, \omega_k^{(i)}$ that share at least a manifold of dimension $d-1$, we assume that the compound patch $\omega_{j,k}^{(i)}$ defined by the union of $\omega_j^{(i)}$ and $\omega_k^{(i)}$ is regular in the sense of Definition 5.8.

Remark 5.11. Note that Assumption 5.10 requires a *covering* only, whereas in Definition 3.13 we have assumed a *non-overlapping* partitioning into patches. Clearly, such a non-overlapping partition is also a covering in the above sense, and if the simplices, which the patches consist of, form a conforming coarse mesh of the boundary layer Ω_η , Part (iv) of Assumption 5.10 is automatically fulfilled.

Theorem 5.12. For each $i \in \mathcal{I}$, let Ω_{i,η_i} be a boundary layer with parameter η_i satisfying Assumption 5.7 and Assumption 5.10. Let $\hat{\alpha}_i = \bar{\alpha}_i^{\eta_i}$, and let the operators D_i and Q be defined according to (5.11)–(5.13). Then the standard one-level and the all-floating FETI method with the preconditioner defined in (5.14) satisfy the condition number estimate

$$\kappa \leq C \max_{k \in \mathcal{I}} \left(\frac{H_k}{\eta_k} \right)^\beta \max_{i \in \mathcal{I}} \frac{\bar{\alpha}_i^{\eta_i}}{\underline{\alpha}_i^{\eta_i}} (1 + \log(H_i/h_i))^2,$$

with the exponent $\beta = 2$. The constant C is independent of the parameters H_i, η_i, h_i , the number of subdomains, and the values of the coefficient $\alpha(\cdot)$. Under the stronger assumption

$$\alpha(x) \gtrsim \underline{\alpha}_i^{\eta_i} \quad \forall x \in \Omega_i \quad \forall i \in \mathcal{I},$$

we have the improved estimate with $\beta = 1$, i. e., linear dependence on H_k/η_k . These statements hold in both two and three dimensions.

Proof. Postponed to Section 5.4. □

Remark 5.13. There are two special cases of Theorem 5.12 concerning the coefficient α and the parameters η_i .

- (i) For the case that $\alpha(\cdot)$ is piecewise constant in the subdomains, Theorem 5.12 reproduces Theorem 2.28, in particular the known result by KLAWONN AND WIDLUND [109]. This is because $\underline{\alpha}_i^{H_i} = \bar{\alpha}_i^{H_i} \equiv \alpha|_{\Omega_i}$.
- (ii) If the η_i can be chosen with $\eta_i \simeq H_i$ and $\alpha(x) \leq C_\eta \alpha(y)$ for $x, y \in \Omega_{i,\eta_i}$ for each $i \in \mathcal{I}$, then we obtain the condition number bound $C_\eta (1 + \log(H/h))^2$, i. e., the method is completely robust to possible coefficient variation in $\Omega_i \setminus \Omega_{i,\eta_i}$.

Remark 5.14. In the subsequent proof we will never use the values of the coefficient $\alpha(\cdot)$ in the subdomain interiors, i. e., any positive values in $(0, \infty)$ are possible. It is therefore interesting to consider also the following two limit cases which correspond to applying our FETI methods to (homogeneous) problems on perforated domains (e. g., bubbly flow).

- (i) The case that the coefficient in the subdomain interiors goes to infinity corresponds to Dirichlet boundary conditions on $\partial\Omega_{i,\eta_i} \setminus \partial\Omega_i$, see e. g., AKSOYLU, GRAHAM, KLIE, AND SCHEICHL [3]. We obtain the condition number bound as in Theorem 5.12 with $\beta = 1$.
- (ii) The case that the coefficient vanishes completely in $\Omega_i \setminus \Omega_{i,\eta_i}$ corresponds to Neumann boundary conditions on $\partial\Omega_{i,\eta_i} \setminus \partial\Omega_i$. Thus in this case we obtain the condition number bound as in Theorem 5.12 with $\beta = 2$.

Remark 5.15. From the proof given in the subsequent section, it will become clear that Theorem 5.12 holds true as well if subdomains where α is constant are treated with BEM.

Corollary 5.16. *Let κ denote the condition number of the preconditioned FETI-DP method from Chapter 4 (Algorithm B or C) where the values $\bar{\alpha}_i^{\eta_i}$ are used in the scaling operators D_i , cf. (4.8). Then we have*

$$\kappa \leq C \max_{k \in \mathcal{I}} \left(\frac{H_k}{\eta_k} \right)^\beta \max_{i \in \mathcal{I}} \frac{\bar{\alpha}_i^{\eta_i}}{\underline{\alpha}_i^{\eta_i}} (1 + \log(H_i/h_i))^2,$$

where $\beta = 2$ in general, and $\beta = 1$ if $\alpha(x) \gtrsim \underline{\alpha}_i^{\eta_i}$ for all $x \in \Omega_i$ and $i = \mathcal{I}$.

Proof. Postponed to Section 5.4.4. □

5.4 Proof of the theoretical results

Due to the discussion in Chapter 2 it is sufficient to show the bound

$$|P_D(w + z_w)|_S^2 \leq \max_{k \in \mathcal{I}} \left(\frac{H_k}{\eta_k} \right)^\beta \max_{i \in \mathcal{I}} \frac{\bar{\alpha}_i^{\eta_i}}{\underline{\alpha}_i^{\eta_i}} (1 + \log(H_i/h_i))^2 |w|_S^2 \quad \forall w \in W^\perp, \quad (5.15)$$

in order to prove Theorem 5.12. In this chapter, we use the definition

$$W^\perp := \left\{ w \in W : \int_{\partial\Omega_i} w_i(x) dx = 0 \quad \forall i \in \mathcal{I}_{\text{float}} \right\}, \quad (5.16)$$

which differs slightly from the one in Chapter 2, but which can be justified by modifying the proof of Lemma 2.41 accordingly. The spaces W_i can be interpreted as spaces of discrete α -harmonic functions, since

$$|v|_{S_i}^2 = \min \left\{ \int_{\Omega_i} \alpha_i |\nabla \tilde{v}|^2 dx : \tilde{v} \in V^h(\Omega_i), \tilde{v}|_{\partial\Omega_i} = v \right\} \quad \forall v \in W_i. \quad (5.17)$$

Note that for a non-floating subdomain, W_i is a genuine subspace of $V^h(\partial\Omega_i)$. Using the above formula, however, we can extend the definition of $|\cdot|_{S_i}$ to the entire space $V^h(\partial\Omega_i)$. The function $\mathcal{H}_i^\alpha v$ for which the minimum is attained is called the *discrete α -harmonic extension* of v from $V^h(\partial\Omega_i)$ to $V^h(\Omega_i)$. For convenience, we also define the discrete trace seminorm

$$|v|_{H_h^{1/2}(\partial\Omega_i)}^2 := \min \left\{ \int_{\Omega_i} |\nabla \tilde{v}|^2 dx : \tilde{v} \in V^h(\Omega_i), \tilde{v}|_{\partial\Omega_i} = v \right\} \quad \text{for } v \in V^h(\partial\Omega_i), \quad (5.18)$$

which coincides with $|v|_{S_i}$ if $\alpha|_{\Omega_i} \equiv 1$. The function $\mathcal{H}_i v$ for which the minimum in (5.18) is attained is the *discrete harmonic extension* of v from $\partial\Omega_i$ to Ω_i , cf. Definition 2.32. Recall also the norm equivalence

$$|u|_{H^1(\Omega_i)}^2 + \frac{1}{H_i^2} \|u\|_{L^2(\Omega_i)}^2 \simeq |u|_{H^1(\Omega_i)}^2 + \frac{1}{H_i} \|u\|_{L^2(\partial\Omega_i)}^2, \quad (5.19)$$

due to Theorem 1.7.

For the proof of (5.15) we will use two main tools which are interesting on their own. As a first tool, in Section 5.4.1 we show an estimate of the form

$$|v|_{S_i}^2 \lesssim \bar{\alpha}_i^{\eta_i} \left\{ |v|_{H_h^{1/2}(\partial\Omega_i)}^2 + \frac{1}{\eta_i} \|v\|_{L^2(\partial\Omega_i)}^2 \right\} \quad \forall v \in V^h(\partial\Omega_i), \quad (5.20)$$

which is proved using a cut-off function as in Lemma 3.16 and in the proof of Theorem 3.15(ii). This result allows us (i) to remove the dependence on $\alpha(\cdot)$ in the interior of the subdomain completely, and (ii) to reuse the known FETI tools which are worked out with harmonic extensions in the H^1 -seminorms, or equivalently in the $H_h^{1/2}$ -seminorms. The price to pay is a factor of $1/\eta_i$ in front of the L^2 -term instead of $1/H_i$ in the piecewise constant case, cf. (5.19). This will lead to a factor H_i/η_i in the condition number estimate.

In the case where $\alpha(\cdot)$ is completely arbitrary in the interior (in particular not bounded from below by $\underline{\alpha}_i^{\eta_i}$), we need a second tool. We estimate the L^2 -term in (5.20) from above by the H^1 -seminorm of v , but restricted to the boundary layer Ω_{i,η_i} . That means, we need Poincaré and Friedrichs type inequalities on boundary layer domains (which are topologically non-trivial) with explicit information on the dependence of the Poincaré/Friedrichs constant on the aspect ratio H_i/η_i . It turns out that the dependence is linear in H_i/η_i which leads to the second factor in the condition number estimate. To get the exact dependence of the constants, we need direct proofs of Friedrichs and Poincaré type inequalities for simple domains, which can be found in the literature. However, we also need discrete estimates similar to the ones in Lemma 2.33 and Lemma 2.34. We generalize an idea which can be found, e. g., in ZHENG AND QI [194] to show all the needed inequalities in Section 5.4.2. The proof of (5.15) is finally given in Section 5.4.3. The proof of Corollary 5.16 concerning the FETI-DP method is briefly discussed in Section 5.4.4.

5.4.1 A cut-off result

Lemma 5.17. *For all $v \in V^h(\partial\Omega_i)$ we have*

$$\begin{aligned} (i) \quad & |v|_{S_i}^2 \lesssim \bar{\alpha}_i^{\eta_i} \left\{ |\tilde{v}|_{H^1(\Omega_{i,\eta_i})}^2 + \frac{1}{\eta_i} \|v\|_{L^2(\partial\Omega_i)}^2 \right\}, \\ (ii) \quad & |v|_{S_i}^2 \lesssim \bar{\alpha}_i^{\eta_i} \left\{ |v|_{H_h^{1/2}(\partial\Omega_i)}^2 + \frac{1}{\eta_i} \|v\|_{L^2(\partial\Omega_i)}^2 \right\}, \end{aligned}$$

where \tilde{v} is an arbitrary extension of v from $V^h(\partial\Omega_i)$ to $V^h(\Omega_i)$.

Proof. By slightly adjusting the proof of Lemma 3.16 we can find a discrete cut-off function $\chi \in V^h(\Omega_i)$ with

$$\chi(x) \in [0, 1], \quad \chi|_{\partial\Omega_i} = 1, \quad \chi|_{\Omega_i \setminus \Omega_{i,\eta_i}} = 0, \quad \text{and} \quad \|\nabla \chi\|_{L^\infty(\Omega_i)} \lesssim \eta_i^{-1}.$$

Let $v \in V^h(\partial\Omega_i)$ be fixed and let $\tilde{v} \in V^h(\Omega_i)$ denote an arbitrary extension of v from $\partial\Omega_i$ to Ω_i . Then, $I^h(\chi\tilde{v}) \in V^h(\Omega_i)$ is also an extension of v from $\partial\Omega_i$ to Ω_i , and because of the minimum property (5.17) we can bound the S_i -energy norm of v by the α -weighted H^1 -seminorm of $I^h(\chi\tilde{v})$. Using the continuity of the nodal interpolator I^h we obtain

$$\begin{aligned} |v|_{S_i}^2 &\leq \int_{\Omega_i} \alpha(x) \underbrace{|\nabla[I^h(\chi\tilde{v})(x)]|^2}_{0 \text{ in } \Omega_i \setminus \Omega_{i,\eta_i}} dx = \int_{\Omega_{i,\eta_i}} \alpha(x) |\nabla[I^h(\chi\tilde{v})(x)]|^2 dx \\ &\leq \int_{\Omega_{i,\eta_i}} \bar{\alpha}_i^{\eta_i} |\nabla[I^h(\chi\tilde{v})(x)]|^2 dx \lesssim \bar{\alpha}_i^{\eta_i} \int_{\Omega_{i,\eta_i}} |\nabla(\chi(x)\tilde{v}(x))|^2 dx \\ &\lesssim \bar{\alpha}_i^{\eta_i} \left\{ \underbrace{\|\nabla\chi\|_{L^\infty(\Omega_i)}^2}_{\lesssim \eta_i^{-2}} \|\tilde{v}\|_{L^2(\Omega_{i,\eta_i})}^2 + \underbrace{\|\chi\|_{L^\infty(\Omega_i)}^2}_{=1} \|\nabla\tilde{v}\|_{L^2(\Omega_{i,\eta_i})}^2 \right\}. \end{aligned} \quad (5.21)$$

As in the proof of TOSELLI AND WIDLUND [184, Lemma 3.10] we cover the boundary layer Ω_{i,η_i} by regular patches $\{\omega_j^{(i)}\}_{j \in \mathcal{J}^{(i)}}$ which satisfy the requirements stated in Assumption 5.10. We have, trivially,

$$\frac{1}{\eta_i^2} \|\tilde{v}\|_{L^2(\Omega_{i,\eta_i})}^2 \leq \sum_{j \in \mathcal{J}^{(i)}} \frac{1}{\eta_i^2} \|\tilde{v}\|_{L^2(\omega_j^{(i)})}^2. \quad (5.22)$$

Due to Assumption 5.10, for each j the intersection $\partial\omega_j^{(i)} \cap \partial\Omega_i$ is a union of shape-regular faces of the patch $\omega_j^{(i)}$ with its diameter proportional to η_i . Thus, we can apply a Friedrichs type inequality on each patch $\omega_j^{(i)}$ which yields

$$\sum_{j \in \mathcal{J}^{(i)}} \frac{1}{\eta_i^2} \|\tilde{v}\|_{L^2(\omega_j^{(i)})}^2 \lesssim \sum_{j \in \mathcal{J}^{(i)}} \left\{ |\tilde{v}|_{H^1(\omega_j^{(i)})}^2 + \frac{1}{\eta_i} \|\tilde{v}\|_{L^2(\partial\omega_j^{(i)} \cap \partial\Omega_i)}^2 \right\}. \quad (5.23)$$

Since the patches have finite overlap, combining (5.21)–(5.23), we easily obtain (i). Choosing \tilde{v} to be the discrete harmonic extension $\mathcal{H}_i v$, we also obtain estimate (ii). \square

5.4.2 Generalized Poincaré, Friedrichs, and discrete Sobolev inequalities

First we consider three inequalities on the regular domain Ω_i . Let $\tilde{\Gamma}$ be a relatively closed part of $\partial\Omega_i$ with diameter H_i and surface measure H_i^{d-1} , such as a union of faces of Ω_i (edges in two dimensions). The Poincaré type inequality

$$\frac{1}{H_i} \|u\|_{L^2(\partial\Omega_i)}^2 \lesssim |u|_{H^1(\Omega_i)}^2 + H_i^{d-2} \left(\frac{1}{|\tilde{\Gamma}|} \int_{\tilde{\Gamma}} u(x) ds_x \right)^2 \quad \forall u \in H^1(\Omega_i), \quad (5.24)$$

can be derived from Theorem 1.7. An immediate consequence thereof is the Friedrichs type inequality

$$\frac{1}{H_i} \|u\|_{L^2(\partial\Omega_i)}^2 \lesssim |u|_{H^1(\Omega_i)}^2 \quad \forall u \in H^1(\Omega_i), \quad u|_{\tilde{\Gamma}=0}. \quad (5.25)$$

For $u \in V^h(\Omega_i)$, let $\zeta(u)$ denote the average of u over an edge (in three dimensions), or a vertex evaluation on $\partial\Omega_i$ (in two dimensions). The discrete Sobolev type inequality

$$\frac{1}{H_i} \|u - \zeta(u)\|_{L^2(\partial\Omega_i)}^2 \lesssim (1 + \log(H_i/h_i)) |u|_{H^1(\Omega_i)}^2 \quad \forall u \in V^h(\Omega_i), \quad (5.26)$$

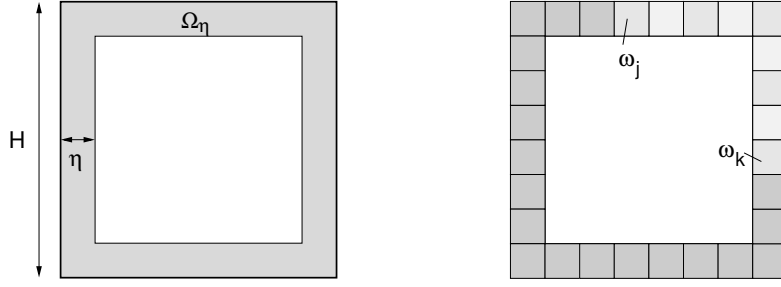


Figure 5.2: *Left:* Boundary layer Ω_η of diameter $\mathcal{O}(H)$ and width η . *Right:* Sketch of partitioning of Ω_η into patches, cf. (5.27) and the path P_{jk} connecting the patches ω_j and ω_k , cf. Definition 5.18.

can be derived from Theorem 1.7, Lemma 2.33, and Lemma 2.34. The left hand side may also be replaced by $\|u - \zeta(u)\|_{L^2(\mathcal{E}_i)}^2$ for an edge \mathcal{E}_i in three dimensions, or by $\|u - \zeta(u)\|_{L^\infty(\partial\Omega_i)}^2$ in two dimensions.

In this section, we provide generalizations of the above inequalities where we replace Ω_i by the boundary layer Ω_{i,η_i} , and we make explicit the dependence of the respective constants on the aspect ratio H_i/η_i . For the sake of simplicity we will occasionally drop the subdomain indices i (in this subsection only) and thus work on a generic domain Ω with boundary $\partial\Omega$ and diameter H , and with the boundary layer Ω_η with parameter η .

5.4.2.1 Auxiliary results

The proofs of all our inequalities are based on the concept of a *path* through the patches due to the partition from Assumption 5.10. Recall that we can cover the boundary layer Ω_η by finitely many patches

$$\Xi_\eta := \{\omega_1, \dots, \omega_s\}. \quad (5.27)$$

The patches ω_j are regular in the sense of Definition 5.8, cf. Figure 5.2. They have uniform diameter η and the intersection $\gamma_j := \partial\omega_j \cap \partial\Omega$ is a union of faces of ω_j with a diameter proportional to η . Due to the finite overlap assumption it is clear that there are at most $s = \mathcal{O}((H/\eta)^{d-1})$ such patches.

Definition 5.18. *Let $\omega_j, \omega_k \in \Xi_\eta$. We call $P_{jk} \subset \Omega_\eta$ a path of length M connecting the patches ω_j and ω_k , if it is a connected union of M patches from Ξ_η such that $\omega_j, \omega_k \subset P_{jk}$.*

The following lemma is essential for the proofs of all the generalized inequalities that will follow.

Lemma 5.19. *Suppose $\Omega \subset \mathbb{R}^d$, $d = 2, 3$. Let $\omega_j, \omega_k \in \Xi_\eta$ and let P_{jk} be a path of length M connecting ω_j, ω_k .*

(i) *Then*

$$\frac{1}{\eta^d} \int_{\gamma_j} \int_{\gamma_k} |u(x) - u(y)|^2 ds_x ds_y \lesssim M |u|_{H^1(P_{jk})}^2 \quad \forall u \in H^1(\Omega_\eta).$$

(ii) Let $d = 2$ and let $x_j \in \gamma_j$ and $x_k \in \gamma_k$ be two points on $\partial\Omega$. Then

$$|u(x_j) - u(x_k)|^2 \lesssim M(1 + \log(\eta/h)) |u|_{H^1(P_{jk})}^2 \quad \forall u \in V^h(\Omega_\eta).$$

(iii) Let $d = 3$ and let $e_j \subset \bar{\gamma}_j$ and $e_k \subset \bar{\gamma}_j$ be two edges on $\partial\Omega$. Then

$$\begin{aligned} \frac{1}{\eta} \int_{e_j} \int_{e_k} |u(x) - u(y)|^2 ds_y ds_x &\lesssim M(1 + \log(\eta/h)) |u|_{H^1(P_{jk})}^2 \quad \forall u \in V^h(\Omega_\eta), \\ \frac{1}{\eta^2} \int_{\gamma_j} \int_{e_k} |u(x) - u(y)|^2 ds_y ds_x &\lesssim M(1 + \log(\eta/h)) |u|_{H^1(P_{jk})}^2 \quad \forall u \in V^h(\Omega_\eta). \end{aligned}$$

Proof. Let j, k and the path P_{jk} be fixed. Without loss of generality, we assume that the patches in Ξ_η and in the path P_{jk} are ordered in such a way that $\{\omega_\ell\}_{j \leq \ell \leq k}$ are exactly the patches in P_{jk} and that $\bar{\omega}_\ell, \bar{\omega}_{\ell+1}$ share at least a manifold of dimension $d-1$ for $j \leq \ell < k$. We define the average values

$$\bar{u}^\ell := \frac{1}{|\gamma_\ell|} \int_{\gamma_\ell} u(x) ds_x \quad \text{for } j \leq \ell \leq k.$$

Proof of Part (i): Let $x \in \gamma_j$ and $y \in \gamma_k$. Using the Cauchy-Schwarz inequality in \mathbb{R}^M and the fact that P_{jk} is a path of length M we obtain

$$\begin{aligned} |u(x) - u(y)|^2 &= \left| [u(x) - \bar{u}^j] + \left[\sum_{\ell=j}^{k-1} \bar{u}^\ell - \bar{u}^{\ell+1} \right] + [\bar{u}^k - u(y)] \right|^2 \\ &\lesssim M \left\{ |u(x) - \bar{u}^j|^2 + \left[\sum_{\ell=j}^{k-1} |\bar{u}^\ell - \bar{u}^{\ell+1}|^2 \right] + |\bar{u}^k - u(y)|^2 \right\}. \end{aligned} \quad (5.28)$$

Since $|\gamma_j| \simeq |\gamma_k| \simeq \eta^{d-1}$ we can conclude that

$$\begin{aligned} \frac{1}{\eta^d} \int_{\gamma_j} \int_{\gamma_k} |u(x) - u(y)|^2 ds_x ds_y \\ \lesssim M \left\{ \frac{1}{\eta} \int_{\gamma_j} |u(x) - \bar{u}^j|^2 ds_x + \eta^{d-2} \left[\sum_{\ell=j}^{k-1} |\bar{u}^\ell - \bar{u}^{\ell+1}|^2 \right] + \frac{1}{\eta} \int_{\gamma_k} |\bar{u}^k - u(y)|^2 \right\}. \end{aligned} \quad (5.29)$$

Using a Poincaré type inequality on ω_ℓ , cf. (5.24), we obtain

$$\frac{1}{\eta} \int_{\gamma_\ell} |u(x) - \bar{u}^\ell|^2 ds_x \lesssim |u|_{H^1(\omega_\ell)}^2, \quad \ell = j, k.$$

For the terms $\eta^{d-2} |\bar{u}^\ell - \bar{u}^{\ell+1}|^2$, $\ell = j, \dots, k-1$, we apply an argument similar to Lemma 1.13 (Bramble-Hilbert). Using that $\omega_{\ell, \ell+1}$ is regular due to Assumption 5.10, we obtain by the Cauchy-Schwarz inequality that

$$\begin{aligned} |\bar{u}^\ell - \bar{u}^{\ell+1}|^2 &\lesssim \left(\frac{1}{|\gamma_\ell|} \int_{\gamma_\ell} u(x) - \bar{u}^{\ell+1} ds_x \right)^2 \lesssim \eta^{1-d} \int_{\gamma_\ell} |u(x) - \bar{u}^{\ell+1}|^2 ds_x \\ &\lesssim \eta^{1-d} \int_{\partial\omega_{\ell, \ell+1}} |u(x) - \bar{u}^{\ell+1}|^2 ds_x. \end{aligned}$$

On the regular domain $\omega_{\ell, \ell+1}$ we can apply another Poincaré type inequality using the fact that γ_ℓ is a union of edges (resp. faces) of $\omega_{\ell, \ell+1}$ in two (resp. three) dimensions. This yields

$$\eta^{d-2} |\bar{u}^\ell - \bar{u}^{\ell+1}|^2 \lesssim \frac{1}{\eta} \|u - \bar{u}^{\ell+1}\|_{L^2(\partial\omega_{\ell, \ell+1})}^2 \lesssim |u|_{H^1(\omega_{\ell, \ell+1})}^2. \quad (5.30)$$

Since all the compound patches $\omega_{\ell, \ell+1}$ have only finite overlap and their union forms the path P_{jk} , we easily obtain the desired result (i) by combining (5.29) and (5.30).

Proof of Part (ii): Suppose $\Omega \subset \mathbb{R}^2$. Let $\tilde{\mathcal{T}}^h(\omega_j)$ be an auxiliary quasi-uniform mesh on ω_j of mesh width h that coincides on γ_j with the original mesh $\mathcal{T}^h(\Omega)$. Note that $\tilde{\mathcal{T}}^h(\omega_j)$ does not have to coincide with $\mathcal{T}^h(\Omega)$ on the rest of ω_j , i. e., the patches ω_j are allowed to cut through triangles/tetrahedra in the original mesh $\mathcal{T}^h(\Omega)$. Let $\Pi_h^{(j)}$ denote the Scott-Zhang quasi-interpolation operator on ω_j with respect to $\tilde{\mathcal{T}}^h(\omega_j)$ such that

$$\begin{aligned} (\Pi_h^{(j)} u)|_{\gamma_j} &= u|_{\gamma_j} & \forall u \in V^h(\omega_j), \\ |\Pi_h^{(j)} u|_{H^1(\omega_j)} &\lesssim |u|_{H^1(\omega_j)} & \forall u \in H^1(\omega_j), \end{aligned}$$

cf. Lemma 1.28.

Assume that the patches in the path P_{jk} are enumerated successively as before. In (5.28), let $x = x_j \in \gamma_j$ and $y = x_k \in \gamma_k$. But now we estimate the first and last term in (5.28) using the discrete Sobolev inequality from Lemma 2.33(ii) and the properties of the Scott-Zhang operator outlined above. Then

$$\begin{aligned} |u(x_j) - \bar{u}^j|^2 + |\bar{u}^k - u(x_k)|^2 &\lesssim (1 + \log(\eta/h)) \left[|\Pi_h^{(j)} u|_{H^1(\omega_j)}^2 + |\Pi_h^{(k)} u|_{H^1(\omega_k)}^2 \right] \\ &\lesssim (1 + \log(\eta/h)) \left[|u|_{H^1(\omega_j)}^2 + |u|_{H^1(\omega_k)}^2 \right]. \end{aligned}$$

The terms $|\bar{u}^\ell - \bar{u}^{\ell+1}|^2 = \eta^{d-2} |\bar{u}^\ell - \bar{u}^{\ell+1}|^2$ can be treated as before. Again because of the finite overlap assumption this immediately proves (ii).

Proof of Part (iii): Suppose $\Omega \subset \mathbb{R}^3$. Let $e_j \subset \bar{\gamma}_j$ and $e_k \subset \bar{\gamma}_k$ be two edges on $\partial\Omega$ (with $|e_j| \simeq |e_k| \simeq \eta$). It follows again from (5.28) that

$$\begin{aligned} &\frac{1}{\eta} \int_{e_j} \int_{e_k} |u(x) - u(y)|^2 ds_y ds_x \\ &\lesssim M \left\{ \int_{e_j} |u(x) - \bar{u}^j|^2 ds_x + \eta \left[\sum_{\ell=j}^{k-1} |\bar{u}^\ell - \bar{u}^{\ell+1}|^2 \right] + \int_{e_k} |u(x) - \bar{u}^k|^2 ds_y \right\}. \end{aligned}$$

For the first and the last term we can use the discrete Sobolev inequality from Lemma 2.34(ii). The remaining terms are treated as in (i). This finishes the proof of the first estimate in (iii). The second estimate is shown analogously, but using the usual Poincaré inequality to bound the term $\int_{\gamma_j} |u(x) - \bar{u}^j|^2 ds_x$. \square

Lemma 5.20. *Let $\omega_j, \omega_k \in \Xi_\eta$. Then there exists a path P_{jk} connecting ω_j and ω_k of length $M = \mathcal{O}(H/\eta)$.*

Proof. This follows directly from Assumption 5.10, in particular from the regularity of the patches and from the finite overlap assumption. \square

With Lemma 5.19 being proved we can state and prove the generalized inequalities.

5.4.2.2 Generalized Poincaré and Friedrichs type inequalities

Lemma 5.21 (Generalized Poincaré type inequality). *Let the boundary layer Ω_{i,η_i} satisfy Assumption 5.10 and let $\tilde{\Gamma}$ be either (a) an edge of Ω_i (in two dimensions), (b) a face of Ω_i (in three dimensions), or (c) the entire boundary $\partial\Omega_i$ of Ω_i . Then*

$$\frac{1}{H_i} \|u\|_{L^2(\partial\Omega_i)}^2 \lesssim \frac{H_i}{\eta_i} |u|_{H^1(\Omega_{i,\eta_i})}^2 + H_i^{d-2} \left(\frac{1}{|\tilde{\Gamma}|} \int_{\tilde{\Gamma}} u(x) ds_x \right)^2 \quad \forall u \in H^1(\Omega_{i,\eta_i}). \quad (5.31)$$

Before we give the proof, we state the following inequality which immediately follows from Lemma 5.21.

Corollary 5.22 (generalized Friedrichs type inequality). *Let the boundary layer Ω_{i,η_i} satisfy Assumption 5.10 and let $\tilde{\Gamma} \subset \partial\Omega_i$ be an edge of Ω_i (in two dimensions) or a face of Ω_i (in three dimensions). Then*

$$\frac{1}{H_i} \|u\|_{L^2(\partial\Omega_i)}^2 \lesssim \frac{H_i}{\eta_i} |u|_{H^1(\Omega_{i,\eta_i})}^2 \quad \forall u \in H^1(\Omega_{i,\eta_i}), \quad u|_{\tilde{\Gamma}} = 0. \quad (5.32)$$

Proof of Lemma 5.21: Assume first that $\tilde{\Gamma} = \partial\Omega$. We start as in many direct proofs of Poincaré's inequality from the literature. For $x, y \in \partial\Omega$, we have

$$u(x)^2 + u(y)^2 - 2u(x)u(y) = [u(x) - u(y)]^2. \quad (5.33)$$

Integrating twice over $\partial\Omega$ and using the patch covering/decomposition from (5.27) yields

$$\begin{aligned} 2|\partial\Omega| \int_{\partial\Omega} u(x)^2 ds_x - 2 \left(\int_{\partial\Omega} u(x) ds_x \right)^2 &= \int_{\partial\Omega} \int_{\partial\Omega} [u(x) - u(y)]^2 ds_x ds_y \\ &\leq \sum_{j,k=1}^s \int_{\gamma_j} \int_{\gamma_k} [u(x) - u(y)]^2 ds_x ds_y. \end{aligned} \quad (5.34)$$

Using Lemma 5.19(i) we can bound each one of the double integrals on the right hand side of (5.34) from above by $\eta^d M |u|_{H^1(P_{jk})}^2$, where P_{jk} is a path of length M connecting ω_j and ω_k . Due to Lemma 5.20 we know that $M \lesssim H/\eta$, and so

$$\sum_{j,k=1}^s \int_{\gamma_j} \int_{\gamma_k} [u(x) - u(y)]^2 ds_x ds_y \lesssim \eta^d \frac{H}{\eta} \sum_{j,k=1}^s |u|_{H^1(P_{jk})}^2. \quad (5.35)$$

Combining (5.34) and (5.35), and using the trivial bound $|u|_{H^1(P_{jk})}^2 \lesssim |u|_{H^1(\Omega_\eta)}^2$ as well as the fact that $s = \mathcal{O}((H/\eta)^{d-1})$ we get

$$\frac{1}{H} \|u\|_{L^2(\partial\Omega)}^2 \lesssim \left(\frac{H}{\eta} \right)^{d-1} |u|_{H^1(\Omega_\eta)}^2 + \frac{1}{H |\partial\Omega|} \left(\int_{\partial\Omega} u ds \right)^2,$$

which is the desired inequality (5.31) for $d = 2$, case (c).

In three dimensions this leads to the suboptimal quadratic factor $(H/\eta)^2$ in front of the H^1 -seminorm. In order to get the linear factor H/η in three dimensions we make use of an overlap argument. In the following we restrict ourselves to the case that Ω is a tetrahedron.

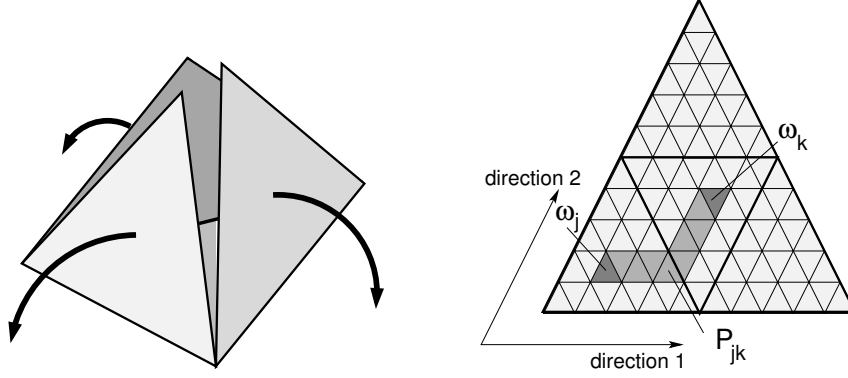


Figure 5.3: *Left:* Unfolding the boundary of a tetrahedron. *Right:* Sketch illustrating the three-dimensional path algorithm from the proof of Lemma 5.21.

It is straightforward to generalize the arguments to more general regular domains. We cover the boundary $\partial\Omega$ by faces of the patches ω_j and unfold and flatten the boundary, essentially as depicted in Figure 5.3. We introduce two main directions (cf. Figure 5.3) and local coordinates $j = (j_1, j_2)$ for each of the patches ω_j . We create a special path P_{jk} by starting from ω_j : first running through patches in the first direction from j_1 to k_1 keeping the second coordinate j_2 fixed, then through patches in the second direction from j_2 to k_2 keeping the first coordinate k_1 fixed, see Figure 5.3. We denote the two parts of P_{jk} by $P_{jk}^{(1)}$ and $P_{jk}^{(2)}$, respectively. To improve our bound on the right hand side of (5.35) we now fix j_1 and $k = (k_1, k_2)$. Then, because of the finite overlap of the patches ω_ℓ , we have

$$\sum_{j_2} |u|_{H^1(P_{jk}^{(1)})}^2 \lesssim |u|_{H^1(\Omega_\eta)}^2.$$

Since the remaining indices j_1 and $k = (k_1, k_2)$ can take $\mathcal{O}((H/\eta)^3)$ possible different values, we conclude that

$$\sum_{j,k=1}^s |u|_{H^1(P_{jk}^{(1)})}^2 \lesssim \left(\frac{H}{\eta}\right)^3 |u|_{H^1(\Omega_\eta)}^2.$$

Similarly, we obtain

$$\sum_{j,k=1}^s |u|_{H^1(P_{jk}^{(2)})}^2 \lesssim \left(\frac{H}{\eta}\right)^3 |u|_{H^1(\Omega_\eta)}^2.$$

Now combining this with (5.34) and (5.35) and using the fact that $P_{jk} = P_{jk}^{(1)} \cup P_{jk}^{(2)}$, we get (5.31) for $d = 3$, case (c).

Cases (a) and (b) are treated as follows. For $\int_{\tilde{\Gamma}} u \, ds = 0$ we obtain

$$\underbrace{|\partial\Omega| \int_{\tilde{\Gamma}} u^2 \, ds}_{\geq 0} + |\tilde{\Gamma}| \int_{\partial\Omega} u^2 \, ds = \int_{\partial\Omega} \int_{\tilde{\Gamma}} [u(x) - u(y)]^2 \, ds_x \, ds_y$$

from (5.33) by integration. With the arguments from before this implies

$$\frac{1}{H_i} \|u\|_{L^2(\partial\Omega)}^2 \lesssim \frac{H}{\eta} |u|_{H^1(\Omega_\eta)}^2.$$

For a general function u , the desired inequality follows immediately by a quotient argument using the mean value $|\tilde{\Gamma}|^{-1} \int_{\tilde{\Gamma}} u \, ds$. \square

5.4.2.3 Generalized discrete Sobolev type inequalities

Lemma 5.23 (generalized discrete Sobolev type inequalities). *Let the boundary layer Ω_{i,η_i} fulfill Assumption 5.10 and suppose $u \in V^h(\Omega_{i,\eta_i})$.*

(i) *Let $\Omega_i \subset \mathbb{R}^2$ and let $\zeta(u)$ be (a) a nodal evaluation of u in $\partial\Omega_i$, (b) the average value of u over an edge \mathcal{E}_i of Ω_i , or (c) the average of u over the entire boundary $\partial\Omega_i$. Then*

$$\|u - \zeta(u)\|_{L^\infty(\partial\Omega_i)}^2 \lesssim \frac{H_i}{\eta_i} \left(1 + \log \frac{\eta_i}{h_i}\right) |u|_{H^1(\Omega_{i,\eta_i})}^2, \quad (5.36)$$

$$\frac{1}{H_i} \|u - \zeta(u)\|_{L^2(\partial\Omega_i)}^2 \lesssim \frac{H_i}{\eta_i} \left(1 + \log \frac{\eta_i}{h_i}\right) |u|_{H^1(\Omega_{i,\eta_i})}^2. \quad (5.37)$$

(ii) *Let $\Omega_i \subset \mathbb{R}^3$ and let $\zeta(u)$ be the average value of u over (a) an edge \mathcal{E}_{ij} of Ω_i , (b) a face \mathcal{F}_{ij} of Ω_i , or (c) all of $\partial\Omega_i$. Then, for all edges \mathcal{E}_{ik} of Ω_i ,*

$$\|u - \zeta(u)\|_{L^2(\mathcal{E}_{ik})}^2 \lesssim \frac{H_i}{\eta_i} \left(1 + \log \frac{\eta_i}{h_i}\right) |u|_{H^1(\Omega_{i,\eta_i})}^2, \quad (5.38)$$

$$\frac{1}{H_i} \|u - \zeta(u)\|_{L^2(\partial\Omega_i)}^2 \lesssim \frac{H_i}{\eta_i} \left(1 + \log \frac{\eta_i}{h_i}\right) |u|_{H^1(\Omega_{i,\eta_i})}^2. \quad (5.39)$$

Proof. Part (i). Let $d = 2$ and let $\zeta(u)$ be a point evaluation at a point $x_i \in \partial\Omega$. Then $x_i \in \partial\omega_i$ for some patch ω_i . Since $u \in V^h(\Omega_{i,\eta_i}) \subset \mathcal{C}(\bar{\Omega}_{i,\eta_i})$ we can also find another distinguished patch $\omega_j \in \Xi_\eta$ and a point $x_j \in \bar{\omega}_j$ where the L^∞ -norm of $u - \zeta(u)$ is attained. Thus it follows from Lemma 5.19(ii) that

$$\|u - \zeta(u)\|_{L^\infty(\partial\Omega)}^2 = |u(x_j) - u(x_i)|^2 \lesssim \frac{H}{\eta} (1 + \log(\eta/h)) |u|_{H^1(P_{ij})}^2.$$

Since the path P_{ij} is a subset of Ω_η this completes the proof of (5.36) for case (a), i. e., point evaluations. However, thanks to the continuity of u we can also find a distinguished point $x_i \in \partial\Omega$ such that $\zeta(u) = u(x_i)$ in the remaining two cases (b) and (c), and so the corresponding estimates follows immediately. Due to $|\partial\Omega_i| \simeq H_i$, (5.37) is also immediate from (5.36).

Part (ii). In three dimensions, we restrict ourselves to the proof of (5.38) in the case of face averages, i. e., we prove

$$\|u - \zeta(u)\|_{L^2(\mathcal{E})}^2 \lesssim \frac{H}{\eta} (1 + \log(\eta/h)) |u|_{H^1(\Omega_\eta)}^2,$$

for the case that $\zeta(u) = \frac{1}{|\mathcal{F}|} \int_{\mathcal{F}} u(x) \, ds_x$, where \mathcal{F} is a face of Ω and \mathcal{E} is an edge of Ω . The proofs of the remaining cases are similar.

Firstly, we can cover the edge \mathcal{E} by $N_\mathcal{E}$ edges $e_1, \dots, e_{N_\mathcal{E}}$ of the patches $\{\omega_j\}$, where $N_\mathcal{E} \lesssim H/\eta$. Similarly, the face \mathcal{F} can be covered by $N_\mathcal{F}$ sets $\gamma_1, \dots, \gamma_{N_\mathcal{F}}$ where $\gamma_j := \partial\omega_j \cap \partial\Omega$

as before and $N_{\mathcal{F}} \lesssim (H/\eta)^2$. Hence, using Lemma 5.19(iii) we obtain

$$\begin{aligned} \|u - \zeta(u)\|_{L^2(\mathcal{E})}^2 &= \int_{\mathcal{E}} \left| u(x) - \frac{1}{|\mathcal{F}|} \int_{\mathcal{F}} u(y) ds_y \right|^2 ds_x = \int_{\mathcal{E}} \left| \frac{1}{|\mathcal{F}|} \int_{\mathcal{F}} u(x) - u(y) ds_y \right|^2 ds_x \\ &\leq \frac{1}{|\mathcal{F}|} \int_{\mathcal{E}} \int_{\mathcal{F}} |u(x) - u(y)|^2 ds_y ds_x \leq \frac{1}{|\mathcal{F}|} \sum_{k=1}^{N_{\mathcal{E}}} \sum_{j=1}^{N_{\mathcal{F}}} \int_{e_k} \int_{\gamma_j} |u(x) - u(y)|^2 ds_y ds_x \\ &\lesssim \frac{1}{|\mathcal{F}|} \sum_{k=1}^{N_{\mathcal{E}}} \sum_{j=1}^{N_{\mathcal{F}}} M_{jk} (1 + \log(\eta/h)) |u|_{H^1(P_{jk})}^2, \end{aligned}$$

where the path P_{jk} of length $M_{jk} \lesssim H/\eta$ is chosen as in the proof of Lemma 5.21. Now using the same arguments as in that proof we obtain the desired estimate. \square

Remark 5.24. For η_i chosen such that $\Omega_{i,\eta_i} = \Omega_i$, i.e., $H_i/\eta_i \simeq 1$, Lemma 5.21, Corollary 5.22, and Lemma 5.23 reproduce the known Poincaré, Friedrichs, and discrete Sobolev type inequalities, cf. (5.24)–(5.26), and the inequalities in Lemma 2.33 and Lemma 2.34, see also TOSELLI AND WIDLUND [184, Sect. A.4, Lemma 4.15, Lemma 4.16, and Lemma 4.21].

5.4.3 Proof of the P_D -estimate (5.15)

We only give a detailed proof for the three-dimensional case. We have to show that

$$|P_D(w + z_w)|_S^2 \lesssim \left\{ \max_{j \in \mathcal{I}} \left(\frac{H_j}{\eta_j} \right)^\beta \max_{i \in \mathcal{I}} \frac{\bar{\alpha}_i^{\eta_i}}{\underline{\alpha}_i^{\eta_i}} (1 + \log(H_i/h_i))^2 \right\} |w|_S^2 \quad \forall w \in W^\perp, \quad (5.40)$$

with $\beta = 2$ in general and $\beta = 1$ if $\alpha(x) \gtrsim \underline{\alpha}_i^{\eta_i}$ for all $x \in \Omega_i$ and for all $i \in \mathcal{I}$. As in Chapter 2, we split the left hand side into two parts

$$|P_D(w + z_w)|_S^2 \lesssim |P_D w|_S^2 + |P_D z_w|_S^2,$$

and treat them separately.

5.4.3.1 Estimating $|P_D w|_S$

We prove that for all $w \in W^\perp$,

$$|P_D w|_S^2 = \sum_{i \in \mathcal{I}} |(P_D w)_i|_{S_i}^2 \lesssim \max_{j \in \mathcal{I}} \left\{ \left(\frac{H_j}{\eta_j} \right)^\beta \frac{\bar{\alpha}_j^{\eta_j}}{\underline{\alpha}_j^{\eta_j}} (1 + \log(H_j/h_j))^2 \right\} \sum_{i \in \mathcal{I}} |w_i|_{S_i}^2. \quad (5.41)$$

By Lemma 5.17(ii), the characterization of $P_D w$ in Lemma 2.16, and the partition of unity on $\partial\Omega_i$ provided by the cut-off functions $\theta_{\mathcal{X}_i}$ from Definition 2.30, we obtain

$$\begin{aligned} |(P_D w)_i|_{S_i}^2 &\lesssim \bar{\alpha}_i^{\eta_i} \left\{ |(P_D w)_i|_{H_h^{1/2}(\partial\Omega_i)}^2 + \frac{1}{\eta_i} \|(P_D w)_i\|_{L^2(\partial\Omega_i)}^2 \right\} \\ &\lesssim \sum_{\mathcal{X}_i \subset \Gamma} \sum_{j \in \mathcal{N}_{\mathcal{X}_i}} \bar{\alpha}_i^{\eta_i} \left\{ |I^h(\theta_{\mathcal{X}_i} \widehat{\delta}_j^\dagger(w_i - w_j))|_{H_h^{1/2}(\partial\Omega_i)}^2 + \frac{1}{\eta_i} \|I^h(\theta_{\mathcal{X}_i} \widehat{\delta}_j^\dagger(w_i - w_j))\|_{L^2(\partial\Omega_i)}^2 \right\} + \\ &\quad + \sum_{\mathcal{X}_i \subset \Gamma_D} \bar{\alpha}_i^{\eta_i} \left\{ |I^h(\theta_{\mathcal{X}_i} w_i)|_{H_h^{1/2}(\partial\Omega_i)}^2 + \frac{1}{\eta_i} \|I^h(\theta_{\mathcal{X}_i} w_i)\|_{L^2(\partial\Omega_i)}^2 \right\}, \end{aligned} \quad (5.42)$$

where the last line can be dropped in the standard one-level formulation. The next steps are almost analogous to the proof of Lemma 2.42. Using the fact that $\widehat{\delta}_j^\dagger(\cdot)$ is constant on edges and faces, as well as the elementary inequality

$$\overline{\alpha}_i^{\eta_i} [\widehat{\delta}_j^\dagger(x)]^2 \leq \min(\overline{\alpha}_i^{\eta_i}, \overline{\alpha}_j^{\eta_j}), \quad (5.43)$$

cf. inequality (2.100), we can show that

$$\begin{aligned} |(P_D w)_i|_{S_i}^2 &\lesssim \sum_{\mathcal{X}_i \subset \Gamma} \sum_{j \in \mathcal{N}_{\mathcal{X}_i}} \overline{\alpha}_j^{\eta_j} \left\{ |I^h(\theta_{\mathcal{X}_i} w_j)|_{H_h^{1/2}(\partial\Omega_i)}^2 + \frac{1}{\eta_i} \|I^h(\theta_{\mathcal{X}_i} w_j)\|_{L^2(\partial\Omega_i)}^2 \right\} \\ &+ \sum_{\mathcal{X}_i \subset \Gamma_D} \left\{ |I^h(\theta_{\mathcal{X}_i} w_i)|_{H_h^{1/2}(\partial\Omega_i)}^2 + \frac{1}{\eta_i} \|I^h(\theta_{\mathcal{X}_i} w_i)\|_{L^2(\partial\Omega_i)}^2 \right\}. \end{aligned} \quad (5.44)$$

Using Lemma 2.34(iii) and the fact that $\|I^h(\theta_{\mathcal{X}_i} w_j)\|_{L^2(\partial\Omega_j)} \lesssim \|w_j\|_{L^2(\partial\Omega_j)}$, the contribution from w_j on a face \mathcal{F}_i can (up to a constant) be estimated by

$$\begin{aligned} &\overline{\alpha}_j^{\eta_j} (1 + \log(H_j/h_j))^2 \left\{ |w_j|_{H_h^{1/2}(\partial\Omega_j)}^2 + \frac{1}{H_j} \|w_j - \overline{w}_j\|_{L^2(\partial\Omega_j)}^2 \right\} + \\ &+ \overline{\alpha}_j^{\eta_j} \left\{ (1 + \log(H_j/h_j)) \frac{1}{H_j} \|w_j\|_{L^2(\partial\Omega_j)}^2 + \frac{1}{\eta_j} \|w_j\|_{L^2(\partial\Omega_j)}^2 \right\}, \end{aligned} \quad (5.45)$$

with $\overline{w}_j = |\Omega_j|^{-1} \int_{\Omega_j} w_j dx$. Here, we have used the same trick as in the proof of Lemma 2.42 (see the paragraph entitled *standard one-level method*) in order not to get a quadratic factor $(1 + \log(H_j/h_j))^2$ in front of the term $\|w_j\|_{L^2(\partial\Omega_j)}^2$.

By Lemma 2.34(i), the contribution of w_j on an edge \mathcal{E}_i is bounded by

$$\overline{\alpha}_h^{\eta_j} \left\{ \|w_j\|_{L^2(\mathcal{E}_i)}^2 + \frac{1}{\eta_j} \|w_j\|_{L^2(\partial\Omega_j)}^2 \right\}. \quad (5.46)$$

This bound also holds for the contribution of w_j on a vertex \mathcal{V}_j which is the endpoint of \mathcal{E}_j , cf. estimate (2.96). In order to complete the proof of (5.41) we need to bound

$$|w_j|_{H_h^{1/2}(\partial\Omega_j)}^2, \quad \|w_j - \overline{w}_j\|_{L^2(\partial\Omega_j)}^2, \quad \|w_j\|_{L^2(\partial\Omega_j)}^2, \quad \text{and} \quad \|w_j\|_{L^2(\mathcal{E}_j)}^2 \quad (5.47)$$

in terms of $|w_j|_{S_j}^2$. To this end, recall that the discrete α -harmonic extension $\mathcal{H}_j^\alpha(w_j - \overline{w}_j)$ of $w_j - \overline{w}_j$ from $\partial\Omega_j$ to Ω_j satisfies

$$\int_{\Omega_j} \alpha(x) |\nabla \mathcal{H}_j^\alpha(w_j - \overline{w}_j)(x)|^2 dx = |w_j - \overline{w}_j|_{S_j}^2 = |w_j|_{S_j}^2. \quad (5.48)$$

Firstly, applying Lemma 5.17(i) with coefficient $\alpha' \equiv 1$ (to bound $|w_j - \overline{w}_j|_{H_h^{1/2}(\partial\Omega_j)}^2$) we can conclude that

$$|w_j|_{H_h^{1/2}(\partial\Omega_j)}^2 = |w_j - \overline{w}_j|_{H_h^{1/2}(\partial\Omega_j)}^2 \lesssim |\mathcal{H}_j^\alpha(w_j - \overline{w}_j)|_{H^1(\Omega_j, \eta_j)}^2 + \frac{1}{\eta_j} \|w_j - \overline{w}_j\|_{L^2(\partial\Omega_j)}^2. \quad (5.49)$$

Secondly, applying Lemma 5.21 (the generalized Poincaré inequality) to $u = \mathcal{H}_j^\alpha(w_j - \bar{w}_j)$ yields

$$\|w_j - \bar{w}_j\|_{L^2(\partial\Omega_j)}^2 \lesssim \frac{H_j^2}{\eta_j} |\mathcal{H}_j^\alpha(w_j - \bar{w}_j)|_{H^1(\Omega_j, \eta_j)}^2, \quad (5.50)$$

which is at the same time a bound for the second term in (5.47). For any of the formulations (standard one-level or all-floating), the function w_j vanishes either at least on an edge, or its mean value over $\partial\Omega_j$ is zero, see the definition (5.16) of W^\perp . Using the discrete Sobolev type inequalities from (5.23) we obtain the following bound for the two remaining terms in (5.47)

$$\frac{1}{H_j} \|w_j\|_{L^2(\partial\Omega_i)}^2 + \|w_j\|_{L^2(\mathcal{E}_j)}^2 \lesssim \frac{H_j}{\eta_j} (1 + \log(\eta_j/h_j)) |\mathcal{H}_j^\alpha w_j|_{H^1(\Omega_j, \eta_j)}^2. \quad (5.51)$$

Combining (5.44)–(5.46), (5.48)–(5.51), and using that

$$H_j \geq \eta_j, \quad \text{and} \quad |\mathcal{H}_j^\alpha(w_j - \bar{w}_j)|_{H^1(\Omega_j, \eta_j)} = |\mathcal{H}_j^\alpha w_j|_{H^1(\Omega_j, \eta_j)},$$

we obtain

$$|(P_D w)_i|_{S_i}^2 \lesssim \sum_{\mathcal{X}_i \subset \Gamma \cup \Gamma_D} \sum_{j \in \mathcal{N}_{\mathcal{X}_i}} \left(\frac{H_j}{\eta_j}\right)^2 (1 + \log(H_j/h_j))^2 \bar{\alpha}_j^{\eta_j} |\mathcal{H}_j^\alpha w_j|_{H^1(\Omega_j, \eta_j)}^2. \quad (5.52)$$

Due to the definition of the discrete α -harmonic extension,

$$\begin{aligned} \bar{\alpha}_j^{\eta_j} |\mathcal{H}_j^\alpha w_j|_{H^1(\Omega_j, \eta_j)}^2 &= \frac{\bar{\alpha}_j^{\eta_j}}{\underline{\alpha}_j^{\eta_j}} \int_{\Omega_j, \eta_j} \underline{\alpha}_j^{\eta_j} |\nabla \mathcal{H}_j^\alpha w_j|^2 dx \\ &\leq \frac{\bar{\alpha}_j^{\eta_j}}{\underline{\alpha}_j^{\eta_j}} \int_{\Omega_j} \alpha(x) |\nabla(\mathcal{H}_j^\alpha w_j)(x)|^2 dx = \frac{\bar{\alpha}_j^{\eta_j}}{\underline{\alpha}_j^{\eta_j}} |w_j|_{S_j}^2. \end{aligned} \quad (5.53)$$

Combining (5.52) and (5.53), and using that each subdomain has a finite number of neighbors, we obtain the desired inequality (5.41) with $\beta = 2$.

Under the additional assumption that $\alpha(x) \gtrsim \underline{\alpha}_j^{\eta_j}$ for all $x \in \Omega_j$, we can estimate the terms in (5.47) more directly:

$$\begin{aligned} |w_j|_{H_h^{1/2}(\partial\Omega_i)} &\lesssim |\mathcal{H}_j^\alpha w_j|_{H^1(\Omega_j)} && \text{by identity (5.18),} \\ \|w_j - \bar{w}_j\|_{L^2(\partial\Omega_j)}^2 &\lesssim H_j |\mathcal{H}_j^\alpha w_j|_{H^1(\Omega_j)}^2 && \text{by Theorem 1.7,} \\ \|w_j\|_{L^2(\partial\Omega_j)}^2 &\lesssim H_j (1 + \log(H_j/h_j)) |\mathcal{H}_j^\alpha w_j|_{H^1(\Omega_j)}^2 && \text{by Lemma 2.38,} \\ \|w_j\|_{L^2(\mathcal{E}_j)}^2 &\lesssim (1 + \log(H_j/h_j)) |\mathcal{H}_j^\alpha w_j|_{H^1(\Omega_j)}^2 && \text{by Lemma 2.34.} \end{aligned} \quad (5.54)$$

Using these bounds instead of (5.49)–(5.51), we obtain

$$|(P_D w)_i|_{S_i}^2 \lesssim \sum_{\mathcal{X}_i \subset \Gamma \cup \Gamma_D} \sum_{j \in \mathcal{N}_{\mathcal{X}_i}} \frac{H_j}{\eta_j} (1 + \log(H_j/h_j))^2 \bar{\alpha}_j^{\eta_j} |\mathcal{H}_j^\alpha w_j|_{H^1(\Omega_j, \eta_j)}^2.$$

Combining this with (5.53) we get (5.41) with $\beta = 1$. \square

5.4.3.2 Estimating $|P_D z_w|_S$

We prove that for all $w \in W^\perp$,

$$\sum_{i \in \mathcal{I}} |(P_D z_w)_i|^2 \lesssim \left\{ \max_{k \in \mathcal{I}} \left(\frac{H_k}{\eta_k} \right)^\beta \max_{j \in \mathcal{I}} \frac{\bar{\alpha}_j^{\eta_j}}{\underline{\alpha}_j} (1 + \log(H_j/h_j))^2 \right\} \sum_{i \in \mathcal{I}} |w_i|_{S_i}^2, \quad (5.55)$$

where z_w is the unique element in $\ker S$ associated with w from Lemma 2.22. Again, we restrict ourselves to the more interesting three-dimensional case. Throughout the proof we denote the (constant) components of z_w by z_i .

Note first that in the standard one-level formulation,

$$\|B z_w\|_Q^2 = \langle B z_w, Q B z_w \rangle \simeq \sum_{\{i, j: \Gamma_{ij} \neq \emptyset\}} \min(\bar{\alpha}_i^{\eta_i}, \bar{\alpha}_j^{\eta_j}) \sum_{x^h \in \Gamma_{ij}^h} q_{ij}(x^h) |z_i - z_j|^2. \quad (5.56)$$

In the all-floating formulation, we have to add

$$\sum_{i: \partial\Omega_i \cap \Gamma_D \neq \emptyset} \bar{\alpha}_i^{\eta_i} \sum_{x^h \in \partial\Omega_i^h \cap \Gamma_D} q_i(x^h) |z_i|^2 \quad (5.57)$$

to the right hand side of (5.56). Now we consider a fixed index i and obtain by formula (5.42) and the elementary inequality (5.43) that

$$\begin{aligned} |(P_D z_w)_i|_{S_i}^2 &\lesssim \sum_{\mathcal{X}_{ij} \subset \Gamma} \min(\bar{\alpha}_i^{\eta_i}, \bar{\alpha}_j^{\eta_j}) \left\{ |I^h \theta_{\mathcal{X}_{ij}}|_{H_h^{1/2}(\partial\Omega_i)}^2 + \frac{1}{\eta_i} \|I^h \theta_{\mathcal{X}_{ij}}\|_{L^2(\partial\Omega_i)}^2 \right\} |z_i - z_j|^2 \\ &\quad + \sum_{\mathcal{X}_i \subset \Gamma_D} \bar{\alpha}_i^{\eta_i} \left\{ |I^h \theta_{\mathcal{X}_i}|_{H_h^{1/2}(\partial\Omega_i)}^2 + \frac{1}{\eta_i} \|I^h \theta_{\mathcal{X}_i}\|_{L^2(\partial\Omega_i)}^2 \right\} |z_i|^2, \end{aligned} \quad (5.58)$$

where the last line is dropped in the standard one-level formulation. Using the estimates (2.107) from page 82 as well as the trivial estimates

$$\|\mathcal{H}_i \theta_{\mathcal{F}_i}\|_{L^2(\partial\Omega_i)}^2 \lesssim H_i^2, \quad \|\mathcal{H}_i \theta_{\mathcal{E}_i}\|_{L^2(\partial\Omega_i)}^2 \lesssim H_i, \quad \|\mathcal{H}_i \theta_{\mathcal{V}_i}\|_{L^2(\partial\Omega_i)}^2 \lesssim h_i,$$

a comparison with (5.56), (5.57), and (5.13) yields

$$|P_D z_w|_S^2 \lesssim \left(\max_{k \in \mathcal{I}} \frac{H_k}{\eta_k} \right) \|B z_w\|_Q^2. \quad (5.59)$$

By Lemma 2.22 and using the accordingly modified formula (2.109) from page 83, we can conclude that

$$|P_D z_w|_S^2 \lesssim \left(\max_{k \in \mathcal{I}} \frac{H_k}{\eta_k} \right) \sum_{i \in \mathcal{I}} \bar{\alpha}_i^{\eta_i} (1 + \log(H_i/h_i)) \left\{ \frac{1}{H_i} \|w_i\|_{L^2(\partial\Omega_i)}^2 + \sum_{\mathcal{E}_i} \|w_j\|_{L^2(\mathcal{E}_i)}^2 \right\}. \quad (5.60)$$

In order to bound the L^2 -terms of w_j we use the same argument as in the proof of (5.41), which finally yields the desired inequality (5.55),

$$|P_D z_w|_S^2 \lesssim \left(\max_{k \in \mathcal{I}} \frac{H_k}{\eta_k} \right)^\beta \sum_{i \in \mathcal{I}} \bar{\alpha}_i^{\eta_i} (1 + \log(H_i/h_i)) |w_i|_{S_i}^2. \quad (5.61)$$

Together with (5.41), this completes the proof of (5.15) for the case of three dimensions. \square

The above proof can easily be adapted to the two-dimensional case using in particular Part (i) instead of Part (ii) in Lemma 5.23, i. e., the discrete Sobolev type inequalities for the case of two dimensions.

5.4.4 Proof of Corollary 5.16

A close inspection of the proof of Theorem 4.3 reveals that we can use the same tools from the proof of Theorem 5.12 to obtain the estimate

$$|P_{\Delta}w|_{\mathcal{S}}^2 \leq C \max_{k \in \mathcal{I}} \left(\frac{H_k}{\eta_k} \right)^{\beta} \max_{i \in \mathcal{I}} \frac{\bar{\alpha}_i^{\eta_i}}{\underline{\alpha}_i^{\eta_i}} (1 + \log(H_i/h_i))^2 |w|_{\mathcal{S}}^2 \quad \forall w \in \widetilde{W},$$

which immediately implies the statement of Corollary 5.16.

5.5 Numerical results

In this section we first give two examples with so-called “island” coefficients that do not vary in the vicinity of the interface, but have a jump or are even randomly distributed in the subdomain interiors. We use these examples mainly to confirm our theoretical results. In particular, we will see from the experiments that the factor H/η in our condition number bound is sharp. However, we also study more complicated multiscale and nonlinear problems where the coefficient varies also in the vicinity of the interface. We will see that our bounds are sharp in these cases as well, and that the condition number does indeed grow with $\bar{\alpha}_i^{\eta_i}/\underline{\alpha}_i^{\eta_i}$. As a remedy we use the pointwise weights $\widehat{\alpha}_i^{\max}$ in Q and D_i (instead of $\bar{\alpha}_i^{\eta_i}$ on all of $\partial\Omega_i$). These are more natural and suitable for boundary layer variation and seem to lead to an extremely robust method even in the case of very high variation near the interface. We compare various weightings for the case of “edge islands” and finish the section with some nonlinear magnetic field computations with huge variation. Note that such problems will be treated in more detail in Chapter 6. All the experiments are two-dimensional although our theory holds true as well in three dimensions.

Interior “island” coefficients

Example 5.1 We choose Ω to consist of 25 squares, with an island coefficient in the center square, cf. Figure 5.4, left. Here, and in what follows, H denotes the subdomain width/height and η denotes the distance of the material interface to the subdomain boundary. We set the coefficient to 1 outside the shaded square and to a constant value α_I inside. We impose Dirichlet boundary conditions on the entire boundary $\partial\Omega$ and choose a constant source f .

In Table 5.1 and Table 5.2 we display the required numbers of PCG iterations (to achieve a relative residual reduction of 10^{-8}) and the condition numbers (estimated by the Lanczos method) for the case of $\alpha_I = 10^{+5}$ as well as $\alpha_I = 10^{-5}$. For comparison we have included also the cases $\alpha_I = 1$ (no jump) as well as $\eta = 0$ (jump aligned with the subdomain boundary). Finally, Figure 5.5 shows various estimated condition numbers when keeping $H/h = 512$ constant, but varying H/η as well as the jump, i. e., the value of α_I . From these figures we see that the linear growth in H/η is asymptotically sharp and that the case of $\alpha_I \ll 1 = \underline{\alpha}_i^{\eta_i}$ is indeed harder than $\alpha_I \gg 1$.

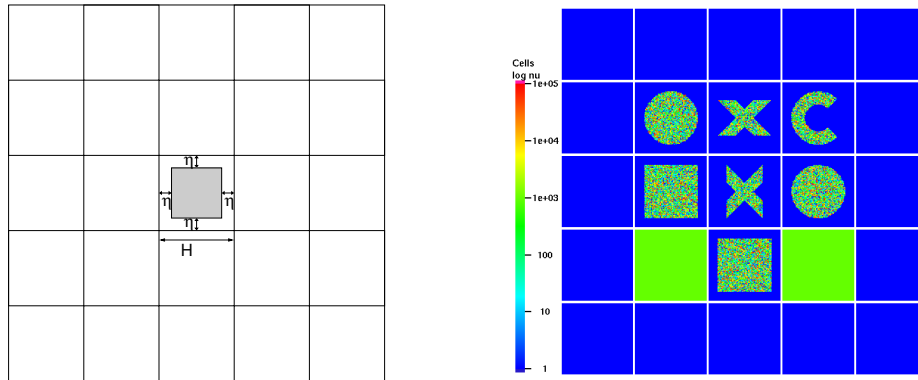


Figure 5.4: *Left:* Coefficient distribution and subdomain partition in Example 5.1. *Right:* Coefficient distribution (logarithmic scale) and subdomain partition in Example 5.2.

	$\frac{H}{h} = 4$	8	16	32	64	128	256	512
$\frac{H}{\eta} = 4$	10(10)	12(12)	14(13)	15(14)	16(15)	17(17)	18(18)	18(18)
8	–	13(12)	14(14)	15(15)	16(16)	17(17)	18(19)	18(18)
16	–	–	14(15)	15(17)	17(17)	18(19)	18(20)	18(21)
32	–	–	–	16(19)	17(19)	19(20)	19(22)	19(21)
64	–	–	–	–	19(23)	19(24)	20(25)	22(27)
128	–	–	–	–	–	24(30)	23(30)	25(31)
256	–	–	–	–	–	–	30(35)	29(36)
512	–	–	–	–	–	–	–	39(48)
$\eta = 0$	10(9)	13(11)	14(11)	15(13)	15(13)	17(15)	17(16)	18(16)
$\alpha_I \equiv 1$	10	12	13	14	15	17	18	17

Table 5.1: Example 5.1: Number of CG iterations; island coefficient with $\alpha_I \equiv 10^{+5}$, in brackets: $\alpha_I \equiv 10^{-5}$

	$\frac{H}{h} = 4$	8	16	32	64	128	256	512
$\frac{H}{\eta} = 4$	2.4(2.4)	3.2(3.2)	4.3(4.3)	5.4(5.5)	6.8(6.8)	8.3(8.3)	9.9(9.9)	11.7(11.7)
8	–	3.2(3.8)	4.3(5.0)	5.4(6.3)	6.8(7.9)	8.3(9.5)	9.9(11.3)	11.7(13.3)
16	–	–	4.3(8.5)	5.4(11.0)	6.8(13.4)	8.3(15.8)	9.9(18.4)	11.7(21.1)
32	–	–	–	5.5(20.7)	6.8(24.8)	8.3(29.0)	9.9(33.3)	11.7(37.8)
64	–	–	–	–	8.7(47.8)	9.4(55.6)	10.4(63.5)	11.9(71.5)
128	–	–	–	–	–	15.6(108.7)	16.0(123.8)	16.6(139.0)
256	–	–	–	–	–	–	29.6(243.8)	29.9(273.4)
512	–	–	–	–	–	–	–	57.7(540.7)
$\eta = 0$	2.4(2.4)	3.2(3.2)	4.3(4.3)	5.4(5.4)	6.8(6.8)	8.2(8.3)	9.9(9.9)	11.7(11.7)
$\alpha_I \equiv 1$	2.4	3.2	4.3	5.4	6.8	8.3	9.9	11.7

Table 5.2: Example 5.1: Estimated condition numbers; island coefficient with $\alpha_I \equiv 10^{+5}$, in brackets: $\alpha_I \equiv 10^{-5}$

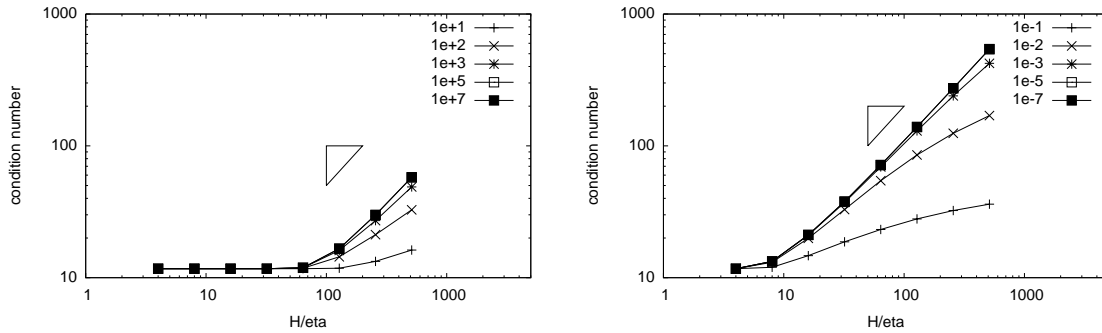


Figure 5.5: Example 5.1: Estimated condition numbers; $H/h = 512$, varying ratio H/η and varying magnitude of the jump α_I . *Left:* $\alpha_I > 1$. *Right:* $\alpha_I < 1$.

Example 5.2 We investigate the behavior of our method in the case of more complexly shaped island coefficients, as depicted in Figure 5.4, right, in order to rule out any symmetry effects. Note that here we have interface jumps (across the interface between subdomains), as well as strong variation in the subdomain interiors. The values in the interior islands are randomly distributed (piecewise constant) such that $\log_{10} \alpha$ is uniformly distributed in $[0, 5]$ or $[-5, 0]$. Again, η denotes the distance of the islands from the interface. In Table 5.3 and Table 5.4 we display again the required number of PCG iterations and the estimated condition numbers. The results are similar to those for Example 5.1.

Using the coefficient distribution from Example 5.2 and setting $\eta = 0$, we get strong coefficient variation along the subdomain boundaries over 5 orders of magnitude. Nevertheless, using $\hat{\alpha}_i^{\max}$ as the new weights in our method the results in Table 5.5 suggest that it is almost coefficient robust even in this case.

	$\frac{H}{h} = 8$	16	32	64	128	256	512
$\frac{H}{\eta} = 8$	15(17)	17(19)	19(21)	22(23)	24(25)	26(27)	27(28)
16	–	28(22)	20(25)	22(28)	24(30)	26(31)	28(33)
32	–	–	22(29)	24(31)	26(34)	28(37)	30(40)
64	–	–	–	27(36)	28(39)	29(41)	31(44)
128	–	–	–	–	32(43)	33(47)	35(51)
256	–	–	–	–	–	41(50)	42(56)
512	–	–	–	–	–	–	53(58)

Table 5.3: Example 5.2: Number of CG iterations; island coefficient with $\alpha_I \in [1, 10^{+5}]$, in brackets: $\alpha_I \in [10^{-5}, 1]$, randomly distributed.

	$\frac{H}{h} = 8$	16	32	64	128	256	512
$\frac{H}{\eta} = 8$	3.8(4.8)	4.7(6.3)	5.8(8.0)	6.9(9.8)	8.3(11.6)	9.7(13.6)	11.3(15.7)
16	–	5.8(9.9)	6.7(13.0)	7.7(15.7)	8.9(18.8)	10.3(22.0)	11.8(25.3)
32	–	–	9.6(19.5)	10.4(23.9)	11.4(29.5)	12.4(35.0)	13.7(40.3)
64	–	–	–	16.9(33.9)	17.7(43.0)	18.5(51.6)	19.4(60.1)
128	–	–	–	–	31.0(58.1)	31.8(69.5)	32.6(81.6)
256	–	–	–	–	–	58.0(86.3)	58.8(101.8)
512	–	–	–	–	–	–	107.7(122.1)

Table 5.4: Example 5.2: Estimated condition numbers; island coefficient with $\alpha_I \in [1, 10^{+5}]$, in brackets: $\alpha_I \in [10^{-5}, 1]$, randomly distributed.

		$\frac{H}{h} = 8$	16	32	64	128	256	512
$\alpha_I \in [1, 10^{+5}]$	it	16	19	25	27	31	40	52
	cond	4.1	5.2	29.1	12.4	22.5	34.5	66.4
$\alpha_I \in [10^{-5}, 1]$	it	32	36	42	44	53	70	86
	cond	205.5	59.3	57.9	58.9	99.1	118.8	218.3

Table 5.5: Example 5.2: Iteration counts and estimated condition numbers; random island coefficient, $\eta = 0$.

“Edge” and “crosspoint” islands

Example 5.3 Here, we investigate the dependence of our method(s) on coefficient variation near the interface. The coefficient distribution is depicted in Figure 5.6. As in Example 5.1 we have 25 subdomains with $\alpha = 1$ everywhere except for the shaded regions. In the interior island we choose $\alpha_I = 10^7$. In the edge islands the coefficients are α_2 and α_3 , respectively, which we will vary in the range of $[10^{-5}, 10^{+5}]$. Table 5.6 displays the iteration and condition numbers for a fixed discretization with $H/h = 64$ and for three different weightings:

1. First we use the subdomain maximum $\bar{\alpha}_i$ (denoted *max*). Here we get a very poor behavior in the condition number (as expected).
2. Then we use $\bar{\alpha}_i^{\eta_i}$ (denoted *layer max*), where η_i is chosen such that the value α_I disappears from the weights. The behavior in this case (albeit slightly better than for the first choice) confirms our theoretical results in Theorem 5.12, i.e., a linear growth of the condition number with $\bar{\alpha}_i^{\eta_i} / \underline{\alpha}_i^{\eta_i}$ but no dependence on jumps across the subdomain interfaces. The iteration numbers do not seem to be affected as badly by the size of the coefficient variation. This is due to clustering effects in the spectrum of the preconditioned matrix, since we only introduce a small number of islands (cf. AKSOYLU, GRAHAM, KLIE, AND SCHEICHL [3], GRAHAM AND HAGGER [72], XU AND ZHU [192]).
3. Finally, using the pointwise weights $\widehat{\alpha}_i^{\max}$ (denoted *pw max*) defined in (5.9) results in a fully robust method with respect to any kind of variation of α_2 , α_3 , and α_I . This is very encouraging, but unfortunately we cannot give a sound theoretical explanation for that robustness in this thesis.

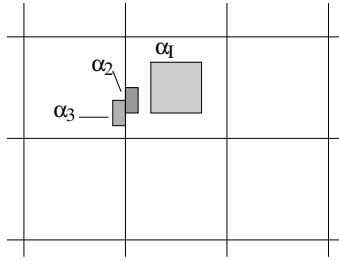


Figure 5.6: Coefficient distribution in Example 5.3.

α_2	<i>max</i>		<i>layer max</i>		<i>pw max</i>		α_2	<i>max</i>		<i>layer max</i>		<i>pw max</i>	
	it	cond	it	cond	it	cond		it	cond	it	cond	it	cond
10^{-5}	61	$1.0 \cdot 10^5$	56	$2.5 \cdot 10^4$	19	6.34	10^{-5}	110	$1.0 \cdot 10^8$	25	$3.2 \cdot 10^3$	20	6.34
10^{-4}	62	$1.0 \cdot 10^4$	52	$2.5 \cdot 10^3$	20	6.34	10^{-4}	141	$1.0 \cdot 10^8$	26	$3.2 \cdot 10^2$	20	6.34
10^{-3}	56	$1.0 \cdot 10^3$	44	$2.5 \cdot 10^2$	21	6.34	10^{-3}	129	$1.0 \cdot 10^6$	27	$3.8 \cdot 10^1$	21	6.34
10^{-2}	44	$1.0 \cdot 10^2$	30	$2.6 \cdot 10^1$	21	6.34	10^{-2}	100	$1.0 \cdot 10^4$	27	$1.6 \cdot 10^1$	21	6.34
10^{-1}	29	$1.5 \cdot 10^1$	21	$6.4 \cdot 10^0$	21	6.34	10^{-1}	50	$1.0 \cdot 10^2$	26	$1.3 \cdot 10^1$	20	6.34
1	25	$1.5 \cdot 10^1$	18	$6.3 \cdot 10^0$	18	6.34	1	25	$1.5 \cdot 10^1$	18	$6.3 \cdot 10^0$	18	6.34
10^{+1}	30	$1.6 \cdot 10^1$	26	$1.3 \cdot 10^1$	21	6.37	10^{+1}	26	$1.5 \cdot 10^1$	24	$1.1 \cdot 10^1$	21	6.34
10^{+2}	47	$1.0 \cdot 10^2$	36	$2.6 \cdot 10^1$	21	6.78	10^{+2}	28	$1.5 \cdot 10^1$	27	$1.4 \cdot 10^1$	21	6.34
10^{+3}	61	$1.0 \cdot 10^3$	60	$2.5 \cdot 10^2$	21	6.88	10^{+3}	28	$3.8 \cdot 10^1$	27	$3.8 \cdot 10^1$	21	6.34
10^{+4}	76	$1.0 \cdot 10^4$	74	$2.5 \cdot 10^3$	21	6.89	10^{+4}	26	$3.2 \cdot 10^2$	27	$3.2 \cdot 10^2$	20	6.34
10^{+5}	86	$1.0 \cdot 10^5$	88	$2.5 \cdot 10^4$	21	6.89	10^{+5}	24	$3.2 \cdot 10^3$	25	$3.2 \cdot 10^3$	20	6.34

Table 5.6: Example 5.3 (with $H/h = 64$). Iteration numbers and estimated condition numbers for different weightings: *max* – global maximum over whole subdomain, *layer max* – maximum over boundary layer (excluding $\alpha_I = 10^{+7}$), *pw max* – pointwise weights $\hat{\alpha}_i^{\max}$ defined in (5.9). *Left*: $\alpha_3 = \alpha_2$. *Right*: $\alpha_3 = (\alpha_2)^{-1}$.

Example 5.4 In this example we study the behavior of our FETI preconditioner with the pointwise weights for an “edge” and a “crosspoint” island, see Figure 5.7. Here we have chosen 4×4 subdomains. The coefficients $\alpha_1 = 1$, $\alpha_2 = 10^5$ are fixed but we vary the characteristic distance η . Figure 5.8 shows the estimated condition numbers for various discretizations (various levels of refined meshes) and different values of η , varying from $\mathcal{O}(h)$ to $\mathcal{O}(H)$. Again, these results are very encouraging. We conjecture the condition number bound $C(H/\eta)^\beta (1 + \log(H/h))^2$, with $\beta = 1$ for this two-dimensional setting. This would be a generalization of Theorem 5.12. However, this issue should be the subject of future investigations; see also PECHSTEIN AND SCHEICHL [148]. Note that numerical experiments on a similar similar three-dimensional problem using FETI-DP methods with α -weighted edge averages can be found in KLAWONN AND RHEINBACH [104].

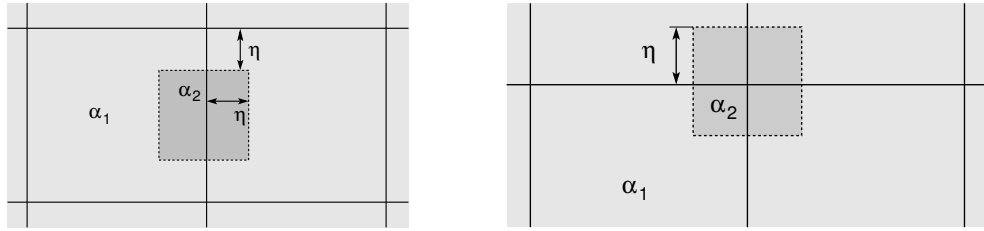


Figure 5.7: Example 5.4: Coefficient configurations. *Left*: “Edge” island. *Right*: “Cross-point” island.

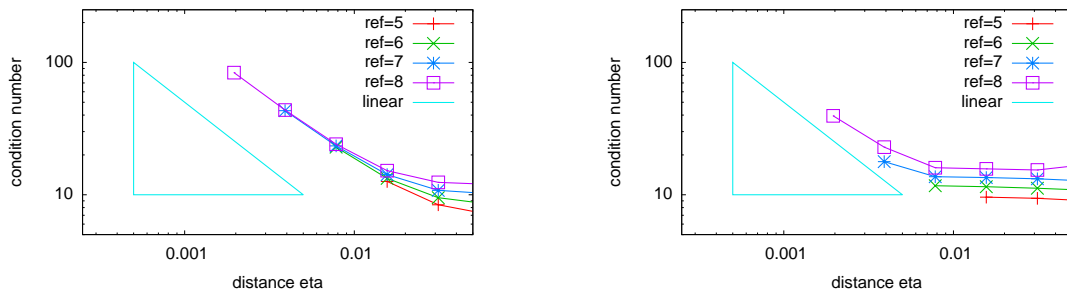


Figure 5.8: Example 5.4: Condition numbers for various values of η and levels of refined meshes ($H/h = 2^{\text{ref}}$). *Left*: “Edge” island. *Right*: “Crosspoint” island.

Nonlinear magnetic field computations

Example 5.5 We test two coefficient distributions coming from nonlinear magnetic field computations, similar to the ones in LANGER AND PECHSTEIN [116]. In the computations we use the piecewise weights $\hat{\alpha}_i^{\max}$ in (5.9). Figure 5.9 displays the coefficient distribution, the subdomain partition, and the coefficient variation along one of the relevant subdomain boundaries for two cases. In both cases the global coefficient variation in the nonlinear material is approximately $7 \cdot 10^3$. However, in the first case we have a mild variation along subdomain boundaries of magnitude $\simeq 10$. In the second case the variation along the subdomain boundary is $7 \cdot 10^3$. For a fixed discretization with $H/h = 128$ the estimated condition numbers are 8.5 and 13.7, respectively. The numbers of PCG iterations are 19 and 16. Since the variation in the boundary layer is mild in the first case, the good behavior in this case is explained by our theory. The robustness in the second case is more surprising. Note also that in contrast to the usual suggestions in the literature it seems to be of benefit not to resolve the material interfaces with the subdomain partition, but rather to put the areas of largest coefficient variation into the center of the subdomains.

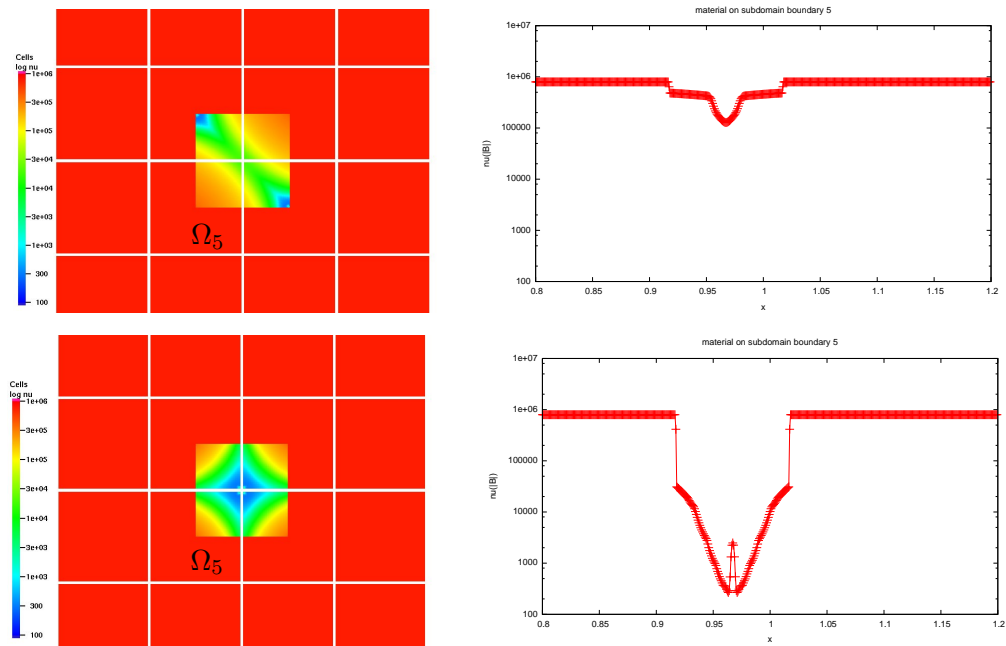


Figure 5.9: Example 5.5. *Left:* Coefficient distribution and subdomain partition. *Right:* Coefficient plotted along a subdomain boundary. *Upper:* Mild boundary layer variation. *Lower:* Strong boundary layer variation.

Chapter 6

Applications to nonlinear magnetic field problems

In this chapter we are treating nonlinear stationary magnetic field problems in two dimensions. In Section 6.1 we describe our nonlinear model problem which can be derived from Maxwell's equations under suitable assumptions. We briefly discuss constitutive laws and the approximation of the underlying B - H -curve. The variational formulation is similar to the problems discussed in previous chapters, but now the coefficient depends nonlinearly on the solution. We briefly discuss the existence of a unique solution and a Newton type method in order to solve the nonlinear equation. Section 6.2 discusses FETI/BETI methods for the solution of the linearized problems. Finally we provide numerical results in Section 6.3.

6.1 Problem formulation

In many industrial applications one is interested in direct electromagnetic field problems, e. g., in the simulation of electrical motors or electromagnetic valves. Under certain conditions, in particular in the low frequency case, the stationary magnetic formulation has indeed some relevance to such problems.

Starting from the full system of Maxwell's equations (see, e. g., one of the monographs by IDA AND BASTOS [92], KALTENBACHER [93], and MONK [136]) we can derive the stationary magnetic equations

$$\mathbf{curl} \mathbf{H} = \mathbf{J} \quad (\text{Ampère's law}), \quad (6.1)$$

$$\mathbf{div} \mathbf{B} = 0 \quad (\text{Gauss' law}), \quad (6.2)$$

$$\mathbf{B} = \boldsymbol{\mu}(\mathbf{H}) \quad (\text{constitutive law}). \quad (6.3)$$

Here, \mathbf{H} denotes the *magnetic field intensity*, \mathbf{J} the *current density*, and \mathbf{B} the *magnetic flux density*, which are all vector fields mapping to \mathbb{R}^3 and depending on the position \mathbf{x} in space. The *magnetic permeability* $\boldsymbol{\mu}$ is in general a nonlinear map. Usually, \mathbf{J} and the permeability are given (at least in form of some measurements), and one wishes to find \mathbf{B} and \mathbf{H} . Note that from (6.1) we obtain the compatibility condition $\mathbf{div} \mathbf{J} = 0$.

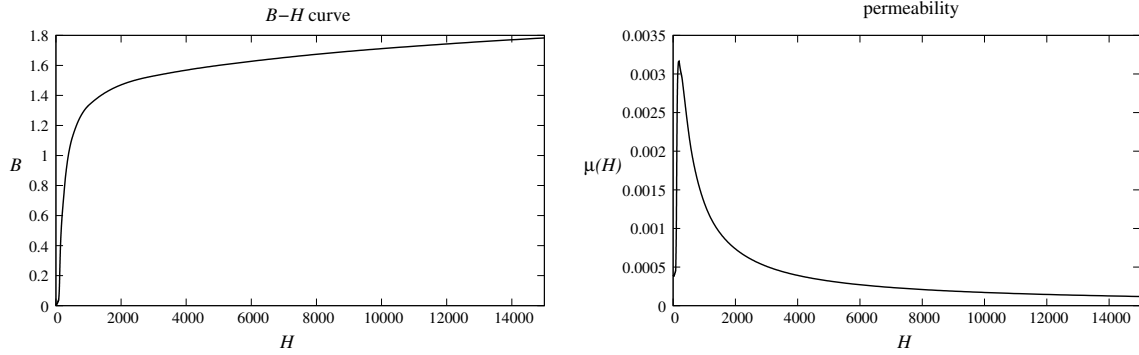


Figure 6.1: Typical material curves for a ferromagnetic material. *Left:* B - H -curve. *Right:* Permeability curve.

6.1.1 Constitutive laws

In what follows we do neither consider hysteresis, nor any material dependency on the temperature (cf. [92, 93]), nor anisotropic materials. In that case, the magnetic permeability μ can be represented by means of a scalar function μ depending only on $|\mathbf{H}|$ and the position \mathbf{x} in space such that

$$\mathbf{B} = \mu(|\mathbf{H}|) \mathbf{H} + \mathbf{B}_0, \quad (6.4)$$

where \mathbf{B}_0 is termed (*permanent*) *magnetization* or *remanent flux density*. We introduce a derived quantity, the *magnetic reluctivity* $\nu(|\mathbf{B}|) = 1/\mu(|\mathbf{H}|)$ such that

$$\mathbf{H} = \nu(|\mathbf{B}|) \mathbf{B} - \mathbf{H}_0, \quad (6.5)$$

where $\mathbf{H}_0 = \nu(|\mathbf{B}|) \mathbf{B}_0$ corresponds to the permanent magnetization.

Linear materials In vacuum (and also air) we have

$$\mu = \mu_0 := 4\pi \cdot 10^{-7}, \quad \nu = \nu_0 := \frac{1}{\mu_0}. \quad (6.6)$$

For other linear materials,

$$\mu = \mu_0 \mu_r, \quad \nu = \frac{1}{\mu_0 \mu_r}, \quad (6.7)$$

with the constant *relative permeability* $\mu_r \geq 1$.

Nonlinear materials If no permanent magnetization is present, we have in general a nonlinear relation of the form

$$|\mathbf{B}| = g(|\mathbf{H}|), \quad (6.8)$$

with a bijective mapping $g : [0, \infty) \rightarrow [0, \infty)$ termed the *B-H-curve*, cf. Figure 6.1. Due to the physical background the following assumptions hold.

Assumption 6.1. *Every B - H -curve g fulfills the following conditions:*

- (i) g is continuously differentiable on $[0, \infty)$,
- (ii) $g(0) = 0$,
- (iii) $g'(s) \geq \mu_0$ for all $s \geq 0$,
- (iv) $g'(s) \rightarrow \mu_0$ for $s \rightarrow \infty$.

Part (iii) states that the amplification of $|\mathbf{B}|$ in case of vacuum is a lower bound for general materials. Part (iv) states that for $|\mathbf{H}| \rightarrow \infty$, the material gets *saturated* and its behavior tends to that of vacuum. Such behavior is typical for ferromagnetic materials.

We will see in Section 6.1.6 that under Assumption 6.1 the functions μ and ν are unique and well-defined by

$$\begin{aligned} \mu(s) &= \frac{g(s)}{s}, & \nu(s) &= \frac{g^{-1}(s)}{s}, & \text{for } s > 0, \\ \mu(0) &= g'(0), & \nu(0) &= (g^{-1})'(0). \end{aligned}$$

Permanent magnetic materials are modeled by relation (6.5), where in many cases $\nu(|\mathbf{B}|)$ can be assumed constant.

6.1.2 Interface and boundary conditions

In general, $\nu(|\mathbf{B}|)$ depends also on the position \mathbf{x} in space. In the following we assume that there exists a partition of the computational domain Ω into finitely many subregions Ω_j , which we call *materials*, such that within a single material the function ν is independent of \mathbf{x} . We write ν_j , μ_j , and g_j for the corresponding restrictions of ν , μ , and the B - H -curve g to Ω_j . Suitable boundary and interface conditions can be found, e. g., in KALTENBACHER [93], MONK [136]. In the following we assume that the boundary $\partial\Omega$ is Lipschitz and consists of only one connected component. Furthermore, let Γ_B and Γ_H be two disjoint parts that together form $\partial\Omega$. We denote the material interface system by Γ and choose \mathbf{n} to be an oriented unit normal vector to $\partial\Omega \cup \Gamma$. Then, we impose the following boundary and interface conditions,

$$\mathbf{B} \cdot \mathbf{n} = 0 \quad \text{on } \Gamma_B, \quad (6.9)$$

$$\mathbf{H} \times \mathbf{n} = 0 \quad \text{on } \Gamma_H, \quad (6.10)$$

$$\llbracket \mathbf{B} \cdot \mathbf{n} \rrbracket = 0, \quad \llbracket \mathbf{H} \times \mathbf{n} \rrbracket = 0, \quad \llbracket \mathbf{J} \cdot \mathbf{n} \rrbracket = 0 \quad \text{on } \Gamma, \quad (6.11)$$

where $\llbracket \cdot \rrbracket$ indicates the jump across Γ .

6.1.3 Vector potential formulation

Due to Gauss' law for magnetism (6.2), the magnetic flux density \mathbf{B} is solenoidal. Since $\partial\Omega$ consists of only one connected component (cf. MONK [136]), we may introduce a vector potential \mathbf{A} , such that

$$\mathbf{curl} \mathbf{A} = \mathbf{B}. \quad (6.12)$$

Using the constitutive law (6.5), the system (6.1)–(6.3) can be rewritten as

$$\mathbf{curl} [\nu(|\mathbf{curl} \mathbf{A}|) \mathbf{curl} \mathbf{A}] = \mathbf{J} + \mathbf{curl} \mathbf{H}_0. \quad (6.13)$$

In order to make \mathbf{A} unique one can use gauging conditions or other regularization techniques. Often, the conditions on \mathbf{B} in (6.9)–(6.11) are replaced by the stronger conditions

$$\mathbf{A} \times \mathbf{n} = 0 \quad \text{on } \Gamma_B \quad \text{and} \quad \llbracket \mathbf{A} \times \mathbf{n} \rrbracket = 0 \quad \text{on } \Gamma, \quad (6.14)$$

in order to exclude surface flows in \mathbf{A} , cf. KALTENBACHER [93], MONK [136].

6.1.4 Reduction to two dimensions

In the following we assume that the domain Ω is of the tensor-product structure $\Omega = \tilde{\Omega} \times \mathbb{R}$, with $\Gamma_B = \Gamma_D \times \mathbb{R}$, $\Gamma_H = \Gamma_N \times \mathbb{R}$, and $\Gamma = \tilde{\Gamma} \times \mathbb{R}$. Under the assumptions that $B_3 = 0$, $H_3 = 0$, $H_{0,3} = 0$, $J_1 = J_2 = 0$ (transverse magnetic mode), and that all fields are independent of x_3 , equation (6.13) can be reduced to

$$-\operatorname{div} [\nu(|\nabla u|) \nabla u] = J_3 + \frac{\partial H_{0,1}}{\partial x_2} - \frac{\partial H_{0,2}}{\partial x_1}, \quad (6.15)$$

where $u = A_3$. Since all the quantities are independent of x_3 we can read (6.15) as an equation in $\tilde{\Omega}$. Note that here, the compatibility condition $\operatorname{div} \mathbf{J} = 0$ is fulfilled, and moreover $\mathbf{A} = (0, 0, u)^\top$ fulfills the *Colomb gauge* condition $\operatorname{div} \mathbf{A} = 0$. The original fields \mathbf{B} and \mathbf{H} can be recovered by the relations

$$\mathbf{B} = \begin{pmatrix} \frac{\partial u}{\partial x_2} \\ -\frac{\partial u}{\partial x_1} \\ 0 \end{pmatrix}, \quad \mathbf{H} = \nu(|\nabla u|) \begin{pmatrix} \frac{\partial u}{\partial x_2} \\ -\frac{\partial u}{\partial x_1} \\ 0 \end{pmatrix} - \mathbf{H}_0. \quad (6.16)$$

The boundary and interface conditions including (6.14) transform to

$$u = 0 \quad \text{on } \Gamma_D, \quad (6.17)$$

$$\nu(|\nabla u|) \nabla u \cdot \mathbf{n} = H_{0,1} n_2 - H_{0,2} n_1 \quad \text{on } \Gamma_N, \quad (6.18)$$

$$\llbracket u \rrbracket = 0, \quad \llbracket \nu(|\nabla u|) \nabla u \cdot \mathbf{n} - H_{0,1} n_2 + H_{0,2} n_1 \rrbracket = 0 \quad \text{on } \tilde{\Gamma}. \quad (6.19)$$

In the sequel we assume that Γ_D is of positive surface measure, and for simplicity we write Ω instead of $\tilde{\Omega}$. Using the above conditions, one derives the following variational formulation.

Find $u \in H_D^1(\Omega) := \{v \in H^1(\Omega) : v|_{\Gamma_D} = 0\}$ such that

$$\int_{\Omega} \nu(|\nabla u|) \nabla u \cdot \nabla v \, dx = \langle F, v \rangle \quad \forall v \in H_D^1(\Omega), \quad (6.20)$$

with the linear form

$$\langle F, v \rangle = \int_{\Omega} J_3 v - H_{0,2} \frac{\partial v}{\partial x_1} + H_{0,1} \frac{\partial v}{\partial x_2} \, dx + \int_{\Gamma_N} (H_{0,1} n_2 - H_{0,2} n_1) v \, ds_x. \quad (6.21)$$

Note that this formulation can be treated in the framework of Theorem 1.17 (Zarantonello) because the underlying bi-form is linear in v . Clearly, under suitable assumptions, e.g.,

$J_3 \in L^2(\Omega)$ and $H_{0,1}, H_{0,2}$ piecewise smooth in $L^2(\Omega)$ and $L^2(\Gamma_N)$, we have $F \in H_D^1(\Omega)^*$. We define the operator $A : H_D^1(\Omega) \rightarrow H_D^1(\Omega)^*$ by

$$\langle A(u), v \rangle = \int_{\Omega} \nu(|\nabla u|) \nabla u \cdot \nabla v \, dx \quad \text{for } v \in H_D^1(\Omega). \quad (6.22)$$

In the following section we show properties of A , in particular that $A(u)$ is really in the dual space $H_D^1(\Omega)^*$.

6.1.5 Existence and uniqueness of solutions

Assume that for each material Ω_j , the underlying B - H -curve g_j satisfies Assumption 6.1. Then the following statements hold.

1. Each g_j is strongly monotonically increasing with monotonicity constant μ_0 , i. e.,

$$(g_j(s) - g_j(t))(s - t) \geq \mu_0(s - t)^2 \quad \forall s, t \geq 0.$$

2. Since g_j' is continuous on $[0, \infty)$, $g_j'(s) \geq \mu_0$, and $g_j'(s)$ tends to μ_0 as $s \rightarrow \infty$, we have that $g_j' \in L^\infty(0, \infty)$ and

$$0 < \mu_0 \leq g_j'(s) \leq L_j := \sup_{s \geq 0} g_j'(s) < \infty \quad \forall s \geq 0.$$

Hence, the B - H -curve g_j is Lipschitz continuous with Lipschitz constant L_j .

3. The inverse function $g_j^{-1} : [0, \infty) \rightarrow [0, \infty)$ exists. It is strongly monotonically increasing with monotonicity constant $1/L_j$, Lipschitz continuous with Lipschitz constant $\nu_0 = 1/\mu_0$, and continuously differentiable where

$$1/L_j \leq (g_j^{-1})'(s) \leq \nu_0 \quad \forall s \geq 0.$$

4. In case of $\mathbf{B}_0 = \mathbf{H}_0 = 0$, the magnetic permeability and reluctivity are given by

$$\mu_j(s) = \frac{g_j(s)}{s}, \quad \nu_j(s) = \frac{g_j^{-1}(s)}{s} \quad \forall s > 0. \quad (6.23)$$

The functions may be continuously extended to $\mu_j(0) = g_j'(0)$ and $\nu_j(0) = (g_j^{-1})'(0)$.

5. We have

$$\begin{aligned} \mu_0 \leq \mu_j(s) \leq L_j \quad \forall s \geq 0, & \quad \mu_j(s) \rightarrow \mu_0 \quad \text{for } s \rightarrow \infty, \\ 1/L_j \leq \nu_j(s) \leq \nu_0 \quad \forall s \geq 0, & \quad \nu_j(s) \rightarrow \nu_0 \quad \text{for } s \rightarrow \infty. \end{aligned}$$

6. The functions μ_j and ν_j are continuously differentiable on $(0, \infty)$. If $g_j''(0)$, or equally $(g_j^{-1})''(0)$, exists, we have

$$\mu_j'(0) = \frac{1}{2} g_j''(0) \quad \nu_j'(0) = \frac{1}{2} (g_j^{-1})''(0) = -\frac{g_j''(0)}{2 g_j'(0)^2}.$$

In short, the functions $g_j^{-1}(s) = \nu_j(s)s$ are strongly monotone and Lipschitz continuous, and the functions $\nu_j(s)$ are uniformly bounded from above. Therefore, $A(u) \in H_D^1(\Omega)^*$ for each $u \in H_D^1(\Omega)$. Using that $\min_j 1/L_j$ is bounded away from zero and $\nu_0 < \infty$, it can be shown that $A(\cdot)$ is strongly monotone and Lipschitz continuous as well. Thus, Theorem 1.17 guarantees the existence of a unique solution to (6.20). For a detailed discussion we refer to PECHSTEIN [142].

6.1.6 Approximation of B - H -curves

In practice, B - H -curves are not available analytically, but must be approximated from measurements. Let $g = \tilde{g}_j$ be one of the B - H -curves and let

$$(H_k, B_k), \quad k = 0, \dots, N \quad (6.24)$$

denote a set of measurements corresponding to absolute values $|\mathbf{H}|$ and $|\mathbf{B}|$ in the material for different settings of the current density \mathbf{J} . Here, $H_0 = B_0 = 0$. Our aim is to construct an approximation \tilde{g} to the unknown curve g . A possible way to achieve this goal is to use spline interpolation. However, we can run into problems since

- (i) the resulting curve must be monotonically increasing, and
- (ii) measurement errors can lead to unphysical, oscillating approximations.

The measurement errors are modeled by the condition

$$|g(H_k) - B_k| \leq \delta_k \quad \forall k = 0, \dots, N. \quad (6.25)$$

Due to (i) we impose the conditions

$$\begin{aligned} 0 &= H_0 < H_1 < H_2 < \dots < H_N < \infty, \\ 0 &= B_0 < B_1 < B_2 < \dots < B_N < \infty \end{aligned} \quad (6.26)$$

on the data. In view of Assumption 6.1(iii) we can additionally use

$$\frac{H_k - H_{k-1}}{B_k - B_{k-1}} \geq (1 - \varepsilon) \mu_0 \quad \forall k = 1, \dots, N, \quad (6.27)$$

for some tolerance parameter ε , in order to check consistency of the data. A method of monotonicity-preserving cubic spline interpolation has been introduced by FRITSCH AND CARLSON [67] and was used by HEISE [84] to reconstruct B - H -curves. Concerning measurement errors, one can approximate the data in the least square sense, minimizing the error

$$\sum_{k=0}^N |\tilde{g}(H_k) - B_k|^2. \quad (6.28)$$

Note that optionally, each term in the above sum can be weighted differently. It is well-known that the cubic interpolating spline minimizes the linearized strain energy

$$\int_{H_0}^{H_N} (\tilde{g}''(x))^2 dx. \quad (6.29)$$

Hence, one can add this energy as a regularization term to the cost functional (6.28), multiplied by a regularization parameter. The larger this parameter, the smoother the optimizing function \tilde{g} will be. Therefore we call (6.29) a smoothing functional. Such an approach is well described in the article by REINSCH [151]. The ideas of monotonicity preserving and cubic smoothing spline approximation were used by REITZINGER, KALTENBACHER, AND KALTENBACHER [152] to approximate B - H -curves. In that article, the authors obtain the

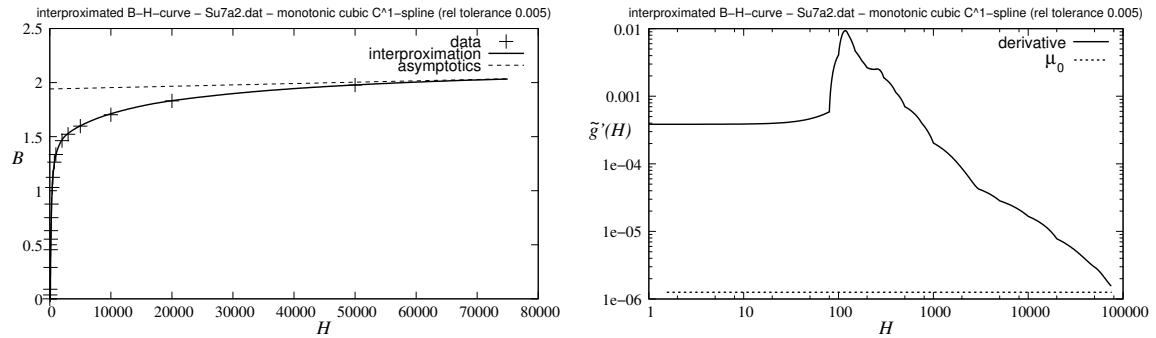


Figure 6.2: Interproximation results for the data set **Su7a2** (Courtesy of Robert Bosch GmbH, Stuttgart). *Left*: Approximated B - H -curve and data. *Right*: Derivative of the approximation, double-logarithmic scale.

regularization parameter iteratively according to the discrepancy principle. During this iteration, monotonicity is checked and the update for the regularization parameter can be adjusted accordingly.

Two key problems of that approach are the following. First, the uniqueness of the solution to the corresponding optimization problem is achieved only by imposing boundary conditions on $\tilde{g}'(H_0)$ and $\tilde{g}'(H_N)$. However, the values of these boundary constraints (e. g., chosen as the first difference quotient of the data points) have a non-negligible influence on the shape of the curve. Second, the authors do not make clear if the method leads to a solution for any data set in the sense that the error (6.28) is in the order of the noise level *and* the curve is monotone. It is also not clear whether the choice of the boundary conditions can have bad influence on the monotonicity.

This was the motivation to use an approach called *interproximation* (cf. CHENG AND BARSKY [32]) for the reconstruction of B - H -curves. In PECHSTEIN AND JÜTTLER [146] we minimize a smoothing functional similar to (6.29) under the side conditions of monotonicity and the approximation conditions

$$|\tilde{g}(H_k) - B_k| \leq c \delta_k \quad \forall k = 0, \dots, N,$$

for some constant c . In other words, we look for an approximation \tilde{g} such that the point-wise error lies in the range of the assumed noise. This results in a quadratic programming problem which can be solved using standard techniques. By using a special B-spline basis, the monotonicity constraints can even be incorporated rather easily. As an advantage of this approach, no artificial boundary conditions have to be used. Since typical B - H -curves start with very steep gradients which get then more and more flat, cf. Figure 6.1(left), we propose to use a data-dependent smoothing functional which introduces suitable weights to the strain energy in each spline interval. In order to ensure a unique solution the smoothing functional is regularized by some additional terms. The existence of solution is then guaranteed automatically unless condition (6.26) is violated. For details see [146].

Another problem is the modeling of the behavior for $|\mathbf{H}| \rightarrow \infty$. Suitable extrapolation techniques are discussed, e. g., in HEISE [84] and REITZINGER ET AL. [152]. In PECHSTEIN AND JÜTTLER [146], we use a suitable nonlinear transformation from the infinite interval

$[H_N, \infty)$ to a finite interval, so that we can incorporate the conditions at infinity simply as boundary conditions.

The resulting B - H -curves are physically plausible and visually pleasing. Figure 6.2 shows an approximation of a data sample. We mention that the underlying code was developed by the author of this thesis, using a quadratic programming solver by Helmut Gfrerer (University of Linz).

6.2 Newton-FETI/BETI methods

This section deals with the discretization and iterative solution of our nonlinear model problem (6.20) by means of Newton's method and the FETI/BETI methods discussed in previous chapters. To this end we consider a shape-regular partitioning of Ω into subdomains $\{\Omega_i\}_{i \in \mathcal{I}}$. Here, we assume that the partitioning resolves the material interfaces, i. e., to each subdomain Ω_i we can associate a function $\nu_i(\cdot)$ which is independent of the position x . If Ω_i corresponds to a linear material ($\nu_i = \text{const}$) with no permanent magnetization and if $(J_3)_{|\Omega_i} = 0$, the subdomain may be discretized by means of BEM; for the remaining subdomains we use FEM. Note, that the partition into *subdomains* may (and usually will) be finer than the partition into homogeneous *materials*. Let \mathcal{I}_{BEM} and $\mathcal{I}_{\text{FEM}} = \mathcal{I} \setminus \mathcal{I}_{\text{BEM}}$ denote the corresponding index sets. On each BEM subdomain we make use of the approximation $S_{i,\text{BEM}}^{\text{int}}$ of the interior Steklov-Poincaré operator S_i^{int} on $\partial\Omega_i$. For this purpose, we introduce the space

$$\tilde{V}_D := \left\{ u \in H_D^1(\Omega) : \int_{\Omega_i} \nabla u \cdot \nabla v \, dx = 0 \quad \forall v \in H_0^1(\Omega_i) \quad \forall i \in \mathcal{I}_{\text{BEM}} \right\}, \quad (6.30)$$

i. e., the functions in $H_D^1(\Omega)$ which are weakly harmonic in the BEM subdomains. In the next step we approximate the nonlinear variational equation (6.20) by the equation

$$\tilde{A}(u) = F \quad \text{in } \tilde{V}_D^*, \quad (6.31)$$

with

$$\langle \tilde{A}(u), v \rangle = \sum_{i \in \mathcal{I}_{\text{FEM}}} \underbrace{\int_{\Omega_i} \nu_i(|\nabla u|) \nabla u \cdot \nabla v \, dx}_{=: \langle A_i(u), v \rangle_{\Omega_i}} + \sum_{i \in \mathcal{I}_{\text{BEM}}} \nu_i \langle S_{i,\text{BEM}}^{\text{int}} u, v \rangle_{\partial\Omega_i}, \quad (6.32)$$

$$\langle F, v \rangle = \sum_{i \in \mathcal{I}_{\text{FEM}}} \underbrace{\int_{\Omega_i} J_3 v - H_{0,2} \frac{\partial v}{\partial x_1} + H_{0,1} \frac{\partial v}{\partial x_2} \, dx + \int_{\partial\Omega_i \cap \Gamma_N} H_{0,1} n_2 - H_{0,2} n_1 \, ds}_{=: \langle f_i, v \rangle}, \quad (6.33)$$

for $u, v \in \tilde{V}_D$.

For a discretization we consider a shape-regular and geometrically conforming triangulation of the skeleton Γ_S and expand it to quasi-uniform triangulations on the subdomains Ω_i for $i \in \mathcal{I}_{\text{FEM}}$. We define $V_D^h(\Omega_i)$ and $V_D^h(\partial\Omega_i)$ as the corresponding spaces of continuous piecewise affine linear functions with respect to the triangulation which fulfill the essential boundary conditions. The discrete analogon to \tilde{V}_D is the space

$$\tilde{V}_D^h := \left\{ u \in \tilde{V}_D : u_{|\Omega_i} \in V_D^h(\Omega_i) \quad \forall i \in \mathcal{I}_{\text{FEM}}, \quad u_{|\partial\Omega_i} \in V_D^h(\partial\Omega_i) \quad \forall i \in \mathcal{I}_{\text{BEM}} \right\}. \quad (6.34)$$

6.2.1 Newton's method

Usually, one discretizes problem (6.20) first and derives a Newton type method in a second step. It turns out, however, that the Jacobian is closely related to the one of the continuous Newton method. For a detailed discussions see, e. g., HEISE [84] or PECHSTEIN [142]. The Fréchet derivative $\tilde{A}'(u) : \tilde{V}_D \rightarrow \tilde{V}_D^*$ of the operator \tilde{A} at u is given by

$$\langle \tilde{A}'(u)w, v \rangle = \sum_{i \in \mathcal{I}_{\text{FEM}}} \langle A'_i(u)w, v \rangle_{\Omega_i} + \sum_{i \in \mathcal{I}_{\text{BEM}}} \nu_i \langle S_{i,\text{BEM}}^{\text{int}} w, v \rangle_{\partial\Omega_i} \quad \text{for } w, v \in \tilde{V}_D, \quad (6.35)$$

with $A'_i(u) : H_D^1(\Omega_i) \rightarrow H_D^1(\Omega_i)^*$ and $\zeta_i : \mathbb{R}^2 \rightarrow \mathbb{R}^{2 \times 2}$ defined by

$$\langle A'_i(u)w, v \rangle_{\Omega_i} = \int_{\Omega_i} [\zeta_i(\nabla u) \nabla w] \cdot \nabla v \, dx \quad \text{for } w, v \in H_D^1(\Omega_i), \quad (6.36)$$

$$\zeta_i(\mathbf{p}) = \begin{cases} \nu_i(|\mathbf{p}|)I + \frac{\nu'_i(|\mathbf{p}|)}{|\mathbf{p}|} \mathbf{p} \mathbf{p}^\top & \text{for } \mathbf{p} \in \mathbb{R}^2 \setminus \{0\}, \\ \nu_i(0)I & \text{for } \mathbf{p} = 0. \end{cases} \quad (6.37)$$

The Jacobian in the k -th step of a discrete Newton method will then be associated to the bilinear form

$$\langle \tilde{A}'(u_h^{(k)})w_h, v_h \rangle, \quad \text{for } w_h, v_h \in \tilde{V}_D^h.$$

Under Assumption 6.1 it can be shown that the Fréchet derivative $\tilde{A}'(u)$ is elliptic and bounded, uniformly in u , which essentially means that the Jacobian matrix is always regular. Finally, the (damped) Newton method reads as follows.

1. Fix a continuous initial guess $u_h^{(0)} \in \tilde{V}_D^h$.
2. Set $k = 0$.
3. Compute the update $w_h^{(k)} \in \tilde{V}_D^h$ by solving

$$\langle \tilde{A}'(u_h^{(k)})w_h^{(k)}, v_h \rangle = \sum_{i \in \mathcal{I}_{\text{FEM}}} \langle r_i^{(k)}, v_h \rangle_{\Omega_i} + \sum_{i \in \mathcal{I}_{\text{BEM}}} \langle r_i^{(k)}, v_h \rangle_{\partial\Omega_i} \quad \forall v_h \in \tilde{V}_D^h, \quad (6.38)$$

with

$$\begin{aligned} r_i^{(k)} &= f_i - \tilde{A}_i(u_h^{(k)}) && \in V_D^h(\Omega_i)^* && \text{for } i \in \mathcal{I}_{\text{FEM}}, \\ r_i^{(k)} &= -S_{i,\text{BEM}}^{\text{int}} u_h^{(k)} && \in V_D^h(\partial\Omega_i)^* && \text{for } i \in \mathcal{I}_{\text{BEM}}. \end{aligned} \quad (6.39)$$

4. Set $u_h^{(k+1)} = u_h^{(k)} + \rho_k w_h^{(k)}$ where the relaxation parameter ρ_k is chosen using a line search algorithm in order to get a reduction in the residual.
5. Check the convergence of the residual in a suitable norm, e. g., use the stopping criterion

$$\sum_{i \in \mathcal{I}} \langle r_i^{(k)}, w_h^{(k)} \rangle \leq \varepsilon \sum_{i \in \mathcal{I}} \langle r_i^{(1)}, w_h^{(1)} \rangle, \quad (6.40)$$

for some relative tolerance ε . It can be shown that the expression on the left hand side is a norm of the residual, spectrally equivalent to the energy-norm of the global error. If the stopping criterion fails, increase k by one and continue with step 3.

A convergence analysis of this Newton method can be found in PECHSTEIN [142]. Under suitable smoothness assumptions on ν' one can show that the above Newton method converges locally quadratic. In order to obtain a good initial guess, we can use a sequence of refined meshes and use the approximation on each level as initial guess for the next level.

Note that in the case of non-homogeneous boundary conditions, the initial guess $u_h^{(0)}$ is chosen such that it satisfies the correct Dirichlet boundary conditions. Therefore, the update $w_h^{(k)}$ must satisfy homogeneous Dirichlet boundary conditions in any case.

6.2.2 The linearized problem

From the previous considerations we see that equation (6.38) is a potential equation with a tensor-valued coefficient $\zeta_i(\nabla u_h^{(k)})$. We are faced with the following two different kinds of phenomena.

1. *Anisotropy*: For a fixed vector $\mathbf{p} \in \mathbb{R}^2$, the matrix $\zeta_i(\mathbf{p})$ has two eigenvalues, $\nu_i(|\mathbf{p}|)$ and $\nu_i(|\mathbf{p}|) + \nu'_i(|\mathbf{p}|)|\mathbf{p}|$. Depending on the derivative $\nu'_i(|\mathbf{p}|)$, the ratio of these eigenvalues may become large. In terms of the B - H -curve g_i , the ratio is given by

$$\max \left\{ \frac{g_i^{-1}(|\mathbf{p}|)}{(g_i^{-1})'(|\mathbf{p}|)|\mathbf{p}|}, \frac{(g_i^{-1})'(|\mathbf{p}|)|\mathbf{p}|}{g_i^{-1}(|\mathbf{p}|)} \right\}.$$

For details see, e. g., PECHSTEIN [142]. Fortunately, for many practically relevant B - H -curves, this ratio stays small, e. g., $\mathcal{O}(10^1)$.

2. *Variation*: Since the approximations $\nabla u_h^{(k)}$ of ∇u are substituted for \mathbf{p} , a subdomain Ω_i may show large variation in $\zeta_i(\cdot)$, since $\nabla u_h^{(k)}$ may vary significantly. In the presence of singularities at corners etc., ∇u can grow arbitrarily large, whereas ∇u is usually small in the interior of a subdomain. This results in the fact that the ration between the largest and the smallest occurring eigenvalue of $\zeta_i(|\nabla u_h^{(k)}|)$ on one subdomain may be $\mathcal{O}(10^3)$ and more, which is not anymore negligible. Iterative solvers for the linearized problems (6.38) should be robust with respect to the variation of $\zeta_i(\nabla u_h^{(k)})$. This shows indeed the relevance and importance of the theory presented in Chapter 5.

6.2.3 Error control

We use FETI/BETI methods to solve the linearized problem in every step of Newton's iteration. In order not to complicate notation, assume that the FETI/BETI saddle point system in step k reads as

$$\begin{pmatrix} S^{(k)} & B^\top \\ B & 0 \end{pmatrix} \begin{pmatrix} w^{(k)} \\ \lambda^{(k)} \end{pmatrix} = \begin{pmatrix} r^{(k)} \\ 0 \end{pmatrix}.$$

Since we do not have exact arithmetics, the update $w^{(k)}$ is discontinuous. We give the following two suggestions to proceed.

- We can enforce continuity of $w^{(k)}$ by averaging, e. g., using the weighted average operator E_D . From Remark 2.47 (page 91) and the preceding discussion, we know that the FETI/BETI PCG iteration controls the residual

$$|P_D w^{(k)}|_{S^{(k)}} = |w^{(k)} - E_D w^{(k)}|_{S^{(k)}}.$$

Consequently, the global error

$$E^\top (S^{(k)} E_D w^{(k)} - r^{(k)}) = \underbrace{E^\top (S^{(k)} u^{(k)} - r^{(k)} - B^\top \lambda^{(k)})}_{=0} - E^\top S^{(k)} P_D w^{(k)}$$

will be of the same order as that residual.

- Alternatively, we can incorporate the discontinuity in $u^{(k)}$ into the right hand side of the FETI/BETI system for the update $w^{(k)}$,

$$\begin{pmatrix} S^{(k)} & B^\top \\ B & 0 \end{pmatrix} \begin{pmatrix} w^{(k)} \\ \lambda^{(k)} \end{pmatrix} = \begin{pmatrix} r^{(k)} \\ -B u^{(k)} \end{pmatrix},$$

i. e., we enforce a jump of $-B u^{(k)}$ to $w^{(k)}$, such that the jump in the new iterate $u^{(k+1)}$ is reduced. However, this strategy works only if the relaxation parameter ρ_k can be chosen to be 1 (or if it is known *a priori*).

For more details and numerical studies see LANGER AND PECHSTEIN [116, Sect. 4].

6.3 Numerical results

In this section we consider two kinds of problems, an electromagnetic valve and an electrical motor. We show the application of one-level FETI, FETI/BETI, and IC-FETI/BETI methods including the incorporation of an exterior domain to the nonlinear problems.

Example 6.1: Electromagnetic valve In our first example we choose the model valve problem from Section 2.3.3 on the square $[0, 0.1]^2$, cf. Figure 6.3, left. The armature and the iron core are considered as nonlinear materials with the B - H -curve according to Figure 6.2. The source term J_3 is chosen as $2.3 \cdot 10^6$ in the coil and zero elsewhere. Furthermore, we have no permanent magnetization, i. e., $\mathbf{H}_0 = 0$. For all the computations in Example 6.1 we have used a globally quasi-uniform triangular mesh.

First, we impose Dirichlet boundary conditions on the whole boundary. The absolute value of the magnetic flux density $|\mathbf{B}|$ is displayed in Figure 6.3, right. The magnetic field intensity $|\mathbf{H}|$ and the values of the reluctivity $\nu(|\mathbf{B}|)$ are shown in Figure 6.3. We see that we get large values of $\nu(|\mathbf{B}|)$ near the material corners. In order to get an idea on the amount of variation of the reluctivity in the nonlinear materials, we have plotted all the occurring values of $\nu(|\mathbf{B}|)$ in the iron core against $|\mathbf{B}|$ in Figure 6.5, left. In the same figure, we display the residual of the global nonlinear equation. The different branches of the graph correspond to different levels of refinement. On the finest level in that graph the number of global DOFs equals 263 169. Here we have chosen a relative accuracy of $\varepsilon = 10^{-6}$ for the reduction of the residual on the coarsest level (0) and on the finest level (5), whereas we stop after two Newton steps on the levels in between. The linearized problems are controlled by a reduction of the residual by a factor of $\varepsilon_{\text{lin}} = 10^{-8}$ in the energy norm, cf. Algorithm 1 (page 65). For this particular example, the nonlinearity seems to be extremely high, and we need seven Newton steps on the finest level, some of them damped. Nevertheless, we can see the quadratic convergence in the last steps.

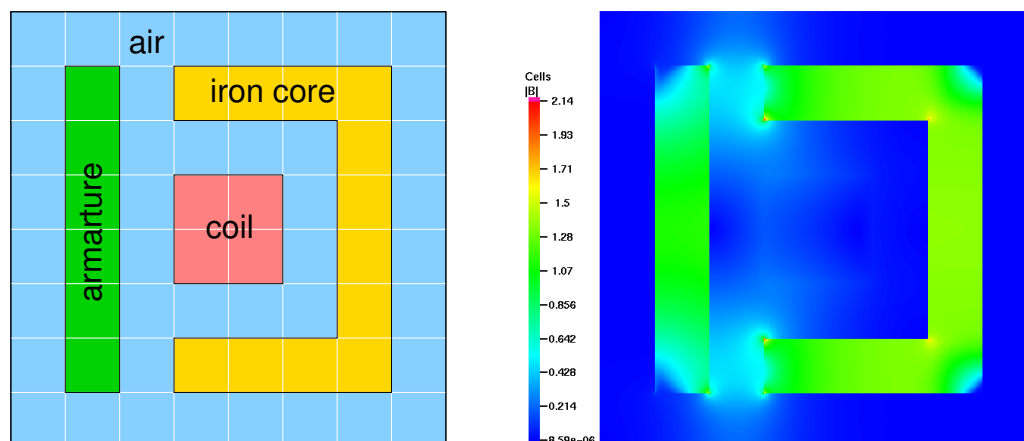


Figure 6.3: Example 6.3: *Left*: Model valve problem. *Right*: Visualization of $|B|$.

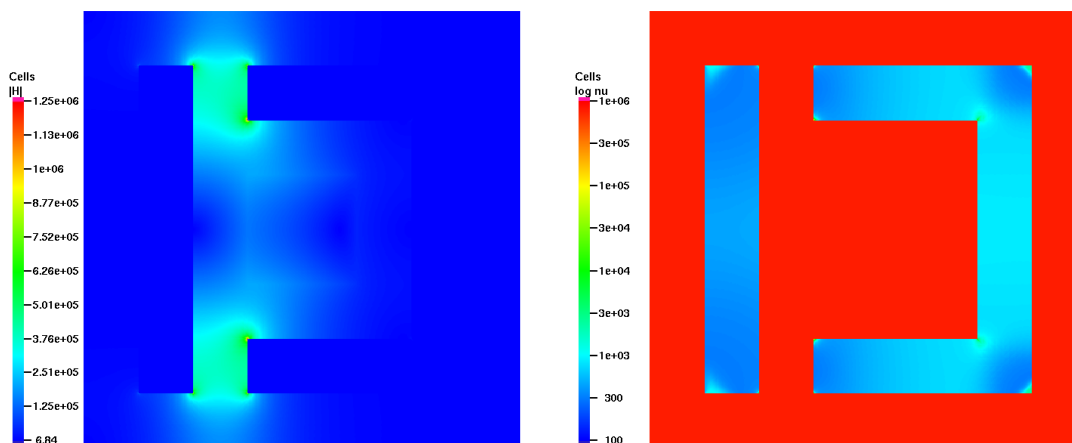


Figure 6.4: Example 6.3: *Left*: Visualization of $|B|$. *Right*: Visualization of $\nu(|B|)$.

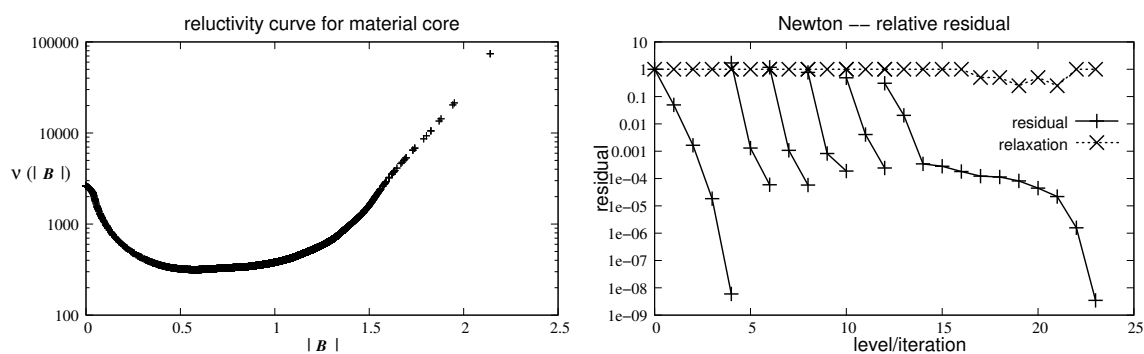


Figure 6.5: Example 6.3: *Left*: Occurring values of $\nu(|B|)$ plotted against $|B|$, logarithmic scale. *Right*: Reduction of the global residual, values of the relaxation parameter ρ_k .

Next we would like to focus on the linearized problems. Since the coefficient $\zeta(\cdot)$ is tensor valued, we choose the largest eigenvalue per element for the pointwise scalings in D_i and Q . In order not to complicate notation, we fix the Newton iteration index k and denote by $\zeta_i|_\tau$ the (matrix) value of $\zeta_i(\nabla u^k|_\tau)$ for an element τ , and by $\lambda_{\max}(\zeta_i|_\tau)$, $\lambda_{\min}(\zeta_i|_\tau)$ the largest, respectively, smallest eigenvalue of that matrix. The weights for the scaling operators (cf. Section 5.2.1) are then chosen as

$$\widehat{\alpha}_i^{\max}(x^h) = \max_{\tau \subset \omega^i(x^h)} \lambda_{\max}(\zeta_i|_\tau) \quad \text{for } x^h \in \partial\Omega_i^h.$$

In order to compare the efficiency of that scaling we introduce the weights

$$\bar{\alpha}_i = \max_{\tau \in \mathcal{T}^h(\Omega_i)} \lambda_{\max}(\zeta_i|_\tau).$$

Furthermore we introduce the *anisotropy measure*

$$m_{\text{anis}}(\zeta) := \max_{i \in \mathcal{I}_{\text{FEM}}} \max_{\tau \in \mathcal{T}^h(\Omega_i)} \frac{\lambda_{\max}(\zeta_i|_\tau)}{\lambda_{\min}(\zeta_i|_\tau)}, \quad (6.41)$$

and the *variation measure*

$$m_{\text{var}}(\zeta) := \max_{i \in \mathcal{I}_{\text{FEM}}} \frac{\max_{\tau \in \mathcal{T}^h(\Omega_i)} \lambda_{\max}(\zeta_i|_\tau)}{\min_{\tau' \in \mathcal{T}^h(\Omega_i)} \lambda_{\min}(\zeta_i|_{\tau'})}. \quad (6.42)$$

Table 6.1 and Table 6.2 show the result for two different settings of J_3 and different discretizations (using 4 up to 7 refinement levels). In Table 6.1, the choice of $J_3 = 1 \cdot 10^6$ leads to a relatively low heterogeneity ($m_{\text{var}} = \mathcal{O}(10^2)$ for the finest discretization). The weights $\bar{\alpha}_i$ still lead to a rather satisfactory number of PCG iterations. Changing the source term to $J_3 = 2.3 \cdot 10^6$ results in a high heterogeneity. In Table 6.2, we see that the weights $\bar{\alpha}_i$ result in a bad condition number of $\mathcal{O}(10^4)$ and an enormous number of PCG iterations. Contrary, the more carefully chosen weights $\widehat{\alpha}_i^{\max}$ result in an acceptable number of PCG iterations. For the finest discretization, however, the condition number is rather large which suggests that a clustering effect has occurred.

global DOFs	H/h			weights $\bar{\alpha}_i$		weights $\widehat{\alpha}_i^{\max}$	
		m_{anis}	m_{var}	PCG	<i>cond.</i>	PCG	<i>cond.</i>
16 641	32	6.1	26.3	20.0	9.9	20.0	9.9
66 049	64	6.9	66.0	24.3	22.6	21.7	18.7
263 169	128	10.2	152.4	29.7	43.9	24.7	35.9
1 050 625	256	11.4	258.1	36.3	84.4	27.7	65.5

Table 6.1: Example 6.1: Comparison of two weights for the one-level FETI preconditioner. Average number of PCG steps and iteration numbers during the Newton iteration on the finest level for the sequence of linearized problems, $J_3 = 1 \cdot 10^6$.

global DOFs	H/h	m_{anis}	m_{var}	weights $\bar{\alpha}_i$		weights $\hat{\alpha}_i^{\max}$	
				PCG	cond.	PCG	cond.
16 641	32	11.7	413.3	29.5	34.9	22.8	11.5
66 049	64	12.0	652.0	68.8	189.5	26.6	19.2
263 169	128	14.2	2 905.7	223.9	3 079.0	32.1	30.3
1 050 625	256	17.9	7 429.7	346.3	7 429.7	40.2	560.7

Table 6.2: Example 6.1: Comparison of two weights for the one-level FETI preconditioner. Average number of PCG steps and iteration numbers during the Newton iteration on the finest level for the sequence of linearized problems, $J_3 = 2.3 \cdot 10^6$.

Finally, we would like to demonstrate the use of a Newton FETI/BETI method including an exterior subdomain. Figure 6.6 displays the solution u and the field $|\mathbf{B}|$. Here, the outer layer of air subdomains has been replaced by an exterior subdomain, and the interior air subdomains have been discretized by BEM. On the left of that figure we show the interfaces between the BEM subdomains

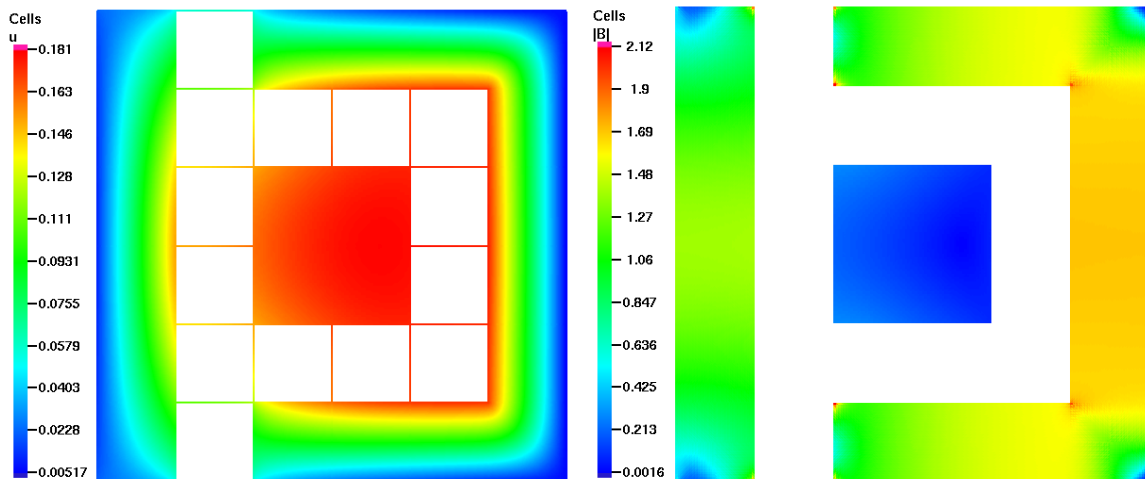


Figure 6.6: Example 6.1: Computational result of a FETI/BETI method including an exterior subdomain. *Left:* Solution u . *Right:* Magnetic flux density $|\mathbf{B}|$.

Example 6.2: Electrical motor Our second example is a model electrical motor, where the data is Courtesy of the ACCM¹. Figure 6.7, left, shows the setup and the subdomain partitioning. We model the surrounding air with an exterior BEM subdomain and the air gap with one single BEM subdomain. The radius of the rotor, which is modeled as a permanent magnet is 20 mm. In the rotor, $H_{0,1} = 0$, $H_{0,2} = 1.2 \nu_0$; elsewhere $\mathbf{H}_0 = 0$. Concerning the source term, we set $J_3 = 10^7$ in the subdomains marked with “+”, $J_3 = -10^7$ in those marked with “-”, and $J_3 = 0$ elsewhere. The yoke is the only ferromagnetic material, where we use the B - H -curve shown in Figure 6.7, right; in all the other materials we set $\nu = \nu_0$.

¹Austrian Center of Competence in Mechatronics – A K2-Center of the COMET/K2 program of the Federal Ministry of Transport, Innovation, and Technology, and the Federal Ministry of Economics and Labour, Austria

In order to compute the solution we have used a Newton IC-FETI/BETI method. Figure 6.8 displays the solution, the field lines and the interface-concentrated mesh (visualized by NetGen/NGSolve). In this example the nonlinearity is not very high because there are no singularities present. However, the small width of the air gap badly influences the condition number of the FETI/BETI system. Finding techniques for FETI/BETI type methods that can cope with such kinds of problems seems to be still an open problem.

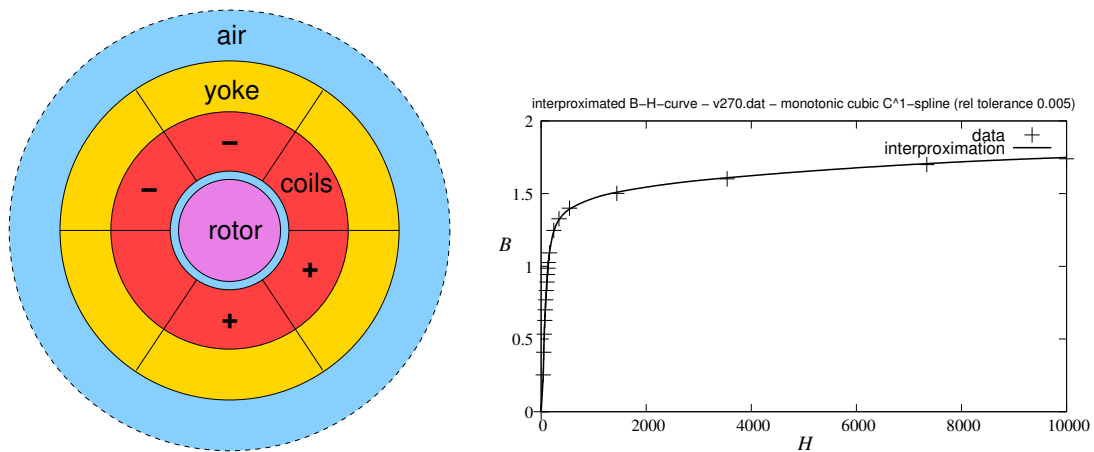


Figure 6.7: Example 6.2: *Left*: Model electric motor setup with subdomain partitioning. *Right*: Approximation of the data set `v270.dat`, Courtesy of the ACCM.

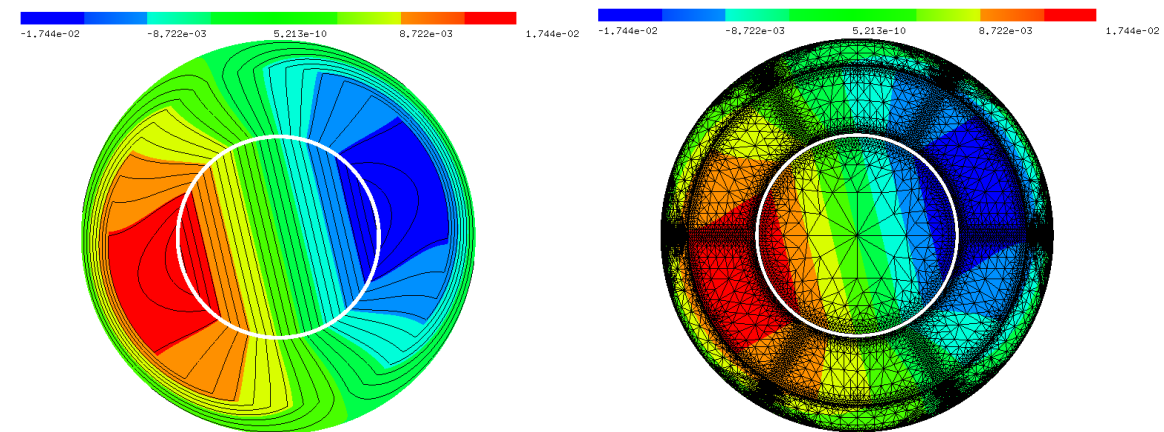


Figure 6.8: Example 6.2: *Left*: Magnetic field lines. *Right*: Solution and interface-concentrated mesh.

Bibliography

- [1] R. A. Adams and J. J. F. Fournier. *Sobolev Spaces*, volume 140 of *Pure and Applied Mathematics*. Academic Press, Amsterdam, Boston, second edition, 2003.
- [2] M. Ainsworth and B. Guo. Analysis of iterative sub-structuring techniques for boundary element approximation of the hypersingular operator in three dimensions. *Appl. Anal.*, 81(2):241–280, 2002.
- [3] B. Aksoylu, I. G. Graham, H. Klie, and R. Scheichl. Towards a rigorously justified algebraic preconditioner for high-contrast diffusion problems. *Comput. Visual Sci.*, 11(4-6):319–331, 2008.
- [4] R. E. Alcouffe, A. Brandt, J. E. Dendy, Jr., and J. W. Painter. The multi-grid method for the diffusion equation with strongly discontinuous coefficients. *SIAM J. Sci. Comput.*, 2(4):430–454, 1981.
- [5] P. Bastian. *Parallele Adaptive Mehrgitterverfahren*. Teubner Skripten zur Numerik. B. G. Teubner, Stuttgart, 1996.
- [6] M. Bebendorf. *Effiziente numerische Lösung von Randintegralgleichungen unter Verwendung von Niedrigrang-Matrizen*. PhD thesis, Universität Saarbrücken, 2000.
- [7] M. Bebendorf. Hierarchical *LU* decomposition based preconditioners for BEM. *Computing*, 74(3):225–247, 2005.
- [8] M. Bebendorf. *Hierarchical Matrices – A Means to Efficiently Solve Elliptic Boundary Value Problems*, volume 63 of *Lecture Notes in Computational Science and Engineering*. Springer, Berlin, Heidelberg, 2008.
- [9] M. Bebendorf and R. Kriemann. Fast parallel solution of boundary integral equations and related problems. *Comput. Visual Sci.*, 8(3-4):121–135, 2005.
- [10] C. Bertoglio, W. Hackbusch, and B. N. Khoromskij. Low rank tensor-product approximation of projected green kernels via sinc-quadratures. Preprint 79/2008, MPI MIS, Leipzig, 2008.
- [11] S. Beuchler, T. Eibner, and U. Langer. Primal and dual interface concentrated iterative substructuring methods. *SIAM J. Numer. Anal.*, 46(6):2818–2842, 2008.
- [12] P. E. Bjørstad, M. Dryja, and E. Vainikko. Additive schwarz methods without subdomain overlap and with new coarse spaces. In *Domain decomposition methods in sciences and engineering (Beijing, 1995)*, pages 141–157. Wiley, Chichester, 1997.

- [13] S. Boerm and J. Bendoraityte. Distributed \mathcal{H}^2 -matrices for non-local operators. *Comput. Visual Sci.*, 11(4-6):237–249, 2008.
- [14] S. Börm, L. Grasedyck, and W. Hackbusch. Hierarchical matrices. Lecture Note 21/2003, Max-Planck-Institut für Mathematik und Naturwissenschaften, Inselstr. 22, 04103 Leipzig, Germany, 2006. revised version, <http://www.mis.mpg.de/preprints/ln/lecturenote-2103.pdf>.
- [15] J.-F. Bourgat, R. Glowinski, P. LeTallec, and M. Vidrascu. Variational formulation and algorithm for trace operator in domain decomposition calculations. In T. Chan, R. Glowinski, J. Périaux, and O. Widlund, editors, *Domain Decomposition Methods. Second International Symposium on Domain Decomposition Methods*, pages 3–16. SIAM, Philadelphia, PA, 1989.
- [16] D. Braess. *Finite elements. Theory, fast solvers, and applications in solid mechanics*. Cambridge University Press, Cambridge, 2001.
- [17] J. H. Bramble and S. R. Hilbert. Estimation of linear functionals on Sobolev spaces with application to Fourier transforms and spline interpolation. *SIAM J. Numer. Anal.*, 7:112–124, 1970.
- [18] J. H. Bramble and X. Zhang. The analysis of multigrid methods. In P. G. Ciarlet and J. Lions, editors, *Handbook of Numerical Analysis*, volume VII, pages 173–415. North-Holland, Amsterdam, 2000.
- [19] J. H. Bramble, J. E. Pasciak, and A. H. Schatz. The construction of preconditioners for elliptic problems by substructuring, I. *Math. Comp.*, 47(175):103–134, 1986.
- [20] J. H. Bramble, J. E. Pasciak, and A. H. Schatz. The construction of preconditioners for elliptic problems by substructuring, II. *Math. Comp.*, 49(179):1–16, 1987.
- [21] J. H. Bramble, J. E. Pasciak, and A. H. Schatz. The construction of preconditioners for elliptic problems by substructuring, III. *Math. Comp.*, 51(184):415–430, 1988.
- [22] J. H. Bramble, J. E. Pasciak, and A. H. Schatz. The construction of preconditioners for elliptic problems by substructuring, IV. *Math. Comp.*, 53(187):1–24, 1989.
- [23] S. C. Brenner. An additive Schwarz preconditioner for the FETI method. *Numerische Mathematik*, 94(1):1–31, 2003.
- [24] S. C. Brenner. Analysis of two-dimensional FETI-DP preconditioners by the standard additive Schwarz framework. *Electron. Trans. Numer. Anal.*, 16:165–185, 2003.
- [25] S. C. Brenner and Q. He. Lower bounds for three-dimensional nonoverlapping domain decomposition algorithms. *Numer. Math.*, 93(3):445–470, 2003.
- [26] S. C. Brenner and L. R. Scott. *The mathematical theory of finite element methods*, volume 15 of *Texts in Applied Mathematics*. Springer, New York, second edition, 2002.
- [27] S. C. Brenner and L. Sung. BDDC and FETI-DP without matrices or vectors. *Comput. Methods Appl. Mech. Engrg.*, 8:1429–1435, 2007.

- [28] S. C. Brenner and L.-Y. Sung. Discrete Sobolev and Poincaré inequalities via Fourier series. *East-West J. Numer. Math.*, 8(2):83–92, 2000.
- [29] F. Brezzi and M. Fortin. *Mixed and Hybrid Finite Element Methods*. Springer Series in Computational Mathematics. Springer, New York, 1991.
- [30] C. Carstensen, M. Kuhn, and U. Langer. Fast parallel solvers for symmetric boundary element domain decomposition equations. *Numer. Math.*, 79:321–347, 1998.
- [31] T. F. Chan and T. P. Mathew. Domain decomposition algorithms. *Acta Numerica*, pages 61–143, 1994.
- [32] F. Cheng and B. A. Barsky. Interproximation: Interpolation and approximation using cubic spline curves. *Computer-Aided Design*, 23(10):700–706, 1991.
- [33] H. Cheng, L. Greengard, and V. Rokhlin. A fast adaptive multipole algorithm in three dimensions. *J. Comput. Phys.*, 155(2):468–498, 1999.
- [34] W. C. Chew, H. Y. Chao, T. J. Cui, C. C. Lu, S. Ohnuki, Y. C. Pan, J. M. Song, S. Velamparambil, and J. S. Zhao. Fast integral equation solvers in computational electromagnetics of complex structures. *Engineering Analysis with Boundary Elements*, 27(8):803–823, 2003.
- [35] P. G. Ciarlet. *The finite element method for elliptic problems*, volume 4 of *Studies in Mathematics and its Applications*. North-Holland, Amsterdam, 1987.
- [36] P. Clément. Approximation by finite element functions using local regularization. *RAIRO Analyse Numérique*, 9(R-2):77–84, 1975.
- [37] *PARDISO. Parallel Sparse Direct Linear Solver. User Guide Version 3.0*. Computer Science Department, University of Basel, Switzerland, 2005. www.computational.unibas.ch/cs/scicomp.
- [38] M. Costabel. Symmetric methods for the coupling of finite elements and boundary elements. In C. A. Brebbia, W. L. Wendland, and G. Kuhn, editors, *Boundary Elements IX*, pages 411–420. Springer, Berlin, Heidelberg, New York, 1987.
- [39] M. Costabel. Some historical remarks on the positivity of boundary integral operators. In M. Schanz and O. Steinbach, editors, *Boundary Element Analysis - Mathematical Aspects and Applications, Lecture Notes in Applied and Computational Mechanics*, volume 29, pages 1–27. Springer, Berlin, 2007.
- [40] M. Costabel and M. Dauge. On representation formulas and radiation conditions. *Math. Meth. Appl. Sci.*, 20(2):133–150, 1997.
- [41] Y.-H. De Roeck and P. LeTallec. Analysis and test of a local domain decomposition preconditioner. In R. Glowinski, Y. A. Kuznetsov, G. A. Meurant, J. Périaux, and O. Widlund, editors, *Fourth International Symposium on Domain Decomposition Methods for Partial Differential Equations*, pages 112–128. SIAM, Philadelphia, PA, 1991.

- [42] C. R. Dohrmann. A preconditioner for substructuring based on constrained energy minimization. *SIAM J. Sci. Comput.*, 25(1):246–258, 2003.
- [43] C. R. Dohrmann. An approximate BDDC preconditioner. *Numer. Linear Algebra Appl.*, 14(2):149–168, 2007.
- [44] C. R. Dohrmann, A. Klawonn, and O. B. Widlund. Extending theory for domain decomposition algorithms to irregular subdomains. In U. Langer, M. Discacciati, O. Widlund, and W. Zulehner, editors, *Domain Decomposition Methods in Science and Engineering XVII*, Lecture Notes in Computational Engineering and Science, pages 255–261. Springer, Berlin, Heidelberg, 2008.
- [45] C. R. Dohrmann, A. Klawonn, and O. B. Widlund. Domain decomposition for less regular subdomains: Overlapping Schwarz in two dimensions. *SIAM J. Numer. Anal.*, 46(4):2153–2168, 2008.
- [46] Z. Dostál, D. Horák, and R. Kučera. Total FETI – An easier implementable variant of the FETI method for numerical solution of elliptic PDE. *Commun. Numer. Methods Eng.*, 22(12):1155–1162, 2006.
- [47] C. C. Douglas, G. Haase, and U. Langer. *A Tutorial on Elliptic PDE Solvers and Their Parallelization*. Software, Environments, and Tools. SIAM, 2003.
- [48] M. Dryja and O. B. Widlund. Schwarz methods of Neumann-Neumann type for three-dimensional elliptic finite element problems. *Comm. Pure Appl. Math.*, 48(2):121–155, 1995.
- [49] M. Dryja, B. F. Smith, and O. B. Widlund. Schwarz analysis of iterative substructuring algorithms for elliptic problems in three dimensions. *SIAM J. Numer. Anal.*, 31(6):1662–1694, 1994.
- [50] T. Eibner. *Adaptive und randkonzentrierte FEM*. PhD thesis, TU Chemnitz, Chemnitz, Germany, June 2006.
- [51] T. Eibner and J. M. Melenk. A local error analysis of the boundary concentrated FEM. *IMA J. Numer. Anal.*, 26(4):752–778, 2006.
- [52] T. Eibner and J. M. Melenk. Multilevel preconditioning for the boundary concentrated hp-FEM. *Comp. Methods Appl. Mech. Engrg.*, 196(37-40):3713–3725.
- [53] L. C. Evans. *Partial Differential Equations*, volume 19 of *Graduate Studies in Mathematics*. American Mathematical Society, Providence, RI, 1998.
- [54] C. Farhat and J. Mandel. The two-level FETI method for static and dynamic plate problems part I: An optimal iterative solver for biharmonic systems. *Comput. Methods Appl. Mech. Engrg.*, 155:129–151, 1998.
- [55] C. Farhat and F.-X. Roux. A method of finite element tearing and interconnecting and its parallel solution algorithm. *Int. J. Numer. Meth. Engrg.*, 32:1205–1227, 1991.

- [56] C. Farhat and F.-X. Roux. Implicit parallel processing in structural mechanics. In J. T. Oden, editor, *Computational Mechanics Advances*, volume 2, pages 1–124. North-Holland, Amsterdam, 1994.
- [57] C. Farhat, J. Mandel, and F.-X. Roux. Optimal convergence properties of the FETI domain decomposition method. *Comput. Methods Appl. Mech. Engrg.*, 115:365–385, 1994.
- [58] C. Farhat, P. Chen, and J. Mandel. A scalable Lagrange multiplier based domain decomposition method for time-dependent problems. *Int. J. Numer. Meth. Engrg.*, 38(22):3831–3853, 1995.
- [59] C. Farhat, P. Chen, J. Mandel, and F.-X. Roux. The two-level FETI method part II: Extensions to shell problems, parallel implementation and performance results. *Comput. Methods Appl. Mech. Engrg.*, 155:153–179, 1998.
- [60] C. Farhat, A. Macedo, and R. Tezaur. FETI-H: A scalable domain decomposition method for high frequency exterior Helmholtz problems. In C.-H. Lai, P. E. Bjørstad, M. Cross, and O. B. Widlund, editors, *Domain Decomposition Methods in Science and Engineering: Eleventh International Conference London, UK*, pages 231–241, 1999. <http://www.ddm.org/DD11/Farhat.pdf>.
- [61] C. Farhat, M. Lesoinne, and K. Pierson. A scalable dual-primal domain decomposition method. *Numer. Linear Algebra Appl.*, 7:687–714, 2000.
- [62] C. Farhat, A. Macedo, and M. Lesoinne. A two-level domain decomposition method for the iterative solution of high-frequency exterior Helmholtz problems. *Numer. Math.*, 85(2):283–303, 2000.
- [63] C. Farhat, M. Lesoinne, P. Le Tallec, K. Pierson, and D. Rixen. FETI-DP: A dual-primal unified FETI method I: A faster alternative to the two-level FETI method. *Internat. J. Numer. Methods Engrg.*, 50:1523–1544, 2001.
- [64] M. Fiedler. Algebraic connectivity of graphs. *Czechoslovak Math. J.*, 23(98):298–305, 1973.
- [65] Y. Fragakis and M. Papadrakakis. The mosaic of high performance domain decomposition methods for structural methanics: Formulation, interrelation and numerical efficiency of primal and dual methods. *Compu. Methods Appl. Mech. Engrg.*, 192:3799–3830, 2003.
- [66] Y. Fragakis and M. Papadrakakis. The mosaic of high performance domain decomposition methods for structural methanics – Part II: Formulation enhancements, multiple right-hand sides and implicit dynamics. *Compu. Methods Appl. Mech. Engrg.*, 193:4611–4662, 2004.
- [67] F. N. Fritsch and R. E. Carlson. Monotone piecewise cubic interpolation. *SIAM J. Numer. Anal.*, 2:235–246, 1980.

- [68] I. Georgiev, J. Kraus, and S. Margenov. On the robustness of hierarchical multilevel splittings for discontinuous galerkin rotated bilinear fe problems. RICAM-Report 2008-09, Johann Radon Institut for Computational and Applied Mathematics, Linz, 2008. <http://www.ricam.oeaw.ac.at/publications/reports/08/rep08-09.pdf>.
- [69] V. Girault and P. A. Raviart. *Finite Element Methods for Navier-Stokes Equations*. Springer, New York, 1986.
- [70] R. Glowinski and M. F. Wheeler. Domain decomposition and mixed finite element methods for elliptic problems. In R. Glowinski, G. H. Golub, G. A. Meurant, and J. Périaux, editors, *First International Symposium on Domain Decomposition Methods for Partial Differential Equations*, pages 144–172. SIAM, Philadelphia, PA, 1988.
- [71] I. G. Graham and M. J. Hagger. Additive schwarz, cg and discontinuous coefficients. In P. E. Bjørstad, M. Espedal, and D. E. Keyes, editors, *Proceedings of 9th International Conference on Domain Decomposition*. Domain Decomposition Press, Bergen, 1999. <http://www.ddm.org/DD9/Graham.pdf>.
- [72] I. G. Graham and M. J. Hagger. Unstructured additive Schwarz-conjugate gradient method for elliptic problems with highly discontinuous coefficients. *SIAM J. Sci. Comput.*, 20(6):2041–2066, 1999.
- [73] I. G. Graham and R. Scheichl. Robust domain decomposition algorithms for multiscale PDEs. *Numerical Methods for Partial Differential Equations*, 23:859–878, 2007.
- [74] I. G. Graham and R. Scheichl. Coefficient-explicit condition number bounds for overlapping additive Schwarz. In U. Langer, M. Discacciati, D. E. Keyes, O. B. Widlund, and W. Zulehner, editors, *Domain Decomposition Methods in Science and Engineering XVII*, volume 60 of *Lecture Notes in Computational Science and Engineering*, pages 365–372. Springer, Berlin Heidelberg, 2008.
- [75] I. G. Graham, P. O. Lechner, and R. Scheichl. Domain decomposition for multiscale PDEs. *Numer. Math.*, 106:589–626, 2007.
- [76] P. Grisvard. *Elliptic Problems on Nonsmooth Domains*. Pitman, Boston, London, Melbourne, 1985.
- [77] G. Haase. *Parallelisierung numerischer Algorithmen für partielle Differentialgleichungen*. Teubner, Stuttgart, Leipzig, 1999.
- [78] G. Haase, B. Heise, M. Kuhn, and U. Langer. Adaptive domain decomposition methods for finite elements and boundary elements. In W. L. Wendland, editor, *Boundary Element Topics*, pages 121–147. Springer, Berlin, 1997. Proceedings of the Final Conference of the Priority Research Programme “Boundary Element Methods, 1989–1995” of the German Research Foundation, Stuttgart, Germany, October 2–4, 1995.
- [79] W. Hackbusch. A sparse matrix arithmetic based on \mathcal{H} -matrices. *Computing*, 62(2): 89–108, 1999.
- [80] W. Hackbusch. *Multi-Grid Methods and Applications*. Springer, Berlin, second edition, 2003.

- [81] W. Hackbusch and B. N. Khoromskij. A sparse \mathcal{H} -matrix arithmetic: II. Approximation to multi-dimensional problems. *Computing*, 64:21–47, 2000.
- [82] W. Hackbusch and Z. P. Nowak. On the fast matrix multiplication in the boundary element method by panel clustering. *Numer. Math.*, 54(4):463–491, 1989.
- [83] P. Hajłasz. Sobolev inequalities, truncation method, and John domains. In *Papers on Analysis*, pages 109–126. Report Univ. Jyväskylä, Dep. Math. Stat. 83, Jyväskylä, 2001.
- [84] B. Heise. Analysis of a fully discrete finite element method for a nonlinear magnetic field problem. *SIAM J. Numer. Anal.*, 31:745–759, 1994.
- [85] N. Heuer. Additive Schwarz method for the p -version of the boundary element method for the single layer potential operator on a plane screen. *Numer. Math.*, 88(3):485–511, 2001.
- [86] N. Heuer and E. P. Stephan. Iterative substructuring for hypersingular integral equations in \mathbf{R}^3 . *SIAM J. Sci. Comput.*, 20(2):739–749, 1998.
- [87] N. Heuer and E. P. Stephan. An additive Schwarz method for the h - p version of the boundary element method for hypersingular integral equations in \mathbf{R}^3 . *IMA J. Numer. Anal.*, 21(1):265–283, 2001.
- [88] G. C. Hsiao and W. L. Wendland. A finite element method for some integral equations of the first kind. *J. Math. Anal. Appl.*, 58:449–481, 1977.
- [89] G. C. Hsiao and W. L. Wendland. Domain decomposition in boundary element methods. In R. Glowinski, Y. A. Kuznetsov, G. Meurant, J. Périaux, and O. B. Widlund, editors, *Proceedings of the Fourth International Symposium on Domain Decomposition Methods for Partial Differential Equations*, pages 41–49. SIAM, Philadelphia, PA, 1991. Moscow, May 21–25, 1990.
- [90] G. C. Hsiao and W. L. Wendland. *Boundary Integral Equations*, volume 164 of *Applied Mathematical Sciences*. Springer, Berlin, Heidelberg, 2008.
- [91] G. C. Hsiao, O. Steinbach, and W. L. Wendland. Domain decomposition methods via boundary integral equations. *J. Comput. Appl. Math.*, pages 521–537, 2000.
- [92] N. Ida and J. P. A. Bastos. *Electromagnetics and Calculation of Fields*. Springer, New York, second edition, 1997.
- [93] M. Kaltenbacher. *Numerical Simulation of Mechatronic Sensors and Actuators*. Springer, Berlin, Heidelberg, 2004.
- [94] G. Karniadakis and S. Sherwin. *Spectral/hp Element Methods for CFD*. Oxford University Press, Oxford, 1999.
- [95] G. Karypis and V. Kumar. A fast and high quality multilevel scheme for partitioning irregular graphs. *SIAM J. Sci. Comp.*, 20(1):359–392, 1998.

- [96] G. Karypis and V. Kumar. *METIS: A Software Package for Partitioning Unstructured Graphs, Partitioning Meshes, and Computing Fill-Reducing Orderings of Sparse Matrices; Version 4.0*. University of Minnesota, Department of Computer Science / Army HPC Research Center Minneapolis, MN 55455, USA, September 1998. <http://people.scs.fsu.edu/~burkardt/pdf/metis.pdf>.
- [97] B. N. Khoromskij. On tensor approximation of green iterations for kohn-sham equations. *Comput. Visual Sci.*, 11(4-6), 2008.
- [98] B. N. Khoromskij. Fast tensor approximation of multi-dimensional convolution with linear scaling. Preprint 36/2008, MPI MIS, Leipzig, 2008.
- [99] B. N. Khoromskij and J. M. Melenk. An efficient direct solver for the boundary concentrated FEM in 2D. *Computing*, 69(2):91–117, 2002.
- [100] B. N. Khoromskij and J. M. Melenk. Boundary concentrated finite element methods. *SIAM J. Numer. Anal.*, 41(1):1–36, 2003.
- [101] H. H. Kim. A FETI-DP preconditioner for mortar methods in three dimensions. *Electron. Trans. Numer. Anal.*, 26:103–120, 2007.
- [102] H. H. Kim. A BDDC algorithm for mortar discretization of elasticity problems. *SIAM J. Numer. Anal.*, 46(4):2090–2111, 2008.
- [103] H. H. Kim and C.-O. Lee. A preconditioner for the FETI-DP formulation with mortar methods in two dimensions. *SIAM J. Numer. Anal.*, 42(5):2159–2175, 2005.
- [104] A. Klawonn and O. Rheinbach. Some computational results for robust FETI-DP methods applied to heterogeneous elasticity problems in 3D. In D. Keyes and O. Widlund, editors, *Domain Decomposition Methods in Sciences and Engineering XVI*, volume 55 of *Lecture Notes in Computational Science and Engineering*. Springer, Heidelberg, Berlin, 2007. Proceedings of the 16th International Conference on Domain Decomposition Methods, New York, January 2005.
- [105] A. Klawonn and O. Rheinbach. A parallel implementation of dual-primal FETI methods for three dimensional linear elasticity using a transformation of basis. *SIAM J. Sci. Comput.*, 28(5):1886–1906, 2006.
- [106] A. Klawonn and O. Rheinbach. Inexact FETI-DP methods. *Inter. J. Numer. Methods Engrg.*, 69:284–307, 2007.
- [107] A. Klawonn and O. Rheinbach. Robust FETI-DP methods for heterogeneous three dimensional elasticity problems. *Comput. Methods Appl. Mech. Engrg.*, 196:1400–1414, 2007.
- [108] A. Klawonn and O. B. Widlund. A domain decomposition method with Lagrange multipliers and inexact solvers for linear elasticity. *SIAM J. Sci. Comput.*, 22(4):1199–1219, 2000.
- [109] A. Klawonn and O. B. Widlund. FETI and Neumann-Neumann iterative substructuring methods: Connections and new results. *Comm. Pure Appl. Math.*, 54(1):57–90, 2001.

- [110] A. Klawonn and O. B. Widlund. Dual-primal FETI methods for linear elasticity. *Comm. Pure Appl. Math.*, 59(11):1523–1572, 2006.
- [111] A. Klawonn, O. B. Widlund, and M. Dryja. Dual-primal FETI methods for three-dimensional elliptic problems with heterogeneous coefficients. *SIAM J. Numer. Anal.*, 40(1):159–179, 2002.
- [112] A. Klawonn, L. Pavarino, and O. Rheinbach. Exact and inexact FETI-DP methods for spectral elements in two dimensions. In *Domain Decomposition Methods in Science and Engineering XVII*, volume 60 of *Lecture Notes in Computational Science and Engineering*, pages 279–286. Springer, Berlin, Heidelberg, 2008.
- [113] A. Klawonn, O. Rheinbach, and O. B. Widlund. An analysis of a FETI-DP algorithm on irregular subdomains in the plane. *SIAM J. Numer. Anal.*, 46(5):2484–2504, 2008.
- [114] J. Kraus and S. Margenov. Multilevel methods for anisotropic elliptic problems. In *Lectures on Advanced Computational Methods in Mechanics*, volume 1 of *Radon Series on Computational and Applied Mathematics*. Walter de Gruyter, Berlin, New York, 2007.
- [115] U. Langer. Parallel iterative solution of symmetric coupled FE/BE-equations via domain decomposition. *Contemporary Mathematics*, 157:335–344, 1994.
- [116] U. Langer and C. Pechstein. Coupled finite and boundary element tearing and interconnecting solvers for nonlinear potential problems. *ZAMM Z. Angew. Math. Mech.*, 86(12), 2006.
- [117] U. Langer and C. Pechstein. All-floating coupled data-sparse boundary and interface-concentrated finite element tearing and interconnecting methods. *Computing and Visualization in Science*, 11(4-6):307–317, 2008.
- [118] U. Langer and O. Steinbach. Boundary element tearing and interconnecting method. *Computing*, 71(3):205–228, 2003.
- [119] U. Langer and O. Steinbach. Coupled boundary and finite element tearing and interconnecting methods. In R. Kornhuber, R. Hoppe, J. Periaux, O. Pironneau, O. Widlund, and J. Xu, editors, *Lecture Notes in Computational Sciences and Engineering*, volume 40, pages 83–97. Springer, Heidelberg, 2004. Proceedings of the 15th International Conference on Domain Decomposition Methods, Berlin, July 2003.
- [120] U. Langer and O. Steinbach. Coupled finite and boundary element domain decomposition methods. In M. Schanz and O. Steinbach, editors, *Boundary Element Analysis - Mathematical Aspects and Applications, Lecture Notes in Applied and Computational Mechanics*, volume 29, pages 61–95. Springer, Berlin, 2007.
- [121] U. Langer, A. Pohořaľa, and O. Steinbach. Dual-primal boundary element tearing and interconnecting methods. Technical report no. 2005/6, Institute for Computational Mathematics, University of Technology, Graz, 2005.

- [122] U. Langer, G. Of, O. Steinbach, and W. Zulehner. Inexact fast multipole boundary element tearing and interconnecting methods. In D. Keyes and O. Widlund, editors, *Domain Decomposition Methods in Sciences and Engineering XVI*, volume 55 of *Lecture Notes in Computational Science and Engineering*. Springer, Heidelberg, Berlin, 2007. Proceedings of the 16th International Conference on Domain Decomposition Methods, New York, January 2005.
- [123] U. Langer, G. Of, O. Steinbach, and W. Zulehner. Inexact data-sparse boundary element tearing and interconnecting methods. *SIAM J. Sci. Comp.*, 29:290–314, 2007.
- [124] P. Le Tallec. Domain decomposition methods in computational mechanics. In J. T. Oden, editor, *Computational Mechanics Advances*, volume 1, pages 121–220. North-Holland, 1994.
- [125] J. Li and O. B. Widlund. FETI-DP, BDDC, and block Cholesky methods. *Int. J. Numer. Meth. Engng.*, 66(2):250–271, 2006.
- [126] J. Li and O. B. Widlund. On the use of inexact subdomain solvers for BDDC algorithms. *Comput. Methods Appl. Mech. Engrg.*, 196(8):1415–1428, 2007.
- [127] J. L. Lions and E. Magenes. *Non-Homogeneous Boundary Value Problems and Applications*, volume I. Springer, Berlin, Heidelberg, New York, 1972.
- [128] Y. Lung-An and L. Ying. *Numerical Methods for Exterior Problems*. World Scientific, 2006.
- [129] J. Mandel and M. Brezina. Balancing domain decomposition for problems with large jumps in coefficients. *Math. Comp.*, 65:1387–1401, 1996.
- [130] J. Mandel and C. R. Dohrmann. Convergence of a balancing domain decomposition by constraints and energy minimization. *Numer. Lin. Alg. Appl.*, 10:639–659, 2003.
- [131] J. Mandel and R. Tezaur. Convergence of a substructuring method with Lagrange multipliers. *Numer. Math.*, 73:473–487, 1996.
- [132] J. Mandel and R. Tezaur. On the convergence of a dual-primal substructuring method. *Numer. Math.*, 88:543–558, 2001.
- [133] J. Mandel, C. R. Dohrmann, and R. Tezaur. An algebraic theory for primal and dual substructuring methods by constraints. *Appl. Numer. Math.*, 54:167–193, 2005.
- [134] W. McLean. *Strongly Elliptic Systems and Boundary Integral Equations*. Cambridge University Press, Cambridge, UK, 2000.
- [135] S. G. Michlin. *Konstanten in einigen Ungleichungen der Analysis*, volume 35 of *Teubner-Texte zur Mathematik*. Teubner, Leipzig, 1981.
- [136] P. Monk. *Finite element methods for Maxwell's equations*. Numerical Mathematics and Scientific Computation. Oxford University Press, Oxford, 2003.
- [137] J. Nečas. *Les méthodes directes en théorie des équations elliptiques*. Masson et Cie, Éditeurs, Paris, 1967.

- [138] G. Of. *BETI-Gebietszerlegungsmethoden mit schnellen Randelementverfahren und Anwendungen*. PhD thesis, Universität Stuttgart, Germany, January 2006.
- [139] G. Of. The all-floating BETI method: Numerical results. In U. Langer, M. Discacciati, D. E. Keyes, O. B. Widlund, and W. Zulehner, editors, *Domain Decomposition Methods in Science and Engineering XVII*, volume 60 of *Lecture Notes in Computational Science and Engineering*, pages 295–302. Springer, Berlin Heidelberg, 2008.
- [140] G. Of, O. Steinbach, and P. Urthaler. Fast evaluation of Newton potentials in the boundary element method. Technical report no. 2008/3, Department for Numerical Mathematics, Graz University of Technology, Austria, 2006.
- [141] L. Pavarino. BDDC and FETI-DP preconditioners for spectral element discretizations. *Comput. Methods Appl. Mech. Engrg.*, 196(8):1380–1388, 2007.
- [142] C. Pechstein. Multigrid-Newton-methods for nonlinear magnetostatic problems. Master’s thesis, Johannes Kepler University of Linz, Institute of Computational Mathematics, Linz, 2004. <http://www.numa.uni-linz.ac.at/Teaching/Diplom/Finished/pechstein>.
- [143] C. Pechstein. Analysis of dual and dual-primal tearing and interconnecting methods in unbounded domains. SFB Report 2007-15, SFB “Numerical and Symbolic Scientific Computing” F013, Johannes Kepler University of Linz, August 2007. http://www.sfb013.uni-linz.ac.at/reports/2007/pdf-files/rep_07-15_pechstein.pdf.
- [144] C. Pechstein. Boundary element tearing and interconnecting methods in unbounded domains. *Applied Numerical Mathematics*, 2008. to appear.
- [145] C. Pechstein. BETI-DP methods in unbounded domains. In K. Kunisch, G. Of, and O. Steinbach, editors, *Numerical Mathematics and Advanced Applications – ENU-MATH 2007*, pages 381–388. Springer, Berlin, Heidelberg, 2008.
- [146] C. Pechstein and B. Jüttler. Monotonicity-preserving interproximation of B-H-curves. *Journal of Computational and Applied Mathematics*, 196(1):45–57, 2006.
- [147] C. Pechstein and R. Scheichl. Analysis of FETI methods for multiscale PDEs. *Numer. Math.*, 111(2):293–333, 2008.
- [148] C. Pechstein and R. Scheichl. Robust FETI solvers for multiscale elliptic PDEs. In *Proceedings of the 7th International Conference on Scientific Computing in Electrical Engineering (SCEE)*. Helsinki, Finland, September 2008; accepted for publication.
- [149] K. H. Pierson. *A Family of Domain Decomposition Methods for the Massively Parallel Solution of Computational Mechanics Problems*. PhD thesis, Aerospace Engineering, University of Colorado at Boulder, Boulder, CO, 2000.
- [150] A. Quarteroni and A. Valli. *Domain Decomposition Methods for Partial Differential Equations*. Oxford Science Publications, Oxford, 1999.
- [151] C. H. Reinsch. Smoothing by spline functions. *Numer. Math.*, 10:177–183, 1967.

- [152] S. Reitzinger, B. Kaltenbacher, and M. Kaltenbacher. A note on the approximation of B - H -curves for nonlinear computations. SFB Report 2002-30, Johannes Kepler University Linz, SFB Numerical and Symbolic Scientific Computing, 2002. <http://www.sfb013.uni-linz.ac.at/reports/2002/pdf-files/sfb02-30.pdf>.
- [153] O. Rheinbach. FETI – A dual iterative substructuring method for elliptic partial differential equations. Master’s thesis, Mathematisches Institut, Universität zu Köln, Germany, 2002.
- [154] O. Rheinbach. *Parallel Scalable Iterative Substructuring: Robust Exact and Inexact FETI-DP Methods with Applications to Elasticity*. PhD thesis, Universität Essen-Duisburg, 2006.
- [155] D. Rixen and C. Farhat. Preconditioning the FETI method for problems with intra- and inter-subdomain coefficient jumps. In P. E. Bjørstad, M. Espedal, and D. E. Keyes, editors, *Proceedings of 9th International Conference on Domain Decomposition*, pages 472–479, 1998. <http://www.ddm.org/DD9/Rixen.pdf>.
- [156] D. Rixen and C. Farhat. A simple and efficient extension of a class of substructure based preconditioners to heterogeneous structural mechanics problems. *Internat. J. Numer. Methods Engrg.*, 44(4):489–516, 1999.
- [157] S. Rjasanow. *Vorkonditionierte iterative Auflösung von Randelementgleichungen für die Dirichlet-Aufgabe*. Wissenschaftliche Schriftenreihe der Technischen Universität Chemnitz, Chemnitz, 1990.
- [158] S. Rjasanow and O. Steinbach. *The Fast Solution of Boundary Integral Equations*. Mathematical and Analytical Techniques with Applications to Engineering. Springer, 2007.
- [159] V. Rokhlin. Rapid solution of integral equations of classical potential theory. *J. Comput. Phys.*, 60(2):187–207, 1985.
- [160] J. Ruge and K. Stüben. Efficient solution of finite difference and finite element equations by algebraic multigrid (AMG). In D. J. Paddon and H. Holstein, editors, *Multigrid Methods for Integral and Differential Equations*, IMA Conference Series, pages 169–212. Clarendon Press, Oxford, 1985.
- [161] M. Sarkis. Nonstandard coarse spaces and Schwarz methods for elliptic problems with discontinuous coefficients using non-conforming elements. *Numer. Math.*, 77(3):383–406, 1997.
- [162] M. V. Sarkis. Two-level Schwarz methods for nonconforming finite elements and discontinuous coefficients. In N. D. Melson, T. A. Manteuffel, and S. F. McCormick, editors, *Proceedings of the Sixth Copper Mountain Conference on Multigrid Methods*, volume 2, pages 543–566. NASA, Hampton, VA, 1993.
- [163] M. V. Sarkis. *Schwarz Preconditioners for Elliptic Problems with Discontinuous Coefficients Using Conforming and Non-Conforming Elements*. PhD thesis, Courant Institute of Mathematical Sciences, 1994. TR-671, Department of Computer Science.

- [164] S. Sauter and C. Schwab. *Randelementmethoden. Analyse, Numerik und Implementierung schneller Algorithmen*. B. G. Teubner, Stuttgart, Leipzig, Wiesbaden, 2004.
- [165] R. Scheichl and E. Vainikko. Additive Schwarz with aggregation-based coarsening for elliptic problems with highly variable coefficients. *Computing*, 80(4):319–343, 2007.
- [166] O. Schenk and K. Gärtner. Solving unsymmetric sparse systems of linear equations with PARDISO. *Journal of Future Generation Computer Systems*, 20(3):475–487, 2004.
- [167] O. Schenk and K. Gärtner. On fast factorization pivoting methods for sparse symmetric indefinite systems. *Elec. Trans. Numer. Anal.*, 23:158–179, 2006.
- [168] R. Schneider. *Multiskalen- und Wavelet-Matrixkompression*. Advances in Numerical Mathematics. B. G. Teubner, Stuttgart, 1998.
- [169] H. A. Schwarz. Ueber einen grenzübergang durch alternirendes verfahren. In *Gesammelte Mathematische Abhandlungen*, volume 2, pages 133–143. Springer, Berlin, 1980. First published in *Vierteljahrsschrift der Naturforschenden Gesellschaft in Zürich*, volume 15, pages 272–286, 1870.
- [170] L. R. Scott and S. Zhang. Finite element interpolation of non-smooth functions satisfying boundary conditions. *Math. Comp.*, 54:483–493, 1990.
- [171] B. F. Smith, P. E. Bjørstad, and W. Gropp. *Domain Decomposition: Parallel Multilevel Methods for Elliptic Partial Differential Equations*. Cambridge University Press, 1996.
- [172] D. Stefanica. A numerical study of FETI algorithms for mortar finite element methods. *SIAM J. Sci. Comput.*, 23(4):1135–1160, 2001.
- [173] D. Stefanica and A. Klawonn. The feti method for mortar finite elements. In *Proceedings of the Eleventh International Conference on Domain Decomposition Methods*, pages 121–129, 1998. Greenwich, UK, July 20–24, 1998, available at <http://www.ddm.org/DD11/Stefanica.pdf>.
- [174] O. Steinbach. *Stability estimates for hybrid coupled domain decomposition methods*, volume 1809 of *Lecture Notes in Mathematics*. Springer, Heidelberg, 2003.
- [175] O. Steinbach. *Numerical Approximation Methods for Elliptic Boundary Value Problems. Finite and Boundary Elements*. Springer, New York, 2008.
- [176] O. Steinbach. OSTBEM – A boundary element software package. Technical report, University of Stuttgart, 2000.
- [177] O. Steinbach and W. L. Wendland. On C. Neumann’s method for second-order elliptic systems in domains with non-smooth boundaries. *J. Math. Anal. Appl.*, 262(2):733–748, 2001.
- [178] E. P. Stephan and T. Tran. Domain decomposition algorithms for indefinite hypersingular integral equations: the h and p versions. *SIAM J. Sci. Comput.*, 19(4):1139–1153 (electronic), 1998.

- [179] R. Tezaur. *Analysis of Lagrange multiplier based domain decomposition*. PhD thesis, University of Colorado at Denver, 1998. <http://www-math.cudenver.edu/graduate/thesis/rtezaur.pdf>.
- [180] A. Toselli. *Domain Decomposition for Vector Field Problems*. PhD thesis, Courant Institute of Mathematical Sciences, New York University, New York, USA, May 1999.
- [181] A. Toselli. Dual-primal FETI algorithms for edge finite-element approximations in 3D. *IMA J. Numer. Anal.*, 26:96–130, 2006.
- [182] A. Toselli and A. Klawonn. A FETI domain decomposition method for edge element approximations in two dimensions with discontinuous coefficients. *SIAM J. Numer. Anal.*, 39(3):932–956, 2001.
- [183] A. Toselli and X. Vasseur. A numerical study on Neumann-Neumann and FETI methods for *hp*-approximations boundary layer meshes in three dimensions. *IMA J. Numer. Anal.*, 24(1):123–156, 2004.
- [184] A. Toselli and O. B. Widlund. *Domain Decomposition Methods – Algorithms and Theory*, volume 34 of *Springer Series in Computational Mathematics*. Springer, Berlin, Heidelberg, 2005.
- [185] P. Urthaler. Schnelle Auswertung von Volumenpotentialen in der Randelementmethode. Master’s thesis, Graz University of Technology, Graz, 2008. available at <http://www.numerik.math.tu-graz.ac.at/berichte/Bericht0108.pdf>.
- [186] P. Vanek, J. Mandel, and M. Brezina. Algebraic multigrid by smoothed aggregation for 2nd and 4th order elliptic problems. *Computing*, 56(3):179–196, 1996.
- [187] P. S. Vassilevski. *Multilevel block factorization preconditioners*. Springer, New York, 2008.
- [188] T. von Petersdorff. *Randwertprobleme der Elastizitätstheorie für Polyeder – Singularitäten und Approximation mit Randelementmethoden*. PhD thesis, Technische Hochschule Darmstadt, Darmstadt, Germany, 1989.
- [189] C. Vuik, A. Segal, and J. A. Meijerink. An efficient preconditioned CG method for the solution of a class of layered problems with extreme contrasts in the coefficients. *J. Comput. Phys.*, 152(1):385–403, 1999.
- [190] O. B. Widlund. Exotic coarse spaces for Schwarz methods for lower order and spectral finite elements. In *Domain decomposition methods in scientific and engineering computing. Seventh International Conference on Domain Decomposition*, volume 180 of *Contemporary Mathematics*, pages 131–136. AMS, 1994.
- [191] O. B. Widlund, May 2008. Private communication.
- [192] J. Xu and Y. Zhu. Uniform convergent multigrid methods for elliptic problems with strongly discontinuous coefficients. *Math. Mod. Meth. Appl. Sci.*, 18(1):77–105, 2008.
- [193] E. Zeidler. *Nonlinear Functional Analysis and Its Applications – Part 2B: Nonlinear Monotone Operators*. Springer, New York, 1990.

- [194] W. Zheng and H. Qi. On Friedrichs–Poincaré-type inequalities. *J. Math. Anal. Appl.*, 304:542–551, 2005.
- [195] O. C. Zienkiewicz, D. M. Kelly, and P. Bettess. Marriage a la mode – the best of both worlds (Finite elements and boundary integrals). In R. Glowinski, E. Y. Rodin, and O. C. Zienkiewicz, editors, *Energy Methods in Finite Element Analysis*, chapter 5, pages 81–106. Wiley and Son, London, 1979.
- [196] W. Zulehner. *Numerische Mathematik – Eine Einführung anhand von Differentialgleichungsproblemen. Band 1: Stationäre Probleme*. Birkhäuser, Basel, 2008.
- [197] G. Zumbusch. *Parallel Multilevel Methods – Adaptive Mesh Refinement and Loadbalancing*. B. G. Teubner, Stuttgart, Leipzig, Wiesbaden, 2003.

Eidesstattliche Erklärung

Ich, Dipl.-Ing. Clemens Pechstein, erkläre an Eides statt, dass ich die vorliegende Dissertation selbständig und ohne fremde Hilfe verfasst, andere als die angegebenen Quellen und Hilfsmittel nicht benutzt bzw. die wörtlich oder sinngemäß entnommenen Stellen als solche kenntlich gemacht habe. Weiters erkläre ich dass ich die vorliegende Dissertation bisher an keiner inländischen oder ausländischen Universität vorgelegt habe.

Linz, December 2008

Clemens Pechstein

Curriculum Vitae

Name:	Clemens Pechstein
Nationality:	Austria
Date/Place of Birth:	9 August, 1979, Schärding, Austria
Education:	
1997	High School Diploma (Matura)
1997–2004	Curriculum “Technische Mathematik”, Johannes Kepler University Linz
March 2004	Diploma
April–Sept. 2004	PhD student at JKU, supported by the FWF project P14953
Oct. 2004–Sept. 2005	Civilian service (Austrian Youth Red Cross)
since Nov. 2005	PhD student at JKU, supported by the Austrian Science Funds (FWF) and the Austrian Grid project
Selected Activities:	
2003–2004	Diploma thesis “Multigrid-Newton-Methods for Nonlinear Magnetostatic Problems”, supported by Robert Bosch GmbH, Gerlingen, Germany
June 2006	17th International Conference on Domain Decomposition Methods (DD17), minisymposium talk
September 2006	SCEE, Sinaia, Romania, talk
May 2007	Conference on Boundary Elements – Theory and Applications (BETA), Hannover, Germany, talk
July 2007	6th International Congress on Industrial and Applied Mathematics (ICIAM), Zürich, Switzerland, invited minisymposium talk
September 2007	7th European Conference on Numerical Mathematics and Advanced Applications (ENUMATH), Graz, Austria, minisymposium talk
May 2008	European Finite Element Fair, Göteborg, Sweden, talk
June 2008	Research visit at the Bath Institute for Complex Systems (BICS), University of Bath, United Kingdom
September 2008	SCEE, Helsinki, Finland, talk; Chemnitz FEM Symposium, Chemnitz, Germany, talk

Further talks at the RWTH Aachen University, University of Duisburg-Essen (Germany), Vienna University of Technology, and Graz University of Technology (Austria), etc.

More information at <http://www.numa.uni-linz.ac.at/~clemens/>

Selected Publications:

C. Pechstein. *Multigrid-Newton-Methods for Nonlinear Magnetostatic Problems*. Master's thesis, Johannes Kepler University of Linz, Institute of Computational Mathematics, Linz, 2004. <http://www.numa.uni-linz.ac.at/Teaching/Diplom/Finished/pechstein>

C. Pechstein and B. Jüttler. Monotonicity-preserving interproximation of B - H -curves. *J. Comp. Appl. Math.* 196(1):45–57 (2006)

U. Langer and C. Pechstein. Coupled finite and boundary element tearing and interconnecting solvers for nonlinear potential problems. *Z. Angew. Math. Mech.* 86(12):915–931 (2006)

J. Schöberl, J. Melenk, C. Pechstein and S. Zangl. Additive Schwarz preconditioning for p -version triangular and tetrahedral finite elements. *IMA J. Numer. Anal.* 28(1):1-24 (2008)

U. Langer and C. Pechstein. All-floating coupled data-sparse boundary and interface-concentrated finite element tearing and interconnecting methods. *Comput. Vis. Sci.* 11(4-6):307–317 (2008)

C. Pechstein. BETI-DP methods in unbounded domains. In K. Kunisch, G. Of, and O. Steinbach, editors, *Numerical Mathematics and Advanced Applications – ENUMATH 2007*, pages 381–388. Springer, Berlin, Heidelberg, 2008.

C. Pechstein and R. Scheichl. Analysis of FETI methods for multiscale PDEs. *Numer. Math.* 111(2):293–333 (2008)

C. Pechstein. Boundary element tearing and interconnecting methods in unbounded domains. *Appl. Num. Math.*, to appear.

C. Pechstein and R. Scheichl. Robust FETI solvers for multiscale elliptic PDEs. Proceedings of the 7th International Conference on Scientific Computing in Electrical Engineering (SCEE 2008), Helsinki, September 2008, accepted for publication.